

**DOKUZ EYLÜL UNIVERSITY  
GRADUATE SCHOOL OF NATURAL AND APPLIED  
SCIENCES**

**DEVELOPMENT OF DESIGN SPECTRA FOR  
İZMİR USING NEW GENERATION  
ATTENUATION RELATIONSHIPS**

**by**

**Siditan ZAGANI**

**July, 2012**

**İZMİR**

**DEVELOPMENT OF DESIGN SPECTRA FOR  
İZMİR USING NEW GENERATION  
ATTENUATION RELATIONSHIPS**

A Thesis Submitted to the  
**Graduate School of Natural and Applied Sciences of Dokuz Eylül University**  
**In Partial Fulfillment of the Requirements for the Degree of Master of Science**  
in  
**Civil Engineering, Geotechnical Engineering Program**

by

**Siditan ZAGANI**

**July, 2012**

**İZMİR**

## M.Sc THESIS EXAMINATION RESULT FORM

We have read the thesis entitled "**DEVELOPMENT OF DESIGN SPECTRA FOR İZMİR USING NEW GENERATION ATTENUATION RELATIONSHIPS**" completed by **SİDİTAN ZAGANI** under supervision of **ASSOC. PROF. GÜRKAN ÖZDEN** and we certify that in our opinion it is fully adequate, in scope and in quality, as a thesis for the degree of Master of Science.



Assoc. Prof. Dr. Gürkan ÖZDEN

---

Supervisor



Prof. Dr. Arif Şengün KAYALAR



Assoc. Prof. Dr. Mustafa AKGÜN

---

(Jury Member)

---

(Jury Member)



---

Prof.Dr. Mustafa SABUNCU  
Director  
Graduate School of Natural and Applied Sciences

## **ACKNOWLEDGMENTS**

I would like to express my indebted appreciation to my supervisor Assoc. Prof. Dr. Gürkan ÖZDEN for his kind guidance and interest, constructive suggestions, and restless supervision throughout every stage of this study.

I am grateful to Dr. Özgür BOZDAĞ for his advices and kind interest. Finally, I offer my grateful thanks to my family, my father, my mother and my brother, for their affectionate love and moral support, which I will need forever.

Siditan ZAGANI

# **DEVELOPMENT OF DESIGN SPECTRA FOR İZMİR USING NEW GENERATION ATTENUATION RELATIONSHIPS**

## **ABSTRACT**

This study is about the development of probabilistic hazard maps of İzmir in terms of ‘ground acceleration’ values for three different probability of exceedance levels in 50 years at the bedrock.

Earthquake magnitudes are defined in different scales all over the world. This causes the collected data to be in different units. In order to use these data correctly, the magnitude data of İzmir and its vicinities were converted to the generally preferred scale of moment of magnitude, after establishment of the correlations between the data pairs.

Next step in the study was to define the seismic zones for İzmir. Using the faults properties taken from several references and the location of earthquake epicenters eleven seismic zones were specified. During risk analyses each zone was taken into consideration separately and the annual reoccurrence relationships for each source zone were obtained.

The earthquake effect was estimated using new generation attenuation relationships postulated by Campbell and Bozorgnia (2008), Brian, Chiou and Youngs (2008) and Boore and Atkinson (2007). The implementation of the probabilistic seismic hazard model was done by using the Seisrisk III software. As they are essential for the development of design spectrum, the calculations were done for two different spectral periods such as  $T=1.0$  second and 0.2 second. It was found that the new attenuation relationships suggested by Campbell and Bozorgnia (2008) and Brian et al (2008) yielded similar results. Among the parameters taken into consideration in the attenuation models the parameter related with the depth to bedrock with 1000 kilometer per second shear wave velocity seems to affect the

obtained results more significantly resulting in the computation of higher values of accelerations along the coastline where the depth to the rock is much deeper.

**Keywords:** İzmir, earthquake hazard map, new generation attenuation relationship, ground acceleration.

## **YENİ NESİL AZALIM İLİŞKİLERİ KULLANILARAK İZMİR İÇİN TASARIM SPEKTRUMLARININ GELİŞTİRİLMESİ**

### **ÖZ**

Bu çalışma, İzmir'e ait probabilistik deprem tehlike haritalarının ivme değerleri cinsinden taban kayasında 50 yıl içinde farklı aşılma olasılıkları için belirlenmesi hakkındadır.

Deprem büyüklükleri dünyada farklı ölçeklerde tanımlanmaktadır. Bu durum toplanan verilerin değişik birimlerde olmasına yol açmaktadır. Bu verilerin doğru bir şekilde kullanılabilmesi için İzmir ve yakın çevresindeki büyüklik verileri veri çiftleri arasındaki ilişkilerin tanımlanmasını takiben moment büyülüğüne çevrilmiştir.

Çalışmada bir sonraki aşama İzmir için sismik zonların tanımlanması olmuştur. Bir çok kaynaktan alınan fay özellikleri ile deprem merkez üslerinin konumları kullanılarak onbir sismik zon tanımlanmıştır.

Risk analizlerinde her zon ayrı ele alınmış ve bunlar her biri için yıllık tekerrür ilişkileri elde edilmiştir. Deprem etkisi Campbell ve Bozorgnia (2008), Brian, Chiou ve Youngs (2008) ile Boore ve Atkinson (2007) tarafından ortaya konmuş yeni nesil azalım ilişkileri yoluyla tahmin edilmiştir. Probabilistik sismik tehlike modelinin uygulaması Seisrisk III yazılımı kullanılarak yapılmıştır. Tasarım spektrumunun kurulmasında gerekli olduğu için hesaplar  $T=1.0$  saniye ve 0.2 saniye spektral periyotları için gerçekleştirılmıştır. Modellerde dikkate alınan parametreler içinde kayma dalgası hızı 1000 metre bölü saniye olan taban kayasına olan derinlikle ilgili parametrenin sonuçları daha belirgin bir şekilde etkilediği, kayaya olan derinliğin çok daha fazla olduğu kıyı şeridinde daha yüksek ivme değerlerinin hesaplanmasına yol açtığı görülmektedir.

**Anahtar Kelimeler:** İzmir, deprem tehlike haritası, yeni nesil azalım ilişkisi, yüzey ivmesi.

## CONTENTS

	Page
THESIS EXAMINATION RESULT FORM.....	ii
ACKNOWLEDGEMENTS .....	iii
ABSTRACT .....	iv
ÖZ.....	vi
 <b>CHAPTER ONE – INTRODUCTION .....</b>	<b>1</b>
1.1 Purpose and Scope .....	1
 <b>CHAPTER TWO – THE STUDY AREA .....</b>	<b>3</b>
2.1 Location of the Study Area .....	3
2.2 Tectonics .....	5
2.2.1 General Geology .....	5
2.2.1.1 Alluvial Geomorphology of Izmir and Surroundings.....	11
2.2.2 Significant Faults .....	13
2.2.3 Seismicity .....	17
2.2.3.1 Historical earthquakes occurred in Izmir and its vicinities before 1900.....	17
2.2.3.2 Significant Earthquakes Occurred in Izmir and its Vicinities after 1900 .....	18
2.3 Soil Characteristics .....	21
2.3.1 Mavişehir Coastal Zone.....	21
2.3.2 Manavkuyu Zone .....	24
 <b>CHAPTER THREE – SEISMIC HAZARD ANALYSIS METHODOLOGY .</b>	<b>26</b>
3.1 Introduction to Seismic Hazard Analysis .....	26
3.2 Identification of the Earthquake Sources.....	26

3.3 Probabilistic Seismic Hazard Analysis.....	27
3.3.1 Introduction to Probabilistic Seismic Hazard Assessment.....	27
3.3.2 Clues of Earthquake Activities .....	31
3.3.2.1 Geologic Evidence.....	31
3.3.2.2 Fault Activity.....	31
3.3.2.3 Magnitude Indicator.....	32
3.3.2.4 Historical Seismicity.....	33
3.4 New Generation Attenuation Relationships.....	33
3.4.1 Campbell-Bozorgnia NGA Ground Motion Relations for the Geometric Mean Horizontal Component of Peak and Spectral Ground Motion Parameters.....	35
3.4.1.1 Median Ground Motion Model .....	35
3.4.1.2 Aleatory Uncertainty Model.....	39
3.4.1.3 General limits of Applicability.....	41
3.4.2 NGA Model for Average Horizontal Component of Peak Ground Motion and Response Spectra suggested by Brian at al. (2008).....	41
3.4.2.1 Ground Motion Model .....	41
3.4.2.2 General Limits of Applicability .....	43
3.4.3 NGA Ground Motion Relations for the Geometric Mean Horizontal Component of Peak and Spectra Ground Motion Parameters suggested by Boore & Atkinson (2007) .....	43
3.4.3.1 General Limits of Applicability .....	46
3.4.4 Advantages of New Generation Attenuation Models .....	46
3.5 Seisrisk III Software .....	47
3.5.1 Model Implementation .....	49
3.5.1.1 Calculation of Ground Motion Exceedance Probability.....	51
3.5.1.2 Outputs.....	52
<b>CHAPTER FOUR – SEISMIC HAZARD ANALYSIS .....</b>	<b>53</b>
4.1 Magnitude Conversion Relationships.....	53
4.2 Earthquake Source Characterization .....	57

4.2.1 Determination of the Source Zones .....	57
4.2.2 Earthquake Recurrence Relationships.....	60
4.3 Determination of Ground Motions Acceleration .....	61
4.4 The Definition of Earthquake Effect .....	64
4.4.1 Earthquake Levels.....	64
4.4.1.1 Earthquake Level D1 .....	64
4.4.1.2 Earthquake Level D2 .....	64
4.4.1.3 Earthquake Level D3 .....	64
4.4.2 Earthquake Design Spectra.....	65
4.5 Discussion of the Results .....	69
<b>CHAPTER FIVE – CONCLUSIONS AND RECOMMANDATIONS.....</b>	<b>72</b>
<b>REFERENCES .....</b>	<b>75</b>
<b>APPENDICES.....</b>	<b>78</b>

## **CHAPTER ONE**

### **INTRODUCTION**

#### **1.1 Purpose and Scope**

By growing of the population of the cities all over the world, the number of high rise buildings is rapidly increasing. As a result, the occurrence of a probable strong earthquake may cause disasters. Some of the recent earthquakes are the Kocaeli (1999), Ceyhan (1998), Erzincan (1992) and Erzurum (1983) Earthquakes that killed thousands of people.

The reality that Turkey is a seismically active country should be taken into consideration. İzmir is one of most important cities of Turkey and its population is rapidly increasing. According to earthquake zonation map of Turkey, İzmir is situated within the first earthquake region.

The aim of this study is to perform a probabilistic seismic hazard analysis for İzmir using new generation attenuation relationships and to create design spectra for two specific sites.

The study is carried out in stages. The first stage is the transformation of earthquake magnitude data to a uniform scale. The second stage is the determination of the seismic source zones and definition of their earthquake recurrence characteristics using the recurrence relationships suggested by Gutenberg & Richter (1954).

The effect of earthquakes on a specified site may be expressed better with the help of new generation attenuation relationships. The third step is about the attenuation relationships. A large number of attenuation relationships have been postulated during the last 50 years. Some of them have been corrected or updated during the time. In this thesis, earthquake effect is estimated using new generation attenuation

relationships postulated by Campbell & Bozorgnia (2008), Brian et al.(2008) and Boore & Atkinson (2007).

The fourth step is about preparation of probabilistic hazard maps for İzmir (ground acceleration values for 1 second and 0.2 seconds spectral period of time) for 2%, 10% and 50% probability of exceedance in 50 years. Probabilistic hazard analysis is implemented using SEISRISK III software.

In the fifth step, design spectra for two specific sites of İzmir region are developed using probabilistic analysis and these design spectra are compared with those suggested by Demiryollar Limanlar Ve Hava Meydanları İnşaat Müdürlüğü [DLH] (2008) and Türkiye deprem Yönetmeliği [DBYBHY] (2007) . Finally, the results are discussed and conclusions are made.

## CHAPTER TWO

### THE STUDY AREA

#### 2.1 Location of the Study Area

The study area is located in the western Anatolia on the Aegean coast. It includes Izmir city and its near vicinity. This area is defined as a rectangle between the longitudes of E  $25.75^{\circ}$  and E  $28.75^{\circ}$  and the latitude of N  $37.75^{\circ}$  and N  $39.5^{\circ}$ , as shown in Figure 2.1.

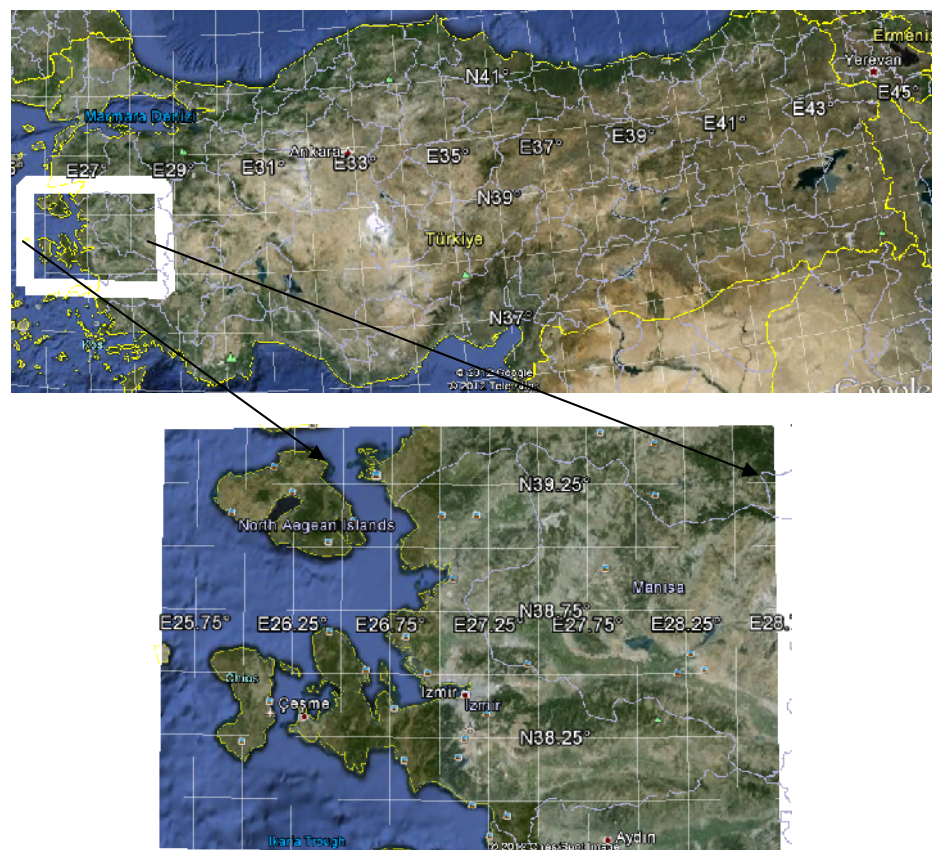


Figure 2.1 Location map of the study area

Additionally, two sites are included in this study. Site\_1 is located in Manavkuyu. It is located at longitude E  $27.17^{\circ}$  and latitude N  $38.458^{\circ}$ . Site\_2 is located in Mavişehir at longitude E  $27.08^{\circ}$  and latitude N  $38.467^{\circ}$ . These two sites are shown in Figure 2.2.



Figure 2.2 Locations of the Site\_1 and Site\_2

## 2.2 Tectonics

### 2.2.1 General Geology

The study area takes place in the central Aegean Sea by the western coast of Anatolia including zmir and its vicinities. As part of Anatolia it includes different kinds of tectonic phenomena such as transform strike-slip faulting, continental collusion, subduction (Nubia, Arabia) etc. A tectonic map of Anatolia and nearby regions is given in Figure 2.3.

Collusion of African plate with Eurasia dominates the tectonic framework of Mediterranean. Subduction of Nubia in Hellenic Arc is the basic reason for N–S extension of Western Anatolia. While the central and Eastern Anatolia have a diffusive deformation, the western of it seems to be extending in N-S with an upper bound speed of 20 mm/year (Aktu & Kilico lu, 2006).

In the history of western Anatolia four major paleotectonic units were developed. These units can be listed from north to south as continental of Sakarya, zmir-Ankara Clamp Zone, Menders Massif and Likya nappes (Özden et al., 2011).

The base unit of Continent of Sakarya is created by a mix of metamorphic and non metamorphic units. The base unit of this continent is covered by Mesozoic and Cenozoic units. zmir-Ankara suture zone takes place between Continent of Sakarya and Menderes massif. It is thought that some parts of zmir-Ankara suture are metamorphosed between the periods of upper Cretaceous and Lower Miocene. This geologic unit that takes place nearby zmir is named as Bornova Melange. Melange is formed from deformed volcanic sedimentary units. These units include basaltic lavas, shale and sand stones. Additionally, limestone and marble blocks can be encountered in Melange units. The age of Bornova Melange is approximately determined as upper Cretaceous. This is done by examining red colored limestone of this Melange (Özden et al., 2011).

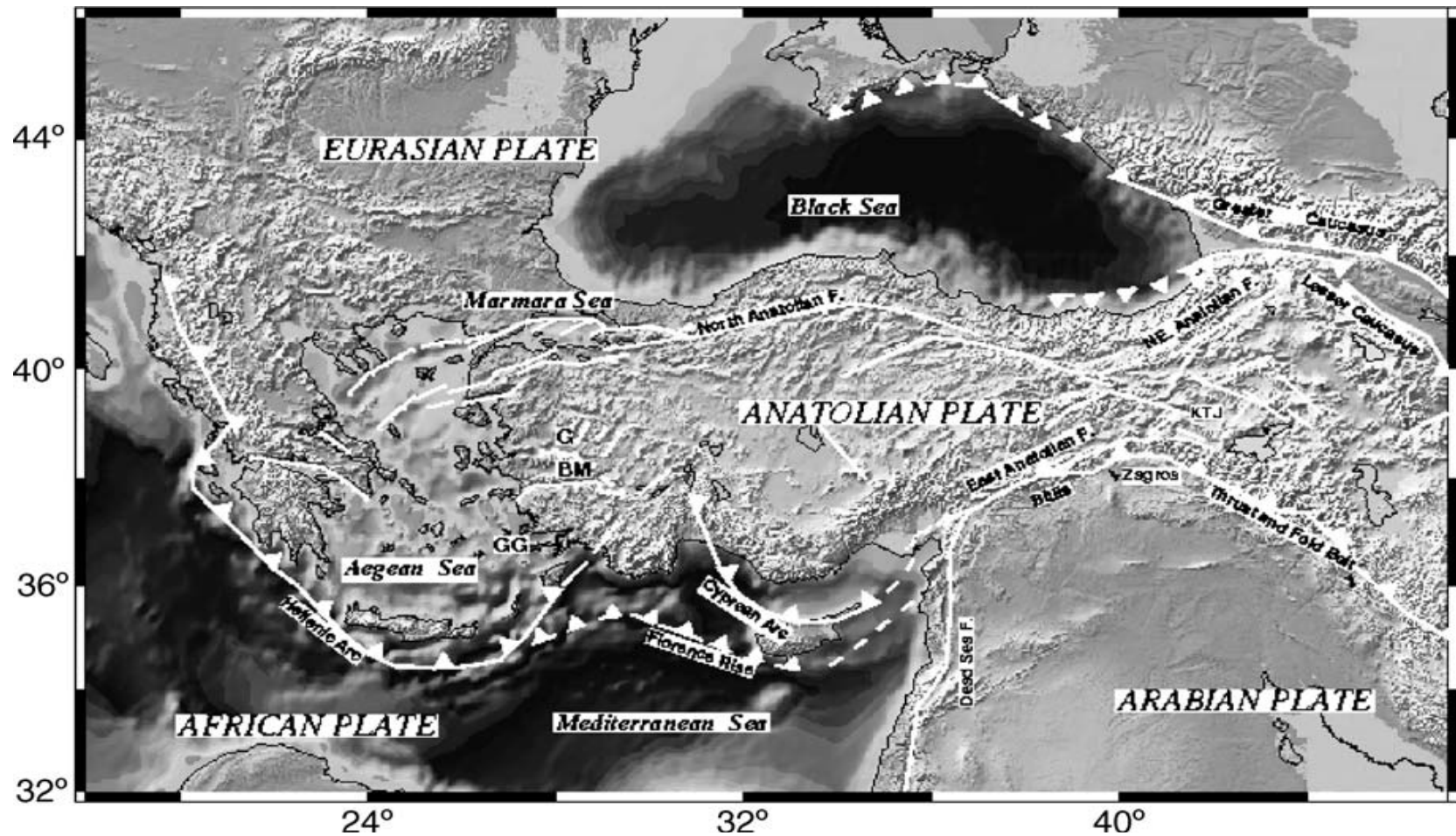


Figure 2.3 General tectonic map of Anatolia and its surroundings. (Aktu & Kılıçlı lu, 2006)

Menderes Massif is one of the most important metamorphic units of western Anatolia. This unit is located between Ankara suture zone and Lycian Nappes. The Menderes Massif has a complicated lithology. Its age is estimated to range from 35 to 40 million years. Lycian nappes extend between Menderes massif and Autochthonous unit of Bey Mountains (Özden et al., 2011).

In the period of upper Cretaceous, ocean crust overlapped Anatolid-Tauride platform during subduction. After that, during the continental collision, occurred during Upper Paleocene-lower Eocene period, this unit changed again reaching its current complex form called Lycian nappes. (RADIUS, 1999; Bozkurt & Sözbilir, 2004; Emre & Sözbilir, 2007). The main Paleotectonic units of pre Mid-Miocene period were united to create geologic structure of western Anatolia. Main geological units of Western Anatolia are shown in Figure 2.4.

Western Anatolia is one of the most deformed regions all over the world. The seismicity presented in this zone is the most important evidence of this deformation. Nowadays geomorphology is created by east-west directed graben systems. These systems can be listed from north to south as Bakırçav, Simav, Gediz, Küçük Menderes, Büyük Menders and Gökova grabens (Özden et al., 2011).

One of the factors for the occurrence of dip-slip normal faults of the region is gravity. One example of this are faults systems of zmir Bay. On the other hand, in horst zones compressive forces are one of the reasons for formation of reverse faults. Most of the east-west directed faults are defined as normal. Dip angle (plane angle) of these normal faults ranges between 45° and 70°. Additionally, the region ( zmir Bay) contains north-south and northeast-south west directed strike-slip faults (Özden et al., 2011). In general, the city of zmir, the districts of Alia a and Menemen are defined as First Degree Earthquake Zones (RADIUS, 1999).

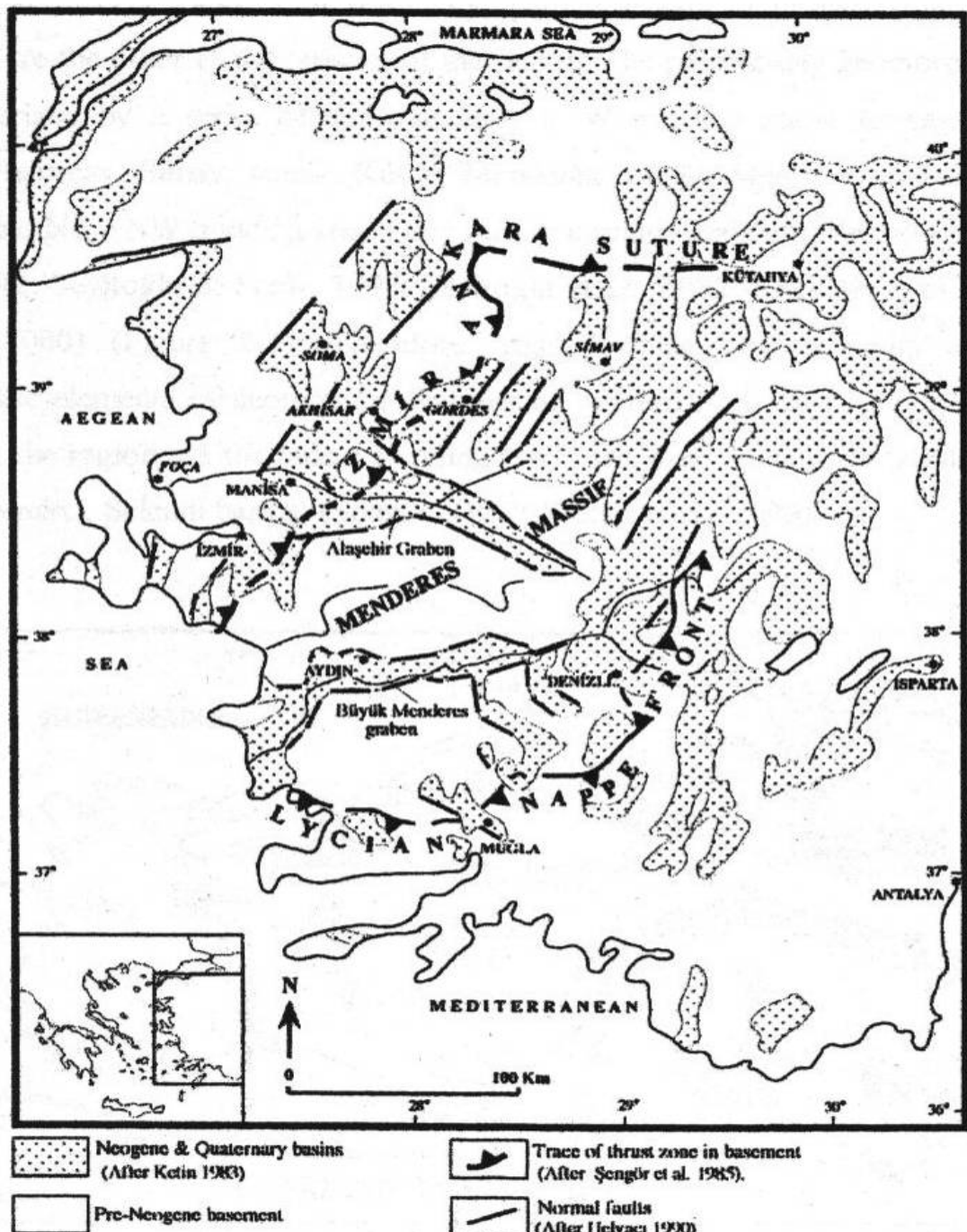


Figure 2.4 Main geological units of western Anatolia (Özden et al., 2011).

There are three different tectonic belts in Izmir Bay. In the east, middle and west of the Izmir Bay are located Menders Massif, Ankara zone and Karaburun Belt respectively. The first descent of Izmir-Ankara zone takes place between Bornova and Seferihisar (Özden et al., 2011). The first deformations at Bornova complexity is thought to get started, by carrying the platform to the basin, between Maestrichtien

and Daniyen during the flysch deposition. Most of the Bornova complexity was pushed over Menderes metamorphic by means of tectonic effects. This deformation extended over all the volume of Bornova complexity taking a squama like geometry. This deformation should have been effective during late Eocene. At the same period of time, the main metamorphism of Menders massif is thought to have been developed (Figure 2.5) (Özden et al., 2011).

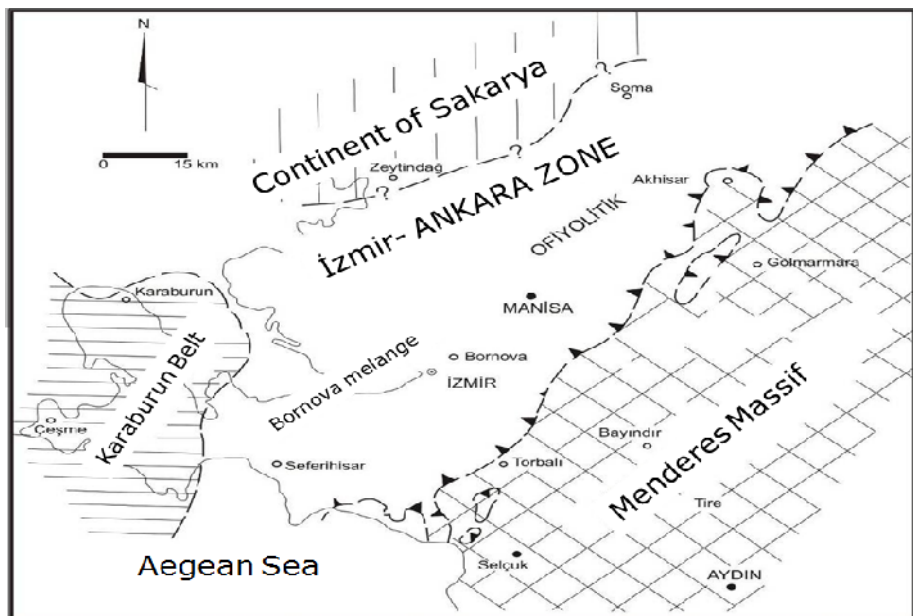


Figure 2.5 Tectonic Belts of Izmir and near vicinity (Özden et al., 2011)

In the second stage of Neotectonics period; with the vanishing of the tension rise of western Anatolia into south Aegean, N-S directed faults effected the development of morphology of current horst-graben system. This movement affected the sediments accumulated in the lake basins of Miocene. Thresholds had been formed between the sediments of the Miocene lake and pre-existing mountain blocks. Sabuncubeli located in the north of Izmir and Buca-Cumaova located in the south are good examples to this formation. One of the most obvious structural ingredients of the Izmir is graben. It is located from Gediz valley to Kemalpasha and is extended to Izmir Bay by passing through Bornova. The existence of hot water in south of Izmir Bay is an evidence of presence of active faults. Similar evidences are seen in northern coasts of the Bay including Ali a, Menemen and Kar iyaka (Özden et al., 2011). Some tectonic sources that are thought to be active are shown in Figure 2.6.

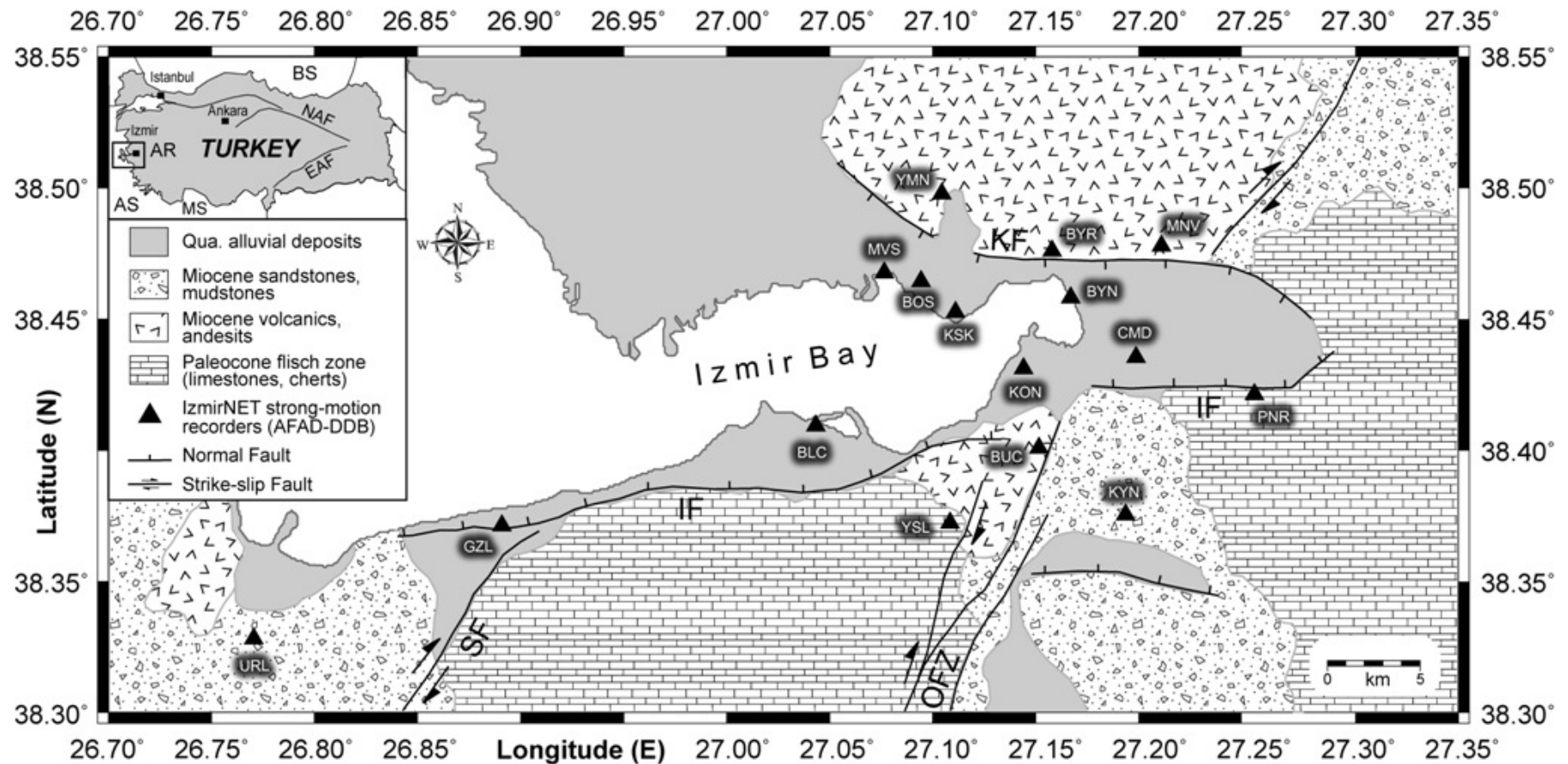


Figure 2.6 Some tectonic sources that are thought to be active nearby Izmir city center (Sözbilir et al., 2008)

### *2.2.1.1 Alluvial Geomorphology of zmir and Surroundings*

The crust movements, occurred during the Neotectonics period, had formed the basement of geomorphologic units around zmir. In the first stage of this period, zmir-Ankara Clamp Zone had been broken. As a result of this NE-SW and NW-SE directed expansions had occurred. After that, the rise of Menderes Massif had been followed by rising block which had caused concavities between them. These concavities had filled the Myosin lakes. A volcanic activity had been detected during this period. With the deepening of valley between rising blocks, E-W directed new broken formations had been created. One of the most important examples of these new formations is Kemalpa a- zmir branch of the Gediz graben (Özden et al., 2011).

Tectonic movements had caused the overlay of the alluvial plans over the coasts of Gulf of zmir. Coarse materials had been carried and accumulated by the rivers. Tectonic movements had increased the amount of accumulated coarse materials. On the other hand, finer materials had been accumulated in the medium part of the lowland (Özden et al., 2011).

At lower levels of the rising blocks, eroded materials had been moved in. This erosion can be seen at the north peaks of Kar ıyaka and Bornova. Volcanic coarse materials or limestone are present in the north of gulf of zmir. These formations are not present in the southern zmir Bay. The presence of this formation in northern Bay is only an evidence of the deepening of Bornova lowland to south direction (Kayan, 2000). Bornova lowland is not a typical delta because there is not a river passing through it. There are three main streams of Bornova lowland that reach the sea. The origins of these streams are the mountains that surround the lowland. These streams are named as Kocaçay, Gökdere and Manda çayı. Kocaçayı forms the cone of alluvial deposits of Bornova. Gökdere stream carries the alluvial sediments of the south of Bornova. Manda çayı forms the sediments of south segment of Bornova lowland. Because insufficient sediments are carried from high levels (mountains) of the east to west, east segment of the lowland is higher than that of the west. This is the reason why Bornova lowland is not a typical delta (Kayan, 2000).

Even though they are accumulations that belong to the same territory, the alluvial plains differ from each other. A river-mouth delta is developed in front of the piedmont of Yamanlar Mountain in Karşıyaka. Located in the northwest of Karşıyaka, Old Gediz River Delta is created by the alluvial sediments that had been brought by the Gediz River (Figure 2.7). The soil profile of the Delta is very complex and contains horizontal discontinuities. These discontinuities can be seen even at close distances (Kayalar, 1991; Özden, 2000).

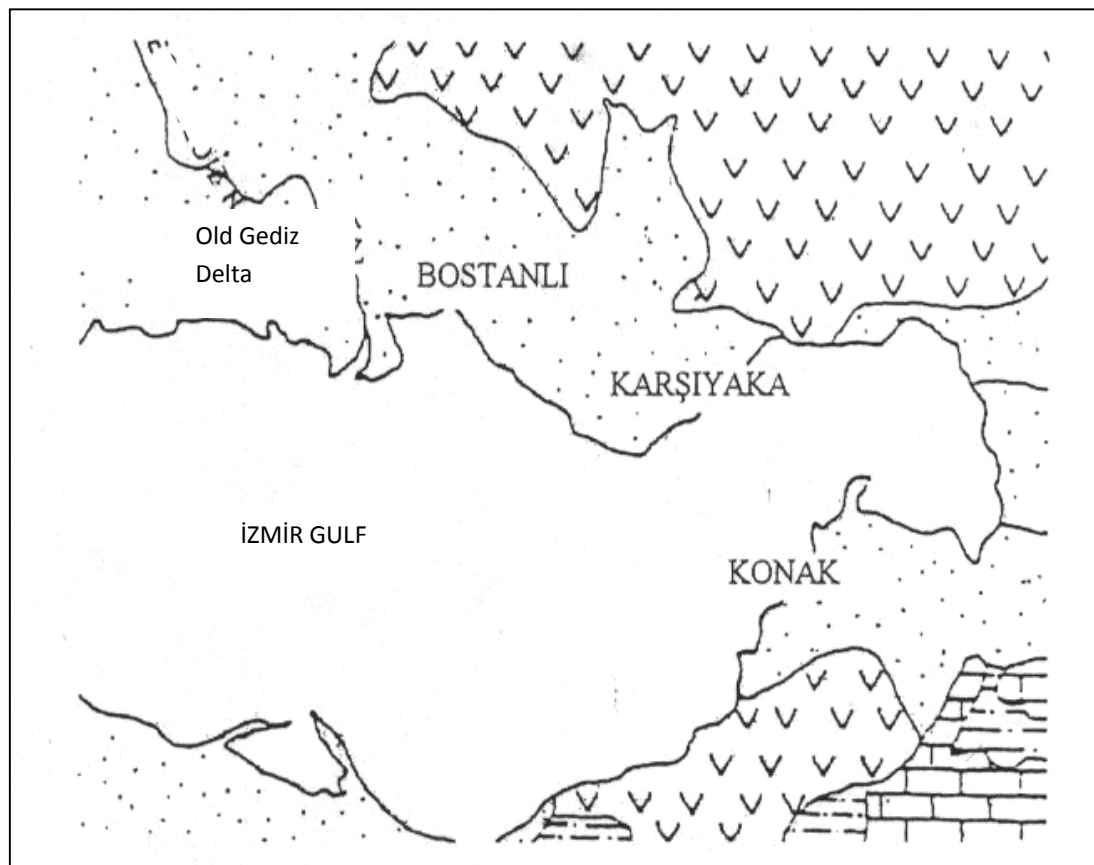


Figure 2.7 Old Gediz River Delta and Bostanlı region (Özden, 2000)

## 2.2.2 Significant Faults

Western Anatolia is one of the regions with high seismic capacity. It is under the action of tectonic N-S trending tension deformations. As a result, many E-W trending graben systems are created. At the center of Western Anatolia, the main grabens, such as Gediz and Menderes, are situated (Figure 2.8). Normal faults are formed parallel to these main grabens.

Generally, the tectonic structures in the Gediz graben system are normal faults. The structures outside this graben, which belongs to neotectonic period, have the characteristics of strike-slip faults. In the south and east of Izmir Bay, normal faults are situated. These faults are named as Izmir fault, Manisa fault, and Bornova fault. Additionally, Tuzla fault, Foça-Bergama fault zones are NE-SW oriented strike-slip faults that are potential earthquake sources.

In the west of the Izmir Bay, Karaburun Fault takes place. This fault is characterized as strike slip fault as well (Sözbilir et al., 2001). Tectonically active sources are shown in Figure 2.8. These sources are specified as faults able to produce potential earthquakes close to the center of the city of Izmir. Some of the critical faults situated around Izmir are drawn in Figure 2.9.

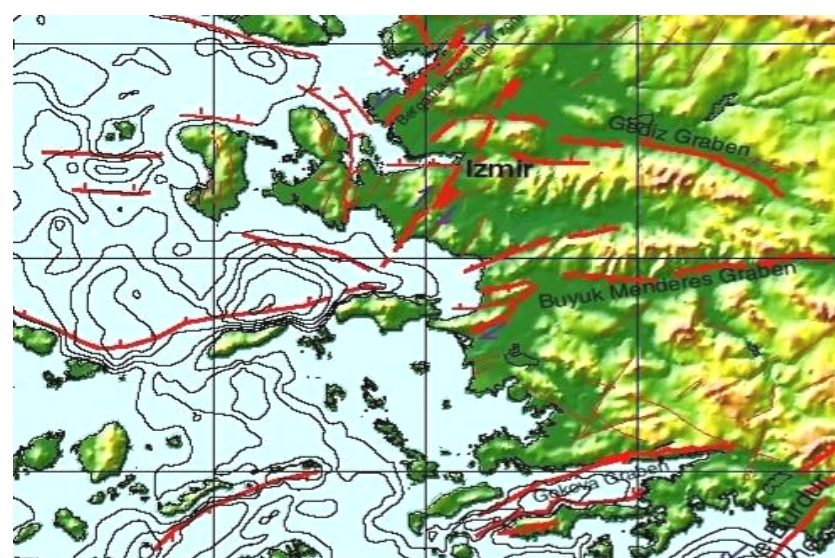


Figure 2.8 Tectonically active sources around Izmir (RADIUS, 1999)

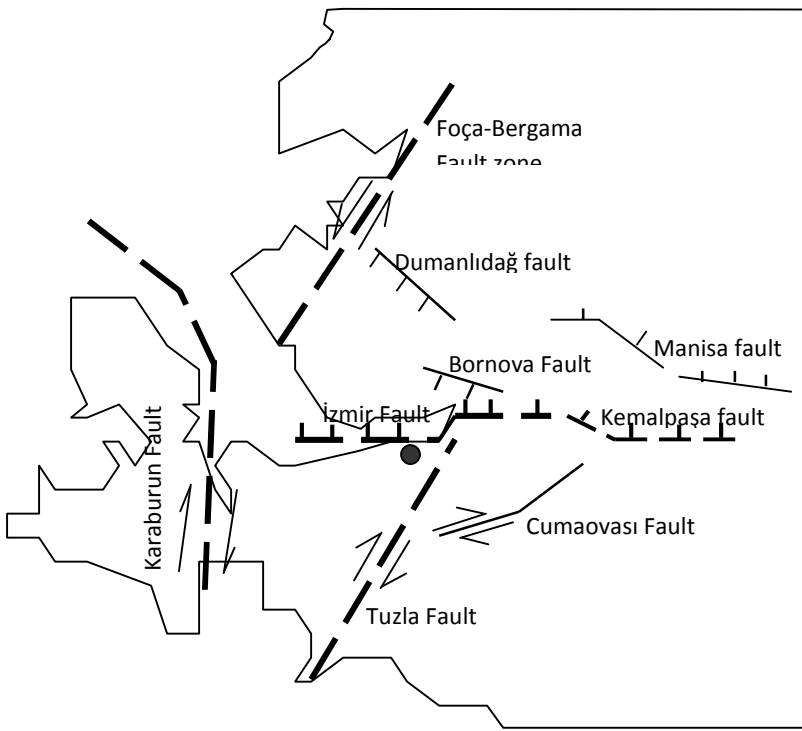


Figure 2.9 Some of the critical fault surrounding the city of Izmir (Özden et al., 2011)

**Izmir Fault:** Izmir fault is an E-W trending fault situated in the south of the Izmir Bay. Its length is approximately 35 km. The main part of this fault consists of two branches such as north and east branches. The North branch of this fault extends between Üçkuyular and Güzelbahçe and it is parallel to the Northern coast of the Bay. Some evidences about the presence of this fault are seen near Balçova. Dip angle of this part of the fault is  $80^\circ$ . The east branch of this fault takes place in southeast of Izmir. This segment of the fault near Pınarba ı consists of two small branches. Along Izmir fault Bornova flysch sediments of Cretaceous, Paleocene sandstone-shale and Quaternary alluvium are found. Normal faulting and hot water can be easily seen. According to history of earthquakes produced by this fault, it can be characterized as active normal fault (RADIUS, 1999; Emre & Barka, 2000). The epicenters of distractive earthquakes in 1688, 1739 and 1778 are thought to have been near the Izmir Fault. The earthquake occurred in 1688 had an epicenter approximately 10 km from the surface and the soil surface in Sancak Burnu is subsided approximately 80 cm (Figure 2.10). The distractions in Sancak Bornu are

evidences to the activity of zmir fault. Even though there is some information about this fault, more should be done in order to do a total specification.

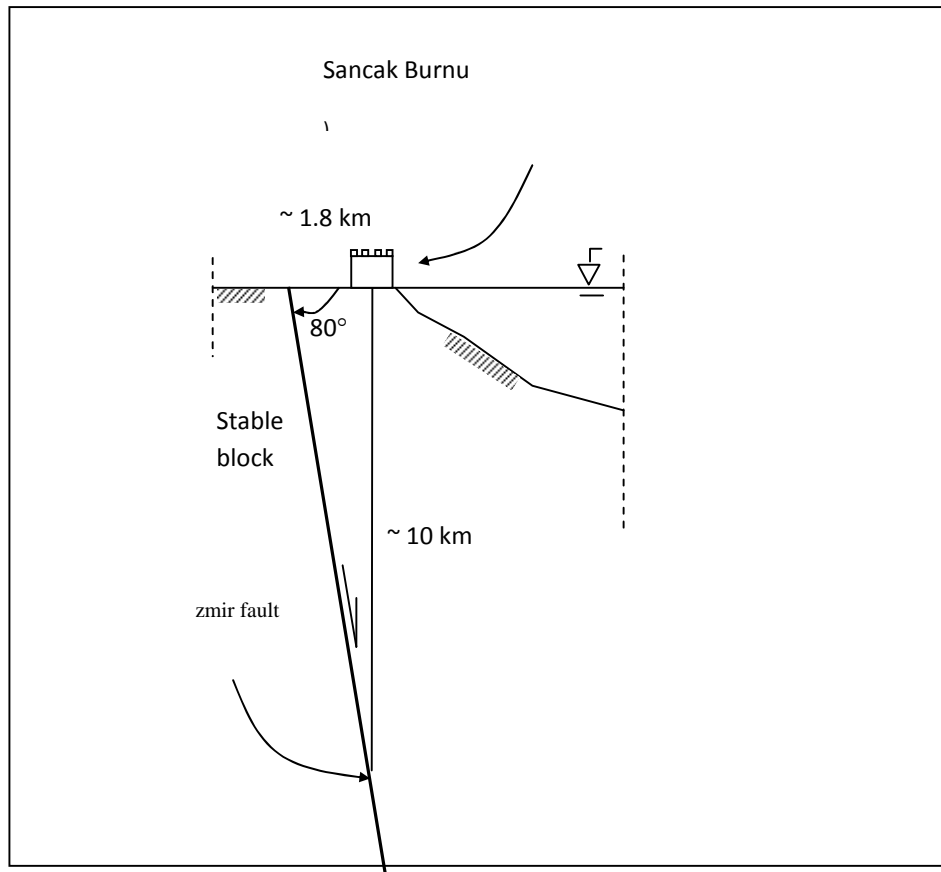


Figure 2.10 The geometric analysis of the epicenter of earthquake occurred near zmir fault in 1688 (Özden et al., 2011).

**Tuzla Fault:** Tuzla fault is situated in south west and extended to the north east of zmir. Its length is about 35-40 km. The south west part of the fault lies from Aegean Sea to the cost of the Gulf of Do anbey. This segment of the fault is about 15 km and consists of three branches. The north-west branch of this segment intersects with Cumaovası Fault which is located in the south of zmir. Do anbey Earthquake occurred on the Tuzla fault segment that lies between the Gulf of Do anbey and Cumaovası. The zone of Seferihisar was highly affected by this earthquake. Tuzla fault carries the characteristic of dextral strike slip fault (RADIUS, 1999).

**Karaburun Fault:** This fault is elongated in N-S direction. It lies parallel to east coast of Karaburun Peninsula and ends off the north of the Gulf of Seferihisar. The length of this fault is about 15 km. This fault can be characterized as strike-slip fault with normal components. According to some indications, the earthquakes with the epicenter on Karaburun fault had caused extensive damages around zmir Bay and Karaburun Peninsula (RADIUS, 1999).

**Foça-Bergama Fault zone:** This fault zone is elongated to NE-SW direction. It is extended between the Bergama and Foça districts. The southwest part of the faults reaches the Aegean Sea. This fault zone is seen as the source of the large scale earthquakes occurred in the south of zmir. Dikili Earthquake is the strongest earthquake occurred in the north of zmir. The epicenter of this earthquake is thought to have been on Foça-Bergama Fault zone. This fault zone possesses the characteristics of left-lateral strike-slip faults (RADIUS, 1999).

**Manisa Fault:** Manisa Fault is prolonged to NW-SE direction. It lies between Turgutlu and Manisa Fault. It can be defined as normal fault. Its length is about 25 km and its dip angle ranges between  $50^{\circ}$  to  $65^{\circ}$  (RADIUS, 1999; Emre & Barka, 2000). In or near the fault zone landslides and rock falls can be seen.

**Kemalpa a Fault:** Kemalpa a has an approximate length of 20 km. This fault intersects the Quaternary sediments in the north and creates a contact between Quaternary and Neogene units. According to morphotectonic findings, this fault had been active in the Holocene area (Emre & Barka, 2000).

**Bornova Fault:** This fault takes place in the south of the zmir Bay and extends to NW-SE direction. It carries the characteristics of normal faults. There is limited information about the activity of this fault. It seems to have similar characteristic with the zmir Fault (RADIUS, 1999).

**Dumanlıda Fault zone:** Dumanlıda Fault zone lies along NW-SE direction. It is situated in the north of Menemen. It follows the west branch of the Manisa Fault.

It has the characteristic of normal faults. Because its morphology is young, this fault is thought to be active. (RADIUS, 1999; Emre & Barka, 2000).

**Cumaovası Fault:** This fault is located in south-east of zmir. The general direction of this fault is NE-SW. It is characterized as dextral strike fault. There is no information about the activity of this fault in Holocene Age (RADIUS, 1999).

### **2.2.3 Seismicity**

#### *2.2.3.1 Historical Earthquakes Occurred in zmir and its Vicinities before 1900*

Several significant earthquakes have occurred in zmir and its vicinities during the time. Since the technology of detection and examination of an earthquake has become available only within the last hundred years, the assessment of historical earthquakes is done approximately by estimating the damages that a specific earthquake did in a defined area. These damages may be material or life loss. The earliest earthquake is thought to have occurred in 17 (A.D) . It is concluded that this earthquake caused big damages in 13 historical cities around zmir, Manisa and Urla. Some of the historical earthquakes occurred around zmir, their locations and magnitudes are shown in Table 2.1 (Özden et al., 2011).

The earthquake occurred in July 1688 was a destructive earthquake which killed more than 15000 people and broke down three quarters of the buildings of the zmir city. Only three of seven large mosques were not collapsed.

The epicenter of the earthquake occurred on April 4 1688 is thought to be in the Gulf of zmir. It killed about 80 people. Foça Fortress and some mosques were seriously damaged.

Another important earthquake is the one that occurred on July 3 1778. It lasted about 15 seconds and killed more than 200 people. A fire ignited after the earthquake burning half of the city in 36 hours (Özden et al., 2011).

Table 2.1 Large historical earthquakes occurred around Izmir before 1900 (Özden et al., 2011)

Date	Latitude	Longitude	Magnitude, I <sub>0</sub>	Location
17	38.40	27.50	IX	İzmir, Manisa, Aydın
110	37.00	26.00	IX	İzmir, Efes
177	38.40	27.10	IX	İzmir, Sakız Adası
688	38.40	27.00	IX	İzmir
20.03.1389	38.40	26.30	IX	İzmir, Sakız Adası
10.07.1688	38.40	27.20	X	İzmir
04.04.1739	38.40	27.20	IX	İzmir
03-05.07.1778	38.40	27.20	IX	İzmir
01.02.1873	37.75	27.00	IX	Sisam Adası, İzmir
29.07.1880	38.60	27.10	IX	Menemen, İzmir
03.04.1881	38.25	26.10	X	Sakız Adası, İzmir
25.10.1889	39.30	26.30	IX	Midilli ve Sakız, İzmir

### 2.2.3.2 Significant Earthquakes Occurred in Izmir and its Vicinities after 1900

Several large earthquakes have occurred in Izmir and vicinities since 1900. Some of them can be seen in Table 2.2. The first important earthquake after 1900 period is the Torbalı Earthquake occurred in 1928. This earthquake caused significant damages in Torbalı district. The epicenter of this earthquake is detected as nearby Torbalı region. This earthquake caused damages in Alsancek, Halkapınar Coast and Konak (Özden et al., 2011).

Table 2.2 Large earthquakes occurred around zmir after 1900 (Özden et al., 2011).

		Date	Year	Earthquake	Latitude	Longitude	Depth (km)	M	Deaths	Collapses	Surface Rupture
		Month	Day								
1	1909	January	19	Foca	38	26.5	60	6	8	700	
2	1914	October	3	Burdur	37.7	30.4	60	7	300	6000	40 km
3	1914	October	4	Bolvadin	38	30	15	5	400	1700	
4	1925	August	7	Dinar	37.4	30.5	60	6	3	2043	
5	1926	February	8	Milas	36.8	27.1	30	5	2	598	
6	1926	March	18	Finike	35.84	29.5	10	7	27	190	
7	1928	March	31	Torbali	38.5	28.1	60	6	50	2100	
8	1933	July	19	Civril	38.2	29.8	40	6	20	200	
9	1935	January	4	Erdek	40	27.5	60	6	5	600	
10	1939	September	22	Dikili	39	26.9	60	7	60	1235	
11	1941	May	23	Mu la	37.1	28.2	40	6	2	500	
12	1941	December	13	Mu la	37.2	28.3	30	6		400	
13	1942	November	15	Bigadiç	39.8	28.6	10	6	7	1262	
14	1944	June	25	Gediz	38.79	29.3	40	6	21	3476	
15	1944	October	6	Ayvalik-Edremit	39.48	26.56	40	7	27	1158	
16	1945	December	21	Denizli	38.04	28	-	-	190	400	
17	1946	February	21	Kadınhanı-IIğın	38.3	31.8	60	6	2	509	
18	1949	February	5	Orhanelli-Harmancık	39.89	29.35	40	5	-	150	
19	1949	July	23	Sakız-Karaburun	38.6	26.3	10	7	1	824	
20	1953	March	18	Yenice-Gönen	39.99	27.36	10	7	265	9670	
21	1953	May	2	Karaburun	38.51	26.55	60	5	-	73	
22	1955	July	16	Söke-Balat	37.9	27.1	40	7	23	470	
23	1956	February	20	Eski ehir	39.7	30.4	24	6	2	1219	
24	1957	April	25	Fethiye	36.47	28.56	53	7	67	3100	
25	1959	April	25	Köyce iz	37	28.5	30	6	-	59	
26	1961	May	23	Marmaris	36.4	28.3	70	6	-	61	
27	1963	March	11	Denizli	38	29.3	33	6	-	54	
28	1963	November	22	Telenni	37.2	29.7	40	5	-	298	
29	1964	October	6	Manyas	40.2	28.1	24	7	23	5398	
30	1965	March	2	Salihi	38.4	28.4	-	6	-	110	
31	1965	June	13	Honaz	37.85	29.32	33	6	14	488	
32	1966	June	19	Menemen	38.55	27.35	9	4.8		100	
33	1967	October	26	Açipayam	37.3	29.1	35	5	-	-	
34	1969	January	14	Fethiye-Ka	36.11	29.19	22	6	-	42	
35	1969	March	25	Yeniköy	39.1	28.45	12	7	-	1826	
36	1969	March	3	Gönen	40.08	27.5	6	6	1	20	
37	1969	March	28	Ala ehir	38.55	28.46	4	7	41	4372	36 km
38	1969	April	6	Karaburun	38.47	26.41	16	6	3	443	
39	1970	March	28	Gediz	39.21	29.51	18	7	1086	9452	40 km
40	1970	April	23	Demirci	39.13	28.65	28	6	43	150	
41	1971	May	12	Burdur	37.65	30	30	6	57	1389	40 km
42	1971	September	21	Bucak	37.27	30.17	42	5	-	-	
43	1974	February	1	zmr	38.55	27.22	24	6	20	47	
44	1976	June	9	Emet	39.24	29.15	12	5	-	-	
45	1976	August	19	Denizli	37.71	29	20	5	4	887	
46	1977	April	11	Antalya	36.91	30.73	90	5	-	-	
47	1977	October	27	Gemencik	37.87	27.88	16	5	-	-	
48	1977	December	16	zmr	38.41	27.19	24	5	-	40	
49	1979	June	14	Foca	38.79	26.57	15	6	-	22	
50	1979	July	18	Kavacik	39.66	28.65	7	5	-	-	
51	1983	April	21	Bala	39.31	33.06	36	5	-	-	
52	1983	July	5	Biga	40.33	27.21	7	5	5	85	
53	1983	October	21	negöl	40	29.35	12	5	-	-	
54	1989	August	15	Mindilli-Edremit	39.18	26.29	10	5	-	-	
55	1992	November	6	Do anbey	38.16	26.99	17	5.7	-	60	
56	1994	January	28	Manisa	38.69	27.49	5	5.2	-	60	
57	1994	May	24	Karaburun	38.66	26.54	17	5	-	10	
58	1995	October	1	Dinar	38.1	30.1	33	6	90	14156	
59	2003	April	10	Urla	38.26	26.83	16	5.6	-	-	
60	2005	October	17-20	Urla-Si acik	38	26.4	-	5.9	-	-	

One of the significant earthquakes is the Dikili Earthquake occurred near the urbanized areas of Dikili and Bergama. It affected these regions and the areas around them such as villages. Some cracks were seen on the surface and thermal sources were created (Özden et al., 2011).

Another large earthquake occurred in zmir is the zmir Earthquake. Its epicenter was in the north of the Gulf of zmir. During this earthquake 47 buildings were seriously damaged and 2 people are killed. Maximum peak acceleration was measured as 0.13g in alluvium soils in Alsancak.

Furthermore, in 1977 two large earthquakes occurred within a short time of one week. Specifically, they occurred on December 9 and 16. Their magnitudes were measured as 4.8 and 5.3 respectively. In total, 40 buildings were damaged and 20 people were wounded (Özden et al., 2011).

Do anbey-Seferihisar Earthquake is another significant earthquake. This earthquake affected alluvial soils of zmir. The maximum peak acceleration was measured as 0.039g. This earthquake affected Alsancak, Kar iyaka and Bornova (Özden et al., 2011).

Urla Earthquake occurred in 2003 and its epicenter was between Urla and Seferihisar. Some buildings in zmir were slightly damaged. Important damages were detected in Urla and Seferihisar (Özden et al., 2011).

A sequence of Earthquakes occurred on October 21 in 2005. The epicenters of these earthquakes were in Gulf of Sı acık and Seferihisar. The magnitude of the first earthquake was 5. The magnitudes of earthquakes that follows are M=5.8, 5.5 and 5.9. Additionally more than 200 small earthquakes occurred in that time. The distribution of the epicenters of all these earthquakes is shown in Figure 2.11. These earthquakes strongly affected the region of Urla and Seferihisar. Especially in these two regions, many building were significantly damaged (Özden et al., 2011).

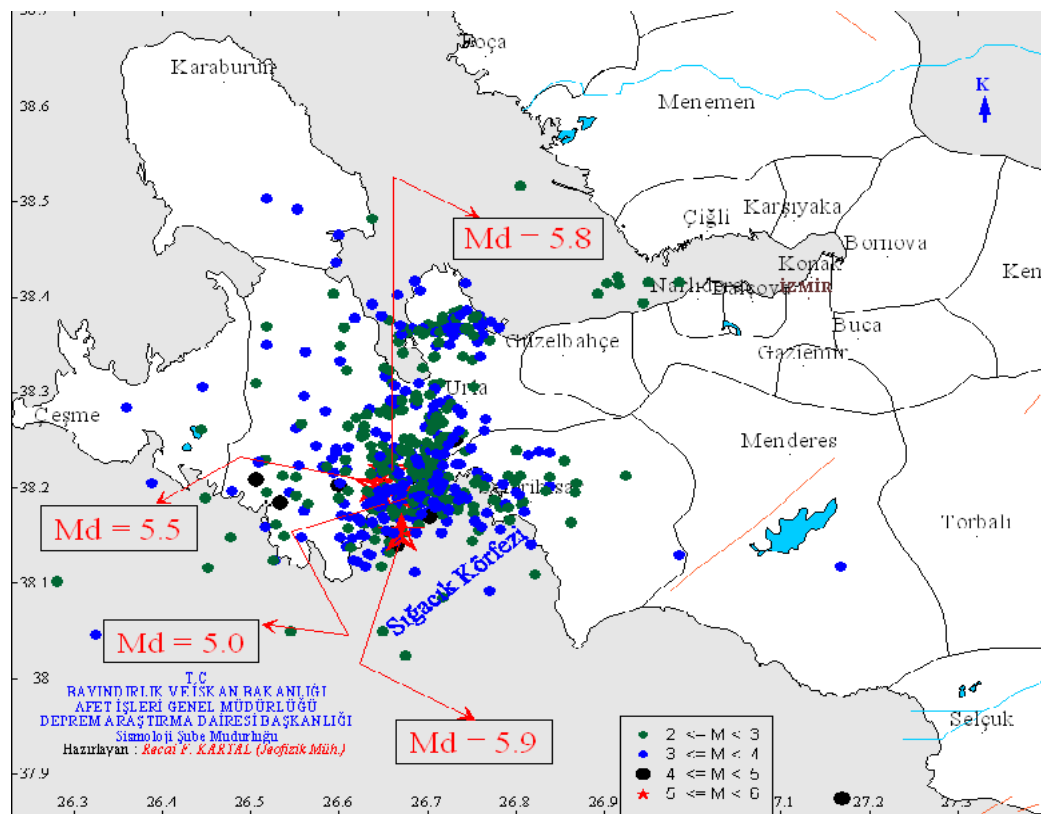


Figure 2.11 Location of epicenters of earthquakes occurred in Gulf of Sı acık and Seferihisar in October 2005 (Özden et al., 2011).

### 2.3 Soil Characteristics

As mentioned at the beginning of this chapter, two defined zones are taken in consideration. One is located in Mavi ehir and the other in Manavkuyu. The soil characteristics and idealized soil profiles of these two sites are given in the sections below.

#### 2.3.1 Mavi ehir Coastal Zone

Mavi ehir Coastal Zone extends between coast line of Bostanlı and Alaybey. Because of some similarities in soil properties, this zone can be defined as part of Old Gediz Delta Area. The water table is determined to range between 0 to 1.2 m. The average water level can be taken as 0.6 m. Some soil parameters of Mavi ehir Coastal Zone are given in Table 2.3 (Özden et al., 2011).

The first zone taken into consideration in this study is located in Mavi ehir Costal Zone. The idealized soil profile of the site is given in detail in Figure 2.12.  $N_{60}$  is equivalent SPT value (Standard penetration Test).

Table 2.3 Index properties of the soil profile in Mavi ehir Costal Zone (Özden et al., 2011).

Depth (m)	-No.4*	- No.200	w <sub>L</sub>	w <sub>P</sub>	I <sub>p</sub>	w <sub>n</sub>	γ <sub>n</sub> (kN/m <sup>3</sup> )	G <sub>s</sub>	USCS
0.0-8.0	68-100	4-44		NP		22-40	18.5	2.62	SM
8.0-19.0	90-100	70-100	56-85	23-49	15-43	43-62	16.5	2.60	MH
19.0-25.0	51-99	6-41		NP		12-36	18	2.61	SM
25.0-35.0	89-100	24-77	54-91	24-35	22-59	14-32	19	2.65	SC/CH
35.0-40.0	91-100	36-79	55	26	29	21-43	19	2.70	CH
40.0-47.0	40-45	1-5	-	-	-	19-25	21	2.65	GC
47.0-51.0	96-100	51-66	45	25	20	14-32	20	2.65	CH
51.0-54.0	-	-	-	-	-	22-28	21	2.65	GC

\*-No.4: Percentage passing No4 sieve ; -No.200: Percentage passing No200 sieve

w<sub>L</sub>: Liquid limit of the soil ; w<sub>P</sub>: Plastic limit of the soil ; γ<sub>n</sub>: Unit weight of the soil

G<sub>s</sub>: Specific Gravity of the soil

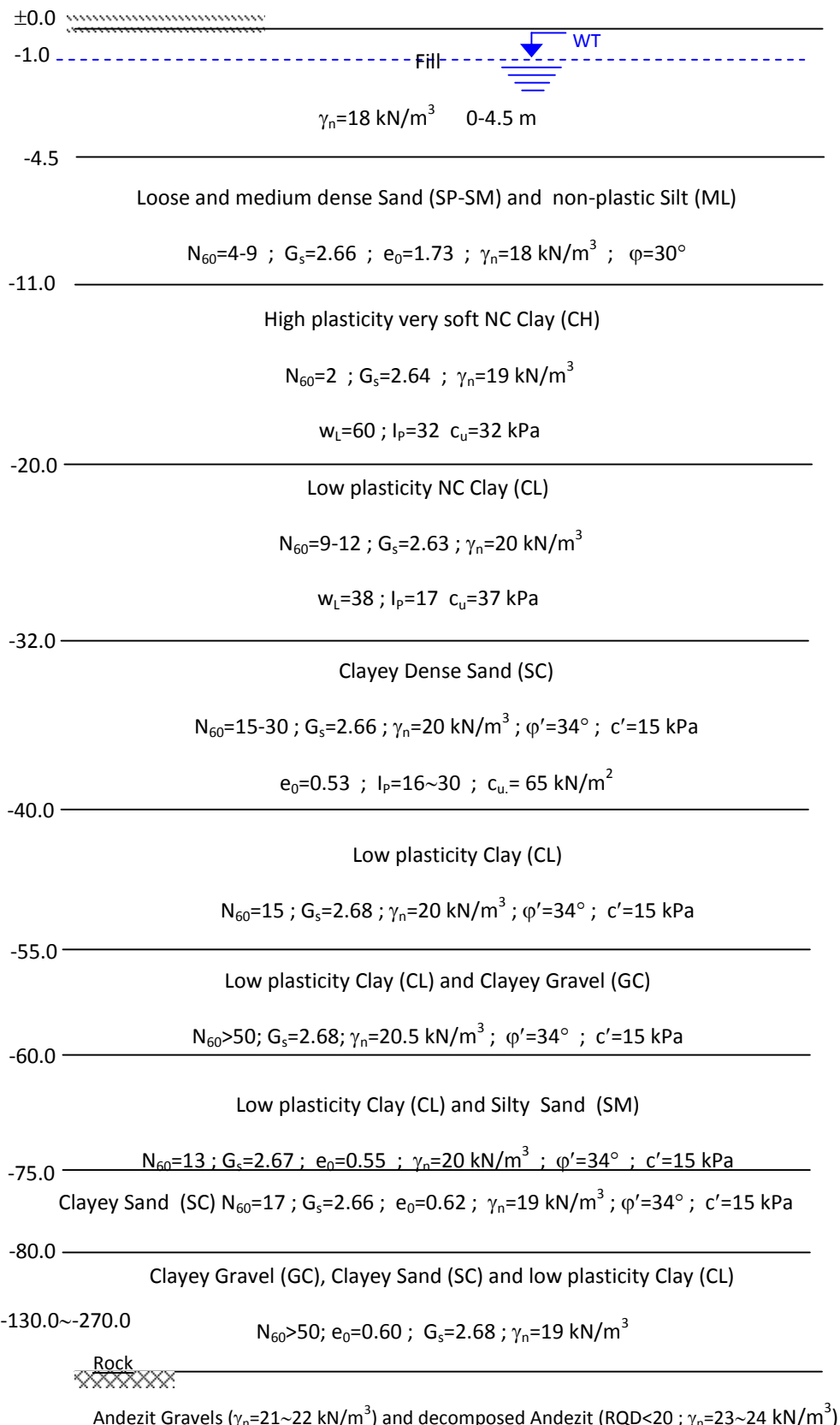


Figure 2.12 Idealized soil profile for Mavi ehir Coastal Zone (Özden et al., 2011).

### 2.3.2 Manavkuyu Zone

This zone consists of alluvial carried by streams of Laka, Bornova and Manda regions. Manavkuyu zone is located in the northeast of the zmir Bay. The water table is determined as 1.8 m below the surface. Index properties of the soil layers in Manavkuyu are given in Table 2.4. The second site included in this study is located in Manavkuyu zone and its idealized soil profile is shown in Figure 2.13

Table 2.4: Index properties of the Manavkuyu Zone (Özden et al., 2011).

Depth (m)	-No.4*	- No.200	w <sub>L</sub> (%)	w <sub>P</sub> (%)	l <sub>p</sub> (%)	w <sub>n</sub> (%)	γ <sub>n</sub> (kN/m <sup>3</sup> )	G <sub>s</sub>	USCS
0.0-3.0	80-94	9-22	-	NP	-	20-27	18	2.65	SM
3.0-13.0	100	90-95	56-63	23-28	30-37	42-62	16	2.69	CL/MH
13.0-30.0	95-100	60-68	37-46	19-22	16-24	24-33	18	2.67	MH/CL
30.0-43.0	75-85	54-62	33-37	20-24	13-16	22-26	19	2.66	CL/MH
43.0-63.0	65-75	51-56	30-34	16-20	14-16	15-18	19	2.65	SC/SM

\*-No.4: Percentage passing No.4 sieve; -No.200: Percentage passing No200 sieve

w<sub>L</sub>: Liquid limit of the soil ; w<sub>P</sub>: Plastic limit of the soil ;γ<sub>n</sub> : Unit weight of the soil

G<sub>s</sub>: Specific Gravity of the soil

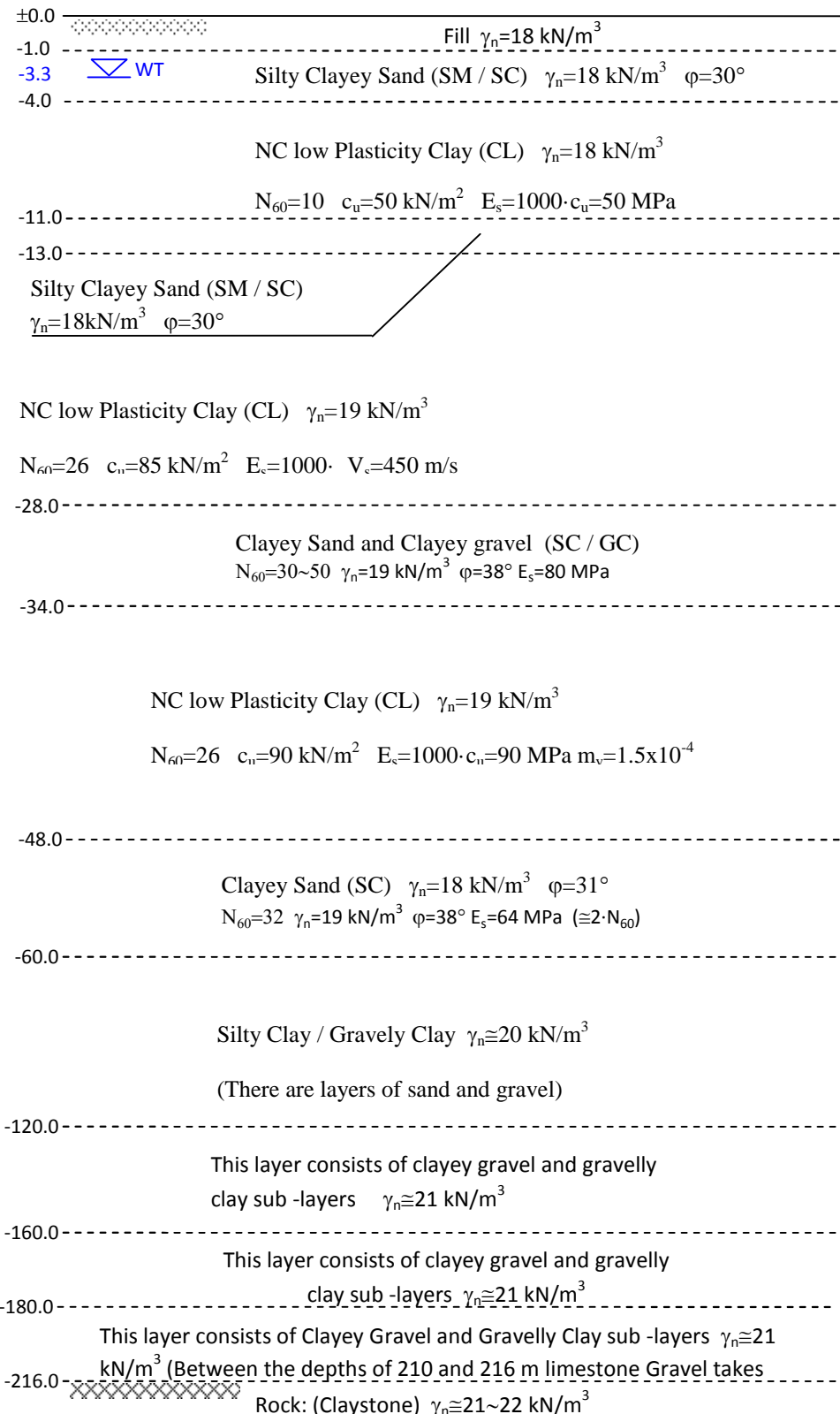


Figure 2.13 Idealized soil profile for Manavkuyu Zone (Özden et al., 2011)

## **CHAPTER THREE**

### **SEISMIC HAZARD ANALYSIS METHODOLOGY**

#### **3.1 Introduction to Seismic Hazard Analysis**

Earthquakes provide serious threat for the human activities, so they should be taken into consideration in the design of structures and facilities. Earthquake resistant design is done in order to create a structure that can withstand the coming seismic shakings without being damaged seriously. The level of shaking is described by a design ground motion which is represented by ground motion parameters. Because of much uncertain and incomplete information, the determination of these parameters is one of the most difficult problems of geotechnical earthquake engineering. Earthquake resistant design is done according to the acceptable and maximum damage that is expected. Sometimes some small damages can be tolerated based on some considerations. These considerations can be economical or functional. On the other hand, there are buildings where no damage can be tolerated. A good example of these can be hospitals, etc.

Seismic hazard analysis includes the estimation of ground motion hazard in specified sites. In general, these analyses can be done using probabilistic or deterministic methods. In this thesis only probabilistic method is taken into consideration.

#### **3.2 Identification of the Earthquake Sources**

Determination of the seismic zones is crucial for the evaluation of the seismic hazards for a specified site. These zones are determined by using nature's clues, which may be obvious or hidden, such as fault ruptures near the surface. Earthquake history of a site can provide lot of information about the possibility of a coming earthquake. However, it does not mean that a site which does not have a seismic history will not experience an earthquake in the future. Currently, earthquake's magnitude, location and time can be detected with the help of seismographs which

are set all over the world. All the significant earthquakes can be recorded instantly. Earthquake data used in this analysis are collected from various organization's websites around the world such as Cosmos Virtual Data Base [Cosmos] (1999), U.S Geological Survey [USGS] (1989), and AFAD (2009).

### 3.3 Probabilistic Seismic Hazard Analysis (PSHA)

#### 3.3.1 Introduction to Probabilistic Seismic Hazard Assessment

Probabilistic Seismic Hazard Analysis allows various competing model to be used with their uncertainties and dilemmas. In this thesis the effects of all earthquakes are taken in consideration. So, Probabilistic Seismic Hazard Analysis (PSHA) is not restricted to the scenario like statements. Additionally, the probability of different magnitude earthquakes can be included in the analysis. Furthermore, it is a flexible method that estimates the probable ground motion at a specific site. This allows comparisons of different options in decision making. This analysis is applied in four steps (Figure 3.1) (Kramer, 1996).

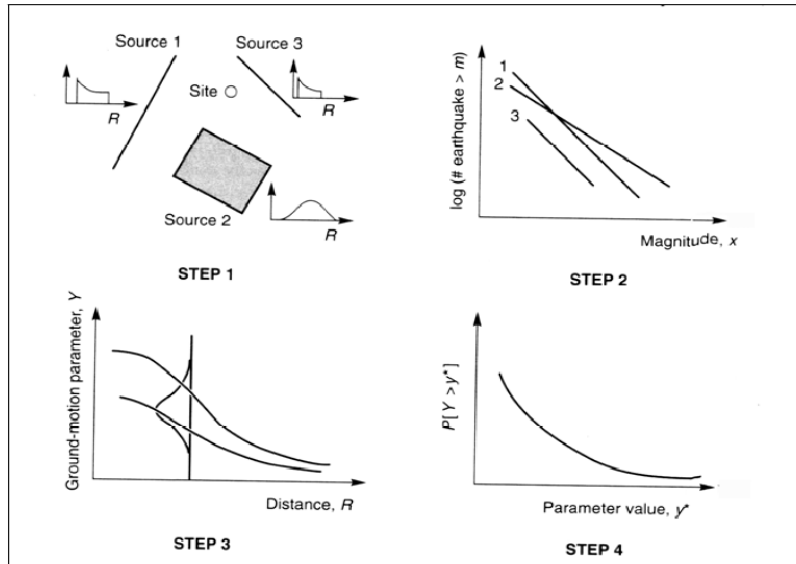


Figure 3.1 Steps of probabilistic hazard analysis (Kramer 1996)

The first step is about the determination and of seismic sources. These sources may be point sources which are represented by a single point, line source, which is represented by line such as faults or zone sources which are represented by a zone or an area. Generally, zone sources are constituted by parallel faults. Every point of a zone source is assumed to have the same earthquake potential. So, we have uniform probability distribution that is combined with the source geometry to obtain the corresponding probability distribution of source to site distance (Figure 3.2). This probability distribution can be defined by probability density function ( $F_R(r)$ ) of source to site distance ( $R$ ). This function for line sources is given by Equation 3.1.

$$F_R(r) = \frac{r}{L_f \sqrt{r^2 - r_{min}^2}} \quad (3.1)$$

For source zones with more complex geometries, numerical methods are more convenient. These zones are divided into a number of equal areas and a histogram (approximately)  $F_R(r)$  can be formatted by tabulating the values of  $R$  which corresponds to the center of each area (Figure 3.2 c).

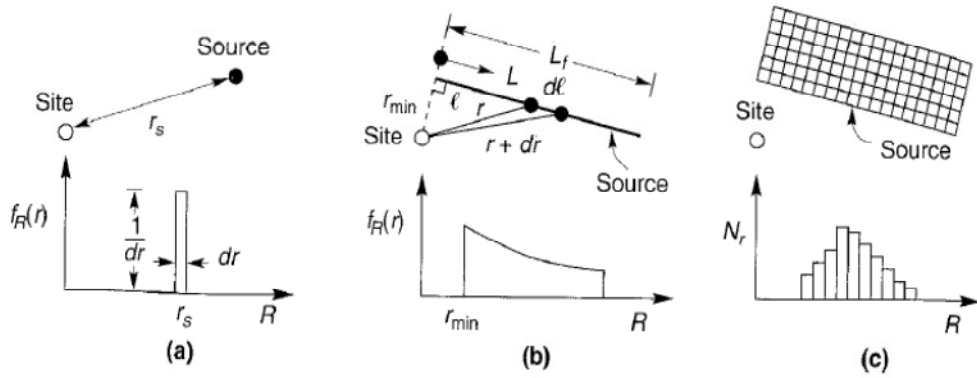


Figure 3.2 Examples of variations to source to site for different source zone geometries (Kramer, 1996)

The second step is about obtaining the recurrence relationships for each source. A recurrence relationship shows the possibility of an earthquake, which magnitude is within a given range ( $m_0 < M < m_u$ ) at a specific size, to occur at any point of the zone during a given period of time. This relationship is represented by a straight line in a

coordinate system whose horizontal axis shows the magnitude values and vertical axis is logarithmic and shows the number of earthquakes in a specific period of time (Kramer, 1996). The recurrence curve has power-law equation:

$$\log N = A - BM \quad (3.2)$$

Where,

N: The number of earthquakes occurred in a defined magnitude interval around M during a specified period of time, M: Magnitude, A, B: are coefficients of recurrence curve equation. B represents the slope of this curve (Kramer, 1996).

All the points inside the source zone should be included into the computations because the earthquakes are supposed to occur at any point of the zone. The probabilistic hazard analyses are done by assuming that all earthquakes occur independently from the others (Kramer, 1996).

In the third step, earthquake effect should be estimated. This is done by using earthquake attenuation relationships. The most decisive parameters of these relationships are distance from the site and earthquake magnitude.

The fourth step is about the probability that a practical ground motion parameter Y exceeds a certain value,  $y^*$ , for an earthquake of a given magnitude, m, occurring at a given distance, r. This is given by

$$P[Y > Y^* | m, r] = 1 - F_Y(y^*) \quad (3.3)$$

$F_Y(y^*)$  is the value of cumulative distribution function of Y at m and r. This value depended on the probability distribution used to present Y (Figure 3.3).

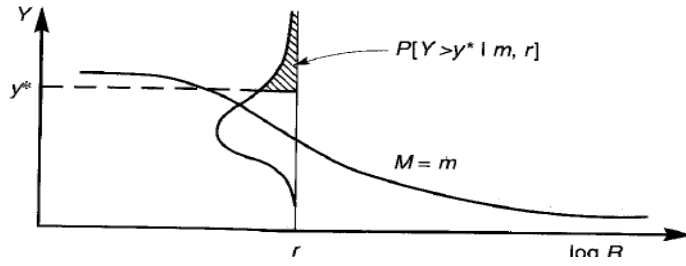


Figure 3.3 Schematic illustration of conditional probability of exceeding a particular value of ground motion parameter for a given magnitude and distance (Kramer, 1996) .

Finally, by integrating the effect of the earthquakes at different sizes occurring at different location within different sources at different probabilities of occurrence, the rate of occurrence of the events can be calculated by using the formulation below:

$$\lambda_{y^*} = \sum_{i=1}^{N_s} \sum_{j=1}^{N_M} \sum_{k=1}^{N_R} v_i P[Y > y^* | m_j] f_{Mi}(M_j) f_{Ri}(r_k) \Delta m \Delta r \quad (3.4)$$

Where:

$N_s$  number of potential earthquake sources

$N_m, N_R$ : number of segments that the ranges of magnitude and distance are divided (Kramer, 1996).

In the equation above, two important probability density functions are included. The first one is a function of magnitude ( $f_{Mi}(M_j)$ ) and the second one is a function of distance  $f_{Ri}(r_k)$ . The second one is explained in the step one. Whereas probability density function of magnitude can be computed using the Equation 3.5. Here  $m_0$  and  $m_{max}$  are the lower and upper limits of magnitude (Kramer, 1996).

$$f_M(m) = \frac{\beta \exp[-\beta(m-m_0)]}{1 - \exp[-\beta(m_{max}-m_0)]} \quad (3.5)$$

Where,  $\beta=2.303B$

### Poisson Model

Poisson model is most commonly used to describe the temporal occurrence of earthquakes. This model is useful for evaluating probabilities of events that follows

a Poisson process. The probability that N earthquakes occurs within a time interval can be calculated as below (Kramer, 1996):

$$P[N = n] = \frac{(\lambda t)^n e^{-\lambda t}}{n!} \quad (3.6)$$

$\lambda$ : is the average rate of occurrence of the event

T: time period of interest.

### 3.3.2 Clues of Earthquake Activities

#### 3.3.2.1 Geologic Evidence

According to the theory of tectonic plate method earthquake occurrence records are related to the offset and displacement of various strata. Sometimes the geologic record of the past earthquakes can be easily detected but there are cases where they are hidden deep in the soil and it is very difficult to detect them. Faults are one of these records that can be very helpful for finding out more about the earthquake history of a given site. Criteria for identification of faults can be summarized as below:

1. Clearly detectable fracture surfaces and indicator of fracturing. These fractures may be observed at the surface or nearby.
2. Observation of dissimilar materials, repeated or missing strata, cutting of strata of structures
3. Changes in the landform surface
4. Sudden changes of water table, gradients and chemical compositions, presence of volcanic vents and hot springs
5. Lineaments seen on remote sensing imagery
6. Fault movements, changing in distance between fixed points. (Kramer, 1996)

#### 3.3.2.2 Fault Activity

The evaluation of faults as indicators of future earthquakes is not exactly correct. Faults can be active or not active. Active faults are faults that posses a current earthquake thread. On the other hand, inactive faults are faults that have an

earthquake history but future earthquakes are unlikely to be produced by these faults. A lot of definitions about the active faults have been suggested. These definitions possess a lot of criteria about the active faults. Most of these criteria are related to the period of time since the recent movement of fault. However, according to the U.S Nuclear Region Commission (Code of Federal regulations, 1978) principal active fault criteria are in the following (Kramer, 1996):

1. Movement at the ground surface of the fault should have occurred within the past 35,000 years or repetition of occurrence of earthquake should have occurred within the past 500,000 years
2. A demonstration of a strong relationship between the faults and earthquakes should be determined.
3. Structural relationships among earthquakes should be observed, so the occurrence of one should be responsible for the occurrence of the others.

On the other hand, faults can pass from active to inactive so the approaches that are related with the period of time are not very realistic. In response to this, Cluff (1984) postulated six classes of fault activity. These are depended on some characteristic of fault such as slip rate, slip per event, rupture length, earthquake size and recurrence interval. This approach is more competitive than others because it includes a satisfying characterization of the fault. However, it is very difficult to be implemented in practice (Kramer, 1996).

### *3.3.2.3 Magnitude Indicators*

Magnitude of the past earthquakes can be estimated by the use of geologic evidences. This can be done by correlating the observed deformation characteristics with magnitudes of recorded earthquakes. According to worldwide studies, the fault does not rupture along the full length but it ruptures along a segment. Some correlation for determining the magnitude of earthquake using only the length of the fault have been suggested by a number of studies such as (e.g., Bonilla et al., 1984; Wells and Coppersmith, 1994. One handicap of these correlations is not involvement of area of the fault. However, the rupture surface has not been taken in account.

Because the seismic moment is thought to be correlated to the area of the fault, it is expected to have major effect to the computation of magnitudes. Especially when the width of the fault is more than 20 km, it may be more convenient to use fault area rather than fault length for the prediction or determination of the earthquake magnitudes. Correlating earthquake magnitudes to the maximum surface displacement may easier than correlating it to average fault displacement since average fault displacement is very difficult to be determined correctly (Kramer, 1996).

#### *3.3.2.4 Historical Seismicity*

Records of historical seismicity may be useful for identification of earthquake sources. Historical earthquakes and their shaking effects on the environment and population can be helpful to estimate the earthquakes' geographic distribution of intensity. Although the peak density may provide important information about the epicenter of an earthquake, the accuracy of location of this epicenter depends on the density of population. Additionally, records of historical seismicity help for the determination of the rate of earthquake recurrence as well. If correct historical information about the population density and environment is provided, rate of earthquake recurrence and epicenter of historical can be determined (Kramer, 1996).

### **3.4 New Generation Attenuation Relationships**

New generation attenuation relationships are recently developed empirical ground motion models that are used for the calculation of expected ground motion at a defined site. Three empirical ground motion models are used in this thesis. These models are presented by Boore & Atkinson (2007), Campbell & Bozorgnia (2008) and Brian et al. (2008). They are developed as part of the PEER Next Generation Attenuation of Ground Motion (NGA) Project. A common database of worldwide strong motion recording is used to develop relationships and predictor variables presented in these models. Both median and aleatory uncertainty models for horizontal peak ground acceleration, response spectral acceleration and displacement

for spectral period ranging from 0.01s -10 s have been developed. Also, the magnitude ranges from 4 to 8 and the distance ranges from 0-200 km. The values calculated using New Generation Attenuation Relationships usually forms a 5% damped pseudo- absolute acceleration response spectra and the values are calculated as median.

The parameters of the models used in this thesis have a significant importance and influence on the obtained results. Even though these parameters and their part on the solution are explained in detail in the next section, a brief summary of them is presented in Table 3.1. Additionally the geometric meaning of some of them is shown in Figure 3.4.

Table 3.1 Brief explanation of parameters of the NGA models

M	Moment magnitude.
R <sub>RUP</sub>	Closest distance to coseismic rupture (km).
R <sub>JB</sub>	Closest distance to surface projection of coseismic rupture (km).
R <sub>X</sub>	Horizontal distance from top of rupture measured perpendicular to fault strike (km).
U	Unspecified-mechanism factor: 1 for unspecified; 0 otherwise.
F <sub>RV</sub>	Reverse-faulting factor: 0 for strike slip, normal, normal-oblique; 1 for reverse, reverse-oblique and thrust.
F <sub>NM</sub>	Normal-faulting factor: 0 for strike slip, reverse, reverse-oblique, thrust and normal-oblique; 1 for normal.
F <sub>HW</sub>	Hanging-wall factor: 1 for site on down-dip side of top of rupture; 0 otherwise.
Z <sub>TOR</sub>	Depth to top of coseismic rupture (km).
d	Average dip of rupture plane (degrees).
V <sub>S30</sub>	Average shear-wave velocity in top 30m of site profile.
F <sub>Measured</sub>	V <sub>S30</sub> Factor: 1 if V <sub>S30</sub> is measured, 0 if V <sub>S30</sub> is inferred.
Z <sub>1.0</sub>	Depth to 1.0 km/sec velocity horizon (m).
Z <sub>2.5</sub>	Depth of 2.5 km/s shear-wave velocity horizon (km).
F <sub>AS</sub>	Aftershock factor: 0 for mainshock; 1 for aftershock.

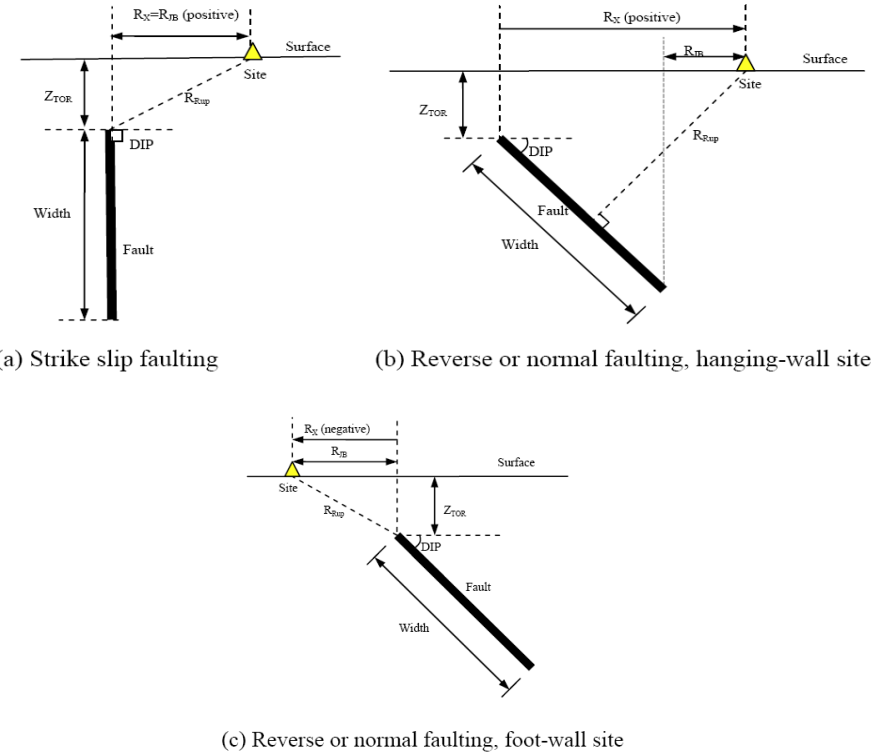


Figure 3.4 Illustration of the geometric mean of some parameters used in the NGA models

### ***3.4.1 Campbell-Bozorgnia NGA Ground Motion Relations for the Geometric Mean Horizontal Component of Peak and Spectral Ground Motion Parameters***

In this section, strong motion parameters used in the model, implementation of median ground motion model and aleatory uncertainty models are explained. All the information and formulation used in this Section 3.4.1 are taken from Campbell-Bozorgnia (2008).

### *3.4.1.1 Median Ground Motion Model*

According to this model, median ground motion model is calculated by the equation below:

$$\widehat{LnY} = f_{mag} + f_{ais} + f_{flt} + f_{hng} + f_{site} + f_{sed} \quad (3.7)$$

Where,

$f_{\text{mag}}$ : magnitude term

- $f_{dis}$ : distance term
- $f_{flt}$ : style of faulting term
- $f_{ng}$ : hanging wall term
- $f_{site}$  shallow site response
- $f_{sed}$ : deep site response term

### Magnitude term

Magnitude term represent the effect of magnitude on the ground motion values. The magnitude term is modeled using trilinear functional form shown below. Trilinear functional form is used to model the relationship between the magnitude and distance. So, with the increases of the distance from the site to the source, the degree of magnitude scaling decreases. Magnitude term is developed as part of analysis of residuals and can be computed as below:

M: Moment magnitude

$c_n$ : correlation's coefficients (Appendix B)

$$f_{mag} = \begin{cases} c_0 + c_1 * M & M \leq 5.5 \\ c_0 + c_1 * M + c_2 * (M - 5.5) & 5.5 < M \leq 6.5 \\ c_0 + c_1 * M + c_2 * (M - 5.5) + c_3 * (M - 6.5); & M > 6.5 \end{cases} \quad (3.8)$$

### Distance term

The effect of distance from source is represented by distance term. Distance term ( $f_{dis}$ ) is a magnitude depended geometrical attenuation term that fits both small and large magnitude recordings. This term is valid to distance of 200 km.

$R_{rup}$ : closest distance to rupture plane

$$f_{dis} = (c_4 + c_5 * M) * \ln(\sqrt{R_{rup}^2 + c_6^2}) \quad (3.9)$$

### Style of faulting term

The style of faulting term represents the effect of type of faulting on the ground motion computation. This term depends on the parameter ( $Z_{tor}$ ) which represents rupture extension to the surface. So  $Z_{tor}$  represents the depth to the top of cosmic rupture plane. According to models developers, for rupture breaks near the surface,

the ground motions for reverse faults are comparable on average to ground motions for strike-slip faults Style of faulting term is given by the correlations below:

$$f_{flt} = c_7 * F_{RV} * f_{flt,Z} + c_8 * F_{NM} \quad (3.10)$$

$$f_{flt,Z} = \begin{cases} Z_{TOR}; & Z_{TOR} < 1 \\ 1; & Z_{TOR} \geq 1 \end{cases} \quad (3.11)$$

$F_{RV}$ : indicator variable of reverse faulting

If  $30^\circ < \lambda < 150^\circ$        $F_{RV}=1$ ;

Otherwise  $F_{RV}=0$ ;

Where  $\lambda$  is the rake angle or the average angle between the strike direction and slip vector (Figure 3.5)

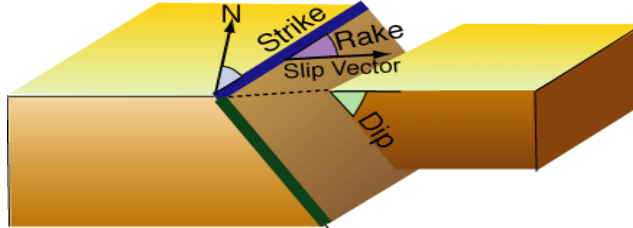


Figure 3.5 Schematic illustration of rake angle

$F_{NM}$ : indicator variable of normal faulting

If  $-30^\circ < \lambda < -150^\circ$        $F_{MN}=1$ ;

Otherwise  $F_{MN}=0$ ;

$c_n$ : correlation's coefficients (Appendix B)

### Hanging wall term

In order to include the hanging wall effect in the models, hanging wall term has been developed. This term depends on terms below:

$f_{hng,R}$ : distance-dependence term

$f_{hng,M}$ : magnitude-dependence term

$f_{hng,Z}$ : rupture depth-dependence term

$f_{hng,\delta}$ : rupture dips-dependence term

The terms above are included to gradually decrease the effect of hanging at small magnitudes.

Hanging wall term can be calculated using the correlation below:

$$f_{hng} = c_9 * f_{hng,R} * f_{hng,M} * f_{hng,Z} * f_{hng,\delta} \quad (3.12)$$

$$f_{hng,R} = \begin{cases} 1; & R_{JB} = 0 \\ \left[ \max(R_{Rup} * \sqrt{R_{JB}^2 + 1}) - R_{JB} \right] / \max(R_{Rup} * \sqrt{R_{JB}^2 + 1}); & R_{JB} > 0; Z_{TOR} < 1 \\ (R_{Rup} - R_{JB}) / R_{Rup} & R_{JB} > 0; Z_{TOR} \geq 1 \end{cases} \quad (3.13)$$

$$f_{hng,M} = \begin{cases} 0; & M \leq 6.0 \\ 2 * (M - 6); & 6.0 < M < 6.5 \\ 1; & M \geq 6.5 \end{cases} \quad (3.14)$$

$$f_{hng,Z} = \begin{cases} 0; & Z_{TOR} \geq 20 \\ \frac{20 - Z_{TOR}}{20}; & 0 \leq Z_{TOR} < 20 \end{cases} \quad (3.15)$$

$$f_{hng,\delta} = \begin{cases} 1; & \delta \leq 70 \\ \frac{90 - \delta}{20}; & \delta > 70 \end{cases} \quad (3.16)$$

Where,

$\delta$ : dip angle

#### Shallow site response term

This term depends on two main parameters. The first one is the average shear wave velocity in the top 30 m of site profile ( $V_{s30}$ ) and the second one is the value of PGA on rock ( $A_{1100}$  (g)) where  $V_{s30} = 1100$  m/s. The term can be computed as below:

$$f_{site} = \begin{cases} c_{10} * \ln\left(\frac{V_{s30}}{k_1}\right) + k_2 \left\{ \ln \left[ A_{1100} + c * \left( \frac{V_{s30}}{k_1} \right)^n \right] - \ln [A_{1100} + c] \right\}; & V_{s30} < k_1 \\ (c_{10} + k_2 * n) * \ln\left(\frac{V_{s30}}{k_1}\right); & k_1 \leq V_{s30} < 1100 \\ (c_{10} + k_2 * n) * \ln\left(\frac{1100}{k_1}\right); & V_{s30} \geq 1100 \end{cases} \quad (3.17)$$

$$c = 1.88;$$

$$n = 1.18;$$

### Deep site response term ( $f_{\text{sed}}$ )

The most important parameter included in deep site response term is depth to the 2.5 km/s shear wave velocity horizon (sediment depth) ( $Z_{2.5}$  (km)).

$$f_{\text{sed}} = \begin{cases} c_{11} * (Z_{2.5} - 1); & Z_{2.5} < 1 \\ 0; & 1 \leq Z_{2.5} \leq 3 \\ c_{12} * k_3 * e^{-0.75} * (1 - e^{-0.25*(Z_{2.5}-3)}); & Z_{2.5} > 3 \end{cases} \quad (3.18)$$

#### *3.4.1.2 Aleatory Uncertainty Model*

Aleatory Uncertainty model is represented by the equation below:

$$\ln Y_{ij} = \widehat{\ln Y_{ij}} + \eta_i + \varepsilon_{ij} \quad (3.19)$$

Where:

$\eta_i$ : Inter- event variation for ith earthquake (random effect)

$\widehat{\ln Y_{ij}}$ : Median estimated value

$\ln Y_{ij}$ : observed value

$\varepsilon_{ij}$ : intra event variation of j recording for ith earthquake

$\eta_i$  and  $\varepsilon_{ij}$  as supposed to be normally distributed variables with variance  $\tau^2$  and  $\sigma^2$  respectively.

Total model residual ( $r_{ij}$ ) can be represented as the sum of inter-event variation ( $\eta$ ) and intra-event variation ( $\varepsilon_{ij}$ ).

So,

$$r_{ij} = \eta_i + \varepsilon_{ij} \quad (3.20)$$

Inter-event and intra-event residuals can be determined as below:

$$r_i^{\text{inter}} = \eta_i = \frac{\tau^2 * \sum_{j=1}^{N_i} r_{ij}}{N_i * \tau^2 + \sigma^2} \quad (3.21)$$

$$r_{ij}^{\text{ultra}} = \varepsilon_{ij} = r_{ij} - r_i^{\text{inter}} \quad (3.22)$$

$N_i$ : Number of recording of ith earthquake

The total aleatory standard deviation of geometric mean is:

$$\sigma_T = \sqrt{\sigma^2 + \tau^2} \quad (3.23)$$

Inter and intra variance values can be computed using the equations below:

$$\sigma^2 = \sigma_{\ln Y}^2 + \alpha^2 * \sigma_{\ln A_{1100,B}}^2 + 2 * \alpha * \rho_\sigma * \sigma_{\ln Y_B} * \sigma_{\ln A_{1100,B}} \quad (3.24)$$

$$\tau^2 = \tau_{\ln Y}^2 + \alpha^2 * \tau_{\ln A_{1100}}^2 + 2 * \alpha * \rho_\tau * \tau_{\ln Y} * \tau_{A_{1100}} \quad (3.25)$$

$\sigma_{\ln Y}$  :: intra-event standard derivation of  $\ln Y$

$\sigma_{A_{1100}}$ ; intra-event standard derivation of  $\ln A_{1100}$

$\tau_{\ln Y}$  :: inter-event standard derivation of  $\ln Y$

$\tau_{A_{1100}}$ ; inter-event standard derivation of  $\ln A_{1100}$

$\sigma_{\ln Y_B}$ : intra-event standard derivation of  $\ln Y$  on rock

$\sigma_{\ln A_{1100,B}}$  : intra-event deviation of  $\ln A_{1100}$  at the base of soil profile

$\rho_b, \rho_r$  : correlations coefficients between inter-events and ,intra-event (Appendix B)

Inter-event standard deviations on rock and at the base of the soil are defined by the equation below:

$$\sigma_{\ln Y_B}^2 = \sigma_{\ln Y}^2 - \sigma_{\ln AMP}^2 \quad (3.26)$$

$$\sigma_{\ln A_{1100,B}}^2 = \sigma_{\ln A_{1100}}^2 - \sigma_{\ln AMP}^2 \quad (3.27)$$

$\sigma_{\ln AMP}$  : standard deviation of the linear part of the shallow site response term  $f_{site}$

It is calculated as  $\sigma_{\ln AMP} = 0.3$  for all periods.

The standard derivations that are explained above are supposed to represent the aleatory uncertainty in the linear site response of ground motion.

The difference between the shallow site response term and rock can be represented by  $\alpha$ .

$$\alpha = \frac{\partial f_{site}}{\partial \ln A_{1100}} = k_2 * A_{1100} * \begin{cases} \left\{ [A_{1100} + c * (\frac{V_{s30}}{k_1})^n]^{-1} - [A_{1100} + c]^{-1} \right\} & V_{s30} < k_1 \\ 0 & V_{s30} \geq k_1 \end{cases} \quad (3.28)$$

### 3.4.1.3 General limits of Applicability

This model can be used for shallow continental earthquakes and the general conditions for using this model are as below:

- a) M>4
- b) M<8.5 for strike slip faulting, and M<7.5 for normal faulting
- c) R<sub>rup</sub><200 km
- d) V<sub>s30</sub>=150-1500 m/s
- e) Z<sub>2.5</sub>=0-10 km
- f) Z<sub>TOR</sub>=0-15 km
- g) δ=15-90 °

If these conditions are not met, the error of the models can become very large and not negligible.

### 3.4.2 NGA Model for Average Horizontal Component of Peak Ground Motion and Response Spectra suggested by Brian et al. (2008).

This model is developed in order to estimate horizontal ground motion amplitudes caused by shallow crustal earthquakes occurring in active tectonic zones. It is a part of the Pacific Earthquake Engineering Research Center's (PEER) Next Generation Attenuation model (NGA) project. Using the relationships suggested by Brian et al. (2008), median peak ground acceleration and 5% damped pseudo-spectral acceleration for spectral period of 0-10 s can be predicted. All the information presented in this section (3.4.2) is taken from Brian et al. (2008).

#### 3.4.2.1 Ground Motion Model

According to this model, computation of expected peak ground motion can be done by using the correlations below:

$$\ln y_{refij} = c_1 + [c_{1a} * F_{Rvi} + c_{1b} * F_{NMI} + c_7 * (Z_{TOR,i} - 4)] * (1 - A * S_i) + [c_{10} + c_{7a} * (Z_{TOR,i} - 4)] * A * S_i + c_2 * (M_i - 6) + \frac{c_2 - c_3}{c_n} * \ln(1 + e^{c_n * (c_M - M_i)}) + c_4 * \ln[R_{Rupij} + c_5 * \cosh\{c_6 * (R_{Rupij} - 1)\}]$$

$$\max(M_i - c_{HM}, 0)\} \] + (c_{4a} - c_4) * \ln\left(\sqrt{R_{RUPij}^2 + c_{RB}^2}\right) + \left\{c_{\gamma 1} + \frac{c_{\gamma 1}}{\cosh[\max(M_i - c_{\gamma 3}, 0)]}\right\} * R_{RUPij} + \\ c_9 * F_{HWij} * \tanh\left(\frac{R_{xij} * \cos^2 \delta_i}{c_{9a}}\right) * \left\{1 - \frac{\sqrt{R_{JBij}^2 + Z_{TOR}^2}}{R_{RUPij} + 0.001}\right\} \quad (3.29)$$

The variability in ground motion is defined with the equation below :

$$\ln(y_{ij}) = \ln(y_{refi,j}) + \phi_1 * \min\left(\ln\left(\frac{V_{S30j}}{1130}\right), 0\right) + \phi_2 * \{e^{\phi_3 * (\min(V_{S30,1130}) - 360)} - e^{\phi_3 * (1130 - 360)}\} * \\ \ln\left(\frac{y_{refij} * e^{\eta_i + \phi_4}}{\phi_4}\right) + \phi_5 * \left(1 - \frac{1}{\cosh[\phi_6 * \max(0, Z_{2.5} - \phi_7)]}\right) + \frac{\phi_8}{\cosh[0.15 * \max(0, Z_{1.0} - 15)]} + \eta_i + \varepsilon_{ij} \quad (3.30)$$

M: Moment magnitude

R<sub>RUP</sub>: Closest distance to the rupture plane (km)

R<sub>JB</sub>: distance from the site to the rupture plane (km)

R<sub>X</sub>: Site coordinate (km) measured perpendicular to the fault strike from the surface projection of the up-dip edge of the fault rupture, with the down-dip direction being positive

F<sub>HW</sub>: Hanging-wall flag: It is 1 for R<sub>X</sub> ≥ 0 and 0 for R<sub>X</sub> < 0

δ : Fault dip angle

Z<sub>TOR</sub>: Depth to top of rupture (km)

F<sub>RV</sub>: Reverse-faulting flag: It is 1 for 30° ≤ λ ≤ 150° and 0 otherwise

λ: is the rake angle.

F<sub>NM</sub>: Normal faulting flag: It is 1 for -120° ≤ λ ≤ -60° (excludes normal-oblique), 0 otherwise.

F<sub>AS</sub>: Aftershock flag: It is 1 if the event is an aftershock, 0 otherwise

V<sub>S30</sub>: Average shear-wave velocity for top 30 m (m/s)

Z<sub>1.0</sub>: Depth to shear-wave velocity of 1.0 km/s (m).

ϕ<sub>n, Cn</sub>: correlation's coefficients (Appendix B)

ε<sub>ij</sub>: intra event variation of j recording for ith earthquake

η<sub>i</sub>: Inter-event variation for ith earthquake (random effect) (Brian et al., 2008).

The values of total standard deviation are given in Appendix B.

### *3.4.2.2 General limits of Applicability*

Data used in this model are related to the earthquakes occurred in California. As a result it is convenient to use this model for the zones with the similar seismicity to that of California.

The application conditions can be listed as below:

- For strike-slip earthquakes  $4 \leq M \leq 8.5$
- For reverse and normal faulting  $4 \leq M \leq 8.0$
- $0 \leq R_{\text{Rup}} \leq 200 \text{ km}$
- $150 \leq V_{s30} \leq 1500 \text{ m/sec}$

### ***3.4.3 NGA Ground Motion Relations for the Geometric Mean Horizontal Component of Peak and Spectral Ground Motion Parameters suggested by Boore & Atkinson (2007).***

As the previous two models, this model is part of the Pacific Earthquake Engineering Research Center's Next Generation Attenuation project. Ground motion prediction equations have been empirically developed by regressing recorded ground motion amplitude data versus magnitude distance and other variables. These equations can be used to predict peak ground acceleration (PGA), peak ground velocity (PGV), and 5%-damped pseudo-absolute acceleration spectra (PSA) at periods between 0.01 s and 10 s. The database of this model includes 1574 records from 58 main shocks. The distances from site to source range from 0 to 400 km (Boore & Atkinson, 2007). All information presented in this section (3.4.3) is taken from Boore & Atkinson (2007). The equation for predicting the ground motions is given as below:

$$\ln Y = F_M(M) + F_D(R_{JB}, M) + F_s(V_{30}, R_{JB}, M) + \varepsilon * \sigma_T \quad (3.31)$$

In this equation  $F_M$  represents the magnitude scaling,  $F_D$  represents distance function and  $F_s$  represent site amplification.

$\varepsilon$ : Fractional number of standard deviations for a single value

$R_{JB}$ : the closest distance from site to the surface projection of the faults or source zone.

$V_{S30}$ : Average shear-wave velocity for top 30 m (m/s)

Magnitude scaling is computed using the Equation (3.32).

For  $M \leq M_h$

$$F_M(M) = e_1 * U + e_2 * SS + e_3 * NS + e_4 * RS + e_5 * (M - M_h) + e_6 * (M - M_h)^2 \quad (3.32a)$$

For  $M \geq M_h$

$$F_M(M) = e_1 * U + e_2 * SS + e_3 * NS + e_4 * RS + e_5 * (M - M_h) + e_6 * (M - M_h)^2 + e_7 * (M - M_h) \quad (3.32b)$$

Where,

U, SS, NS and RS are dummy variables that represent the effect of different fault types (Table 3.2).

The distance function is given by the equation below:

$$F_D(R_{JB}, M) = [c_1 + c_2 * (M - M_f)] * \ln\left(\frac{R}{R_{Ref}}\right) + c_3 * (R - R_{Ref}) \quad (3.33)$$

Here R is computed as below:

$$R = \sqrt{R_{JB}^2 + h^2} \quad (3.34)$$

$c_1, c_2, c_3, M_{Ref}, R_{Ref}, e_1, e_2, e_3, e_4, e_5, e_6, e_7, M_h$  and  $h$  are coefficients which are determined empirically (Appendix B).

Table 3.2 Values of dummy variables according to the type of fault

Fault type	U	SS	NS	RS
Unspecified	0	0	0	0
Strike-slip	0	1	0	0
Normal	0	0	1	0
Reverse	0	0	0	1

.

Site amplification is given as the sum of linear and non-linear terms.

$$F_S = F_{LIN} + F_{NL} \quad (3.35)$$

$F_{LIN}$ : Linear term

$F_{NL}$ : Non-linear term

The linear term is determined using the equation below:

$$F_{LIN} = b_{LIN} * \ln(V_{s30}/V_{Ref}) \quad (3.36)$$

$b_{LIN}$ : Period dependent coefficient

$V_{ref}$ : Specified reference velocity (760 m/s)

Non linear term is given by:

$$F_{NL} = b_{nl} * \ln\left(\frac{pga\_low}{0.1}\right) \quad for \quad pga4nl \leq a_1 \quad (3.37)$$

$$F_{NL} = b_{nl} * \ln\left(\frac{pga\_low}{0.1}\right) + c * \left[\ln\left(\frac{pga4nl}{a_1}\right)\right]^2 + d * \left[\ln\left(\frac{pga4nl}{a_1}\right)\right]^3 \quad for \quad a_1 \leq pga4nl \leq a_2 \quad (3.38)$$

$$F_{NL} = b_{nl} * \ln\left(\frac{pga4nl}{0.1}\right) \quad for \quad a_2 < pga4nl \quad (3.39)$$

The coefficients of these equations are determined as below:

$$a_1 = 0.3 \text{ g}$$

$$a_2 = 0.6 \text{ g}$$

$$pga\_low = 0.6 \text{ g}$$

$pga4nl$ : initial estimate of predicted PGA in g for  $V_{ref}=760$  m/s,  $F_s=0$  and  $\epsilon=0$  at equation (3.34)

The value of  $b_{nl}$  depends on both period and  $V_{s30}$ . It is determined by the relationships shown below:

For  $V_{s30} \leq V_1$  :

$$b_{nl}=b_1$$

For  $V_1 \leq V_{s30} \leq V_2$  :

$$b_{nl} = (b_1 - b_2) * \frac{\ln\left(\frac{V_{s30}}{V_2}\right)}{\ln\left(\frac{V_1}{V_2}\right)} + b_2 \quad (3.40)$$

For  $V_2 \leq V_{s30} \leq V_{ref}$  :

$$b_{nl} = b_2 * \ln\left(\frac{V_{s30}}{V_{ref}}\right) / \ln\left(\frac{V_2}{V_{ref}}\right) \quad (3.41)$$

For  $V_{ref} \leq V_{s30}$

$$b_{nl}=0.0$$

Where,  $V_1=180$  m/s,  $V_2=300$  m/s and  $b1, b2$  are period depended coefficients given in Table 3.3

The coefficients  $c, d$  are given below:

$$c= (3*\Delta y - b_{nl}*\Delta x)/\Delta x^2$$

$$d=-(2*\Delta y - b_{nl}*\Delta x)/\Delta x^3$$

$$\Delta x = \ln(a_2/a_1)$$

$$\Delta y = b_{nl} * \ln(a_2/\text{pga\_low})$$

Table 3.3 Period-dependent site-amplification coefficients (Boore & Atkinson, 2007).

Period	$b_{lin}$	$b_1$	$b_2$
PGV	-0.6	-0.5	-0.06
PGA	-0.36	-0.64	0.14
0.01	-0.36	-0.64	-0.14
0.02	-0.34	-0.63	-0.12
0.03	-0.33	-0.62	-0.11
0.05	-0.29	-0.64	-0.11
0.075	-0.23	-0.64	-0.11
0.1	-0.25	-0.6	-0.13
0.15	-0.28	-0.53	-0.18
0.2	-0.31	-0.52	-0.19
0.25	-0.39	-0.52	-0.16
0.3	-0.44	-0.52	-0.14
0.4	-0.5	-0.51	-0.1
0.5	-0.6	-0.5	-0.06
0.75	-0.69	-0.47	0
1	-0.7	-0.44	0
1.5	-0.72	-0.4	0
2	-0.73	-0.38	0
3	-0.74	-0.34	0
4	-0.75	-0.31	0
5	-0.75	-0.291	0
7.5	-0.692	-0.247	0
10	-0.650	-0.215	0

#### 3.4.3.1 General limits of Applicability

The equation presented should be used for predictable variables in these ranges:

M=5~8

R<sub>Jb</sub><200 km

V<sub>s30</sub>=180-1300 m/s

#### 3.4.4 Advantages of New Generation Attenuation Models and their Comparisons with Older Models

The first advantage of New Generation Attenuation models, as compared with the previous models, is the number of data. As the technology is developing, the possibility to collect more data than before is increasing. As a result, the New

Generation Attenuation (NGA) models are supposed to be more complete than the old models.

Additionally, according to Campbell & Bozorgnia (2008), the results obtained by older versions give approximately the same results as NGA models. However, the limits of applicability change. For example, the previous models of Campbell & Bozorgnia such as Campbell and Bozorgnia, (2003) and Campbell and Bozorgnia, (97) are not convenient to be used for the sites that are farther than 60 km from the source. So the results taken from these models at distance of 150 km from the source significantly change from the results obtained by NGA models. Contrary, if the site is nearer than 60 km than the results of old models are compatible with those of NGA models (Campbell & Bozorgnia 2008).

Furthermore, the previous models of Campbell & Bozorgnia are useful for magnitude that ranges from 5 to 6.5. So if magnitudes, which are out of this range, are used, than the results differ from those obtained from NGA model.

Another difference between previous models NGA model Campbell & Bozorgnia is the effect of buried faults rupture. Since the previous models don't distinguish between reverse faulting earthquakes with surface and buried fault rupture, the values of NGA models are higher when the fault rupture is defined as buried.

Additionally, hanging wall effect has its own effect on results. NGA model predicts significantly higher ground motion than the CB03 (Campbell & Bozorgnia 2003) model at short and mid periods, because of the inclusion of hanging-wall effects. This represents a worst-case scenario for strike-slip faults (Campbell & Bozorgnia 2008).

For nearly the same reasons, the NGA model postulated by Boore & Atkinson (2007) gives different results (especially for high magnitudes) from previous models. Because of the lack of data, the previous models do not include high earthquake magnitudes. A big difference between the old and NGA model is seen for  $T = 1$  s ( $T$ : spectral period) and  $M = 7.5$ . NGA model gives lower values than previous model.

When the parameters are suitable for both models, similar solutions are obtained (Boore & Atkinson, 2007).

Finally, according to some comparisons between NGA model of Brian et al. (2008) and that of Sadigh et al. (1997), the values of both older and NGA models are similar. However, the difference between the two models increases for longer period motions, with the new model generally indicating lower motions (Brian et al., 2008).

### 3.5 Seisrisk III Software

Seisrisk III program is used to calculate maximum ground motion levels with the condition of not exceeding a specified probability during fixed period of time. The basics of this software are probabilistic calculations. Generally in seismic hazard analysis, earthquakes are represented either as points distributed randomly in seismically homogeneous zones or as ruptures with limited length that occurs randomly along faults. Earthquakes cannot be predicted exactly, therefore probabilistic models are acceptable solutions for predicting them. Because the place of the epicenter of the earthquakes is not known, the zone, that each point of it is assumed to have the same probability of being epicenter of an earthquake, is called source zone. An important point of this program is earthquake location uncertainty. The location of occurred earthquakes is normally distributed using a standard deviation. This averts big differences between the magnitudes in the center and near a boundary. If  $\sigma$  is the standard derivation in location and if an earthquake is expected in point  $(x,y)$ , the probability that an earthquake occurs at a point  $(x+\Delta x, y+\Delta y)$  can be found by using the formulation below (Equation 3.42) (Bender, 1987).

$$P(\Delta x, \Delta y) = \frac{A}{2\pi\sigma^2} \exp\left(-\frac{\Delta x^2 + \Delta y^2}{2\sigma^2}\right) \quad (3.42)$$

When  $A(\sigma=0)$  the source zone is assumed to be homogeneous, so the expected earthquake locations are equal in every point of the zone. However, if  $\sigma=0$ , the probability that an earthquake occurs outside this zone is zero. As we mentioned above, the expected location of an earthquake is unpredictable, so the possibility that

earthquakes may occurs outside a zone is always present. Standard deviation is used in order to obtain more approximation in calculation. The standard deviation effect can be seen in Figure 3.6 where the values of standard deviation varies from 0 at A to 50 at D (Figure 3.6). If the value of standard deviation is too much, then distribution may become exaggerated. The default value of the program is  $\sigma=0$  km. The effect of standard deviation can be seen in Figure 3.6.

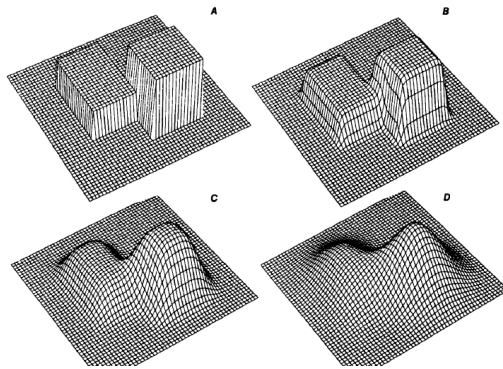


Figure 3.6 The effect of standard deviation on the earthquake locations distribution (Bender, 1987)

### ***3.5.1 Model Implementation***

The creation of the model is done in three main steps. The first step is creating transformed coordinate system for all the other next inputs. According to Bender (1987) coordinate system is determined by specifying two points of a great circle which creates the equator in this system. The circle should include all the zones or faults entered in this system. The new equator becomes the x-axis of the system. During the calculations all zones and faults coordinates are transformed according to the new equator (Figure 3.7a).

The second step is forming the grid area whose points are used in calculations. Even though new coordinate system is established according to an equator, the calculations are done using rectangular coordinate system (Figure 3.7b). So the upper left and lower right corners of this rectangular coordinate system should be specified. Additionally the grid space is decisive for the calculations of ground motion. The

grid space should be adjusted according to the fact that program do not accept grids that have more than 55 column and 55 rows (Bender, 1987). All the inputs should be in decimal degree because they should be in accordance with map programs such as google earth etc.

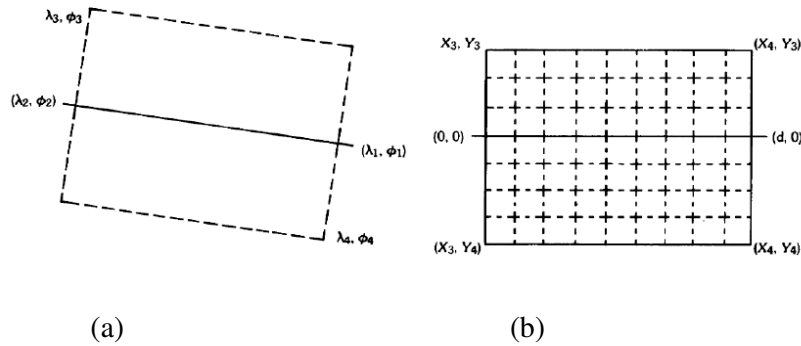


Figure 3.7 New coordinate system and grid creation (Bender, 1987).

The third step is definition of attenuation relationships that are going to be used for the calculation of peak ground acceleration. As it is explained in the sections above, we use three types of attenuation relationships. These attenuation relationships are represented by an acceleration table. Ground motion computation is done by interpolating this table of acceleration as a function of magnitude and distance. Interpolations are linear in distance, magnitude and log acceleration (Bender, 1987).

The fourth step is determination of seismic zones. Seismic zonation is done according to the density of epicenters of occurred earthquakes and existing ruptures such as faults or faults zone. Input of seismic zone into the program is done by defining the real coordinates of these zones as set of quadrilaterals (Figure 3.8) (Bender, 1987).

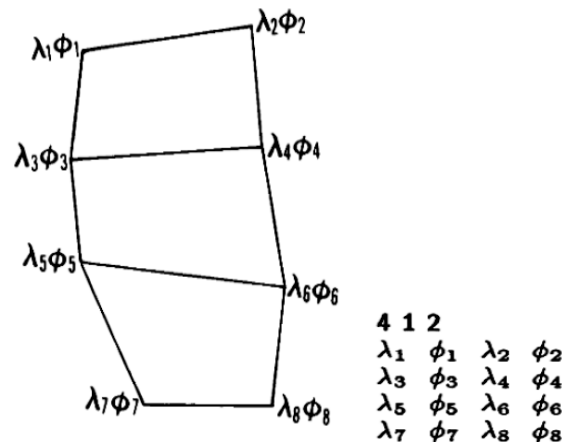


Figure 3.8 Definition of seismic zones in Seisrisk III software (Bender, 1987)

$\lambda_n$ : Longitude coordinates of the corner points of the seismic zone

$\phi_n$ : Latitude coordinates of the corner points of the seismic zone

n: subscript of corner points (Figure 3.8).

### 3.5.1.1 Calculation of Ground Motion Exceedance Probability (Bender, 1987)

Average annual acceleration occurrences for each zone are entered into the program for a set of magnitude values. Earthquake occurrences are supposed to be distributed according to Poisson distribution. According to Poisson distribution, the probability of occurrence of k events during time t is computed as:

$$P(k, t) = \frac{(\mu*t)^k * \exp(-\mu*t)}{k!} \quad (3.43)$$

$\mu$ : mean rate of distribution

k: Exactly number of events

t: Time of occurrence of k events

### *3.5.1.2 Outputs*

The Seisrisk III software computes the ground motion for each site on the grid. This software calculates and displays the occurrence and exceedance rate per year, the average number of events needed to produce a specific exceedance per year. The calculations are displayed in two files such as file 6 and 2. In file 6 all the calculation results are displayed. In file 2 only the peak acceleration values can be seen. File 2 is created in order to simplify drawing of contour maps (Bender, 1987).

## **CHAPTER FOUR**

### **RESULTS AND DISCUSSIONS**

#### **4.1 Magnitude Conversion Relationships**

In Turkey, modern time acceleration recorders have been installed since 1973. These installations were realized in relation with the project of Strong Ground Motion Network of Turkey, under the responsibility of the Earthquake Research Department (ERD) of the General Directorate of Disaster Affairs (GDDA). The first strong motion recording of an earthquake was obtained in Denizli on 19 August 1976, western Turkey. The records used in this thesis were downloaded from different websites such as Emergency Management Presidency [AFAD] (2009), USGS (1879). The magnitude of an earthquake can be represented in different scales. These may be listed as:

$M_L$ : Local magnitude scale

$M_d$ : Duration magnitude scale

$M_w$ : Moment magnitude scale

$M_s$ : Surface magnitude scale

The most useful scale for engineering purpose is the moment magnitude ( $M_w$ ) since it is related to the rupture parameters. For this reason, in this study, earthquake size is defined by means of  $M_w$ . Magnitudes smaller than 4 do not present a significant importance for engineering purpose. Therefore, only earthquakes of which magnitudes were greater than 4 have been taken into consideration. Locations of epicenters of earthquakes with a magnitude greater than 4 that are included in this study are shown in Figure 4.1.

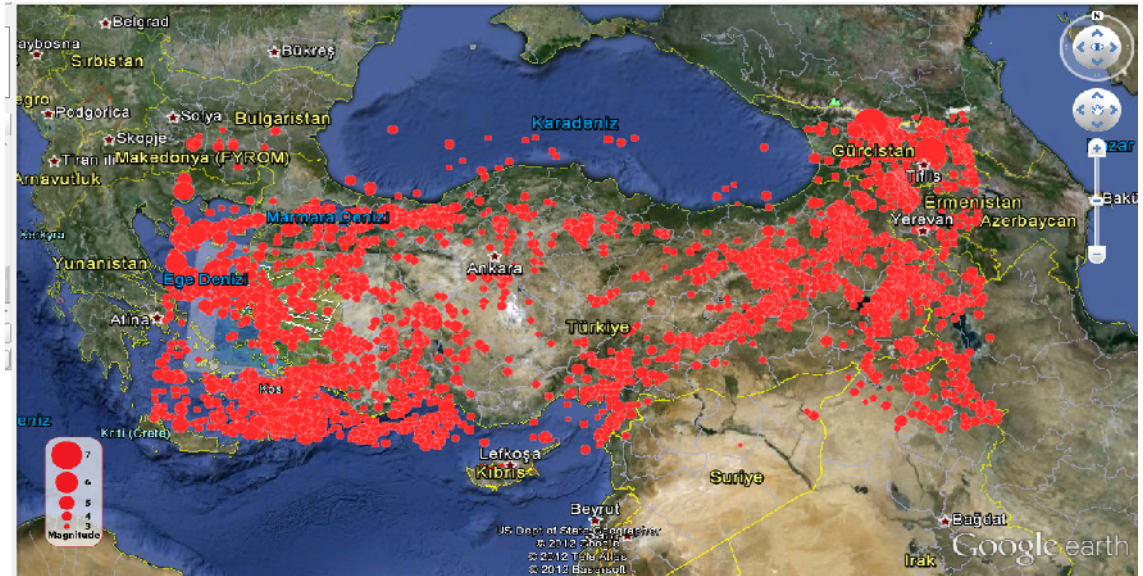


Figure 4.1 The locations of the epicenters of earthquakes greater than 4 occurred in Turkey since 1976

Some of the earthquake magnitudes were recorded using different scales.  $M_w$  data are not available for all the events included in this study. So, all the data should be transformed to  $M_w$ . In order to do this, values of  $M_w$  are correlated to  $M_s$ ,  $M_L$ ,  $M_b$  and  $M_d$  using data pairs of 404, 331, 364, 290 between  $M_w$ - $M_b$ ,  $M_w$ - $M_s$ ,  $M_w$ - $M_L$ ,  $M_w$ - $M_d$ , respectively. These correlations are developed using linear regression technique (Figure 4.2)

$$M_w = 1.0541 * M_b + 0.4286 \quad (R^2 = 0.71)$$

$$M_w = 0.911 * M_d + 0.6502 \quad (R^2 = 0.57)$$

$$M_w = 0.753 * M_s + 1.376 \quad (R^2 = 0.72)$$

$$M_w = 0.6508 * M_L + 1.8223 \quad (R^2 = 0.52)$$

$R^2$ : linear regression

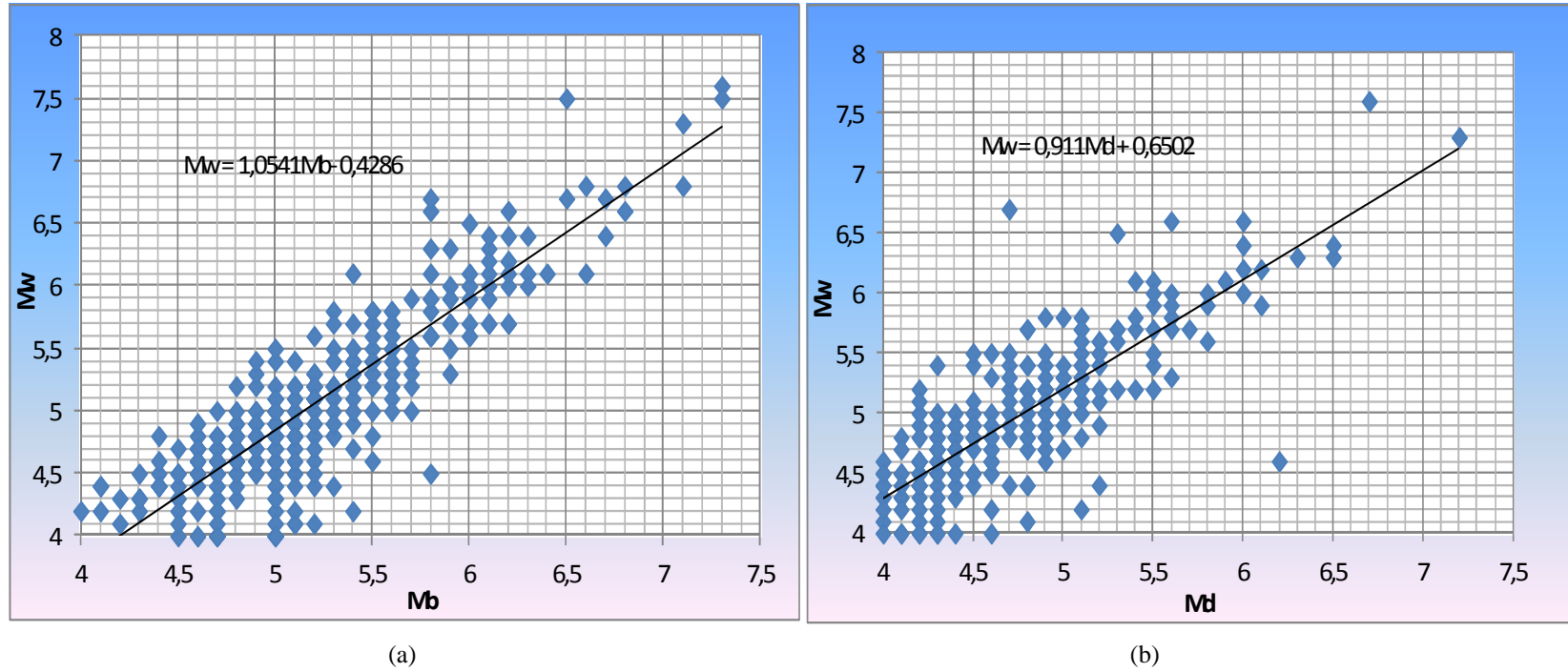


Figure 4.2 Correlations between the magnitudes scale  $M_w$ , and the magnitude scales  $M_s$ ,  $M_b$ ,  $M_d$  and  $M_L$  values for Turkish earthquakes,

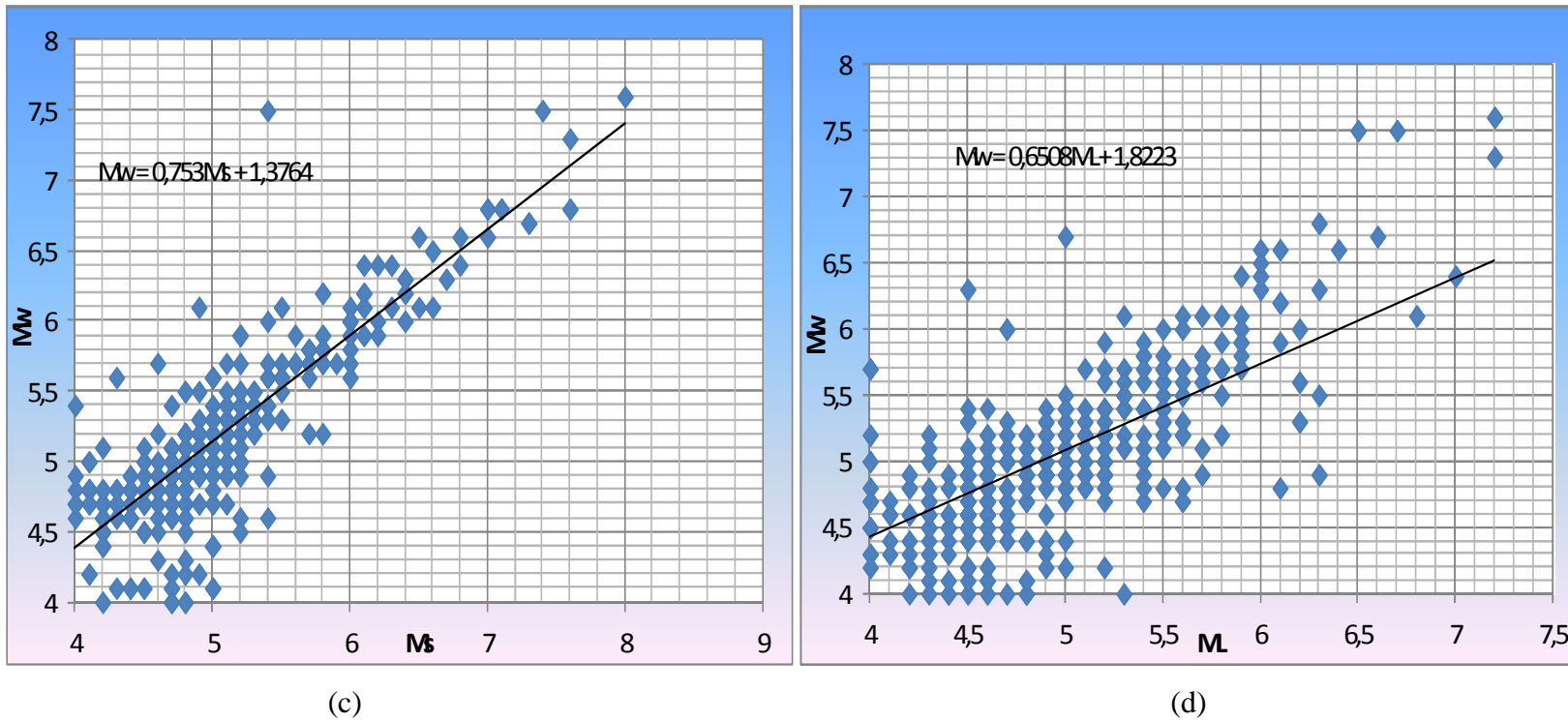


Figure 4.2 (continued)

## 4.2 Earthquake Source Characterization

Earthquake source characterization is related to the seismicity of the region. Existed faults and earthquake history of the region have main importance in the characterizations of the seismic sources. Earthquake source characterization of the study area and its vicinities consists of two stages. The first stage is determination of the source zones and the second stage is determination of the earthquake occurrence within them.

### 4.2.1 Determination of the Source Zones

Probabilistic hazard analyses are related to the earthquake occurrences in a specific zone. Because of the lack of information about the fault presented in the study area, earthquake recurrence information about these faults is scarce. However, taking in account the location density of the epicenters of occurred earthquakes and the location of presented faults, we zonated the study area and its vicinities in 11 zones (Figure 4.3). Characterization of these zones as normal, reverse or strike slip is done according to the specification of the faults within or near these zones. The earthquakes that occurred in each zone can be seen in the Appendix D. Created seismic source zones and occurred earthquakes are shown in Figure 4.4. Most of the information about the earthquakes occurred in Izmir region are taken from AFAD (2009) website.



Figure 4.3 Created Seismic Source Zones

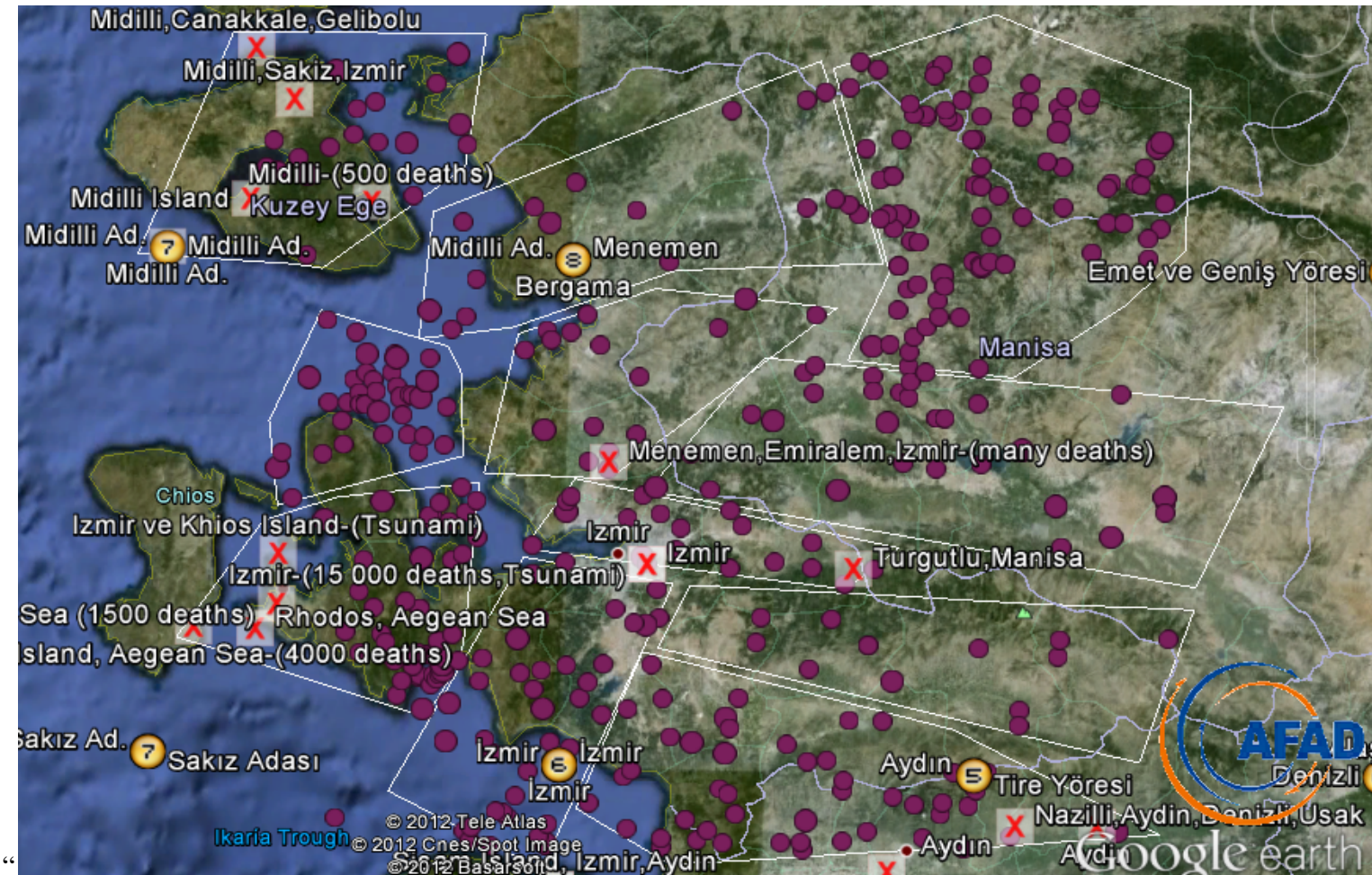


Figure 4.4 Seismic source zones and occurred earthquakes (earthquake list is provided in the Appendix A)

#### **4.2.2. Earthquake Recurrence Relationships**

As it is explained in chapter three, Gutenberg- Richter recurrence relationship is used to define quantitative distribution of earthquake records of last 1000 years. One of these distributions is shown in Figure 4.5. Recurrence relationships of other zones are given in detail in the Appendix D. The value that corresponds to a magnitude in Table 4.1 gives the number of earthquakes that have a magnitude larger than this magnitude and smaller the next magnitude on the table. For example the number of earthquakes of the last ten years with the magnitude that range between 4.2 and 4.7 is 3. After calculating annual earthquake occurrence the maximum values is chosen in order to obtain the earthquake recurrence relationship of each zone. Annual earthquake occurrence and selected and adjusted rate of occurrence are shown in the Table 4.1, 4.2 and 4.3

Table 4.1 Total earthquake occurrence (Zone 1)

Time (Year)	Magnitude								
	4,2	4,7	5,2	5,7	6,2	6,7	7,2	7,7	8,2
10	3	1	3						
20	11	2	3	1					
40	16	4	3	1					
50	17	4	3	1					
100	17	6	4	1					
1000				4		5		7	4

Table 4.2 Annual earthquake occurrence (Zone 1)

Time (Year)	Magnitude								
	4,2	4,7	5,2	5,7	6,2	6,7	7,2	7,7	8,2
10	0,3	0,1	0,3						
20	0,55	0,1	0,15						
40	0,4	0,1	0,075						
50	0,34	0,08	0,06	0,02					
100	0,17	0,06	0,04	0,01					
1000	0	0	0	0,004	0	0,005	0	0,007	0,004

Table 4.3 Selected and adjusted rate of occurrence (Zone 1)

Magnitude								
4,2	4,7	5,2	5,7	6,2	6,7	7,2	7,7	8,2
0,55	0,1	0,3	0,02		0,005		0,007	0,004
0,314	0,1717	0,0939	0,0514	0,0281	0,0154	0,0084	0,0046	0,0025

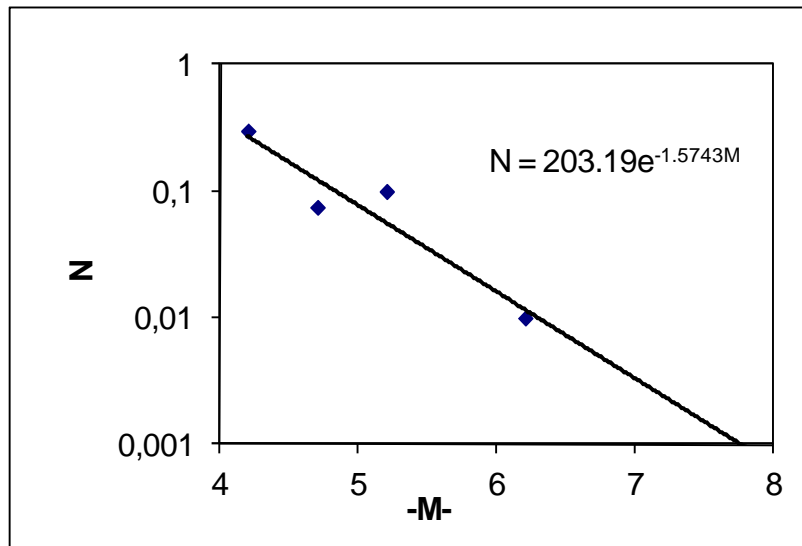


Figure 4.5 Recurrence relationships for zone 1.

The Recurrence relationships for all zones are given in Table 4.4 and their earthquake occurrences are given in the Appendix D.

Table 4.4 Recurrence relationships for each seismic zone

Zone name	Recurrence relationships	Zone name	Recurrence relationships
Zone 1	$N=45.95e^{-1.207M}$	Zone 7	$N=1153.6e^{-1.937M}$
Zone 2	$N=1.5343e^{-0.783M}$	Zone 8	$N=3.6288e^{-0.968M}$
Zone 3	$N=62.35e^{-1.169M}$	Zone 9	$N=16.778e^{-1.247M}$
Zone 4	$N=0.7194e^{-0.67M}$	Zone 10	$N=4.5155e^{-1.044M}$
Zone 5	$N=26.48e^{-1.271M}$	Zone 11	$N=203.19e^{-1.57M}$
Zone 6	$N=8.0274e^{-1.071M}$		

#### 4.3. Determination of Ground Motion Accelerations

Ground motion acceleration is calculated using the New Attenuation Relationships postulated by Campbell & Bozorgnia (2008), Brian et al. (2008) and Boore & Atkinson (2007).

The parameters of these relationships are chosen as below:

$$V_{s30}=760 \text{ m/s}$$

$$\delta=90^\circ$$

$$Z_{1.0}=500 \text{ m for sites near the coast of Izmir city}$$

$$Z_{1.0}=100 \text{ km for sites at the where the rock is near the surface}$$

$$Z_{2.5}=2.32 \text{ km for sites near the coast of Izmir city}$$

$$Z_{2.5}=0.87 \text{ km for sites at the where the rock is near the surface}$$

$$Z_{TOR}=0 \text{ km;}$$

These parameters are explained in chapter three. As it is explained in detail in the previous chapter the type of the fault or seismic zone should be defined. Zone No 1, 10 and 11 are characterized as strike slip because they contain strike slip faults. In general, other zones are characterized as normal.

Probabilistic analyses are done with the help of SIESRISK III software. As it is explained in chapter three, the NGA relationships are defined as values on a table that correspond to a pair of source-site distance ( $R$ ) and magnitude ( $M_w$ ) (Appendix C). Additionally, the recurrence relationships are defined as annual values related to the magnitudes. The coordinates of each site are defined as well. Calculated ground motion accelerations have return periods of 72 years (50% probability in 50 years), 475 years (10% probability in 50 years), and 2475 years (2% probability in 50 years). Two critical spectral periods are taken in consideration such as  $T=1\text{s}$  and  $T=0.2\text{s}$ . These are necessary for constructing of Design Spectrum. In order to do a detailed analysis, 30 sites around situated in different zones of Izmir city are accounted for. About twenty of them are chosen nearby urbanized areas (Figure 4.6).

All the calculations are done with respect to according to the bed rock level. So the average shear wave velocity in top 30 m of the site profile ( $V_{s30}$ ) is taken as 760 m/s.

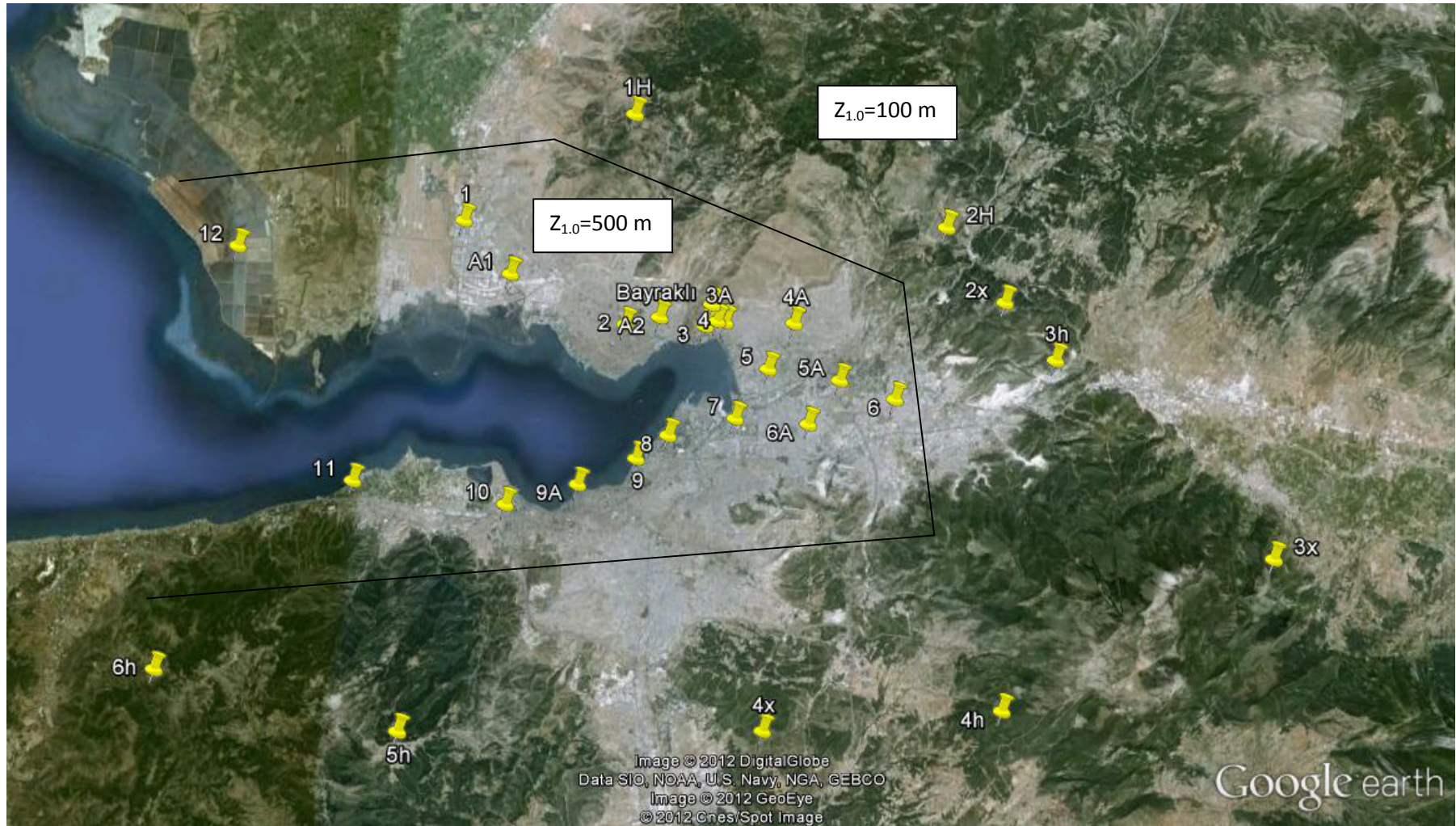


Figure 4.6 Sites chosen for the calculation of ground acceleration (The acceleration value of these points are provided in the Appendix C)

After calculating the ground motion accelerations at these sites for different return periods and spectral periods, we plotted and generated contour maps for Izmir city. We obtained maps for each return period and for spectral periods such as T=1s and T=0.2s. Additionally contour maps are created using median +1 standard deviation values (SA median  $+\sigma$ ) as well (Appendix E).

## **4.4 The Definition of the Earthquake Effect**

### ***4.4.1 Earthquake levels***

#### ***4.4.1.1 Earthquake level D1***

This earthquake level represents all earthquakes that produce relatively small values of ground motion accelerations and have a high probability to occur within a specific period of time. D1 earthquake is defined as having a return period of 72 years or occurrence of probability 50% in 50 years (DLH, 2008).

#### ***4.4.1.2 Earthquake level D2***

D2 level earthquake represents all earthquakes that produce an average ground motion with relatively low energy and have a return period of 475 years. This corresponds to an occurrence of probability 10% in 50 years (DLH, 2008).

#### ***4.4.1.3 Earthquake level D3***

This earthquake level represents any earthquake that produces high value ground accelerations. These earthquakes can be destructive and have a return period of 2475 years. This return period corresponds to occurrence of probability 2% in 50 years (DLH, 2008).

#### 4.4.2 Earthquake Design Spectra (DLH, 2008)

The design spectra (Figure 4.7) are created using the formulations below:

$$S_{MS} = F_a x S_S \quad (4.1)$$

$$S_{M1} = F_v x S_1 \quad (4.2)$$

$S_s$  (g): is the value of ground acceleration with a natural spectral period of 0.2s.

$S_1$  (g): is the value of ground acceleration with a natural spectral period of 1s.

$F_a$  and  $F_v$  are coefficients depended on the soil class (Table 4.5, Table 4.6 and Table 4.7).

Earthquake design spectra are developed using the equations below:

$$S_{ae}(T) = 0.4 S_{MS} + 0.6 \frac{S_{MS}}{T_0} T \quad (T > T_0) \quad (4.3)$$

$$S_{ae}(T) = S_{MS} \quad (T_0 \leq T \leq T_s) \quad (4.4)$$

$$S_{ae}(T) = S_{M1}/T \quad (T_s \leq T \leq T_L) \quad (4.5)$$

$$S_{ae}(T) = S_{M1}xT_L/T^2 \quad (T > T_L) \quad (4.6)$$

$$T_L=12 \text{ s}$$

$$T_s=S_{M1}/S_{MS} \quad (4.7)$$

$$T_0=0.2xT_s \quad (4.8)$$

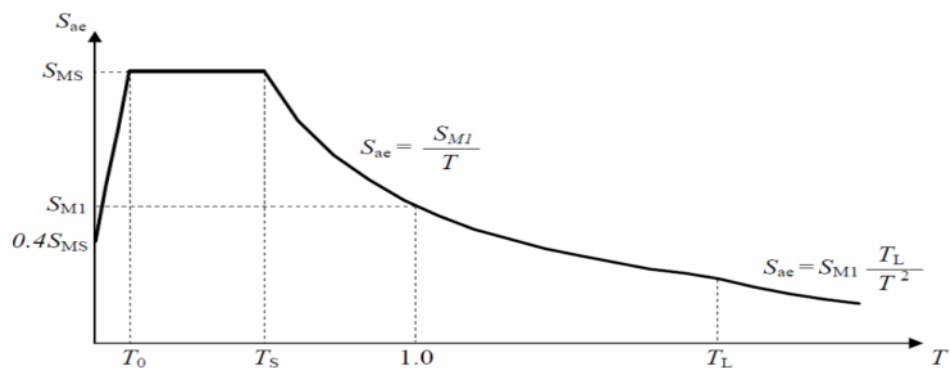


Figure 4.7 Formation of Design Spectra

Table 4.5 Soil classes explanation

Soil classification	Explanation
A	Hard rock Vs>1500 m/s
B	Rock 760 m/s <Vs 1500 m/s
C	Soft Rock 360 m/s <Vs 760 m/s
D	Solid Soils (180 m/sn < Vs 360 m/sn)
E	Vs< 180 m/sn
F	Special site investigations should be done

Table 4.6 Values of  $F_a$  coefficient according to soil classification

Soil Classification	Short Period Spectral Acceleration (g)				
	$S_s \leq 0,25$	$S_s = 0,5$	$S_s = 0,75$	$S_s = 1$	$S_s \geq 1,25$
A	0,8	0,8	0,8	0,8	0,8
B	1	1	1	1	1
C	1,2	1,2	1,1	1	1
D	1,6	1,4	1,2	1,1	1
E	2,5	1,7	1,2	0,9	0,9
F	-	-	-	-	-

Table 4.7 Values of  $F_v$  coefficient according to soil classification

Soil Classification	1s Period Spectral Accelerations				
	$S_1 \leq 0,1$	$S_1 = 0,2$	$S_1 = 0,3$	$S_1 = 0,4$	$S_1 \geq 0,5$
A	0,8	0,8	0,8	0,8	0,8
B	1	1	1	1	1
C	1,7	1,6	1,5	1,4	1,3
D	2,4	2	1,8	1,6	1,5
E	3,5	3,2	2,8	2,4	2,4
F	-	-	-	-	-

As we mentioned before, our calculations are performed for rock. So our soil is classified as C (But is close to B as well). As a result all coefficients are taken as 1.

The Design spectra for two sites are shown in Figure 4.7. These design spectra are developed using three NGA models and the solutions are compared with those suggested by DLH and Specification for Structures to be Built in Disaster Areas (2007) (Deprem Bölgelerinde Yapılacak Binalar Hakkında Yönetmelik) . As design spectra are important for the design of buildings, they are developed only for median+1 standard derivation acceleration values and return periods of 475 and 2475 years (Figure 4.8-4.11).

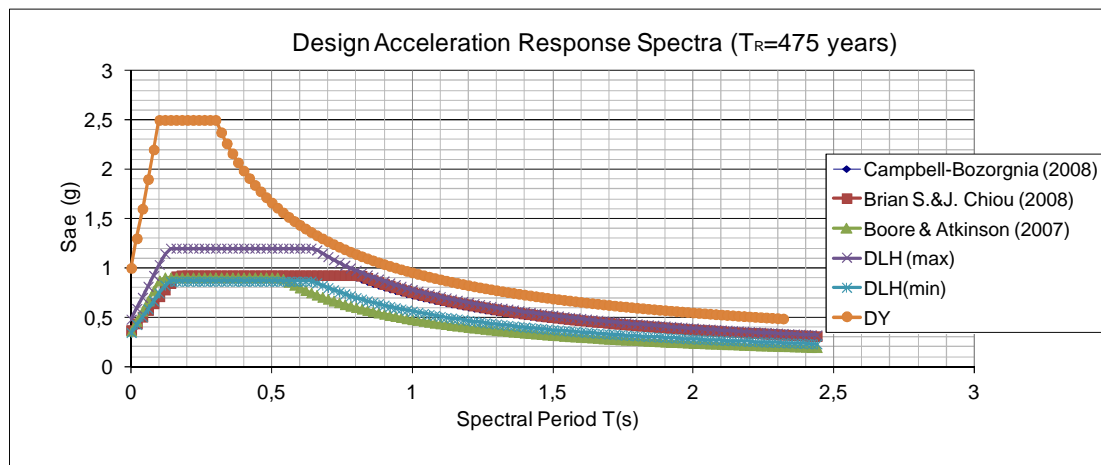


Figure 4.8 Design Spectra for site\_1 (Return period  $T=475$ ) (Manavkuyu)

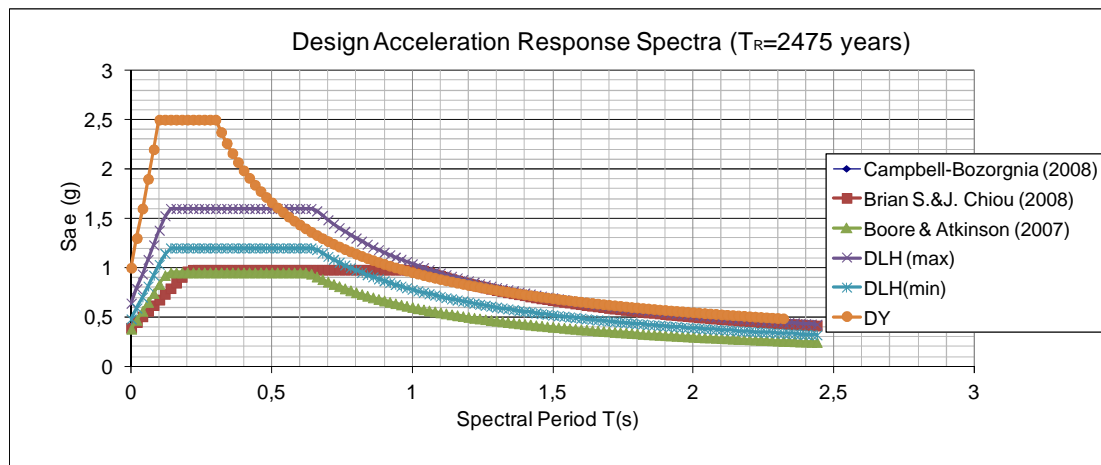


Figure 4.9 Design Spectra for site\_1 (Return period  $T=2475$ ) (Manavkuyu)

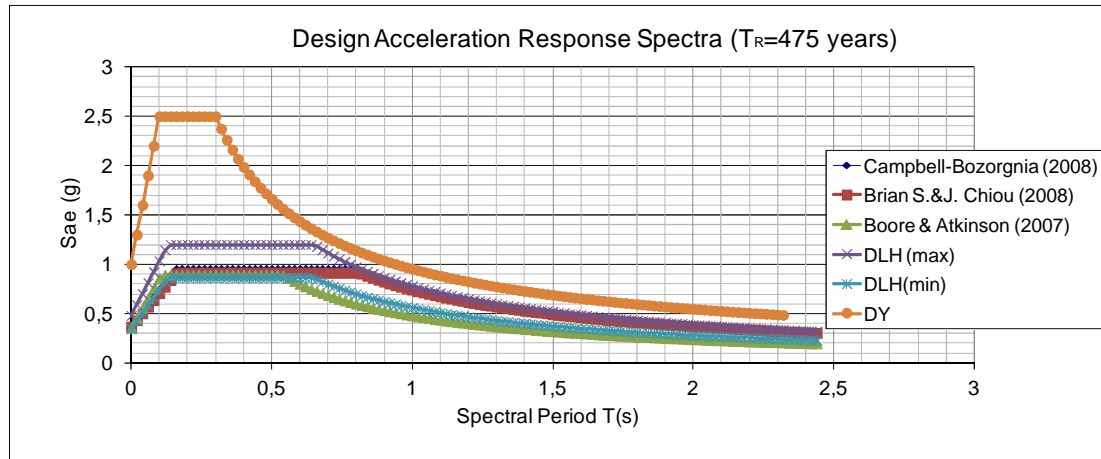


Figure 4.10 Design Spectra for site\_2 (Return period  $T=475$  years) (Mavi ehir)

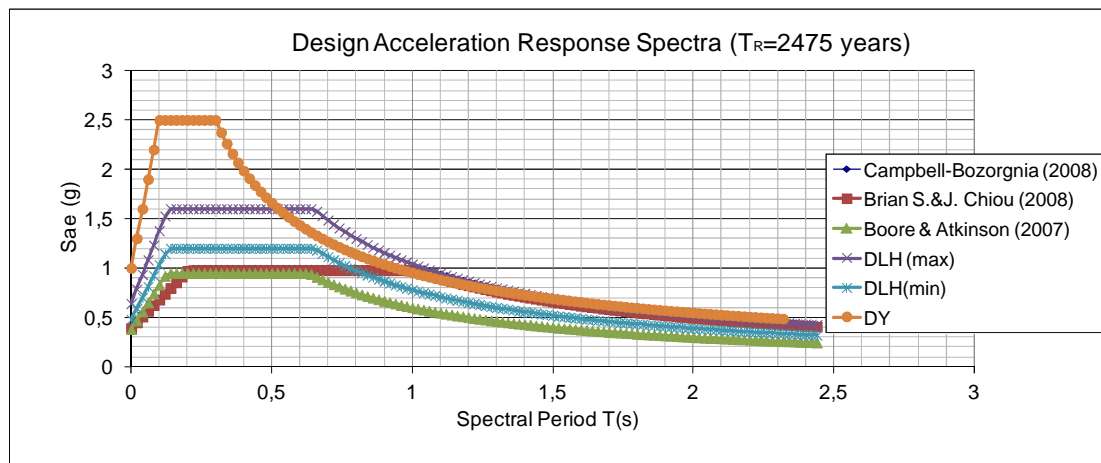


Figure 4.11 Design Spectra for site\_2 (Return period  $T=2475$  years) (Mavi ehir)

(Note: The design spectra created using attenuation relationships of Brian et al. (2008) (or Brian & Chiou) and Cambell & Bozorgia (2008) overlap each other in Figures above)

Where,

DY: DBYBHY (2007)

In order to see better the effect of  $Z_{1.0}$ , we obtained the design spectra of the site named as 2h in Figure 4.6. This site is situated in the highland (Mountains) of zmir (Figure 4.12). The value of the depth of 1.0 km/s shear-wave velocity ( $Z_{1.0}$ ) at this site is assumed as 100 m, whereas the value of this parameter in Manavkuyu and Mavi ehir is taken as 500 m. The design spectra of site 2h are shown in Figure 4.12 and Figure 4.13. These spectra are obtained using the three NGA relationships used in this thesis.

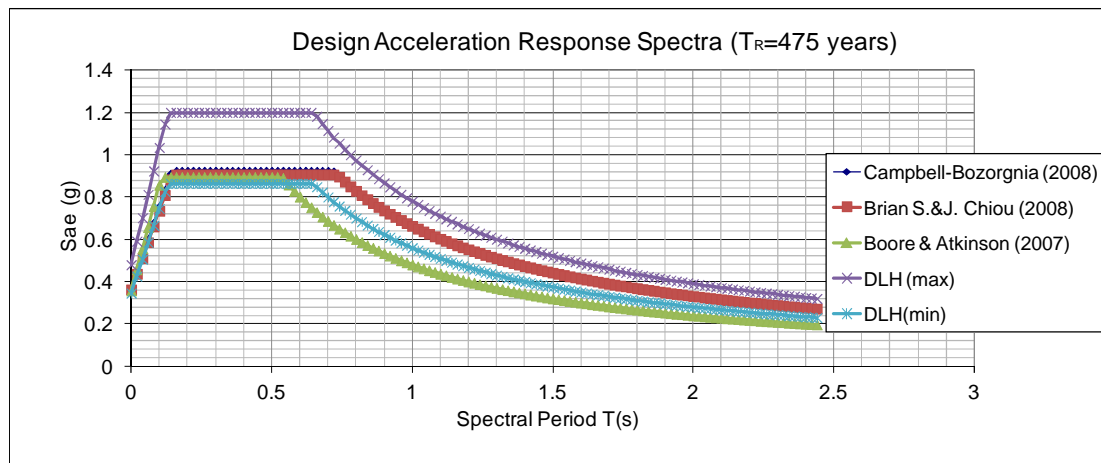


Figure 4.12 The design spectra of site 2h (Return period  $T=475$  years).

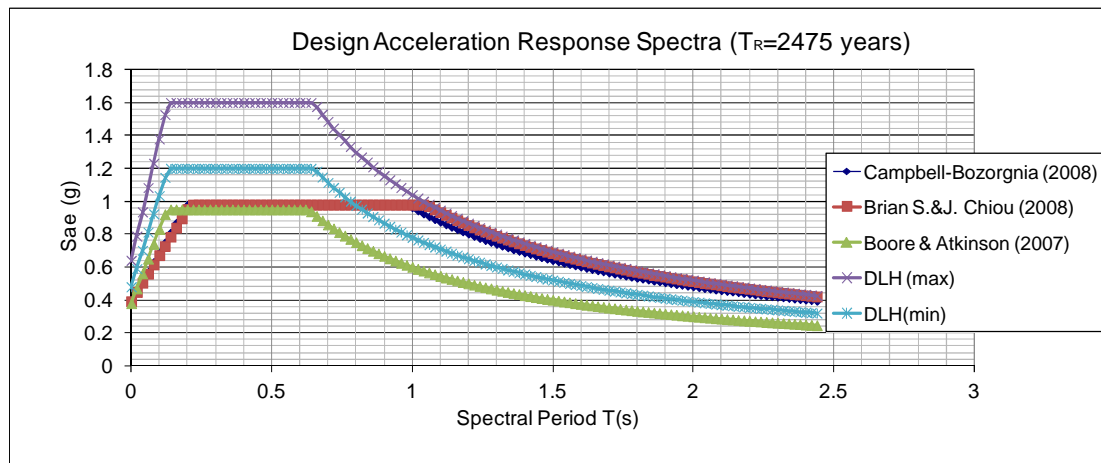


Figure 4.13 The design spectra of site 2h (Return period  $T=2475$  years).

#### 4.5 Discussion of the Results

As we only use earthquakes with the magnitude greater than 4 in our calculations, the earthquake magnitude scales differs slightly from each other. For this reason magnitude conversion relationships obtained in this thesis have small effect on the results of probabilistic analysis.

The most important step of probabilistic analysis is the use of attenuation relations. All three attenuation relationships used in this thesis, use some common parameters such as source zone characterization (strike slip, normal, reverse) and distance from source to site. However, there are other parameters that are unique for

each attenuation relationship. These parameters are the depth of 2.5 km/s shear-wave velocity horizon ( $Z_{2.5}$ ) and the depth of 1.0 km/s shear-wave velocity horizon ( $Z_{1.0}$ ). These two parameters have a significant effect on the results. The first parameter ( $Z_{2.5}$ ) is used in the relationship postulated by Campbell & Bozorgnia (2008). The effect of this parameter can be seen when the spectral period is 1s. The acceleration values of sites near the coastline of Izmir, where the depth of 2.5 km/s shear-wave velocity horizon is thought to be around 2.32 km, are higher than those located at areas where this depth is about 0.87 km.

The results obtained from the attenuation relationship proposed by Campbell & Bozorgnia (2008) are similar to those of the attenuation relationships suggested by Brian et al. (2008). This can be clearly seen in the maps given in the Appendix E. However, the values calculated using the attenuation relationships of Boore & Atkinson (2007) vary from the values calculated by the other two models. This happens because of the lack of the parameter of depth of 2.5 km/s or 1 km/s in the model.

As it is clearly seen from Figure 4.7, 4.8, 4.9, 4.10, the design spectra of sites 1 and 2 are almost the same. If we compare our values with the values DLH (2008), we see that our values are almost the averages of the values of DLH (2008) for the Return period of 475 years. On the other hand, when return period is 2475 years the values taken from DLH (2008) are larger than our values.

Finally, the period range of constant acceleration plateau is significant especially for high rise buildings as their natural period is high. According to the spectra obtained above, our solutions yield a wider constant acceleration plateau than those of DHL (2008) and DBYBHY (2007). Additionally, the constant acceleration plateau is wider at lowland than at highland. This may happened because of the basin effect. This effect should be taken into consideration especially in alluvial areas. The alluvial soils that have been deposited can trap body waves and make them pass through the alluvium as surface waves. This can generate stronger shaking and longer duration that can be predicted. So the sites near the center of the city such as

Manavkuyu and Mavi ehir seems more critical than those at mountains especially for high rise buildings.

## **CHAPTER FIVE**

### **CONCLUSIONS AND RECOMMANDATIONS**

In the scope of this study, probabilistic seismic hazard maps have been developed for the city of Izmir. This is the first time that a detailed probabilistic analysis, which include information about a range of predicted ground acceleration values in almost every urbanized district of Izmir is performed. About 36 maps are created during the study (Appendix E). These maps are developed using three different New Generation Attenuation (NGA) relationships. The probabilistic analysis is done with the help of Seismic III software. These analyses are done for different return periods and for two main spectral periods such as 1s and 0.2s. With the help of these values, design spectra are readily developed for two specific sites such as Mavişehir and Manavkuyu. All the calculations are done at bed rock level. The lack of information about the seismic zone leads to the need of the creation of some seismic zones which help us to obtain some information about reoccurrence of earthquakes. Using the existing information about the faults near each source zone, we did the characterization (normal, reverse, strike slip) of these zones. Earthquake history is very important for doing some predictions about the occurrence of earthquakes within these zones. In total, 11 source zone are created and they include a major part of the earthquakes occurred in Izmir and its vicinities. The annual recurrence relationships for each zone are obtained.

Three New Generation Attenuation models are used in order to calculate the ground motion for each site of the study area. Since we do not have enough information about the source zone (faults), we did some assumptions. The first assumption is that the depth to the top of the rupture is zero ( $Z_{Top}=0$ ) for each source zone. The second assumption is about the characterization of the zones. As each zone is nearby a fault, it is thought that earthquakes occurred in a zone are caused by the nearby faults. For these reasons we characterized the zone according to the most dominant fault.

One of the important parameters of NGA models is the dip angle. Similar to  $Z_{\text{Tor}}$ , this value is taken as  $90^\circ$  for all zones. Other parameters that affect the results are the depth to 1.0 km/s shear wave velocity horizon ( $Z_1$ ) and the depth to 2.5 km/s ( $Z_{2.5}$ ) shear wave velocity horizon. These two parameters are used in NGA models postulated by Campbell-Bozorgnia (2008) and Brian et al. (2008). From 30 calculation points taken in consideration, 10 of them are located at the highland and the others are located at the coast or lowlands of Izmir.  $Z_{1.0}$  is chosen as 100 m in highlands and 500 m in coast. The effect of these parameters can be seen in Map 1 (Appendix E). The values of ground acceleration are about  $0.16g$  on the coastline and it decreases to  $0.14g$  at the mountains. This effect cannot be seen at short spectral periods such as  $T=0.25$  s, where we have the same value in both lowlands and highlands (Appendix E, Map 4). Since all the points are taken inside or nearby Izmir city, the ground motions at the site where there are not enough points shall not be considered as exact.

The effect of the source zones and faults is obvious. Izmir and Tuzla faults created significant earthquakes in the past, so their effect can be seen at the values of ground acceleration near these zones. In general, the maximum ground acceleration value is especially obtained near the center (Manavkuyu) which is under the threat of both Tuzla and Izmir faults. According to the results, the ground acceleration values obtained by Boore & Atkinson (2007) model gives slightly different (lower) results from other two models. This is thought to happen because of the lack of  $Z_1$  and  $Z_{2.5}$  parameters in this model. The maps obtained from the attenuation relationships developed by Brian et al. (2008) and Campbell & Bozorgnia (2008) seems to be more realistic as they produce similar results.

Using maps provided in this thesis, the design spectra at bed rock level can be obtained. Design spectra for two sites are formed and a comparison is made with the DLH (2008) and Specification for Structures to be Built in Disaster Areas (2007) solutions. DLH (2008) maps are obtained by using only few points around Izmir and DHL gives only a range (min and max) of values for Izmir. According to these values, a minimum and maximum design spectrum is formed. For return period of

475 years, our results seem to be within the range given by DLH (2008). However, when the return period is 2475 years, the values of DLH (2008) are much higher. On the other hand, the spectra suggested by DBYBHY (2007) provide high acceleration values as well. However, the constant acceleration plateaus of both spectra suggested by these two organizations are narrower than some of constant acceleration plateaus of our spectra. This may be related to the difference in relationships, methods and especially in the model expressing distribution of probability with time. Plateau is important especially for high rise building because these building have long natural period. The data used in the analysis are very important as well. In our analyses, we used all the earthquakes until the year of 2012. On the other hand, the maps taken from DLH (2008) are created in the year of 2008. Even though only few earthquakes occurred in Izmir after 2008, this may cause some differences in the results.

One shall notice that when the depth to bedrock increases, the constant acceleration plateau of the design spectrum widens. This fact is observed in NGA models suggested by Brian et al. (2008) and Campbell & Bozorgnia (2008) and it may be attributed to the basin effect where earthquake waves can be trapped and magnified in deep alluvial sites where the bedrock is at large distance to ground surface. Influence of  $Z_{1.0}$  and  $Z_{2.5}$  may be quite significant at sites where saturated deep alluvial with large fundamental exists since such soils are expected to amplify high period harmonics of the ground motion at the bedrock level. This fact shall be investigated in detail (2D or 3D numerical simulation, etc) by future researchers who are expected to clarify several fault parameters as well.

## REFERENCES

- Afet ve Acil durum yönetimi başkanlığı [AFAD]. (2009). Depremler. *Afet ve Acil durum yönetimi başkanlığı dairesi başkanlığı (AFAD)*. Retrieved 2012, <http://www.deprem.gov.tr/sarbis/Veritabani/DDA.aspx?param=3>.
- Aktuğ, B., & Kılıçoğlu, A. (2006), Recent crustal deformation of Izmir, Western Anatolia and surrounding regions as deduced from repeated GPS measurements and strain field. *Journal of Geodynamics, Geodesy Department, General Command of Mapping*.
- Bender, B. (1987). A computer program for seismic hazard estimation. *U.S Geological Survey for seismic hazard estimation Bulletin 1772*.
- Boore, D. M., & Atkinson, G. M. (2007). Boore-Atkinson NGA ground motion relations for the geometric mean horizontal component of peak and spectral ground motion parameters. *PEER Report 2007/01*. Berkeley, Calif.: Pacific Earthquake Engineering Research Center, University of California.
- Bozkurt, E., Sözbilir, H. (2004). Tectonic Evolution of the Gediz Graben: Field Evidence for an Episodic, two-stage extension in Western Turkey. *Geological Magazine, 141*, 63-79.
- Brian, S., Chiou, J., & Youngs, R. (2008). NGA Model for Average Horizontal Component of Peak Ground Motion and Response Spectra. *Peer Report 2008/09 Pacific Engineering Research Center College of Engineering University of California, Berkeley*.
- Campbell, K.W.,& Bozorgnia,Y. (2008). Campbell-Bozorgnia NGA Ground Motion Relations for the Geometric Mean Horizontal Component of Peak and Spectral Ground Motion Parameters. *Pacific Earthquake Engineering Research Center College of Engineering University of California*. Berkeley.

Code of Federal Regulations. (1978). Title 10, Energy; Part 100 [10 CFR] Reactor Site Criteria; Appendix A, Seismic and geologic siting criteria for nuclear power plants. *Nuclear Regulatory Commission*, Washington, D.C.

Cosmos Virtual Data Base (Cosmos). *Earthquakes within each Region*. Retrieved January , 2012, from <http://db.cosmos-eq.org/scripts/earthquakes.plx#TURK>.

DBYBHY (2007). Deprem Bölgelerinde Yapılacak Binalar Hakkında Yönetmelik, *T.C. Bayındırılık ve İskan Bakanlığı*, Ankara.

Demiryollar Limanlar Ve Hava Meydanları İnşaat Müdürlüğü (DLH). (2008). Kıyı ve Liman Yapıları, Demiryolları, Hava meydanları İnşaatlarına İlişkin Deprem Teknik Yönetmeliği. *Ulaştırma Bakanlığı*, Türkiye.

Emre, T., Sözbilir, H. (2007). Tectonic Evolution of Kiraz Basin, Küçük Menderes Graben: Evidence of Compression/Uplift Related Basin Formation Overprinted by Extension Tectonics in West Anatolia. *Turkish Journal of Earth Sciences*, 16 (4), 441-470.

Emre, Ö. ve Barka, A. (2000). Gediz Grabeni - Ege Denizi Arasının (İzmir Yöresi) Aktif Fayları. *Bati Anadolu'nun Depremseliği Sempozyumu (BADSEM)*, İzmir, Bildiriler Kitabı, ISBN: 975-585-148-8, 131-132.

Gutenberg, B., & Richter, C. F. (1954). Seismicity of the earth and associated phenomena. *Princeton, N.J., Princeton University Press, 1954*.

Kayalar, A.Ş. (1991). Eski Gediz Deltası ve Melez Çayı kıyı sedimanlarının oturma özellikleri ve bu sedimanların üzerindeki yapılarda görülen oturma problemleri. *İnşaat Mühendisliğinde Zemin Sempozyumu, İzmir, İMO İzmir Şubesi, Bildiriler Kitabı*, 115-131.

- Kayan, İ. (2000). İzmir çevresinin morfotektonik birimleri ve alüvyal jeomorfolojisi. *Batı Anadolu'nun Depremselligi Sempozyumu (BADSEM), İzmir, Bildiriler Kitabı*, 103-111.
- Kramer, S. L. (1996). Geotechnical Earthquake Engineering, *Prentice Hall, ISBN: 0-13-374943-6*.
- Özden, G., et al. (2011). İzmir Metropolü ile Aliağa ve Menemen İlçelerinde Güvenli Yapı Tasarımı için. *TC Başbakanlık Afet ve Acil Durum Yönetimi, Tübitak Kamag 106G159, İş Paketi No.4 Sonuç Raporu*.
- Özden, G. (2000). Marjinal Zeminlerde Temel Problemleri. *ESBAŞ Sempozyumu, İzmir, Bildiriler Kitabı*, 1-16.
- RADIUS (1999). İzmir Deprem Senaryosu ve Deprem Master Planı. *Final Raporu, Boğaziçi Üniversitesi, İstanbul*. Retrieved Mars 25, 2012, From <http://www.izmir.bel.tr/izmirdeprem/izmirrapor.htm>.
- Sözbilir, H., Uzel, B., Sümer, Ö., İnci, U., Ersoy, E., Koçer, T., Demirtaş, R., Özkaraymak, Ç. (2008). D-B uzanımlı İzmir Fayı ile KD-uzanımlı Seferihisar Fayı'nın birlikte çalışlığına dair veriler: İzmir Körfezi'ni oluşturan Aktif Faylarda Kinematik ve Paleosismolojik Çalışmalar, Batı Anadolu. *Türkiye Jeoloji Bülteni*, 52 (2), 91-114.
- Sözbilir, H. (2001). Extensional Tectonics and the Geometry of Related Macroscopic Structures: Field Evidence from the Gediz Detachment, Western Turkey. *Turkish Journal of Earth Sciences*, 10 (2), 51-67.
- U.S. Geological Survey (USGS).1989. *Turkey Earthquake information*, Retrieved 2012, From <http://www.usgs.gov/>.

## APPENDICES

## **APPENDIX A**

The earthquakes occurred in zmir and its  
vicinities from 1900 to 2012

A.1 The earthquakes occurred in İzmir and its vicinities from 1900 to 2012 (AFAD,2009)

Date	Time	Latitude	Longitude	Author	Mtype1	Mag1	Country	City	District
10.02.1900 00:00	05:00	37,88	27,75	(Ambraseys)	MS	4	TURKIYE	AYDIN	INCIRLOVA
22.05.1900 00:00	21:00	38,3	27,65	(Ambraseys)	MS	4,1	TURKIYE	IZMIR	BAYINDIR
16.07.1900 00:00	06:00	39,34	26,65	(Ambraseys)	MS	4,5	TURKIYE		
29.10.1900 00:00	24:00:00	38,05	27,55	(Ambraseys)	MS	4,8	TURKIYE	IZMIR	TIRE
30.12.1900 00:00	19:00	37,95	27,41	(Ambraseys)	MS	4,2	TURKIYE	IZMIR	SELÇUK
23.02.1901 00:00	00:00	37,86	27,69	(Ambraseys)	MS	4	TURKIYE	AYDIN	INCIRLOVA
10.07.1901 00:00	03:45	38,4	26,65	(Ambraseys)	MS	5	TURKIYE		
18.12.1901 00:00	03:51	39,4	26,7	(Ambraseys)	MS	5,9	TURKIYE		
10.01.1902 00:00	18:50	38,41	27,51	(Ambraseys)	MS	4,7	TURKIYE	IZMIR	KEMALPASA
29.05.1902 00:00	00:00	38,37	27,68	(Ambraseys)	MS	4	TURKIYE	IZMIR	KEMALPASA
23.11.1902 00:00	20:14	38,28	27,2	(Ambraseys)	MS	5,5	TURKIYE	IZMIR	MENDERES
13.01.1903 00:00	23:00	38,45	28,2	(Ambraseys)	MS	4,8	TURKIYE	MANISA	SALIHLI
08.02.1903 00:00	21:40	38,48	27,43	(Ambraseys)	MS	4,4	TURKIYE	IZMIR	KEMALPASA
02.04.1903 00:00	00:00	38,62	27,3	(Ambraseys)	MS	4,5	TURKIYE	MANISA	MERKEZ
24.09.1903 00:00	02:25	38,49	27,15	(Ambraseys)	MS	4,6	TURKIYE	IZMIR	BORNOVA
19.05.1904 00:00	20:27	38,25	27,74	(Ambraseys)	MS	4	TURKIYE	IZMIR	BAYINDIR
19.05.1904 00:00	22:20	38,25	27,74	(Ambraseys)	MS	4,5	TURKIYE	IZMIR	BAYINDIR
15.08.1904 00:00	12:30	38,1	27,1	(Ambraseys)	MS	4,6	TURKIYE	IZMIR	MENDERES
15.12.1904 00:00	00:10	38,4	27,75	(Ambraseys)	MS	4,5	TURKIYE	MANISA	TURGUTLU
15.04.1907 00:00	00:30	38,25	27,47	(Ambraseys)	MS	4,6	TURKIYE	IZMIR	TORBALI
21.06.1907 00:00	22:47	38,45	27,6	(Ambraseys)	MS	4,7	TURKIYE	MANISA	TURGUTLU
22.06.1907 00:00	16:00	38,6	27,9	(Ambraseys)	MS	4,5	TURKIYE	MANISA	AHMETLI
20.12.1907 00:00	00:00	39,15	27	(Ambraseys)	MS	4,3	TURKIYE	IZMIR	DIKILI
04.02.1908 00:00	00:00	38,87	27,36	(Ambraseys)	MS	4,7	TURKIYE	MANISA	MERKEZ
16.02.1908 00:00	21:57	38,08	27,41	(Ambraseys)	MS	4	TURKIYE	IZMIR	TORBALI
08.03.1908 00:00	20:00	37,88	28,09	(Ambraseys)	MS	4,4	TURKIYE	AYDIN	KÖSK
08.04.1908 00:00	03:00	38,14	27,43	(Ambraseys)	MS	4,3	TURKIYE	IZMIR	TORBALI
28.04.1908 00:00	17:17	38,1	27,78	(Ambraseys)	MS	4,8	TURKIYE	IZMIR	TIRE
23.06.1908 00:00	14:15	38,75	26,65	(Ambraseys)	MS	5,1	TURKIYE		
23.06.1908 00:00	14:42	38,75	26,65	(Ambraseys)	MS	5	TURKIYE		
23.06.1908 00:00	16:03	38,75	26,65	(Ambraseys)	MS	5	TURKIYE		
25.06.1908 00:00	11:32	38,75	26,65	(Ambraseys)	MS	4,6	TURKIYE		
03.07.1908 00:00	01:42	38,25	28	(Ambraseys)	MS	4,5	TURKIYE	IZMIR	ÖDEMIS
19.01.1909 00:00	04:56	38,66	26,94	(Ambraseys)	MS	5,8	TURKIYE	IZMIR	FOÇA
16.02.1909 00:00	02:55	38,6	27,05	(Ambraseys)	MS	4,8	TURKIYE	IZMIR	MENEMEN
22.01.1910 00:00	16:00	38,77	27,17	(Ambraseys)	MS	4,1	TURKIYE	MANISA	MERKEZ
14.07.1910 00:00	02:35	38,86	27,84	(Ambraseys)	MS	4,4	TURKIYE	MANISA	AKHISAR
27.07.1910 00:00	14:51	38,88	27,87	(Ambraseys)	MS	4,9	TURKIYE	MANISA	AKHISAR
17.03.1912 00:00	23:30	38,3	27,48	(Ambraseys)	MS	4,8	TURKIYE	IZMIR	KEMALPASA
02.02.1913 00:00	06:30	38,79	27,87	(Ambraseys)	MS	4,6	TURKIYE	MANISA	AKHISAR
07.01.1915 00:00	07:19	38,3	26,65	(Ambraseys)	MS	4,3	TURKIYE	IZMIR	URLA
18.01.1915 00:00	00:03	38,3	26,65	(Ambraseys)	MS	4	TURKIYE	IZMIR	URLA
08.08.1917 00:00	03:41:10	39	27	(ALSAN)	MS	4,5	TURKIYE	IZMIR	DIKILI
18.11.1919 00:00	21:54:50	39,26	26,71	(ALSAN)	MS	7	TURKIYE		
28.09.1920 00:00	15:17:37	37,89	28,35	(ALSAN)	MS	5,7	TURKIYE	AYDIN	NAZILLI
27.11.1920 00:00	16:26:20	39,3	26,5	(ALSAN)	MS	4,9	YUNANISTAN		
24.07.1921 00:00	19:20:00	38,8	26,5	(ALSAN)	MS	5,2	TURKIYE		
14.04.1924 00:00		39	27,8	(ALSAN)	MS	4,7	TURKIYE	MANISA	AKHISAR
13.01.1926 00:00	01:47:04	38,64	28,11	(ALSAN)	MS	5,8	TURKIYE	MANISA	SALIHLI
13.01.1926 00:00	08:08:44	38,53	28,19	(ALSAN)	MS	5,7	TURKIYE	MANISA	SALIHLI
31.03.1928 00:00	00:29:49	38,18	27,8	(ALSAN)	MS	6,5	TURKIYE	IZMIR	TIRE
31.03.1928 00:00	05:12:24	38,1	27,4	(ALSAN)	MS	5,2	TURKIYE	IZMIR	TORBALI
15.07.1928 00:00	09:33:33	38,05	27,32	(ALSAN)	MS	5,5	TURKIYE	IZMIR	TORBALI
12.07.1931 00:00	22:24:20	39,15	26,34	(ALSAN)	MS	5,2	YUNANISTA	M?D?LL? ADASI	
16.06.1932 00:00	12:09:25	39,3	27,38	(ALSAN)	MS	4,8	TURKIYE	IZMIR	BERGAMA
23.05.1937 00:00	10:57:30	38,69	27,78	(ALSAN)	MS	5,4	TURKIYE	MANISA	SARUHANLI
02.01.1939 00:00	04:35:22	38,5	27	(ALSAN)	MS	5,3	TURKIYE	IZMIR	ÇIGLI
22.09.1939 00:00	00:36:37	39,07	26,94	(ALSAN)	MS	6,6	TURKIYE	IZMIR	DIKILI
09.01.1941 00:00	18:13:34	38,03	27,4	(ALSAN)	MS	5,2	TURKIYE	IZMIR	SELÇUK
05.02.1941 00:00	01:15:59	38,84	27,74	(ALSAN)	MS	5,4	TURKIYE	MANISA	AKHISAR

## A.1 (Continue)

23.06.1941 00:00	08:00:38	37,95	27,81	(ALSAN)	MS	4,9	TURKIYE	AYDIN	MERKEZ
12.08.1941 00:00	20:38:46	39,13	27,64	(ALSAN)	MS	4,8	TURKIYE	MANISA	KIRKAGAÇ
12.08.1941 00:00	21:52:46	39,1	27,7	(ALSAN)	MS	4,8	TURKIYE	MANISA	KIRKAGAÇ
28.10.1942 00:00	00:31:52	39,27	28,19	(ALSAN)	MS	5,4	TURKIYE	BALIKES	SINDIRGI
28.10.1942 00:00	02:22:53	39,1	27,8	(ALSAN)	MS	6	TURKIYE	MANISA	KIRKAGAÇ
07.10.1944 00:00	21:34:25	39,22	26,58	(ALSAN)	MS	5,2	YUNANISTAN		
04.01.1949 00:00	20:30	38,9	27,9	(ALSAN)	MS	4,5	TURKIYE	MANISA	AKHISAR
21.05.1949 00:00	17:41:12	38,6	26,3	(ALSAN)	MS	4,8	TURKIYE		
23.07.1949 00:00	15:03:33	38,57	26,29	(ALSAN)	MS	6,6	TURKIYE		
30.07.1949 00:00	17:47:13	38,62	26,45	(ALSAN)	MS	4,8	TURKIYE	IZMIR	KARABURUN
23.11.1949 00:00	16:51:05	38,75	26,36	(ALSAN)	MS	5,2	TURKIYE		
03.05.1950 00:00	07:13:48	38,67	27,06	(ALSAN)	MS	4,9	TURKIYE	IZMIR	MENEMEN
26.01.1952 00:00	02:50	39,1	26,9	(ALSAN)	MS	4,6	TURKIYE	IZMIR	DIKILI
13.04.1953 00:00	23:15:18	38	27	(ALSAN)	MS	4,7	TURKIYE		
01.05.1953 00:00	20:06:45	38,41	26,75	(ALSAN)	MS	4,9	TURKIYE		
02.05.1953 00:00	05:41:56	38,48	26,67	(ALSAN)	MS	5	TURKIYE		
02.05.1953 00:00	10:06:43	38,7	26,5	(ALSAN)	MS	4,7	TURKIYE		
02.05.1953 00:00	18:37:44	38,51	26,55	(ALSAN)	MS	5,1	TURKIYE	IZMIR	KARABURUN
14.05.1953 00:00	13:00:24	38,7	26,5	(ALSAN)	MS	4,8	TURKIYE		
09.06.1953 00:00	16:28:25	39,34	28,21	(ALSAN)	MS	4,6	TURKIYE	BALIKES	SINDIRGI
22.07.1953 00:00	15:09:38	39,24	28,43	(ALSAN)	MS	5,2	TURKIYE	BALIKES	SINDIRGI
20.11.1956 00:00	23:21:01	39,36	26,4	(ALSAN)	MS	5,4	YUNANISTA	M'D?LL?	ADASI
11.10.1957 00:00	07:33:05	39,32	28,19	(ALSAN)	MS	4,9	TURKIYE	BALIKES	SINDIRGI
03.09.1958 00:00	02:58:38	38,27	28,19	(ALSAN)	MS	4,6	TURKIYE	IZMIR	KIRAZ
19.11.1959 00:00	14:00:32	38,89	26,65	(ALSAN)	MS	5,3	TURKIYE		
28.04.1963 00:00	00:41:52	39,32	27,82	(ALSAN)	MS	4,7	TURKIYE	BALIKES	SAVASTEPE
02.03.1965 00:00	22:00:07,2	38,47	28,33	ISC	mb	5	TURKIYE	MANISA	SALIHLI
03.03.1965 00:00	01:37:18,3	38,27	28,47	ISC	mb	4,5	TURKIYE	MANISA	ALASEHIR
17.03.1965 00:00	14:05:01,0	38,1	28,1	ISC	mb	4,4	TURKIYE	IZMIR	ÖDEMIS
07.04.1965 00:00	23:33:46,0	38,1	27,7	ISC	mb	4,3	TURKIYE	IZMIR	TIRE
19.09.1965 00:00	14:03:30,6	38,9	27,95	ISC	mb	4,3	TURKIYE	MANISA	AKHISAR
30.09.1965 00:00	19:36:41,0	38,8	28	BCIS	MS?	4,3	TURKIYE	MANISA	AKHISAR
18.10.1965 00:00	14:32:48,3	38,83	27,83	ISC	mb	4	TURKIYE	MANISA	AKHISAR
22.05.1966 00:00	07:37:29,0	38,7	27,92	ISC	mb	4,4	TURKIYE	MANISA	GÖLMARMARA
02.06.1966 00:00	22:51:28,0	38,5	27,23	ISC	mb	4,5	TURKIYE	IZMIR	BORNOVA
19.06.1966 00:00	17:55:30,0	38,55	27,35	ISC	mb	4,6	TURKIYE	IZMIR	BORNOVA
28.06.1966 00:00	17:01:04,0	39	27	ISC	MS?	4,3	TURKIYE	IZMIR	DIKILI
19.07.1966 00:00	02:33:23,0	38,4	27	ISC	mb	4,3	TURKIYE	IZMIR	NARLIDERE
19.02.1968 00:00	23:17:07,0	38,7	27,9	LAO	MS?	4,5	TURKIYE	MANISA	GÖLMARMARA
19.02.1968 00:00	23:19:34,0	38,7	27,9	LAO	MS?	4,3	TURKIYE	MANISA	GÖLMARMARA
20.02.1968 00:00	05:16:58,0	38,4	27,2	LAO	MS?	4,1	TURKIYE	IZMIR	BORNOVA
21.02.1968 00:00	20:41:42,0	38,7	26,5	LAO	MS?	4,1	TURKIYE		
22.02.1968 00:00	11:00:05,0	38,7	26,5	LAO	MS?	4	TURKIYE		
21.03.1968 00:00	09:42:51,0	38,8	27,6	ISC	mb	4,4	TURKIYE	MANISA	SARUHANLI
28.08.1968 00:00	06:02:44,0	38,6	26,4	ISC	mb	4,1	TURKIYE	IZMIR	KARABURUN
17.02.1969 00:00	22:49:04,0	38,9	27,6	ISC	MS?	4	TURKIYE	MANISA	AKHISAR
23.03.1969 00:00	00:15:45,0	39,17	28,32	ISC	mb	4,4	TURKIYE	BALIKES	SINDIRGI
23.03.1969 00:00	03:50:58,0	39,3	28	ISC	mb	4,6	TURKIYE	BALIKES	SINDIRGI
23.03.1969 00:00	21:11:25,0	37,9	27,6	LAO	MS?	5	TURKIYE	AYDIN	GERMENCIK
24.03.1969 00:00	08:13:05,4	39,02	28,41	ISC	mb	4,7	TURKIYE	MANISA	GÖRDES
25.03.1969 00:00	10:05:27,7	38,75	27,81	ISC	mb	4,3	TURKIYE	MANISA	SARUHANLI
25.03.1969 00:00	13:21:12,0	39,06	28,41	ISC	mb	4,9	TURKIYE	MANISA	GÖRDES
25.03.1969 00:00	13:21:34,2	39,25	28,44	ISC	mb	5,5	TURKIYE	BALIKES	SINDIRGI
25.03.1969 00:00	13:37:53,0	39	28	ISC	mb	5	TURKIYE	MANISA	AKHISAR
25.03.1969 00:00	16:13:30,4	39,08	28,44	ISC	mb	4,7	TURKIYE	MANISA	GÖRDES
25.03.1969 00:00	17:51:24,0	39,16	28	ISC	mb	4,4	TURKIYE	MANISA	AKHISAR
26.03.1969 00:00	03:31:26,5	39,03	28,27	ISC	mb	4,6	TURKIYE	MANISA	GÖRDES
26.03.1969 00:00	09:00:11,0	39,3	28,1	ISC	mb	4,7	TURKIYE	BALIKES	SINDIRGI
26.03.1969 00:00	13:50:41,0	39,3	28,2	ISC	mb	4,3	TURKIYE	BALIKES	SINDIRGI
27.03.1969 00:00	18:07:03,0	39,12	28,2	ISC	mb	4,5	TURKIYE	BALIKES	SINDIRGI
28.03.1969 00:00	01:48:29,5	38,55	28,46	ISC	mb	5,9	TURKIYE	MANISA	ALASEHIR

## A.1 (Continue)

28.03.1969 00:00	10:02:17.4	39,13	28,45	ISC	mb	4,9	TURKIYE	BALIKES	SINDIRGI
06.04.1969 00:00	03:49:33.9	38,47	26,41	ISC	mb	5,6	TURKIYE	IZMIR	KARABURUN
06.04.1969 00:00	12:50:29.0	38,33	26,5	ISC	mb	4,3	TURKIYE	IZMIR	URLA
12.04.1969 00:00	15:33:06.0	39,33	28,1	ISC	mb	4,3	TURKIYE	BALIKES	SINDIRGI
20.04.1969 00:00	04:59:29.0	39,2	28	ISC	mb	4,1	TURKIYE	MANISA	AKHISAR
30.04.1969 00:00	23:08:11.0	39,09	28,31	ISC	mb	4,6	TURKIYE	BALIKES	SINDIRGI
01.05.1969 00:00	01:14:46.0	39,1	28	ISC	MS?	4,1	TURKIYE	MANISA	AKHISAR
06.05.1969 00:00	06:36:06.0	39,3	28,1	ISC	MS?	4	TURKIYE	BALIKES	SINDIRGI
07.10.1969 00:00	05:09:12.0	39,2	28,4	ISC	mb	4,9	TURKIYE	BALIKES	SINDIRGI
13.10.1969 00:00	03:24:26.0	39,17	28,38	ISC	mb	4,9	TURKIYE	BALIKES	SINDIRGI
23.10.1969 00:00	13:37:15.0	38,2	27,6	ISC	MS?	4	TURKIYE	IZMIR	BAYINDIR
24.10.1969 00:00	23:00:46.0	38,4	27,6	ISC	MS?	4	TURKIYE	IZMIR	KEMALPASA
20.01.1970 00:00	01:41:56.0	38,7	26,7	ISC	mb	4,7	TURKIYE		
09.03.1970 00:00	17:28:17.3	38,43	27,27	ISC	mb	4,2	TURKIYE	IZMIR	BORNOVA
23.03.1970 00:00	07:56:08.0	39,2	28,2	ISC	mb	4,1	TURKIYE	BALIKES	SINDIRGI
29.03.1970 00:00	14:37:19.6	38,74	27,83	ISC	mb	4,5	TURKIYE	MANISA	SARUHANLI
29.03.1970 00:00	14:40:26.6	38,73	28	ISC	mb	4,5	TURKIYE	MANISA	GÖLMARMARA
07.04.1970 00:00	10:55:02.0	39	27,8	ISC	mb	4,2	TURKIYE	MANISA	AKHISAR
09.04.1970 00:00	09:23:16.0	39,4	27,9	ISC	mb	4,7	TURKIYE	BALIKES	MERKEZ
13.04.1970 00:00	05:58:15.0	39,4	28	ISC	mb	4,2	TURKIYE	BALIKES	BIGADIÇ
06.05.1970 00:00	03:14:29.0	38,16	26,8	ISC	mb	4,8	TURKIYE		
17.05.1970 00:00	04:33:47.4	38,13	28,1	ISC	mb	4	TURKIYE	IZMIR	ÖDEMIS
25.02.1971 00:00						4			
31.05.1971 00:00	14:56:53.9	38,2374	28,1866	ISC	MS?	4,1	TURKIYE	IZMIR	KIRAZ
06.10.1971 00:00	23:16:04.7	38,0595	27,267	ISC	MS?	4,4	TURKIYE	IZMIR	MENDERES
02.12.1971 00:00	09:40:58.4	39,2336	26,4494	ISC	mb	4,5	YUNANISTA	M?D?LL?	ADASI
03.09.1972 00:00	08:38:46.3	39,1624	27,9848	ISC	mb	4,6	TURKIYE	MANISA	AKHISAR
08.04.1973 00:00	09:52:47.4	39,1658	28,3922	ISC	ML	4,2	TURKIYE	BALIKES	SINDIRGI
19.04.1973 00:00	22:13:54.5	38,2877	26,9419	ISC	mb	4,4	TURKIYE	IZMIR	GÜZELBAHÇE
21.04.1973 00:00	02:05:16.6	38,4314	26,9192	ISC	ML	4	TURKIYE		
01.02.1974 00:00	00:01:02.1	38,5522	27,2172	ISC	mb	5,2	TURKIYE	IZMIR	BORNOVA
14.02.1974 00:00	09:17:14.1	38,5356	27,1865	ISC	MS?	4,5	TURKIYE	IZMIR	BORNOVA
25.11.1974 00:00	23:54:38.6	38,9632	27,8468	ISC	ML	4	TURKIYE	MANISA	AKHISAR
26.01.1975 00:00	12:36:44.6	39,2851	26,4549	ISC	ML	4,2	YUNANISTAN		
07.02.1975 00:00	03:21:13.2	38,7524	28,3495	ISC	ML	4,1	TURKIYE	MANISA	KÖPRÜBASI
30.05.1975 00:00	05:13:44.8	39,119	27,675	ISC	ML	4	TURKIYE	MANISA	KIRKAGAÇ
30.05.1975 00:00	14:22:42.1	38,7458	27,5985	ISC	ML	4,2	TURKIYE	MANISA	SARUHANLI
04.09.1975 00:00	04:55:16.2	38,1344	27,2464	ISC	ML	4	TURKIYE	IZMIR	MENDERES
15.09.1975 00:00	18:40:25.2	38,3954	27,4019	ISC	mb	4,3	TURKIYE	IZMIR	KEMALPASA
25.02.1976 00:00	00:36:41.8	38,8652	26,3999	ISC	Md	4	YUNANISTAN		
03.09.1976 00:00	20:53:26.9	39,2108	28,1608	ISC	ML	4,5	TURKIYE	BALIKES	SINDIRGI
03.10.1976 00:00	00:53:48.1	38,2375	26,6958	ISC	ML	4	TURKIYE	IZMIR	URLA
04.10.1976 00:00	05:22:16.9	38,3753	26,9218	ISC	ML	4	TURKIYE	IZMIR	GÜZELBAHÇE
21.10.1976 00:00	01:45:24.7	38,6418	26,547	ISC	Md	4,1	TURKIYE		
12.11.1976 00:00	09:51:11.2	38,5418	26,7423	ISC	mb	4,6	TURKIYE		
12.11.1976 00:00	09:55:32.9	38,4738	26,715	ISC	mb	4,9	TURKIYE		
13.11.1976 00:00	11:54:48.3	38,6249	26,6964	ISC	mb	4,5	TURKIYE		
17.11.1976 00:00	00:48:33.9	38,5167	26,7797	ISC	ML	4	TURKIYE		
21.11.1976 00:00	23:10:35.4	38,4436	26,7845	ISC	mb	4,2	TURKIYE		
24.02.1977 00:00	20:47:18.1	38,5544	27,661	ISC	mb	5	TURKIYE	MANISA	TURGUTLU
13.03.1977 00:00	20:42:22.9	39,1563	26,2668	ISC	Md	4,1	YUNANISTA	M?D?LL?	ADASI
27.10.1977 00:00	22:43:32.2	37,8712	27,8827	ISC	mb	4,7	TURKIYE	AYDIN	MERKEZ
28.10.1977 00:00	00:31:52.9	38,0049	28,0308	ISC	Md	4,2	TURKIYE	IZMIR	ÖDEMIS
28.10.1977 00:00	00:41:10.5	37,9685	28,0062	ISC	Md	4,3	TURKIYE	AYDIN	KÖSK
10.11.1977 00:00	04:12:22.9	37,9418	27,9277	ISC	mb	4	TURKIYE	AYDIN	MERKEZ
23.11.1977 00:00	09:08:16.5	37,9185	27,923	ISC	ML	4	TURKIYE	AYDIN	MERKEZ
26.11.1977 00:00	00:12:09.5	37,937	27,9886	ISC	ML	4,3	TURKIYE	AYDIN	MERKEZ
09.12.1977 00:00	15:53:37.9	38,3512	27,2254	ISC	mb	4,8	TURKIYE	IZMIR	BUÇA
09.12.1977 00:00	21:32:10.7	39,363	27,9904	ISC	Md	4,2	TURKIYE	BALIKES	BIGADIÇ
16.12.1977 00:00	07:37:29.3	38,414	27,1882	ISC	mb	5,3	TURKIYE	IZMIR	BORNOVA
16.12.1977 00:00	07:40:46.1	38,5371	28,462	ISC	Md	4,4	TURKIYE	MANISA	ALASEHIR

## A.1 (Continue)

16.12.1977 00:00	07:44:22.1	38,473	27,2801	ISC	Md	4,2	TURKIYE	IZMIR	BORNOVA
19.01.1978 00:00	12:08:17.6	38,9321	27,8959	ISC	ML	4,1	TURKIYE	MANISA	AKHISAR
07.02.1978 00:00	07:34:33.4	38,0168	27,6006	ISC	Md	4	TURKIYE	IZMIR	TIRE
24.02.1978 00:00	18:47:33.8	39,2055	26,392	ISC	Md	4,3	YUNANISTAN		
09.04.1978 00:00	06:53:07.2	38,201	27,0997	ISC	MS	4,6	TURKIYE	IZMIR	MENDERES
10.06.1978 00:00	14:42:45.4	38,9984	27,2359	ISC	Md	4,1	TURKIYE	IZMIR	BERGAMA
14.06.1979 00:00	11:44:45.0	38,7943	26,5731	ISC	MS	5,7	TURKIYE		
15.06.1979 00:00	07:31:24.4	38,7268	26,5257	ISC	mb	4	TURKIYE		
16.06.1979 00:00	18:41:59.4	38,7168	26,6352	ISC	MS	5	TURKIYE		
17.06.1979 00:00	23:08:35.8	38,7203	26,6146	ISC	MS	4,1	TURKIYE		
18.06.1979 00:00	03:25:57.8	38,6814	26,5921	ISC	mb	4,6	TURKIYE		
19.06.1979 00:00	23:09:56.8	38,6428	26,607	ISC	MS	4,4	TURKIYE		
26.06.1979 00:00	22:38:15.4	38,7228	26,6081	ISC	mb	4,6	TURKIYE		
27.06.1979 00:00	10:38:20.6	38,9548	26,7629	ISC	mb	4,6	TURKIYE		
25.04.1980 00:00	17:26:04.7	38,7489	26,5175	ISC	mb	4	TURKIYE		
02.08.1980 00:00	00:52:11.8	38,9287	27,4247	ISC	mb	5,3	TURKIYE	IZMIR	KINIK
07.08.1980 00:00	22:54:09.7	39,3662	28,1221	ISC	Md	4	TURKIYE	BALIKESI	BIGADIC
15.11.1980 00:00	15:21:49.2	39,3239	27,5636	ISC	ML	4,3	ISC	TURKIYE	MANISA
27.11.1980 00:00	15:49:51.3	39,2307	27,7136	ISC	Md	4,1	TURKIYE	MANISA	SOMA
16.12.1980 00:00	17:13:25.2	38,7958	26,6544	ISC	mb	4,6	TURKIYE		
19.12.1980 00:00	07:49:21.5	38,0199	27,6483	ISC	mb	4,7	TURKIYE	IZMIR	TIRE
09.07.1981 00:00	18:24:32.8	38,9825	27,906	ISC	ML	5	ISC	TURKIYE	MANISA
17.09.1982 00:00	06:03:02.4	37,9023	26,8491	ISC	Md	4	YUNANISTAN		
02.11.1982 00:00	05:58:48.2	38,5192	28,461	ISC	mb	4,6	TURKIYE	MANISA	ALASEHIR
26.12.1982 00:00	17:48:01.0	39,3247	28,2618	ISC	mb	4,9	TURKIYE	BALIKESI	SINDIRGI
27.12.1982 00:00	02:04:47.6	38,9609	27,9116	ISC	ML	4,2	TURKIYE	MANISA	AKHISAR
27.12.1982 00:00	11:02:44.3	39,3389	28,2675	ISC	mb	4,8	TURKIYE	BALIKESI	SINDIRGI
27.12.1982 00:00	15:32:05.9	38,9542	27,8235	ISC	ML	4	TURKIYE	MANISA	AKHISAR
06.04.1983 00:00	14:48:05.1	38,1125	27,1623	ISC	ML	4,1	TURKIYE	IZMIR	MENDERES
13.07.1983 00:00	20:09:59.3	38,2061	26,6187	ISC	mb	4,5	TURKIYE	IZMIR	URLA
04.08.1983 00:00	20:39:15.0	37,8417	27,5938	ISC	mb	4,7	TURKIYE	AYDIN	GERMENCIK
03.09.1983 00:00	12:45:23.1	39,1111	27,5704	ISC	ML	4	ISC	TURKIYE	MANISA
23.09.1983 00:00	08:32:54.0	38,8305	27,0718	ISC	Md	4	TURKIYE	IZMIR	ALIAGA
25.02.1984 00:00	22:01:00.8	39,3776	27,8795	ISC	ML	4	TURKIYE	BALIKESI	MERKEZ
01.03.1984 00:00	06:39:32.9	39,254	27,9772	ISC	Md	4	TURKIYE	BALIKESI	SINDIRGI
23.04.1984 00:00	16:50:50.2	37,8337	26,8384	ISC	Md	4	YUNANISTAN		
30.05.1984 00:00	15:00:29.3	38,8538	26,7061	ISC	Md	4,1	TURKIYE		
07.11.1984 00:00	11:39:43.6	38,9127	27,8001	ISC	mb	4	TURKIYE	MANISA	AKHISAR
29.11.1984 00:00	15:28:57.1	37,8797	26,9754	ISC	mb	4,7	YUNANISTAN		
29.03.1985 00:00	09:24:08.4	38,8013	26,5684	ISC	mb	4,8	TURKIYE		
01.05.1985 00:00						4,9			
17.10.1985 00:00	19:15:26.2	38,7714	27,8342	ISC	mb	4,1	TURKIYE	MANISA	SARUHANLI
23.10.1985 00:00	06:14:32.0	38,8017	27,8284	ISC	mb	4,3	TURKIYE	MANISA	AKHISAR
19.12.1985 00:00	09:27:41.4	39,1639	26,2362	ISC	mb	4,1	YUNANISTAN		
20.05.1986 00:00	07:43:35.9	38,3979	26,7239	ISC	Md	4	TURKIYE	IZMIR	URLA
01.06.1986 00:00	06:43:09.8	37,9595	27,3894	ISC	mb	4	TURKIYE	IZMIR	SELÇUK
27.06.1986 00:00	06:54:55.0	37,8519	27,4004	ISC	ML	4,2	NEIC	TURKIYE	IZMIR
18.08.1986 00:00	08:11:31.2	38,5862	27,0994	ISC	mb	4,6	TURKIYE	IZMIR	MENEMEN
23.09.1986 00:00	08:41:25.1	39,0929	27,7526	ISC	Md	4	TURKIYE	MANISA	KIRKAGAC
29.09.1986 00:00	17:38:03.8	39,0738	27,7866	ISC	ML	4,1	TURKIYE	MANISA	KIRKAGAC
30.11.1986 00:00	05:29:18.2	38,7517	27,7444	ISC	mb	4,3	TURKIYE	MANISA	SARUHANLI
29.01.1987 00:00	11:58:07.1	38,817	26,8873	ISC	ML	4	TURKIYE		
25.04.1987 00:00	22:10:59.9	39,2963	27,9151	ISC	mb	4,2	TURKIYE	MANISA	KIRKAGAC
15.09.1987 00:00	16:02:05.3	37,8549	26,955	ISC	mb	4,6	YUNANISTAN		
23.04.1988 00:00	17:54:45.0	39,1	28,1	NAO	mb	4	TURKIYE	MANISA	AKHISAR
04.08.1988 00:00	08:25:17.9	38,8552	26,9991	ISC	mb	4,5	TURKIYE	IZMIR	ALIAGA
26.10.1988 00:00	10:10:27.5	37,9608	27,688	ISC	mb	4,8	TURKIYE	IZMIR	TIRE
16.07.1989 00:00	16:48:23.9	39,1166	26,6014	ISC	mb	4,5	YUNANISTAN		
15.08.1989 00:00	16:08:08.2	39,1829	26,3161	ISC	mb	4,4	YUNANISTAN		
15.08.1989 00:00	17:03:30.4	39,2158	26,2533	ISC	MS	4,5	YUNANISTAN		
23.12.1989 00:00	14:59:02.9	38,2994	26,5375	ISC	mb	4,6	TURKIYE	IZMIR	URLA

## A.1 (Continue)

19.12.1990 00:00	09:46:47.6	38,61	28,01	DDA	Md	4,4	TURKIYE	MANISA	SALIHLİ
29.12.1990 00:00	13:33:58.1	37,852	27,9792	ISC	ML	4,1	TURKIYE	AYDIN	MERKEZ
26.02.1991 00:00	22:30:47.4	38,4844	26,6658	ISC	mb	4,9	TURKIYE		
18.04.1991 00:00	11:56:57.7	39,22	26,51	DDA	Md	4,2	YUNANISTAN		
15.06.1991 00:00	21:33:23.5	38,52	27	DDA	Md	4,2	TURKIYE	IZMIR	MENEMEN
15.06.1991 00:00	22:08:31.6	38,53	27,01	DDA	Md	4,1	TURKIYE	IZMIR	MENEMEN
22.07.1991 00:00	00:49:52.1	39,31	27,91	DDA	Md	4,4	TURKIYE	MANISA	KIRKAGAC
10.11.1991 00:00	19:40:27.2	38,4927	26,7544	ISC	ML	4	TURKIYE		
30.11.1991 00:00	15:57:53.7	39,3284	28,1192	ISC	md	4,2	TURKIYE	BALIKESI	SINDIRGI
04.03.1992 00:00	05:15:22.0	39	28	DDA	Md	4	TURKIYE	MANISA	AKHISAR
25.04.1992 00:00	18:17:25.3	38,6669	26,444	ISC	mb	4,3	TURKIYE	IZMIR	KARABURUN
19.07.1992 00:00	11:51:49.0	38	28	DDA	Md	4	TURKIYE	IZMIR	ODEMIS
06.08.1992 00:00	19:10:14.0	39	27	DDA	Md	4	TURKIYE	IZMIR	DIKILI
06.08.1992 00:00	20:58:49.0	38	28	DDA	Md	4	TURKIYE	IZMIR	ODEMIS
01.09.1992 00:00	22:08:03.0	38	28	DDA	Md	4	TURKIYE	IZMIR	ODEMIS
06.11.1992 00:00	19:08:09.4	38,1091	26,956	ISC	MS	6	TURKIYE	IZMIR	SEFERIHISAR
06.11.1992 00:00	19:13:54.9	38,2019	27,2166	ISC	ML	4,4	TURKIYE	IZMIR	MENDERES
06.11.1992 00:00	19:22:10.6	37,8429	26,7887	ISC	mb	4,1	YUNANISTAN		
06.11.1992 00:00	20:05:59.1	38,0323	27,025	ISC	mb	4,6	TURKIYE		
06.11.1992 00:00	22:03:46.3	38,311	27,1243	ISC	mb	4,6	TURKIYE	IZMIR	GAZIEMIR
07.11.1992 00:00	03:25:45.7	38,1964	27,0098	ISC	mb	4,8	TURKIYE	IZMIR	MENDERES
07.11.1992 00:00	04:36:34.4	38,1323	27,0449	ISC	mb	4,4	TURKIYE	IZMIR	MENDERES
08.11.1992 00:00	14:26:32.3	38,1639	27,0633	ISC	ML	4	TURKIYE	IZMIR	MENDERES
08.11.1992 00:00	18:21:19.6	38,1783	26,8985	ISC	mb	4,2	TURKIYE	IZMIR	SEFERIHISAR
08.11.1992 00:00	19:28:11.2	38,1472	26,9319	ISC	mb	4,7	TURKIYE	IZMIR	SEFERIHISAR
10.11.1992 00:00	15:52:14.5	37,9838	26,924	ISC	ML	4	TURKIYE		
12.11.1992 00:00	15:11:11.0	39	27	DDA	Md	5	TURKIYE	IZMIR	DIKILI
12.11.1992 00:00	15:19:12.4	38,7653	26,5628	ISC	mb	4,3	TURKIYE		
12.11.1992 00:00	17:48:22.3	38,723	26,4847	ISC	mb	4,5	TURKIYE		
05.12.1992 00:00	06:26:16.4	38,0426	26,976	ISC	mb	4,4	TURKIYE		
10.12.1992 00:00	10:17:58.6	38,0442	26,8171	ISC	mb	4,1	TURKIYE		
11.12.1992 00:00	19:12:56.0	38	27	DDA	Md	4	TURKIYE		
19.12.1992 00:00	12:42:51.0	39	27	DDA	Md	4	TURKIYE	IZMIR	DIKILI
29.03.1993 00:00	18:06:33.2	38,9912	26,3453	ISC	mb	4,1	YUNANISTAN		
31.03.1993 00:00	18:20:42.5	39,142	28,0419	ISC	MS	4	TURKIYE	MANISA	AKHISAR
02.06.1993 00:00	10:19:45.5	38,7853	27,5747	ISC	ML	4,3	TURKIYE	MANISA	SARUHANLI
26.07.1993 00:00	08:05:59.6	38,8388	26,9515	ISC	mb	4,2	TURKIYE		
16.10.1993 00:00	21:18:14.8	38,749	26,4705	ISC	ML	4	TURKIYE		
16.10.1993 00:00	21:32:34.3	38,7007	26,4875	ISC	ML	4,2	TURKIYE		
09.01.1994 00:00	12:48:33.4	39,22	26,73	DDA	Md	4,3	TURKIYE		
26.01.1994 00:00	10:07:34.9	39,0941	27,8242	ISC	ML	4,2	TURKIYE	MANISA	KIRKAGAC
28.01.1994 00:00	15:45:25.4	38,6891	27,5004	ISC	MS	5,1	TURKIYE	MANISA	MERKEZ
28.01.1994 00:00	22:59:07.5	38,6864	27,4979	ISC	ML	4	TURKIYE	MANISA	MERKEZ
18.02.1994 00:00	20:58:49.5	38,7013	27,4474	ISC	ML	4	TURKIYE	MANISA	MERKEZ
19.02.1994 00:00	00:20:41.2	38,8904	27,0384	ISC	mb	4	TURKIYE		
24.05.1994 00:00	02:05:35.5	38,6863	26,5335	ISC	MS	5,2	TURKIYE		
24.05.1994 00:00	02:18:33.8	38,7162	26,5892	ISC	MS	5,1	TURKIYE		
24.05.1994 00:00	03:35:33.1	38,7028	26,4568	ISC	MS	4,6	TURKIYE		
24.05.1994 00:00	06:05:54.3	38,6094	26,6346	ISC	mb	4,6	TURKIYE		
12.06.1994 00:00	01:22:33.7	39,01	28,02	DDA	Md	4,1	TURKIYE	MANISA	AKHISAR
09.08.1994 00:00	05:28:18.8	38,51	27,4	DDA	Md	4,7	TURKIYE	IZMIR	KEMALPASA
09.08.1994 00:00	16:59:09.3	38,6406	26,6461	ISC	MS	4,2	TURKIYE		
05.09.1994 00:00	11:25:51.2	39,1013	27,7703	ISC	md	4	TURKIYE	MANISA	KIRKAGAC
07.10.1994 00:00	19:31:35.2	38,7024	26,4105	ISC	mb	4,4	TURKIYE		
09.01.1995 00:00	17:39:53.0	39	27	DDA	Md	4	TURKIYE	IZMIR	DIKILI
12.01.1995 00:00	00:21:32.7	38,62	27,1	DDA	Md	4,3	TURKIYE	IZMIR	MENEMEN
01.02.1995 00:00	19:57:38.0	38	27	DDA	Md	4	TURKIYE		
24.02.1995 00:00	16:14:40.0	39	28	DDA	Md	4	TURKIYE	MANISA	AKHISAR
14.09.1995 00:00	04:41:34.2	39,4009	27,6947	ISC	md	4	TURKIYE	BALIKESI	SAVASTEPE
02.04.1996 00:00	07:59:23.9	37,8411	26,9725	ISC	MS	5	YUNANISTAN		
04.04.1996 00:00	09:27:06.3	37,891	26,8785	ISC	mb	4,1	YUNANISTAN		

## A.1 (Continue)

08.05.1996 00:00	00:20:10.2	37,9102	27,429	ISC	md	4	TURKIYE	IZMIR	SELÇUK
20.05.1996 00:00	09:09:13.3	38,295	27,232	ISC	md	4,1	TURKIYE	IZMIR	BUÇA
30.05.1997 00:00	01:12:21.9	37,8958	27,3093	ISC	md	4	TURKIYE	IZMIR	SELÇUK
07.04.1998 00:00	19:17:47.2	37,9358	27,8608	ISC	md	4	TURKIYE	AYDIN	MERKEZ
09.07.1998 00:00	17:36:47.3	37,8692	26,7908	ISC	MS	4,4	YUNANISTAN		
24.07.1999 00:00	16:05:50.3	39,33	27,95	DDA	Md	4,3	TURKIYE	BALIKESI	SINDIRGI
24.07.1999 00:00	22:31:04.7	39,387	27,739	ISC	ML	4,1	TURKIYE	BALIKESI	SAVASTEPE
25.07.1999 00:00	06:56:54.9	39,3	27,86	DDA	Md	4,3	TURKIYE	MANISA	KIRKAGAÇ
26.09.1999 00:00	06:38:40.8	39,05	27,83	DDA	Md	4,1	TURKIYE	MANISA	AKHISAR
15.02.2000 00:00	18:57:35.1	38,51	26,69	DDA	Md	4	TURKIYE		
23.04.2000 00:00	13:53:34.2	37,98	27,69	DDA	Md	4,4	TURKIYE	IZMIR	TIRE
08.09.2000 00:00	05:46:55.0	39,34	27,61	DDA	Md	4,6	TURKIYE	MANISA	SOMA
09.09.2000 00:00	08:18:49.2	39,35	27,67	DDA	Md	4	TURKIYE	BALIKESI	SAVASTEPE
27.02.2001 00:00	06:14:55.9	39,067	26,726	ISC	mb	4	TURKIYE		
01.03.2001 00:00	13:31:17.5	37,88	26,46	DDA	Md	4,1		EGE DEN?Z?	
24.05.2001 00:00	03:18:10.2	39,3	27,83	DDA	Md	4	TURKIYE	MANISA	KIRKAGAÇ
22.06.2001 00:00	11:54:51.1	39,25	27,8	DDA	Md	4,7	TURKIYE	MANISA	KIRKAGAÇ
22.06.2001 00:00	19:56:21.3	39,295	27,861	ISC	MD	4,1	TURKIYE	MANISA	KIRKAGAÇ
23.06.2001 00:00	12:18:22.2	39,389	27,882	ISC	MS	4	TURKIYE	BALIKESI	MERKEZ
21.01.2002 00:00	14:34:24.2	38,61	27,82	DDA	Md	4,7	TURKIYE	MANISA	AHMETLI
19.05.2002 00:00	10:45:57.4	38,393	26,509	ISC	mb	4,1	TURKIYE	IZMIR	URLA
23.05.2002 00:00	04:48:01.6	38,763	26,5	ISC	mb	4,1	TURKIYE		
16.01.2003 00:00	02:17:54.2	38,2837	27,1711	ISC	ML	4	TURKIYE	IZMIR	MENDERES
10.04.2003 00:00	00:40:15.9	38,2466	26,8895	ISC	MS	5,5	TURKIYE	IZMIR	SEFERIHISAR
10.04.2003 00:00	00:53:46.0	38,25	26,47	DDA	Md	4,1	TURKIYE	IZMIR	ÇESME
10.04.2003 00:00	01:32:19.1	38,2053	26,806	ISC	MD	4	TURKIYE	IZMIR	SEFERIHISAR
17.04.2003 00:00	22:34:26.2	38,1855	26,9492	ISC	MS	4,6	TURKIYE	IZMIR	SEFERIHISAR
15.06.2003 00:00	08:26:40.8	39,16	28,31	DDA	Md	4	TURKIYE	BALIKESI	SINDIRGI
22.06.2003 00:00	23:46:19.7	39,01	27,98	DDA	Md	4,6	TURKIYE	MANISA	AKHISAR
16.12.2003 00:00	10:41:09.3	38,88	26,74	DDA	Md	4,6	TURKIYE		
24.03.2004 00:00	04:38:43.3	38,8572	26,9403	DDA	Md	4,2	TURKIYE		
05.11.2004 00:00	17:30:22.9	39,1694	27,7502	DDA	Md	4,3	TURKIYE	MANISA	KIRKAGAÇ
02.12.2004 00:00	15:51:49.6	39,2545	27,9856	DDA	Md	4,3	TURKIYE	BALIKESI	SINDIRGI
13.01.2005 00:00	11:00:49.5	39,1763	27,772	DDA	Md	4,1	TURKIYE	MANISA	KIRKAGAÇ
13.01.2005 00:00	13:39:04.0	39,1772	27,7817	DDA	Md	4,2	TURKIYE	MANISA	KIRKAGAÇ
20.01.2005 00:00	23:27:35.5	38,6559	27,166	ISC	ML	4	TURKIYE	IZMIR	MENEMEN
29.01.2005 00:00	18:52:25.7	38,0166	26,839	ISC	MS	4	TURKIYE		
24.03.2005 00:00						4,2			
13.05.2005 00:00	22:30:27.8	37,9237	27,0745	ISC	ML	4	TURKIYE		
17.10.2005 00:00	05:45:16.5	38,1012	26,6641	ISC	MS	5,1	TURKIYE		
17.10.2005 00:00	08:28:52.3	38,1638	26,6529	ISC	MS	4,4	TURKIYE		
17.10.2005 00:00	09:46:56.2	38,1889	26,7087	ISC	MS	5,7	TURKIYE		
17.10.2005 00:00	09:55:30.5	38,1773	26,7105	ISC	MS	5,5	TURKIYE		
17.10.2005 00:00	09:58:37.0	38,169	26,6871	ISC	mb	4,3	TURKIYE		
17.10.2005 00:00	10:07:54.2	38,1555	26,6113	ISC	ML	4	TURKIYE	IZMIR	URLA
18.10.2005 00:00	04:10:17.6	38,2504	26,7309	DDA	Md	4	TURKIYE	IZMIR	URLA
18.10.2005 00:00	16:00:47.8	38,2087	26,5062	DDA	Md	4,1	TURKIYE	IZMIR	URLA
19.10.2005 00:00	10:11:30.8	38,1698	26,7027	DDA	Md	4,5	TURKIYE		
19.10.2005 00:00	22:38:58.6	37,8747	27,1683	DDA	Md	4,1	TURKIYE		
20.10.2005 00:00	21:40:02.0	38,1139	26,728	ISC	MS	5,6	TURKIYE		
20.10.2005 00:00	21:44:00.0	38,2076	26,6865	ISC	ML	4,3	TURKIYE		
20.10.2005 00:00	22:15:55.6	38,2087	26,669	ISC	ML	4	TURKIYE	IZMIR	URLA
20.10.2005 00:00	23:16:49.7	38,199	26,7474	ISC	ML	4	TURKIYE		
23.10.2005 00:00	14:59:38.1	38,1268	26,6001	ISC	ML	4	TURKIYE	IZMIR	URLA
29.10.2005 00:00	14:48:41.6	38,1852	26,6369	DDA	Md	4,2	TURKIYE		
29.10.2005 00:00	19:49:30.2	38,2018	26,7143	DDA	Md	4,1	TURKIYE		
31.10.2005 00:00	05:26:39.7	38,1495	26,6823	ISC	MS	4,3	TURKIYE		
31.10.2005 00:00	06:48:22.5	38,1674	26,6545	DDA	Md	4,3	TURKIYE		
24.12.2005 00:00	03:56:07.4	38,8446	27,7826	DDA	Md	4,5	TURKIYE	MANISA	AKHISAR
09.03.2006 00:00	03:18:23.4	37,8617	26,7736	ISC	mb	4	YUNANISTAN		
13.04.2006 00:00	16:18:34.2	38,2473	26,5579	DDA	Md	4,2	TURKIYE	IZMIR	URLA

## A.1 (Continue)

12.06.2006 00:00	08:07:03.2	38,1688	26,7025	DDA	Md	4	TURKIYE		
21.11.2006 00:00	12:14:14.0	38,0385	26,7227	ISC	MD	5,4	TURKIYE		
23.04.2007 00:00	05:20:02.0	38,314	26,6147	ISC	ML	4,1	TURKIYE	IZMIR	URLA
02.08.2007 00:00	10:11:22.9	38,2128	26,6469	ISC	ML	4	TURKIYE	IZMIR	URLA
10.12.2007 00:00	21:50:06.1	38,7812	27,742	DDA	Md	4	TURKIYE	MANISA	SARUHANLI
01.03.2008 00:00	07:01:10.0	37,9	26,867	DDA	Md	4	YUNANISTAN		
15.03.2008 00:00	11:52:13.6	39,0476	27,8478	ISC	ML	4,8	TURKIYE	MANISA	AKHISAR
08.04.2008 00:00	01:13:04.5	38,2311	26,5691	ISC	ML	4,4	TURKIYE	IZMIR	URLA
18.04.2008 00:00	13:49:04.4	37,9338	26,8954	ISC	ML	4,1	TURKIYE		
22.04.2008 00:00	05:12:00.0	38,1613	26,696	ISC	ML	4,5	TURKIYE		
09.05.2008 00:00	10:16:25.6	38,1948	26,5924	ISC	ML	4	TURKIYE	IZMIR	URLA
20.07.2008 00:00	10:15:25.8	38,7375	26,5762	DDA	ML	4,1	TURKIYE		
08.01.2009 00:00	15:43:58.4	37,8568	27,5892	DDA	ML	4,1	TURKIYE	AYDIN	GERMENCIK
03.05.2009 00:00	02:34:08.4	37,8558	27,54	DDA	ML	4,1	TURKIYE	AYDIN	GERMENCIK
07.05.2009 00:00	23:46:42.7	39,2883	27,9308	DDA	ML	4,1	TURKIYE	MANISA	KIRKAGAC
30.08.2009 00:00	00:42:24.8	38,5108	26,3293	DDA	ML	4,2	TURKIYE		
05.10.2010 00:00	23:43:13.6	38,0022	27,952	DDA	ML	4,1	TURKIYE	IZMIR	ODEMIS
11.11.2010 00:00	20:08:00.3	37,8757	27,3632	DDA	ML	4,7	TURKIYE	IZMIR	SELCUK
14.11.2010 00:00	05:21:44.4	37,8558	27,3385	DDA	ML	4,1	TURKIYE	AYDIN	KUSADASI
05.02.2011 00:00	02:37:51.9	37,8392	27,2527	DDA	ML	4,1	TURKIYE	AYDIN	KUSADASI
06.02.2011 00:00	02:08:58.1	37,8567	27,2522	DDA	ML	4,1	TURKIYE	AYDIN	KUSADASI
01.05.2011 00:00	15:04:28.3	39,0602	28,0227	DDA	ML	4,1	TURKIYE	MANISA	AKHISAR
23.05.2011 00:00	10:06:38.0	39,0988	27,1522	DDA	MI	4	TURKIYE	IZMIR	BERGAMA
10.06.2011 00:00	22:47:05.1	39,09	28,35	NEIC	mb	4,4	TURKIYE	BALIKESI	SINDIRGI
08.10.2011 00:00	22:10:53.1	39,0052	28,057	DDA	MI	4	TURKIYE	MANISA	AKHISAR
05.12.2011 00:00	08:17:27.8	38,8424	26,472	MDD	mb	4,8	TURKIYE		
27.12.2011 00:00	05:59:17.4	37,9908	27,1748	DDA	MI	4,1	TURKIYE	IZMIR	MENDERES
27.12.2011 00:00	07:51:46.4	37,9778	27,1563	DDA	MI	4,4	TURKIYE		

## **APPENDIX B**

Coefficients of NGA models

Table B.1 Campbell-Bozorgnia NGA model coefficients (Campbell & Bozorgnia, 2008).

$T(s)$	$c_0$	$c_1$	$c_2$	$c_3$	$c_4$	$c_5$	$c_6$	$c_7$	$c_8$	$c_9$	$c_{10}$	$c_{11}$	$c_{12}$	$k_1$	$k_2$	$k_3$	$c$	$n$	$\sigma_{lnY}$	$\tau_{lnY}$	$\sigma_{lnAF}$	$\sigma_c$	$\rho$
0,010	-1,715	0,500	-0,530	-0,262	-2,118	0,170	5,60	0,280	-0,120	0,490	1,058	0,040	0,610	865	-1,186	1,839	1,88	1,18	0,478	0,219	0,300	0,166	1,000
0,020	-1,680	0,500	-0,530	-0,262	-2,123	0,170	5,60	0,280	-0,120	0,490	1,102	0,040	0,610	865	-1,219	1,840	1,88	1,18	0,480	0,219	0,300	0,166	0,999
0,030	-1,552	0,500	-0,530	-0,262	-2,145	0,170	5,60	0,280	-0,120	0,490	1,174	0,040	0,610	908	-1,273	1,841	1,88	1,18	0,489	0,235	0,300	0,165	0,989
0,050	-1,209	0,500	-0,530	-0,267	-2,199	0,170	5,74	0,280	-0,120	0,490	1,272	0,040	0,610	1054	-1,346	1,843	1,88	1,18	0,510	0,258	0,300	0,162	0,963
0,075	-0,657	0,500	-0,530	-0,302	-2,277	0,170	7,09	0,280	-0,120	0,490	1,438	0,040	0,610	1086	-1,471	1,845	1,88	1,18	0,520	0,292	0,300	0,158	0,922
0,10	-0,314	0,500	-0,530	-0,324	-2,318	0,170	8,05	0,280	-0,099	0,490	1,604	0,040	0,610	1032	-1,624	1,847	1,88	1,18	0,531	0,286	0,300	0,170	0,898
0,15	-0,133	0,500	-0,530	-0,339	-2,309	0,170	8,79	0,280	-0,048	0,490	1,928	0,040	0,610	878	-1,931	1,852	1,88	1,18	0,532	0,280	0,300	0,180	0,890
0,20	-0,486	0,500	-0,446	-0,398	-2,220	0,170	7,60	0,280	-0,012	0,490	2,194	0,040	0,610	748	-2,188	1,856	1,88	1,18	0,534	0,249	0,300	0,186	0,871
0,25	-0,890	0,500	-0,362	-0,458	-2,146	0,170	6,58	0,280	0,000	0,490	2,351	0,040	0,700	654	-2,381	1,861	1,88	1,18	0,534	0,240	0,300	0,191	0,852
0,30	-1,171	0,500	-0,294	-0,511	-2,095	0,170	6,04	0,280	0,000	0,490	2,460	0,040	0,750	587	-2,518	1,865	1,88	1,18	0,544	0,215	0,300	0,198	0,831
0,40	-1,466	0,500	-0,186	-0,592	-2,066	0,170	5,30	0,280	0,000	0,490	2,587	0,040	0,850	503	-2,657	1,874	1,88	1,18	0,541	0,217	0,300	0,206	0,785
0,50	-2,569	0,656	-0,304	-0,536	-2,041	0,170	4,73	0,280	0,000	0,490	2,544	0,040	0,883	457	-2,669	1,883	1,88	1,18	0,550	0,214	0,300	0,208	0,735
0,75	-4,844	0,972	-0,578	-0,406	-2,000	0,170	4,00	0,280	0,000	0,490	2,133	0,077	1,000	410	-2,401	1,906	1,88	1,18	0,568	0,227	0,300	0,221	0,628
1,0	-6,406	1,196	-0,772	-0,314	-2,000	0,170	4,00	0,255	0,000	0,490	1,571	0,150	1,000	400	-1,955	1,929	1,88	1,18	0,568	0,255	0,300	0,225	0,534
1,5	-8,692	1,513	-1,046	-0,185	-2,000	0,170	4,00	0,161	0,000	0,490	0,406	0,253	1,000	400	-1,025	1,974	1,88	1,18	0,564	0,296	0,300	0,222	0,411
2,0	-9,701	1,600	-0,978	-0,236	-2,000	0,170	4,00	0,094	0,000	0,371	-0,456	0,300	1,000	400	-0,299	2,019	1,88	1,18	0,571	0,296	0,300	0,226	0,331
3,0	-10,556	1,600	-0,638	-0,491	-2,000	0,170	4,00	0,000	0,000	0,154	-0,820	0,300	1,000	400	0,000	2,110	1,88	1,18	0,558	0,326	0,300	0,229	0,289
4,0	-11,212	1,600	-0,316	-0,770	-2,000	0,170	4,00	0,000	0,000	0,000	-0,820	0,300	1,000	400	0,000	2,200	1,88	1,18	0,576	0,297	0,300	0,237	0,261
5,0	-11,684	1,600	-0,070	-0,986	-2,000	0,170	4,00	0,000	0,000	0,000	-0,820	0,300	1,000	400	0,000	2,291	1,88	1,18	0,601	0,359	0,300	0,237	0,200
7,5	-12,505	1,600	-0,070	-0,656	-2,000	0,170	4,00	0,000	0,000	0,000	-0,820	0,300	1,000	400	0,000	2,517	1,88	1,18	0,628	0,428	0,300	0,271	0,174
10,0	-13,087	1,600	-0,070	-0,422	-2,000	0,170	4,00	0,000	0,000	0,000	-0,820	0,300	1,000	400	0,000	2,744	1,88	1,18	0,667	0,485	0,300	0,290	0,174
0	-1,715	0,500	-0,530	-0,262	-2,118	0,170	5,60	0,280	-0,120	0,490	1,058	0,040	0,610	865	-1,186	1,839	1,88	1,18	0,478	0,219	0,300	0,166	1,000
-1	0,954	0,696	-0,309	-0,019	-2,016	0,170	4,00	0,245	0,000	0,358	1,694	0,092	1,000	400	-1,955	1,929	1,88	1,18	0,484	0,203	0,300	0,190	0,691
-2	-5,270	1,600	-0,070	0,000	-2,000	0,170	4,00	0,000	0,000	0,000	-0,820	0,300	1,000	400	0,000	2,744	1,88	1,18	0,667	0,485	0,300	0,290	0,174

Table B.2 Standard deviations and correlation coefficients for CB-NGA aleatory uncertainty model (Campbell & Bozorgnia, 2008).

Period $T$ (s)	Standard Deviation			$\sigma_T$ for $V_{530} \geq k_1^{(3)}$		Correlation Coeff.	
	$\sigma_{\ln Y}$	$\tau_{\ln Y}$	$\sigma_c$	Geometric Mean <sup>(1)</sup>	Arbitrary Comp. <sup>(2)</sup>	$\rho_\sigma$	$\rho_\tau$
0.010	0.478	0.219	0.166	0.526	0.551	1.000	1.000
0.020	0.480	0.219	0.166	0.528	0.553	0.999	0.994
0.030	0.489	0.235	0.165	0.543	0.567	0.989	0.979
0.050	0.510	0.258	0.162	0.572	0.594	0.963	0.927
0.075	0.520	0.292	0.158	0.596	0.617	0.922	0.880
0.10	0.531	0.286	0.170	0.603	0.627	0.898	0.871
0.15	0.532	0.280	0.180	0.601	0.628	0.890	0.885
0.20	0.534	0.249	0.186	0.589	0.618	0.871	0.913
0.25	0.534	0.240	0.191	0.585	0.616	0.852	0.873
0.30	0.544	0.215	0.198	0.585	0.618	0.831	0.848
0.40	0.541	0.217	0.206	0.583	0.618	0.785	0.756
0.50	0.550	0.214	0.208	0.590	0.626	0.735	0.631
0.75	0.568	0.227	0.221	0.612	0.650	0.628	0.442
1.0	0.568	0.255	0.225	0.623	0.662	0.534	0.290
1.5	0.564	0.296	0.222	0.637	0.675	0.411	0.290
2.0	0.571	0.296	0.226	0.643	0.682	0.331	0.290
3.0	0.558	0.326	0.229	0.646	0.686	0.289	0.290
4.0	0.576	0.297	0.237	0.648	0.690	0.261	0.290
5.0	0.601	0.359	0.237	0.700	0.739	0.200	0.290
7.5	0.628	0.428	0.271	0.760	0.807	0.174	0.290
10.0	0.667	0.485	0.290	0.825	0.874	0.174	0.290
PGA	0.478	0.219	0.166	0.526	0.551	1.000	1.000
PGV	0.484	0.203	0.190	0.525	0.558	0.691	0.538
PGD	0.667	0.485	0.290	0.825	0.874	0.174	0.290

Table B.3 Chiou-Youngs NGA model coefficients (Brian et al., 2008)

<b>T (s)</b>	<b>c<sub>2</sub></b>	<b>c<sub>3</sub></b>	<b>c<sub>4</sub></b>	<b>c<sub>4a</sub></b>	<b>c<sub>RB</sub></b>	<b>c<sub>HM</sub></b>	<b>c<sub>γ3</sub></b>	<b>c<sub>1</sub></b>	<b>c<sub>1a</sub></b>	<b>c<sub>1b</sub></b>	<b>c<sub>n</sub></b>	<b>c<sub>M</sub></b>	<b>c<sub>5</sub></b>	<b>c<sub>6</sub></b>	<b>c<sub>7</sub></b>	<b>c<sub>7a</sub></b>	<b>c<sub>9</sub></b>	<b>c<sub>9a</sub></b>
0,010	1,06	3,45	-2,1	-0,5	50	3,0	4,0	-1,2687	0,1000	-0,2550	2,996	4,1840	6,1600	0,4893	0,0512	0,0860	0,7900	1,5005
0,020	1,06	3,45	-2,1	-0,5	50	3,0	4,0	-1,2515	0,1000	-0,2550	3,292	4,1879	6,1580	0,4892	0,0512	0,0860	0,8129	1,5028
0,030	1,06	3,45	-2,1	-0,5	50	3,0	4,0	-1,1744	0,1000	-0,2550	3,514	4,1556	6,1550	0,4890	0,0511	0,0860	0,8439	1,5071
0,040	1,06	3,45	-2,1	-0,5	50	3,0	4,0	-1,0671	0,1000	-0,2550	3,563	4,1226	6,1508	0,4888	0,0508	0,0860	0,8740	1,5138
0,050	1,06	3,45	-2,1	-0,5	50	3,0	4,0	-0,9464	0,1000	-0,2550	3,547	4,1011	6,1441	0,4884	0,0504	0,0860	0,8996	1,5230
0,075	1,06	3,45	-2,1	-0,5	50	3,0	4,0	-0,7051	0,1000	-0,2540	3,448	4,0860	6,1200	0,4872	0,0495	0,0860	0,9442	1,5597
0,10	1,06	3,45	-2,1	-0,5	50	3,0	4,0	-0,5747	0,1000	-0,2530	3,312	4,1030	6,0850	0,4854	0,0489	0,0860	0,9677	1,6104
0,15	1,06	3,45	-2,1	-0,5	50	3,0	4,0	-0,5309	0,1000	-0,2500	3,044	4,1717	5,9871	0,4808	0,0479	0,0860	0,9660	1,7549
0,20	1,06	3,45	-2,1	-0,5	50	3,0	4,0	-0,6352	0,1000	-0,2449	2,831	4,2476	5,8699	0,4755	0,0471	0,0860	0,9334	1,9157
0,25	1,06	3,45	-2,1	-0,5	50	3,0	4,0	-0,7766	0,1000	-0,2382	2,658	4,3184	5,7547	0,4706	0,0464	0,0860	0,8946	2,0709
0,30	1,06	3,45	-2,1	-0,5	50	3,0	4,0	-0,9278	0,0999	-0,2313	2,505	4,3844	5,6527	0,4665	0,0458	0,0860	0,8590	2,2005
0,40	1,06	3,45	-2,1	-0,5	50	3,0	4,0	-1,2176	0,0997	-0,2146	2,261	4,4979	5,4997	0,4607	0,0445	0,0850	0,8019	2,3886
0,50	1,06	3,45	-2,1	-0,5	50	3,0	4,0	-1,4695	0,0991	-0,1972	2,087	4,5881	5,4029	0,4571	0,0429	0,0830	0,7578	2,5000
0,75	1,06	3,45	-2,1	-0,5	50	3,0	4,0	-1,9278	0,0936	-0,1620	1,812	4,7571	5,2900	0,4531	0,0387	0,0690	0,6788	2,6224
1,0	1,06	3,45	-2,1	-0,5	50	3,0	4,0	-2,2453	0,0766	-0,1400	1,648	4,8820	5,2480	0,4517	0,0350	0,0450	0,6196	2,6690
1,5	1,06	3,45	-2,1	-0,5	50	3,0	4,0	-2,7307	0,0022	-0,1184	1,511	5,0697	5,2194	0,4507	0,0280	0,0134	0,5101	2,6985
2,0	1,06	3,45	-2,1	-0,5	50	3,0	4,0	-3,1413	-0,0591	-0,1100	1,470	5,2173	5,2099	0,4504	0,0213	0,0040	0,3917	2,7085
3,0	1,06	3,45	-2,1	-0,5	50	3,0	4,0	-3,7413	-0,0931	-0,1040	1,456	5,4385	5,2040	0,4501	0,0106	0,0010	0,1244	2,7145
4,0	1,06	3,45	-2,1	-0,5	50	3,0	4,0	-4,1814	-0,0982	-0,1020	1,465	5,5977	5,2020	0,4501	0,0041	0,0000	0,0086	2,7164
5,0	1,06	3,45	-2,1	-0,5	50	3,0	4,0	-4,5187	-0,0994	-0,1010	1,478	5,7276	5,2010	0,4500	0,0010	0,0000	0,0000	2,7172
7,5	1,06	3,45	-2,1	-0,5	50	3,0	4,0	-5,1224	-0,0999	-0,1010	1,498	5,9891	5,2000	0,4500	0,0000	0,0000	0,0000	2,7177
10,0	1,06	3,45	-2,1	-0,5	50	3,0	4,0	-5,5872	-0,1000	-0,1000	1,502	6,1930	5,2000	0,4500	0,0000	0,0000	0,0000	2,7180
0,0	1,06	3,45	-2,1	-0,5	50	3,0	4,0	-1,2687	0,1000	-0,2550	2,996	4,1840	6,1600	0,4893	0,0512	0,0860	0,7900	1,5005
-1,0	1,06	3,45	-2,1	-0,5	50	3,0	4,0	2,2884	0,1094	-0,0626	1,648	4,2979	5,1700	0,4407	0,0207	0,0437	0,3079	2,6690

Table B.4 Chiou-Youngs NGA model coefficients (Brian et al., 2008)

T (s)	$c_{10}$	$c_{\gamma 1}$	$c_{\gamma 2}$	$\phi_1$	$\phi_2$	$\phi_3$	$\phi_4$	$\phi_5$	$\phi_6$	$\phi_7$	$\phi_8$	$\tau_1$	$\tau_2$	$\sigma_1$	$\sigma_2$	$\sigma_3$	$\sigma_4$
0,010	-0,3218	-0,00804	-0,00785	-0,4417	-0,1417	-0,007010	0,102151	0,2289	0,014996	580,0	0,0700	0,3437	0,2637	0,4458	0,3459	0,8000	0,0663
0,020	-0,3323	-0,00811	-0,00792	-0,4340	-0,1364	-0,007279	0,108360	0,2289	0,014996	580,0	0,0699	0,3471	0,2671	0,4458	0,3459	0,8000	0,0663
0,030	-0,3394	-0,00839	-0,00819	-0,4177	-0,1403	-0,007354	0,119888	0,2289	0,014996	580,0	0,0701	0,3603	0,2803	0,4535	0,3537	0,8000	0,0663
0,040	-0,3453	-0,00875	-0,00855	-0,4000	-0,1591	-0,006977	0,133641	0,2289	0,014996	579,9	0,0702	0,3718	0,2918	0,4589	0,3592	0,8000	0,0663
0,050	-0,3502	-0,00912	-0,00891	-0,3903	-0,1862	-0,006467	0,148927	0,2290	0,014996	579,9	0,0701	0,3848	0,3048	0,4630	0,3635	0,8000	0,0663
0,075	-0,3579	-0,00973	-0,00950	-0,4040	-0,2538	-0,005734	0,190596	0,2292	0,014996	579,6	0,0686	0,3878	0,3129	0,4702	0,3713	0,8000	0,0663
0,10	-0,3604	-0,00975	-0,00952	-0,4423	-0,2943	-0,005604	0,230662	0,2297	0,014996	579,2	0,0646	0,3835	0,3152	0,4747	0,3769	0,8000	0,0663
0,15	-0,3565	-0,00883	-0,00862	-0,5162	-0,3113	-0,005845	0,266468	0,2326	0,014988	577,2	0,0494	0,3719	0,3128	0,4798	0,3847	0,8000	0,0612
0,20	-0,3470	-0,00778	-0,00759	-0,5697	-0,2927	-0,006141	0,255253	0,2386	0,014964	573,9	-0,0019	0,3601	0,3076	0,4816	0,3902	0,8000	0,0530
0,25	-0,3379	-0,00688	-0,00671	-0,6109	-0,2662	-0,006439	0,231541	0,2497	0,014881	568,5	-0,0479	0,3522	0,3047	0,4815	0,3946	0,7999	0,0457
0,30	-0,3314	-0,00612	-0,00598	-0,6444	-0,2405	-0,006704	0,207277	0,2674	0,014639	560,5	-0,0756	0,3438	0,3005	0,4801	0,3981	0,7997	0,0398
0,40	-0,3256	-0,00498	-0,00486	-0,6931	-0,1975	-0,007125	0,165464	0,3120	0,013493	540,0	-0,0960	0,3351	0,2984	0,4758	0,4036	0,7988	0,0312
0,50	-0,3189	-0,00420	-0,00410	-0,7246	-0,1633	-0,007435	0,133828	0,3610	0,011133	512,9	-0,0998	0,3353	0,3036	0,4710	0,4079	0,7966	0,0255
0,75	-0,2702	-0,00308	-0,00301	-0,7708	-0,1028	-0,008120	0,085153	0,4353	0,006739	441,9	-0,0765	0,3429	0,3205	0,4621	0,4157	0,7792	0,0175
1,0	-0,2059	-0,00246	-0,00241	-0,7990	-0,0699	-0,008444	0,058595	0,4629	0,005749	391,8	-0,0412	0,3577	0,3419	0,4581	0,4213	0,7504	0,0133
1,5	-0,0852	-0,00180	-0,00176	-0,8382	-0,0425	-0,007707	0,031787	0,4756	0,005544	348,1	0,0140	0,3769	0,3703	0,4493	0,4213	0,7136	0,0090
2,0	0,0160	-0,00147	-0,00143	-0,8663	-0,0302	-0,004792	0,019716	0,4785	0,005521	332,5	0,0544	0,4023	0,4023	0,4459	0,4213	0,7035	0,0068
3,0	0,1876	-0,00117	-0,00115	-0,9032	-0,0129	-0,001828	0,009643	0,4796	0,005517	324,1	0,1232	0,4406	0,4406	0,4433	0,4213	0,7006	0,0045
4,0	0,3378	-0,00107	-0,00104	-0,9231	-0,0016	-0,001523	0,005379	0,4799	0,005517	321,7	0,1859	0,4784	0,4784	0,4424	0,4213	0,7001	0,0034
5,0	0,4579	-0,00102	-0,00099	-0,9222	0,0000	-0,001440	0,003223	0,4799	0,005517	320,9	0,2295	0,5074	0,5074	0,4420	0,4213	0,7000	0,0027
7,5	0,7514	-0,00096	-0,00094	-0,8346	0,0000	-0,001369	0,001134	0,4800	0,005517	320,3	0,2660	0,5328	0,5328	0,4416	0,4213	0,7000	0,0018
10,0	1,1856	-0,00094	-0,00091	-0,7332	0,0000	-0,001361	0,000515	0,4800	0,005517	320,1	0,2682	0,5542	0,5542	0,4414	0,4213	0,7000	0,0014
0,0	-0,3218	-0,00804	-0,00785	-0,4417	-0,1417	-0,007010	0,102151	0,2289	0,014996	580,0	0,0700	0,3437	0,2637	0,4458	0,3459	0,8000	0,0663
-1,0	-0,1166	-0,00275	-0,00625	-0,7861	-0,0699	-0,008444	5,410000	0,2899	0,006718	459,0	0,1138	0,2539	0,2381	0,4496	0,3554	0,7504	0,0133

Table B.5 Boore-Atkinson NGA model coefficients (Boore & Atkinson, 2007)

$T$ (s)	$e_1$	$e_2$	$e_3$	$e_4$	$e_5$	$e_6$	$e_7$	$M_h$	$c_1$	$c_2$	$c_3$	$M_{ref}$	$R_{ref}$	$h$	$b_{lin}$	$V_{ref}$
0,010	-0,52883	-0,49429	-0,74551	-0,49966	0,28897	-0,10019	0,00000	6,75	-0,66220	0,12000	-0,01151	4,5	1,0	1,35	-0,360	760
0,020	-0,52192	-0,48508	-0,73906	-0,48895	0,25144	-0,11006	0,00000	6,75	-0,66600	0,12280	-0,01151	4,5	1,0	1,35	-0,340	760
0,030	-0,45285	-0,41831	-0,66722	-0,42229	0,17976	-0,12858	0,00000	6,75	-0,69010	0,12830	-0,01151	4,5	1,0	1,35	-0,330	760
0,050	-0,28476	-0,25022	-0,48462	-0,26092	0,06369	-0,15752	0,00000	6,75	-0,71700	0,13170	-0,01151	4,5	1,0	1,35	-0,290	760
0,075	0,00767	0,04912	-0,20578	0,02706	0,01170	-0,17051	0,00000	6,75	-0,72050	0,12370	-0,01151	4,5	1,0	1,55	-0,230	760
0,10	0,20109	0,23102	0,03058	0,22193	0,04697	-0,15948	0,00000	6,75	-0,70810	0,11170	-0,01151	4,5	1,0	1,68	-0,250	760
0,15	0,46128	0,48661	0,30185	0,49328	0,17990	-0,14539	0,00000	6,75	-0,69610	0,09884	-0,01113	4,5	1,0	1,86	-0,280	760
0,20	0,57180	0,59253	0,40860	0,61472	0,52729	-0,12964	0,00102	6,75	-0,58300	0,04273	-0,00952	4,5	1,0	1,98	-0,310	760
0,25	0,51884	0,53496	0,33880	0,57747	0,60880	-0,13843	0,08607	6,75	-0,57260	0,02977	-0,00837	4,5	1,0	2,07	-0,390	760
0,30	0,43825	0,44516	0,25356	0,51990	0,64472	-0,15694	0,10601	6,75	-0,55430	0,01955	-0,00750	4,5	1,0	2,14	-0,440	760
0,40	0,39220	0,40602	0,21398	0,46080	0,78610	-0,07843	0,02262	6,75	-0,64430	0,04394	-0,00626	4,5	1,0	2,24	-0,500	760
0,50	0,18957	0,19878	0,00967	0,26337	0,76837	-0,09054	0,00000	6,75	-0,69140	0,06080	-0,00540	4,5	1,0	2,32	-0,600	760
0,75	-0,21338	-0,19496	-0,49176	-0,10813	0,75179	-0,14053	0,10302	6,75	-0,74080	0,07518	-0,00409	4,5	1,0	2,46	-0,690	760
1,0	-0,46896	-0,43443	-0,78465	-0,39330	0,67880	-0,18257	0,05393	6,75	-0,81830	0,10270	-0,00334	4,5	1,0	2,54	-0,700	760
1,5	-0,86271	-0,79593	-1,20902	-0,88085	0,70689	-0,25950	0,19082	6,75	-0,83030	0,09793	-0,00255	4,5	1,0	2,66	-0,720	760
2,0	-1,22652	-1,15514	-1,57697	-1,27669	0,77989	-0,29657	0,29888	6,75	-0,82850	0,09432	-0,00217	4,5	1,0	2,73	-0,730	760
3,0	-1,82979	-1,74690	-2,22584	-1,91814	0,77966	-0,45384	0,67466	6,75	-0,78440	0,07282	-0,00191	4,5	1,0	2,83	-0,740	760
4,0	-2,24656	-2,15906	-2,58228	-2,38168	1,24961	-0,35874	0,79508	6,75	-0,68540	0,03758	-0,00191	4,5	1,0	2,89	-0,750	760
5,0	-1,28408	-1,21270	-1,50904	-1,41093	0,14271	-0,39006	0,00000	8,50	-0,50960	-0,02391	-0,00191	4,5	1,0	2,93	-0,750	760
7,5	-1,43145	-1,31632	-1,81022	-1,59217	0,52407	-0,37578	0,00000	8,50	-0,37240	-0,06568	-0,00191	4,5	1,0	3,00	-0,692	760
10,0	-2,15446	-2,16137	-2,53323	-2,14635	0,40387	-0,48492	0,00000	8,50	-0,09824	-0,13800	-0,00191	4,5	1,0	3,04	-0,650	760
0	-0,53804	-0,50350	-0,75472	-0,50970	0,28805	-0,10164	0,00000	6,75	-0,66050	0,11970	-0,01151	4,5	1,0	1,35	-0,360	760
-1	5,00121	5,04727	4,63188	5,08210	0,18322	-0,12736	0,00000	8,50	-0,87370	0,10060	-0,00334	4,5	1,0	2,54	-0,600	760

Table B.6 Boore-Atkinson NGA model coefficients (Boore & Atkinson, 2007)

T (s)	b <sub>1</sub>	b <sub>2</sub>	V <sub>1</sub>	V <sub>2</sub>	a <sub>1</sub>	pga_low	a <sub>2</sub>	σ	τ <sub>U</sub>	σ <sub>τU</sub>	τ <sub>M</sub>	σ <sub>τM</sub>
0,010	-0,640	-0,14	180	300	0,03	0,06	0,09	0,502	0,267	0,569	0,262	0,566
0,020	-0,630	-0,12	180	300	0,03	0,06	0,09	0,502	0,267	0,569	0,262	0,566
0,030	-0,620	-0,11	180	300	0,03	0,06	0,09	0,507	0,276	0,578	0,274	0,576
0,050	-0,640	-0,11	180	300	0,03	0,06	0,09	0,516	0,286	0,589	0,286	0,589
0,075	-0,640	-0,11	180	300	0,03	0,06	0,09	0,513	0,322	0,606	0,320	0,606
0,10	-0,600	-0,13	180	300	0,03	0,06	0,09	0,520	0,313	0,608	0,318	0,608
0,15	-0,530	-0,18	180	300	0,03	0,06	0,09	0,518	0,288	0,592	0,290	0,594
0,20	-0,520	-0,19	180	300	0,03	0,06	0,09	0,523	0,283	0,596	0,288	0,596
0,25	-0,520	-0,16	180	300	0,03	0,06	0,09	0,527	0,267	0,592	0,267	0,592
0,30	-0,520	-0,14	180	300	0,03	0,06	0,09	0,546	0,272	0,608	0,269	0,608
0,40	-0,510	-0,10	180	300	0,03	0,06	0,09	0,541	0,267	0,603	0,267	0,603
0,50	-0,500	-0,06	180	300	0,03	0,06	0,09	0,555	0,265	0,615	0,265	0,615
0,75	-0,470	0,00	180	300	0,03	0,06	0,09	0,571	0,311	0,649	0,299	0,645
1,0	-0,440	0,00	180	300	0,03	0,06	0,09	0,573	0,318	0,654	0,302	0,647
1,5	-0,400	0,00	180	300	0,03	0,06	0,09	0,566	0,382	0,684	0,373	0,679
2,0	-0,380	0,00	180	300	0,03	0,06	0,09	0,580	0,398	0,702	0,389	0,700
3,0	-0,340	0,00	180	300	0,03	0,06	0,09	0,566	0,410	0,700	0,401	0,695
4,0	-0,310	0,00	180	300	0,03	0,06	0,09	0,583	0,394	0,702	0,385	0,698
5,0	-0,291	0,00	180	300	0,03	0,06	0,09	0,601	0,414	0,730	0,437	0,744
7,5	-0,247	0,00	180	300	0,03	0,06	0,09	0,626	0,465	0,781	0,477	0,787
10,0	-0,215	0,00	180	300	0,03	0,06	0,09	0,645	0,355	0,735	0,477	0,801
0	-0,640	-0,14	180	300	0,03	0,06	0,09	0,502	0,265	0,566	0,260	0,564
-1	-0,500	-0,06	180	300	0,03	0,06	0,09	0,500	0,286	0,576	0,256	0,560

## **APPENDIX C**

### **SEISRISK III**

## C.1 SEISRISK III

The SEISRISK III software consists of four files such as file 15, file 16, file 2, file 3. File 15 is an input file where the problem is defined. Source zone can be defined as quadrilateral areas or lines. Quadrilateral areas are source zone which are used in this thesis. Faults can be represented as line. Faults are not included in our calculation because of the lack of earthquake reoccurrence information. Attenuation relationships are defined in file 2 as tables where the ground motion is tabulated as a function of magnitude and site- source distance. Source zone coordinates are input as pair of lines that form quadrilateral areas. Finally, the earthquake reoccurrence relationships are given as tables as where annual earthquakes are tabulated as a function of magnitude.

File 16 is a file that all the calculations are given in detail. All the information about even a single point is given in this file. File 2 and File 3 are output files as well. This file can only be written by additional programs. File 2 gives the exact information needed to draw contour maps such as location of each calculated point and its ground motion value for chosen return period. Examples of file 15, file 16 and File 2 are given below: The ground motion acceleration values for 30 points chosen inside of Izmir City are shown in the tables of this appendix.( $T_R$  is the return period).

**File 15 (Input file)**

SEISRISK III Sample Problem

0 20 → (0- for new run), (20 the standard deviation of each zone )

.50 1 50 (0.5- the probability of not being exceeded),(number of calculations), (50 -number of years)

25.75 38.625 28.75 38.625 (Equator of circle coordinates)

25.75 39.50 28.75 37.75 0.100 0.100 (Study area coordinates and grid spaces)

5 25 4 40 (the range of the rows and colons taken in consideration)

5 (number of line segments containing additional points that are to be calculated)

2 (number of part that a segment should be devided)

27.109 38.538 27.257 38.508  
 27.287 38.483 27.313 38.464  
 27.415 38.399 27.301 38.337  
 27.193 38.321 27.030 38.314  
 27.032 38.314 27.912 38.325 } Segment's coordinates

motion values)

5 8 (column and rows)

'Cambel 2008'	7.6	6.6	5.6	5.2
4.2				
3.22	.908	.720	.462	.177
6.43	.728	.536	.307	.104
16.09	.435	.277	.130	.0368
32.18	.256	.143	.0582	.0145
64.3	.154	.0769	.0277	.00617
96.5	.0118	.0560	.0190	.0040
160.9	.0830	.0373	.0119	.00230
200.0	.0696	.0306	.0095	.00178

00 1.0 -1 zn01 (standard deviation of the zone is the same as it is defined line 2,

1.0 means annual year , -1 means don't show the solutions, zn01 is the name of zone).

2 1 1 (2 is the number line that create zones, 1 sequence of subzones and 1 number of subzones)

26.918 38.392 27.264 38.362 } Segment pair of source zones  
 26.555 37.909 26.964 37.789 }  
 .0025 .0046 .0084 .0154 .0281 .0514 .0939 .1717 .3140  
 8.200 7.700 7.200 6.700 6.200 5.700 5.200 4.700 4.200  
 00 1.0 -1 zn10 → Earthquake

3 1 1  
 reoccurrence

27.212 39.939 27.653 38.911  
 26.875 38.846 27.385 38.784  
 26.793 38.572 27.108 38.563  
 .0009 .0015 .0025 .0041 .0070 .0117 .0198 .0334 .0562  
 8.200 7.700 7.200 6.700 6.200 5.700 5.200 4.700 4.200

00 1.0 2 zn11  
 3 1 1  
 26.379 38.882 26.696 38.820  
 26.262 38.660 26.734 38.770  
 26.293 38.498 26.749 38.599  
 .0005 .0011 .0024 .0053 .0117 .0257 .0566 .1243 .2731  
 8.200 7.700 7.200 6.700 6.200 5.700 5.200 4.700 4.200

99

### File 16 (Output file)

```

1SEISRISK III Sample Problem
isw=0: new run--no previous results included
extreme probability 0.500
    for exposure times (years)      50
scale factor for ground motion "box" levels=     1.00
coordinates input in decimal degrees
    coordinates are printed in decimal degrees
variability in attenuation, sigma=  0.50
grid oriented parallel to great circle thru (  25.75,
38.63),( 28.75, 38.63)
corners of gridded area-upper left= 25.75, 39.50
                                lower right= 28.75, 37.75
longitude increment= 0.1000 (decimal degrees)
latitude increment = 0.1000 (decimal degrees)
gridded region contains 24 rows, 30 cols including border
3 rows and cols
for this run begin at row   5 end row  25, begin col   4 end
col  40
new coordinates (km) gridded area
upper left= -33.40  259.30; lower right=  130.78
-97.39
sites are also located on 5 line(s)
2 sites per line
line 1 end points at 27.109, 38.538 and 27.257, 38.508
line 2 end points at 27.287, 38.483 and 27.313, 38.464
line 3 end points at 27.415, 38.399 and 27.301, 38.337
line 4 end points at 27.193, 38.321 and 27.030, 38.314
line 5 end points at 27.032, 38.314 and 27.912, 38.325
attenuation function watashh79
                               magnitude
dist(km)    7.60      6.60      5.60      5.20      4.20
            3.22  0.90800  0.72000  0.46200  0.17700  0.02380
            6.43  0.72800  0.53600  0.30700  0.10400  0.01270
           16.09  0.43500  0.27700  0.13000  0.03680  0.00387
           32.18  0.25600  0.14300  0.05820  0.01450  0.00139
           64.30  0.15400  0.07690  0.02770  0.00617  0.00055
           96.50  0.01180  0.05600  0.01900  0.00400  0.00034
          160.90  0.08300  0.03730  0.01190  0.00230  0.00018
          200.00  0.06960  0.03060  0.00950  0.00178  0.00013
0yrnoc= 1. iprint=-1 for area zn01
        26.918  38.392  27.264  38.362
        26.555  37.909  26.964  37.789
nr of levels of seismicity = 9
zn01 beta= -1.2073
earthquake rate / year
occurrences= 0.314000  0.171700  0.093900  0.051400
0.028100  0.015400  0.008400  0.004600  0.002500
magnitudes=      4.20      4.70      5.20      5.70
6.20      6.70      7.20      7.70      8.20
zn01 area= 2187. sq km, rate/sq km= 0.14360E-03 for mags
3.95- 4.45

```

```

0yrnoc= 1. iprint=-1 for area zn14
      27.212    39.939    27.653    38.911
      26.875    38.846    27.385    38.784
      26.793    38.572    27.108    38.563
nr of levels of seismicity = 9
zn14 beta= -1.0407
earthquake rate / year
occurrences= 0.056200 0.033400 0.019800 0.011700
0.007000 0.004100 0.002500 0.001500 0.000900
magnitudes= 4.20      4.70      5.20      5.70
6.20      6.70      7.20      7.70      8.20
zn14 area= 5436. sq km, rate/sq km= 0.10338E-04 for mags
3.95- 4.45
0yrnoc= 1. iprint= 2 for area zn15
      26.379    38.882    26.696    38.820
      26.262    38.660    26.734    38.770
      26.293    38.498    26.749    38.599
nr of levels of seismicity = 9
zn15 beta= -1.5743
earthquake rate / year
occurrences= 0.273100 0.124300 0.056600 0.025700
0.011700 0.005300 0.002400 0.001100 0.000500
magnitudes= 4.20      4.70      5.20      5.70
6.20      6.70      7.20      7.70      8.20
zn15 area= 1280. sq km, rate/sq km= 0.21338E-03 for mags

```

**File 44 (Output file)**

Number of years

long	lat	50
28.232	38.156	0.042
28.104	38.157	0.042
27.977	38.157	0.049
27.850	38.158	0.058
27.723	38.159	0.077
27.596	38.159	0.106
27.468	38.159	0.137
27.341	38.160	0.180
27.087	38.160	0.367
26.960	38.159	0.395
26.833	38.159	0.376
26.705	38.158	0.282

**Table C.1 Attenuation relationship:** Campbell & Bozorgnia (2008). . **Values:**  
Ground Acceleration (g) (Median) **Spectral period T=1s**

Long	Lat	Ground acceleration $T_R=2475$	Ground acceleration $T_R=475$	Ground acceleration $T_R=72$
26,928	38,481	0,375	0,259	0,152
27,033	38,497	0,456	0,312	0,161
27,057	38,479	0,457	0,321	0,164
27,113	38,464	0,457	0,327	0,167
27,129	38,468	0,457	0,327	0,166
27,15	38,466	0,457	0,327	0,166
27,156	38,468	0,457	0,327	0,166
27,159	38,468	0,457	0,327	0,166
27,192	38,47	0,457	0,327	0,166
27,182	38,452	0,457	0,328	0,168
27,216	38,45	0,457	0,327	0,167
27,168	38,433	0,449	0,322	0,167
27,203	38,433	0,45	0,322	0,166
27,137	38,425	0,442	0,317	0,166
27,138	38,425	0,442	0,317	0,166
27,123	38,415	0,432	0,31	0,166
27,124	38,415	0,432	0,31	0,166
27,064	38,394	0,404	0,292	0,164
27,097	38,404	0,415	0,3	0,164
26,99	38,398	0,401	0,281	0,163
27,109	38,538	0,389	0,27	0,136
27,257	38,508	0,396	0,279	0,141
27,287	38,483	0,406	0,289	0,145
27,313	38,464	0,408	0,291	0,146
27,415	38,399	0,391	0,274	0,141
27,301	38,337	0,288	0,219	0,129
27,193	38,321	0,356	0,246	0,142
27,03	38,314	0,366	0,259	0,15
27,032	38,314	0,366	0,259	0,15
27,912	38,325	0,338	0,221	0,116

**Table C.2 Attenuation relationship:** Campbell & Bozorgnia (2008). . **Values:**  
Ground Acceleration (g) (Median) **Spectral period T=0.2 s**

Long	Lat	Ground acceleration $T_R=2475$	Ground acceleration $T_R=475$	Ground acceleration $T_R=72$
26,928	38,481	0,869	0,692	0,385
27,033	38,497	0,934	0,823	0,481
27,057	38,479	0,934	0,825	0,506
27,113	38,464	0,934	0,824	0,526
27,129	38,468	0,934	0,825	0,528
27,15	38,466	0,934	0,825	0,528
27,156	38,468	0,934	0,825	0,528
27,159	38,468	0,934	0,825	0,528
27,192	38,47	0,934	0,825	0,529
27,182	38,452	0,934	0,824	0,526
27,216	38,45	0,934	0,824	0,525
27,168	38,433	0,933	0,809	0,502
27,203	38,433	0,934	0,812	0,505
27,137	38,425	0,926	0,792	0,487
27,138	38,425	0,926	0,792	0,487
27,123	38,415	0,915	0,77	0,468
27,124	38,415	0,915	0,77	0,468
27,064	38,394	0,855	0,694	0,405
27,097	38,404	0,891	0,735	0,439
26,99	38,398	0,849	0,681	0,396
27,109	38,538	0,917	0,772	0,452
27,257	38,508	0,924	0,789	0,483
27,287	38,483	0,931	0,814	0,502
27,313	38,464	0,931	0,818	0,506
27,415	38,399	0,92	0,778	0,467
27,301	38,337	0,707	0,544	0,353
27,193	38,321	0,92	0,776	0,448
27,03	38,314	0,921	0,795	0,527
27,032	38,314	0,921	0,795	0,527
27,912	38,325	0,858	0,647	0,349

**Table C.3 Attenuation relationship:** Campbell & Bozorgnia (2008). . **Values:**  
**Ground Acceleration (g) (Median +Standard Deviation) Spectral period T=0.2s**

Long	Lat	Ground acceleration $T_R=2475$	Ground acceleration $T_R=475$	Ground acceleration $T_R=72$
26,928	38,481	0,975	0,895	0,616
27,033	38,497	0,974	0,901	0,619
27,057	38,479	0,974	0,906	0,631
27,113	38,464	0,974	0,918	0,663
27,129	38,468	0,973	0,92	0,67
27,15	38,466	0,973	0,921	0,678
27,156	38,468	0,973	0,921	0,68
27,159	38,468	0,973	0,921	0,681
27,192	38,47	0,973	0,921	0,692
27,182	38,452	0,973	0,921	0,692
27,216	38,45	0,973	0,921	0,695
27,168	38,433	0,974	0,918	0,679
27,203	38,433	0,973	0,918	0,686
27,137	38,425	0,974	0,918	0,666
27,138	38,425	0,974	0,918	0,666
27,123	38,415	0,974	0,92	0,657
27,124	38,415	0,974	0,92	0,658
27,064	38,394	0,975	0,941	0,71
27,097	38,404	0,975	0,93	0,68
26,99	38,398	0,975	0,945	0,708
27,109	38,538	0,964	0,9	0,648
27,257	38,508	0,966	0,91	0,684
27,287	38,483	0,966	0,908	0,683
27,313	38,464	0,966	0,907	0,681
27,415	38,399	0,965	0,905	0,682
27,301	38,337	0,949	0,864	0,621
27,193	38,321	0,964	0,902	0,656
27,03	38,314	0,971	0,932	0,746
27,032	38,314	0,971	0,932	0,746
27,912	38,325	0,945	0,841	0,581

**Table C.4 Attenuation relationship:** Campbell & Bozorgnia (2008). . **Values:**  
Ground Acceleration (g) (Median +Standard Deviation) **Spectral period T=1 s**

Long	Lat	Ground acceleration $T_R=2475$	Ground acceleration $T_R=475$	Ground acceleration $T_R=72$
26,928	38,481	0,669	0,467	0,274
27,033	38,497	0,794	0,56	0,291
27,057	38,479	0,798	0,575	0,297
27,113	38,464	0,798	0,586	0,303
27,129	38,468	0,798	0,586	0,303
27,15	38,466	0,798	0,585	0,303
27,156	38,468	0,798	0,585	0,303
27,159	38,468	0,798	0,585	0,303
27,192	38,47	0,798	0,585	0,303
27,182	38,452	0,796	0,586	0,306
27,216	38,45	0,796	0,585	0,305
27,168	38,433	0,783	0,574	0,304
27,203	38,433	0,785	0,575	0,303
27,137	38,425	0,772	0,567	0,303
27,138	38,425	0,772	0,567	0,303
27,123	38,415	0,759	0,555	0,302
27,124	38,415	0,759	0,555	0,302
27,064	38,394	0,719	0,525	0,299
27,097	38,404	0,737	0,539	0,299
26,99	38,398	0,715	0,506	0,297
27,109	38,538	0,712	0,499	0,253
27,257	38,508	0,725	0,516	0,262
27,287	38,483	0,745	0,535	0,269
27,313	38,464	0,748	0,539	0,27
27,415	38,399	0,716	0,506	0,263
27,301	38,337	0,535	0,406	0,238
27,193	38,321	0,657	0,455	0,264
27,03	38,314	0,676	0,48	0,279
27,032	38,314	0,676	0,48	0,279
27,912	38,325	0,623	0,41	0,215

**Table C.5 Attenuation relationship:** Brian et al. (2008). . **Values:** Ground Acceleration (g) (Median) **Spectral period T=1 s**

Long	Lat	Ground acceleration $T_R=2475$	Ground acceleration $T_R=475$	Ground acceleration $T_R=72$
26,928	38,481	0,336	0,222	0,108
27,033	38,497	0,409	0,293	0,121
27,057	38,479	0,409	0,299	0,125
27,113	38,464	0,409	0,301	0,129
27,129	38,468	0,409	0,302	0,13
27,15	38,466	0,409	0,301	0,131
27,156	38,468	0,409	0,301	0,131
27,159	38,468	0,409	0,301	0,131
27,192	38,47	0,409	0,302	0,133
27,182	38,452	0,409	0,3	0,132
27,216	38,45	0,409	0,3	0,134
27,168	38,433	0,405	0,291	0,127
27,203	38,433	0,406	0,293	0,129
27,137	38,425	0,4	0,283	0,124
27,138	38,425	0,4	0,283	0,124
27,123	38,415	0,386	0,271	0,12
27,124	38,415	0,386	0,271	0,12
27,064	38,394	0,344	0,232	0,109
27,097	38,404	0,359	0,252	0,114
26,99	38,398	0,346	0,229	0,107
27,109	38,538	0,364	0,254	0,109
27,257	38,508	0,371	0,264	0,118
27,287	38,483	0,378	0,274	0,123
27,313	38,464	0,379	0,277	0,124
27,415	38,399	0,367	0,259	0,121
27,301	38,337	0,251	0,186	0,096
27,193	38,321	0,388	0,255	0,108
27,03	38,314	0,395	0,28	0,132
27,032	38,314	0,395	0,28	0,132
27,912	38,325	0,317	0,204	0,098

**Table C.6 Attenuation relationship:** Brian et al. (2008). . **Values:** Ground Acceleration (g) (Median) **Spectral period T=0.2 s**

Long	Lat	Ground acceleration $T_R=2475$	Ground acceleration $T_R=475$	Ground acceleration $T_R=72$
26,928	38,481	0,79	0,568	0,293
27,033	38,497	0,893	0,723	0,361
27,057	38,479	0,894	0,731	0,377
27,113	38,464	0,894	0,733	0,391
27,129	38,468	0,894	0,734	0,394
27,15	38,466	0,894	0,733	0,396
27,156	38,468	0,894	0,733	0,397
27,159	38,468	0,894	0,733	0,398
27,192	38,47	0,894	0,734	0,402
27,182	38,452	0,894	0,73	0,399
27,216	38,45	0,894	0,73	0,4
27,168	38,433	0,888	0,714	0,379
27,203	38,433	0,889	0,717	0,385
27,137	38,425	0,88	0,699	0,361
27,138	38,425	0,88	0,699	0,361
27,123	38,415	0,864	0,674	0,342
27,124	38,415	0,865	0,674	0,343
27,064	38,394	0,847	0,621	0,326
27,097	38,404	0,827	0,631	0,318
26,99	38,398	0,848	0,617	0,327
27,109	38,538	0,872	0,683	0,345
27,257	38,508	0,881	0,702	0,378
27,287	38,483	0,892	0,724	0,395
27,313	38,464	0,894	0,73	0,398
27,415	38,399	0,875	0,692	0,373
27,301	38,337	0,702	0,495	0,272
27,193	38,321	0,91	0,726	0,382
27,03	38,314	0,925	0,775	0,436
27,032	38,314	0,925	0,775	0,436
27,912	38,325	0,795	0,559	0,283

**Table C.7 Attenuation relationship:** Brian et al. (2008). **Values:** Ground Acceleration (g) (Median+ Standard Deviation) **Spectral period T=0.2 s**

Long	Lat	Ground acceleration $T_R=2475$	Ground acceleration $T_R=475$	Ground acceleration $T_R=72$
26,928	38,481	0,943	0,826	0,506
27,033	38,497	0,958	0,874	0,554
27,057	38,479	0,96	0,883	0,569
27,113	38,464	0,962	0,889	0,586
27,129	38,468	0,962	0,891	0,589
27,15	38,466	0,962	0,892	0,591
27,156	38,468	0,962	0,892	0,593
27,159	38,468	0,962	0,892	0,593
27,192	38,47	0,963	0,896	0,601
27,182	38,452	0,963	0,894	0,598
27,216	38,45	0,963	0,895	0,603
27,168	38,433	0,961	0,886	0,578
27,203	38,433	0,961	0,889	0,586
27,137	38,425	0,959	0,876	0,563
27,138	38,425	0,959	0,877	0,564
27,123	38,415	0,956	0,867	0,55
27,124	38,415	0,956	0,867	0,551
27,064	38,394	0,956	0,871	0,548
27,097	38,404	0,951	0,853	0,529
26,99	38,398	0,955	0,868	0,547
27,109	38,538	0,956	0,869	0,546
27,257	38,508	0,961	0,885	0,587
27,287	38,483	0,962	0,892	0,602
27,313	38,464	0,962	0,893	0,606
27,415	38,399	0,959	0,882	0,589
27,301	38,337	0,937	0,808	0,487
27,193	38,321	0,963	0,897	0,597
27,03	38,314	0,969	0,922	0,689
27,032	38,314	0,969	0,922	0,689
27,912	38,325	0,941	0,815	0,485

**Table C.8 Attenuation relationship:** Brian et al. (2008). . **Values:** Ground Acceleration (g) (Median+ Standard Deviation) **Spectral period T=1 s**

Long	Lat	Ground acceleration $T_R=2475$	Ground acceleration $T_R=475$	Ground acceleration $T_R=72$
26,928	38,481	0,645	0,429	0,209
27,033	38,497	0,778	0,563	0,235
27,057	38,479	0,778	0,574	0,242
27,113	38,464	0,778	0,578	0,251
27,129	38,468	0,778	0,578	0,252
27,15	38,466	0,778	0,578	0,254
27,156	38,468	0,778	0,578	0,254
27,159	38,468	0,778	0,578	0,255
27,192	38,47	0,778	0,579	0,258
27,182	38,452	0,778	0,576	0,257
27,216	38,45	0,778	0,575	0,259
27,168	38,433	0,77	0,559	0,247
27,203	38,433	0,772	0,562	0,25
27,137	38,425	0,758	0,544	0,24
27,138	38,425	0,758	0,544	0,24
27,123	38,415	0,734	0,521	0,233
27,124	38,415	0,734	0,521	0,233
27,064	38,394	0,657	0,447	0,211
27,097	38,404	0,688	0,485	0,22
26,99	38,398	0,661	0,44	0,207
27,109	38,538	0,784	0,784	0,291
27,257	38,508	0,795	0,795	0,318
27,287	38,483	0,806	0,806	0,331
27,313	38,464	0,807	0,807	0,334
27,415	38,399	0,789	0,789	0,317
27,301	38,337	0,578	0,562	0,251
27,193	38,321	0,827	0,62	0,295
27,03	38,314	0,839	0,657	0,365
27,032	38,314	0,839	0,657	0,365
27,912	38,325	0,702	0,702	0,255

**Table C.9 Attenuation relationship:** Boore & Atkinson (2007). **Values:** Ground Acceleration (g) (Median) **Spectral period T=1 s**

Long	Lat	Ground acceleration $T_R=2475$	Ground acceleration $T_R=475$	Ground acceleration $T_R=72$
26,928	38,481	0,193	0,135	0,082
27,033	38,497	0,242	0,173	0,08
27,057	38,479	0,242	0,175	0,082
27,113	38,464	0,242	0,176	0,085
27,129	38,468	0,242	0,176	0,086
27,15	38,466	0,242	0,176	0,086
27,156	38,468	0,242	0,176	0,086
27,159	38,468	0,242	0,176	0,087
27,192	38,47	0,242	0,176	0,088
27,182	38,452	0,242	0,175	0,088
27,216	38,45	0,242	0,175	0,089
27,168	38,433	0,24	0,17	0,086
27,203	38,433	0,24	0,171	0,087
27,137	38,425	0,235	0,166	0,085
27,138	38,425	0,235	0,166	0,085
27,123	38,415	0,226	0,159	0,088
27,124	38,415	0,226	0,159	0,088
27,064	38,394	0,247	0,178	0,096
27,097	38,404	0,229	0,167	0,091
26,99	38,398	0,25	0,176	0,097
27,109	38,538	0,231	0,161	0,08
27,257	38,508	0,236	0,167	0,087
27,287	38,483	0,241	0,173	0,089
27,313	38,464	0,242	0,175	0,089
27,415	38,399	0,233	0,164	0,089
27,301	38,337	0,2	0,141	0,078
27,193	38,321	0,302	0,201	0,099
27,03	38,314	0,304	0,221	0,116
27,032	38,314	0,304	0,221	0,116
27,912	38,325	0,197	0,133	0,077

**Table C.10 Attenuation relationship:** Boore & Atkinson (2007). **Values:** Ground acceleration (g) (Median) **Spectral period** T=0.2 s

Long	Lat	Ground acceleration T <sub>R</sub> =2475	Ground acceleration T <sub>R</sub> =475	Ground acceleration T <sub>R</sub> =72
26,928	38,481	0,665	0,48	0,273
27,033	38,497	0,81	0,611	0,295
27,057	38,479	0,81	0,613	0,307
27,113	38,464	0,81	0,613	0,328
27,129	38,468	0,81	0,613	0,332
27,15	38,466	0,81	0,613	0,336
27,156	38,468	0,81	0,613	0,336
27,159	38,468	0,81	0,613	0,337
27,192	38,47	0,81	0,613	0,34
27,182	38,452	0,81	0,612	0,339
27,216	38,45	0,81	0,612	0,339
27,168	38,433	0,81	0,596	0,327
27,203	38,433	0,81	0,6	0,33
27,137	38,425	0,805	0,579	0,317
27,138	38,425	0,805	0,579	0,317
27,123	38,415	0,779	0,554	0,306
27,124	38,415	0,779	0,554	0,306
27,064	38,394	0,722	0,543	0,308
27,097	38,404	0,713	0,52	0,288
26,99	38,398	0,732	0,539	0,307
27,109	38,538	0,794	0,565	0,304
27,257	38,508	0,806	0,582	0,328
27,287	38,483	0,81	0,607	0,334
27,313	38,464	0,81	0,613	0,334
27,415	38,399	0,801	0,571	0,324
27,301	38,337	0,593	0,417	0,274
27,193	38,321	0,852	0,625	0,326
27,03	38,314	0,854	0,664	0,391
27,032	38,314	0,854	0,664	0,391
27,912	38,325	0,681	0,462	0,266

**Table C.11 Attenuation relationship: Boore & Atkinson (2007). Values: Ground Acceleration (g) (Median +Standard Deviation) Spectral period T=0.2 s**

Long	Lat	Ground acceleration $T_R=2475$	Ground acceleration $T_R=475$	Ground acceleration $T_R=72$
26,928	38,481	0,922	0,754	0,513
27,033	38,497	0,948	0,844	0,509
27,057	38,479	0,953	0,863	0,511
27,113	38,464	0,954	0,871	0,514
27,129	38,468	0,954	0,872	0,521
27,15	38,466	0,954	0,871	0,53
27,156	38,468	0,954	0,871	0,532
27,159	38,468	0,954	0,871	0,533
27,192	38,47	0,955	0,873	0,545
27,182	38,452	0,953	0,869	0,545
27,216	38,45	0,953	0,868	0,549
27,168	38,433	0,949	0,857	0,533
27,203	38,433	0,949	0,859	0,54
27,137	38,425	0,946	0,848	0,517
27,138	38,425	0,946	0,848	0,518
27,123	38,415	0,943	0,837	0,512
27,124	38,415	0,943	0,837	0,512
27,064	38,394	0,944	0,83	0,521
27,097	38,404	0,941	0,822	0,515
26,99	38,398	0,938	0,815	0,537
27,109	38,538	0,943	0,837	0,503
27,257	38,508	0,947	0,853	0,546
27,287	38,483	0,951	0,864	0,547
27,313	38,464	0,952	0,863	0,543
27,415	38,399	0,945	0,847	0,546
27,301	38,337	0,899	0,741	0,505
27,193	38,321	0,942	0,832	0,582
27,03	38,314	0,958	0,878	0,611
27,032	38,314	0,958	0,879	0,61
27,912	38,325	0,91	0,737	0,469

**Table C.12 Attenuation relationship:** Boore & Atkinson (2007). **Values:** Ground Acceleration (g) (Median +Standard Deviation) **Spectral period** T=1.0 s

Long	Lat	Ground acceleration T <sub>R</sub> =2475	Ground acceleration T <sub>R</sub> =475	Ground acceleration T <sub>R</sub> =72
26,928	38,481	0,367	0,257	0,157
27,033	38,497	0,446	0,33	0,155
27,057	38,479	0,446	0,335	0,157
27,113	38,464	0,446	0,336	0,162
27,129	38,468	0,446	0,337	0,163
27,15	38,466	0,446	0,336	0,164
27,156	38,468	0,446	0,336	0,164
27,159	38,468	0,446	0,336	0,164
27,192	38,47	0,446	0,337	0,167
27,182	38,452	0,446	0,335	0,167
27,216	38,45	0,446	0,335	0,169
27,168	38,433	0,444	0,326	0,163
27,203	38,433	0,445	0,327	0,165
27,137	38,425	0,438	0,316	0,164
27,138	38,425	0,438	0,316	0,164
27,123	38,415	0,424	0,304	0,169
27,124	38,415	0,424	0,304	0,169
27,064	38,394	0,473	0,339	0,184
27,097	38,404	0,438	0,32	0,175
26,99	38,398	0,478	0,335	0,185
27,109	38,538	0,431	0,307	0,155
27,257	38,508	0,439	0,318	0,165
27,287	38,483	0,446	0,331	0,169
27,313	38,464	0,446	0,334	0,17
27,415	38,399	0,435	0,313	0,169
27,301	38,337	0,382	0,269	0,149
27,193	38,321	0,577	0,384	0,189
27,03	38,314	0,581	0,422	0,22
27,032	38,314	0,581	0,422	0,22
27,912	38,325	0,375	0,253	0,149

## **APPENDIX D**

### Recurrence Relationship of Seismic Zones

**ZONE 1**

Time (Year)	Magnitude								
	4,2	4,7	5,2	5,7	6,2	6,7	7,2	7,7	8,2
10	3	1	3						
20	11	2	3	1					
40	16	4	3	1					
50	17	4	3	1					
100	17	6	4	1					
1000				4	5		7	4	

Table D.1 Total earthquake occurrences

Time (Year)	Magnitude								
	4,2	4,7	5,2	5,7	6,2	6,7	7,2	7,7	8,2
10	0,3	0,1	0,3						
20	0,55	0,1	0,15						
40	0,4	0,1	0,075						
50	0,34	0,08	0,06	0,02					
100	0,17	0,06	0,04	0,01					
1000	0	0	0	0,004	0	0,005	0	0,007	0,004

Table D.2 Annual earthquake occurrences

Magnitude							
4,2	4,7	5,2	5,7	6,2	6,7	7,2	7,7
0,55	0,1	0,3	0,02		0,005		0,007
0,314	0,1717	0,0939	0,0514	0,0281	0,0154	0,0084	0,0046

Table D.3 Selected and adjusted rates of occurrences

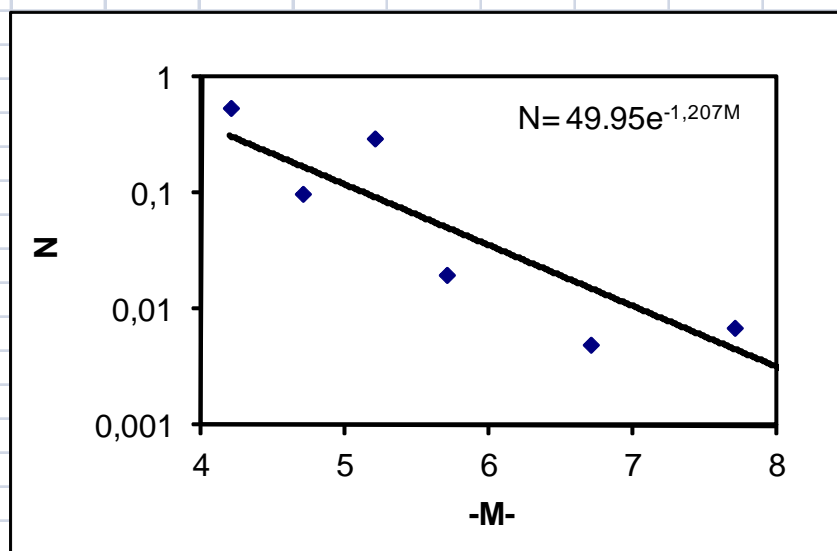


Figure D.1 Recurrence relationship for Source Zone 1

**ZONE 2**

Time (Year)	Magnitude								
	4,2	4,7	5,2	5,7	6,2	6,7	7,2	7,7	8,2
10									
20			1						
40	2		2						
50	4		2						
100	5	6	1						
1000								3	

Table D.4 Total earthquake occurrences

Time (Year)	Magnitude								
	4,2	4,7	5,2	5,7	6,2	6,7	7,2	7,7	8,2
10									
20									
40	0,05	0,05							
50	0,08	0,04							
100	0,05	0,06	0,01						
1000	0	0	0	0	0	0	0	0,003	

Table D.5 Annual earthquake occurrences

Magnitude								
4,2	4,7	5,2	5,7	6,2	6,7	7,2	7,7	8,2
0,08	0,06	0,01						0,003
0,0572	0,0387	0,0261	0,0177	0,0119	0,0081	0,0055	0,0037	0,0025

Table D.6 Selected and adjusted rates of occurrences

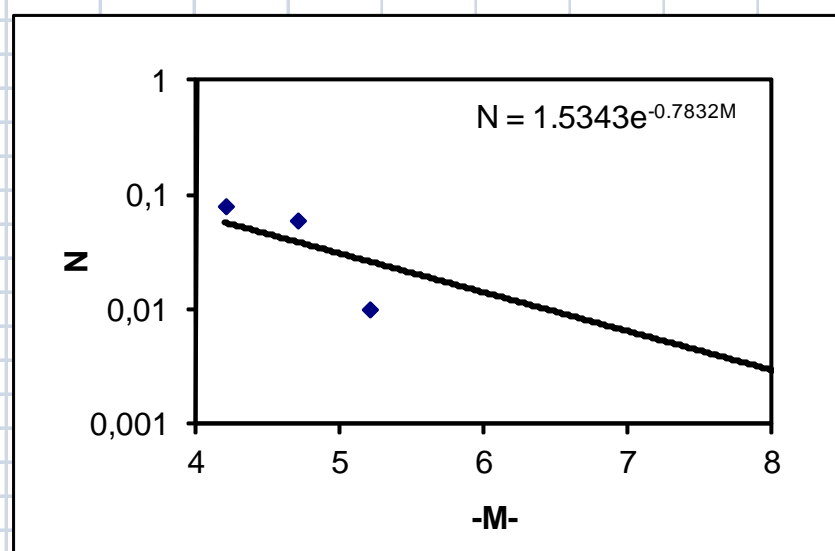


Figure D.2 Recurrence relationship for Source Zone 2

**ZONE 3**

Time (Year)	Magnitude								
	4,2	4,7	5,2	5,7	6,2	6,7	7,2	7,7	8,2
10	6	1	3						
20	6	1	3						
40	6	2	4						
50	6	2	4						
100	18	9	5						
1000									4

Table D.7 Total earthquake occurrences

Time (Year)	Magnitude								
	4,2	4,7	5,2	5,7	6,2	6,7	7,2	7,7	8,2
10	0,6	0,1	0,3						
20	0,3	0,05	0,15		0				
40	0,15	0,05	0,1		0				
50	0,12	0,04	0,08		0				
100	0,18	0,09	0,05	0	0				
1000	0	0	0	0	0	0	0	0,004	

Table D.8 Annual earthquake occurrences

MERKEZ BUYUKLUK							
4,2	4,7	5,2	5,7	6,2	6,7	7,2	7,7
0,6	0,1	0,3					0,004
0,4596	0,2561	0,1428	0,0796	0,0443	0,0247	0,0138	0,0077

Table D.9 Selected and adjusted rates of occurrences

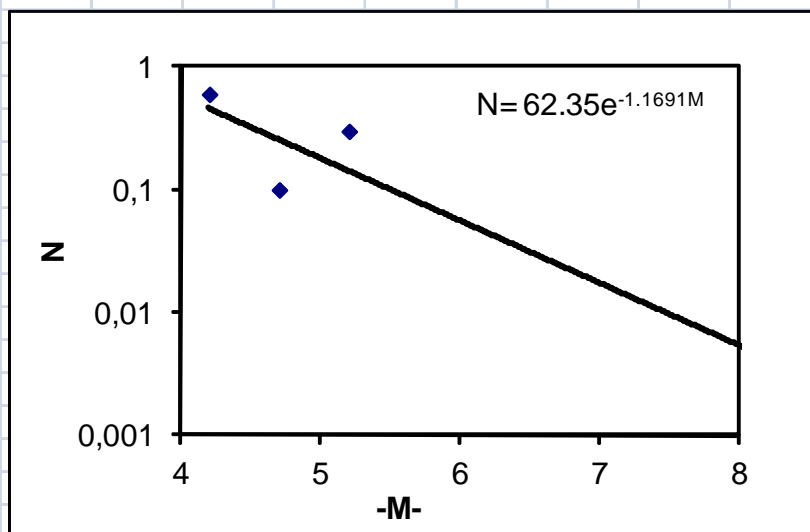


Figure D.3 Recurrence relationship for Source Zone 3

**ZONE 4**

Time (Year)	Magnitude								
	4,2	4,7	5,2	5,7	6,2	6,7	7,2	7,7	8,2
10									
20									
40	1								
50	1								
100	3	5				1			
1000									

Table D.10 Total earthquake occurrences

Time (Year)	Magnitude								
	4,2	4,7	5,2	5,7	6,2	6,7	7,2	7,7	8,2
10	0	0	0						
20	0	0	0						
40	0,025	0	0						
50	0,02	0	0						
100	0,03	0,05	0	0	0,01				
1000									

Table D.11 Annual earthquake occurrences

Magnitude								
4,2	4,7	5,2	5,7	6,2	6,7	7,2	7,7	8,2
0,03	0,05			0,01				
0,0431	0,0308	0,0221	0,0158	0,0113	0,0081	0,0058	0,0041	0,003

Table D.12 Selected and adjusted rates of occurrences

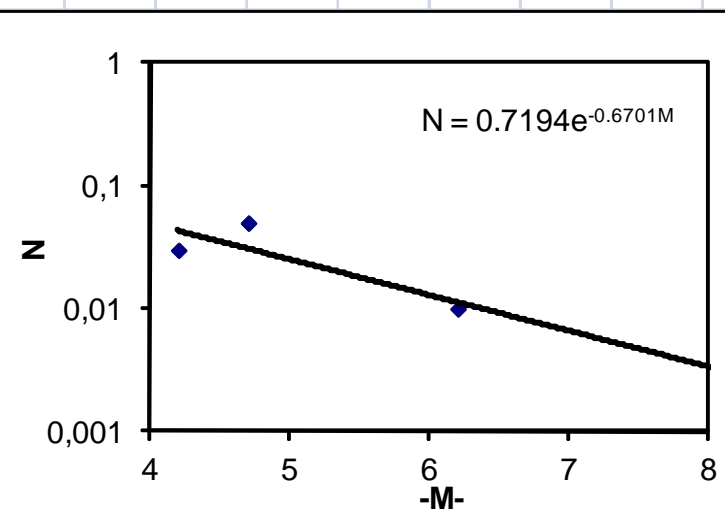


Figure D.4 Recurrence relationship for Karaburun Source Zone 4

**ZONE 5**

Time (Year)	Magnitude								
	4,2	4,7	5,2	5,7	6,2	6,7	7,2	7,7	8,2
10	1	1							
20	1	1	1						
40	3	3	1						
50	6	4	1						
100	6	8	3	2					
1000									

Table D.13 Total earthquake occurrences

Time (Year)	Magnitude								
	4,2	4,7	5,2	5,7	6,2	6,7	7,2	7,7	8,2
10									
20	0,05	0,05							
40	0,075	0,075							
50	0,12	0,08							
100	0,06	0,08	0,03	0,02	0				
1000									

Table D.14 Annual earthquake occurrences

Magnitude								
4,2	4,7	5,2	5,7	6,2	6,7	7,2	7,7	8,2
0,12	0,08	0,03	0,02					
0,1271	0,0673	0,0357	0,0189	0,01	0,0053	0,0028	0,0015	0,0008

Table D.15 Selected and adjusted rates of occurrences

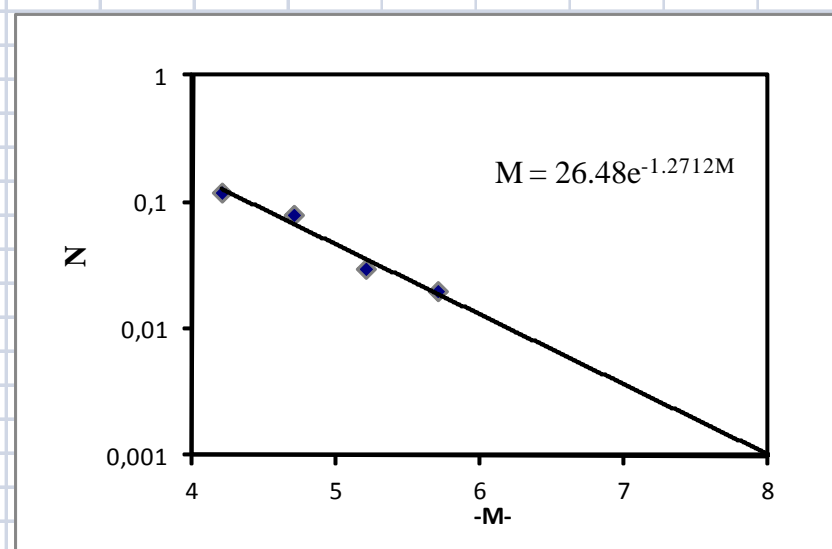


Figure D.5 Recurrence relationship for Source Zone 5

### ZONE 6

Time (Year)	Magnitude								
	4,2	4,7	5,2	5,7	6,2	6,7	7,2	7,7	8,2
10	1								
20	7								
40	14								
50	14		1						
100	21	4	4						
1000				2				3	2

Table D.16 Total earthquake occurrences

Time (Year)	Magnitude								
	4,2	4,7	5,2	5,7	6,2	6,7	7,2	7,7	8,2
10	0,1	0	0						
20	0,35	0	0						
40	0,35	0	0						
50	0,28	0	0,02						
100	0,21	0,04	0,04						
1000	0	0	0	0,002	0	0	0	0,003	0,002

Table D.17 Annual earthquake occurrences

Magnitude								
4,2	4,7	5,2	5,7	6,2	6,7	7,2	7,7	8,2
0,35	0,04	0,04	0,002				0,003	0,002
0,0894	0,0524	0,0307	0,0179	0,0105	0,0062	0,0036	0,0021	0,0012

Table D.18 Selected and adjusted rates of occurrences

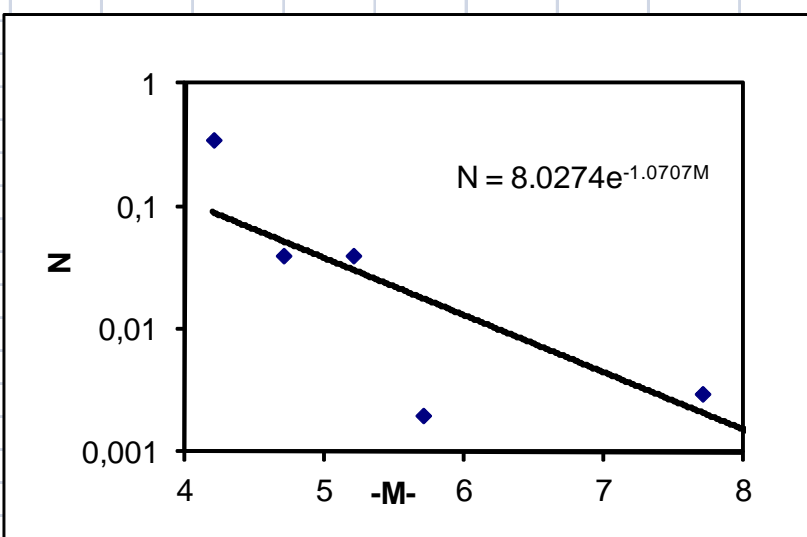


Figure D.6 Recurrence relationship for Source Zone 6

### ZONE 7

Time (Year)	Magnitude								
	4,2	4,7	5,2	5,7	6,2	6,7	7,2	7,7	8,2
10	5	2							
20	6	3							
40	6	3							
50	15	5	1						
100	39	10	4	1					
1000						1		1	

Table D.19 Total earthquake occurrences

Time (Year)	Magnitude								
	4,2	4,7	5,2	5,7	6,2	6,7	7,2	7,7	8,2
10	0,5	0,2	0						
20	0,3	0,15	0		0				
40	0,15	0,075	0		0				
50	0,3	0,1	0,02	0	0				
100	0,39	0,1	0,04	0,01	0				
1000	0	0	0	0	0	0,001	0	0,001	0

Table D.20 Annual earthquake occurrences

Magnitude								
4,2	4,7	5,2	5,7	6,2	6,7	7,2	7,7	8,2
0,5	0,2	0,04	0,01		0,001		0,001	
0,338	0,1283	0,0487	0,0185	0,007	0,0027	0,001	0,0004	0,0001

Table D.21 Selected and adjusted rates of occurrences

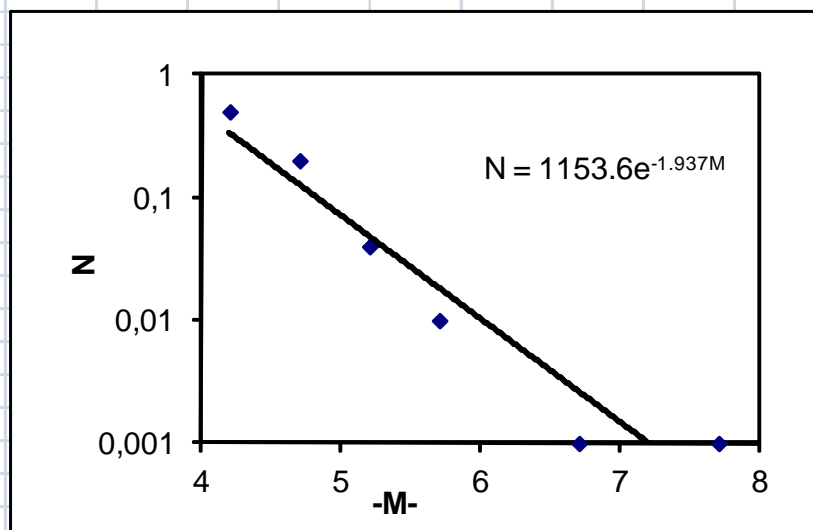


Figure D.7 Recurrence relationship for Source Zone 7

**ZONE 8**

Time (Year)	Magnitude								
	4,2	4,7	5,2	5,7	6,2	6,7	7,2	7,7	8,2
10									
20	1								
40	5	1							
50	6	1							
100	6	3	3	1	1				
1000				2		2	1	5	

Table D.22 Total earthquake occurrences

Time (Year)	Magnitude								
	4,2	4,7	5,2	5,7	6,2	6,7	7,2	7,7	8,2
10	0	0	0						
20	0,05	0	0		0				
40	0,125	0,025	0		0				
50	0,12	0,02	0		0				
100	0,06	0,03	0,03	0,01	0,01				
1000	0	0	0	0,002	0	0,002	0	0,001	0,005

Table D.23 Annual earthquake occurrences

Magnitude								
4,2	4,7	5,2	5,7	6,2	6,7	7,2	7,7	8,2
0,125	0,03	0,03	0,01	0,01	0,002		0,001	0,005
0,0623	0,0384	0,0237	0,0146	0,009	0,0055	0,0034	0,0021	0,0013

Table D.24 Selected and adjusted rates of occurrences

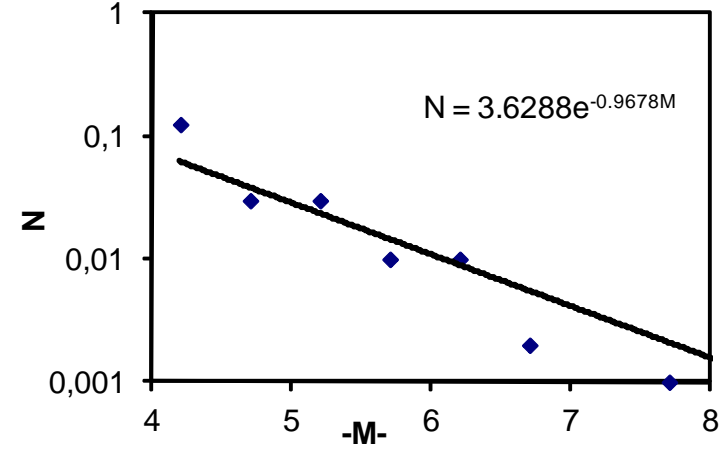


Figure D.8 Recurrence relationship for Source Zone 8

**ZONE 9**

Time (Year)	Magnitude								
	4,2	4,7	5,2	5,7	6,2	6,7	7,2	7,7	8,2
10			1						
20	3	2	1						
40	6	2	1						
50	7	2	1						
100	8	6	2		1				
1000		1		1		2		2	1

Table D.25 Total earthquake occurrences

Time (Year)	Magnitude								
	4,2	4,7	5,2	5,7	6,2	6,7	7,2	7,7	8,2
10	0	0,1	0						
20	0,15	0,1	0,05		0				
40	0,15	0,05	0,025		0				
50	0,14	0,04	0,02		0				
100	0,08	0,06	0,02		0,01				
1000	0	0,001	0	0,001	0	0,002	0	0,002	0,001

Table D.26 Annual earthquake occurrences

Magnitude								
4,2	4,7	5,2	5,7	6,2	6,7	7,2	7,7	8,2
0,15	0,1	0,05	0,001	0,01	0,002		0,002	0,001
0,0892	0,0478	0,0256	0,0137	0,0074	0,0039	0,0021	0,0011	0,0006

Table D.27 Selected and adjusted rates of occurrences

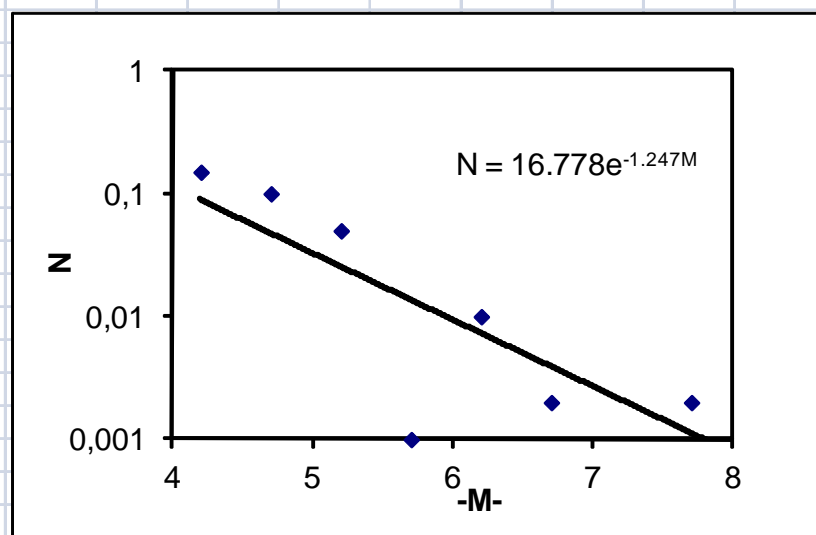


Table D.9 Recurrence relationship for Source Zone 9

### ZONE 10

Time (Year)	Magnitude								
	4,2	4,7	5,2	5,7	6,2	6,7	7,2	7,7	8,2
10									
20	1								
40	3	1							
50	4	1							
100	5	4	1						
1000								1	

Table D.28 Total earthquake occurrences

Time (Year)	Magnitude								
	4,2	4,7	5,2	5,7	6,2	6,7	7,2	7,7	8,2
10	0	0	0						
20	0,05	0	0		0				
40	0,075	0,025	0		0				
50	0,08	0,02	0	0	0				
100	0,05	0,04	0,01	0	0				
1000	0	0	0	0	0	0	0	0,001	

Table D.29 Annual earthquake occurrences

Magnitude								
4,2	4,7	5,2	5,7	6,2	6,7	7,2	7,7	8,2
0,08	0,04	0,01						0,001
0,0562	0,0334	0,0198	0,0117	0,007	0,0041	0,0025	0,0015	0,0009

Table D.30 Selected and adjusted rates of occurrences

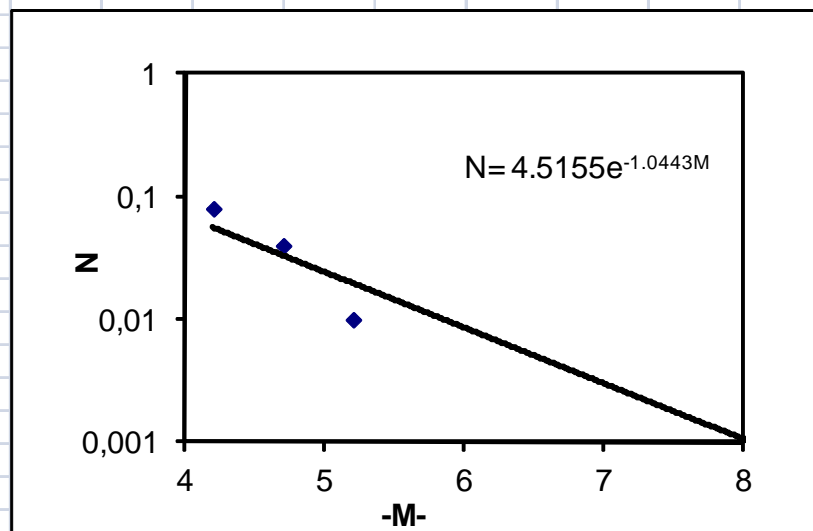


Figure D.10 Recurrence relationship for Source Zone 10

### ZONE 11

Time (Year)	Magnitude								
	4,2	4,7	5,2	5,7	6,2	6,7	7,2	7,7	8,2
10	1								
20	4	1	2						
40	12	3	2						
50	12	3	2						
100	13	7	5		1				
1000									

Table D.31 Total earthquake occurrences

Time (Year)	Magnitude								
	4,2	4,7	5,2	5,7	6,2	6,7	7,2	7,7	8,2
10	0,1	0	0						
20	0,2	0,05	0,1		0				
40	0,3	0,075	0,05		0				
50	0,24	0,06	0,04	0	0				
100	0,13	0,07	0,05	0	0,01				
1000	0	0	0	0	0	0	0	0	

Table D.32 Annual earthquake occurrences

Magnitude								
4,2	4,7	5,2	5,7	6,2	6,7	7,2	7,7	8,2
0,3	0,075	0,1		0,01				
0,2731	0,1243	0,0566	0,0257	0,0117	0,0053	0,0024	0,0011	0,0005

Table D.33 Selected and adjusted rates of occurrences

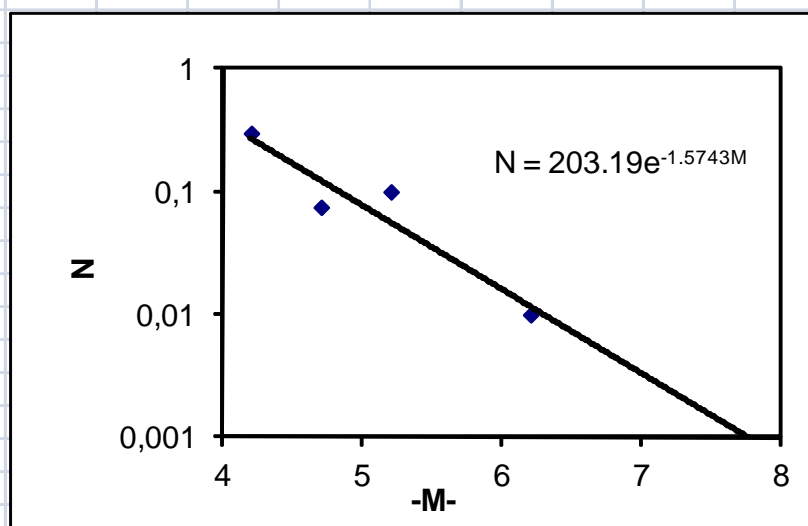
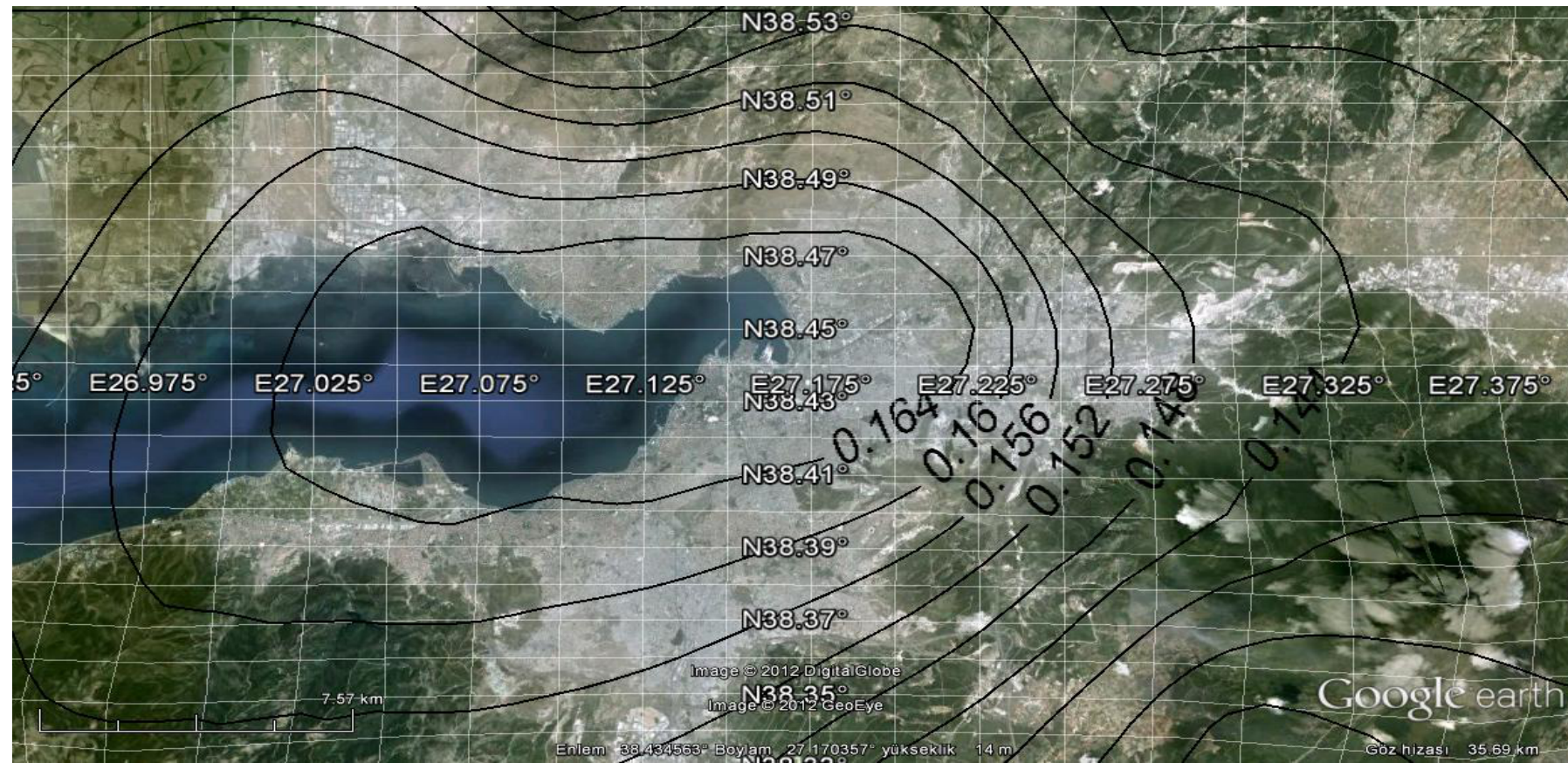
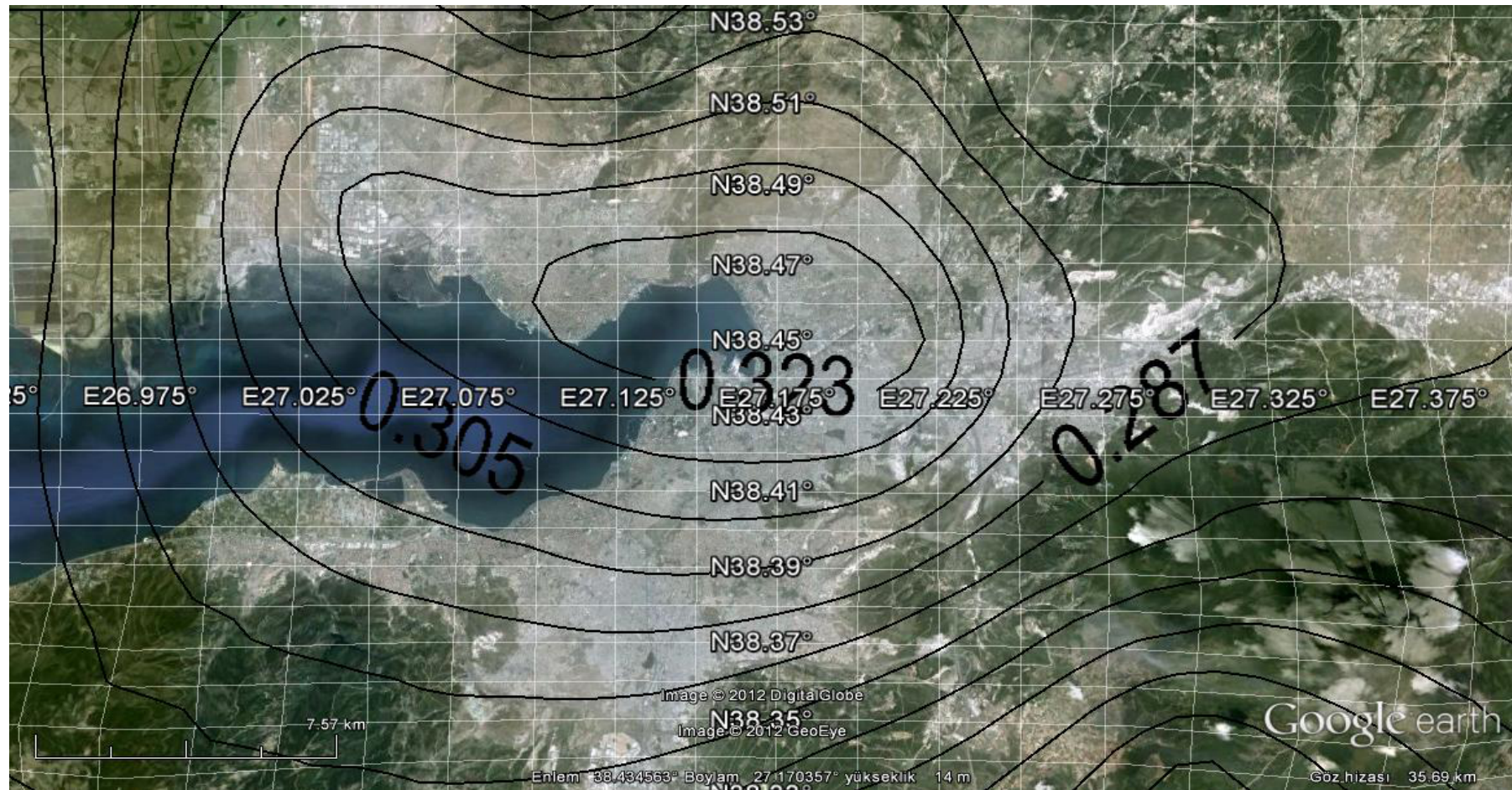


Figure D.11 Recurrence relationship for Source Zone 11

## **APPENDIX E**

### Seismic Hazard Maps





**Figure E.2 (MAP 2): Attenuation relationship:** Campbell & Bozorgnia (2008). **Probability of exceedance in 50 years:** 10%  
**Values:** Ground Acceleration (g) (Median)      **Spectral period T=1s**       $V_{s30}=760 \text{ m/s}$

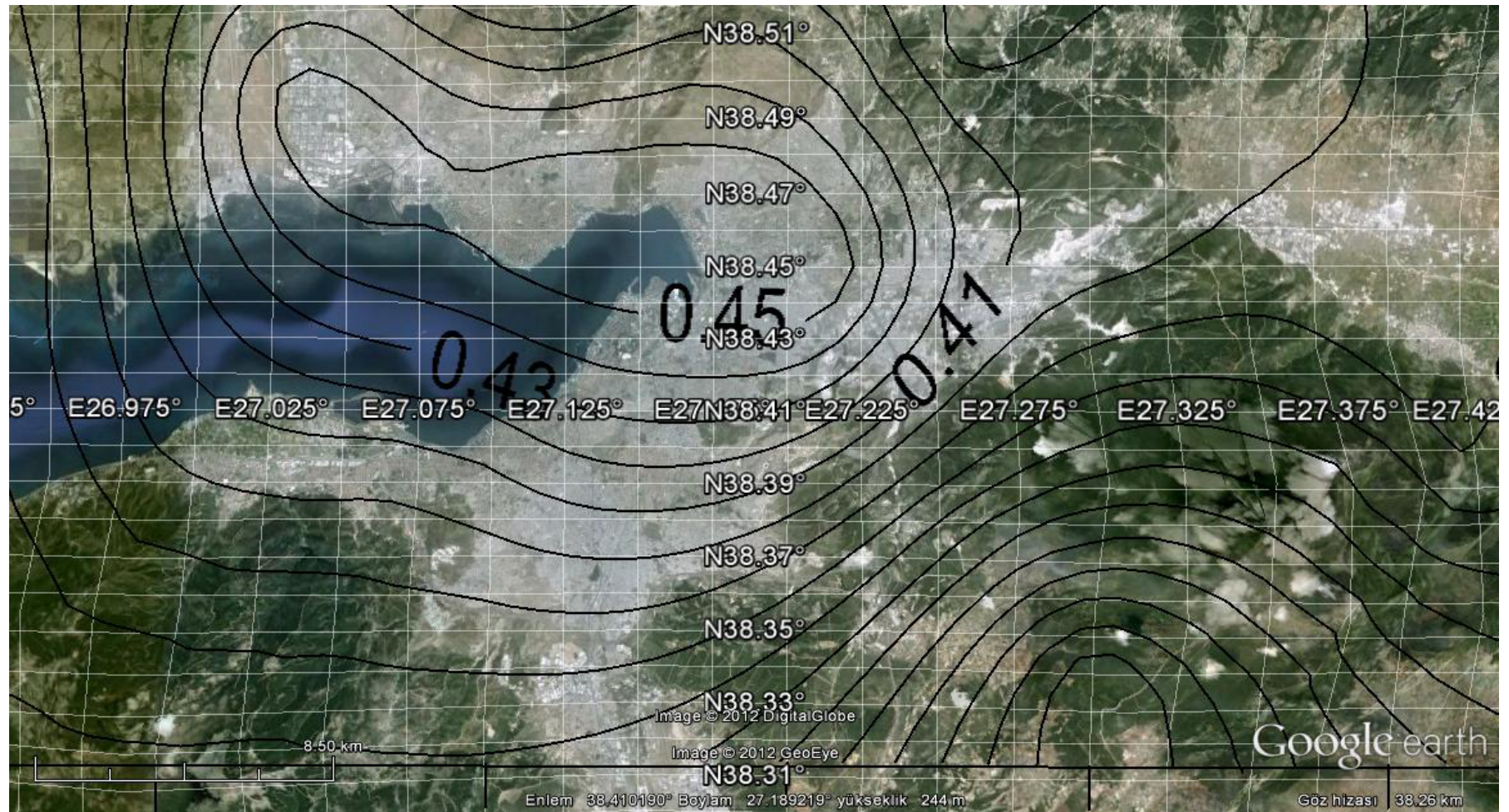


Figure E.3 (MAP 3): Attenuation relationship: Campbell & Bozorgnia (2008). Probability of exceedance in 50 years: 2%  
Values: Ground Acceleration (g) (Median)      Spectral period T=1s       $V_{s30}=760 \text{ m/s}$

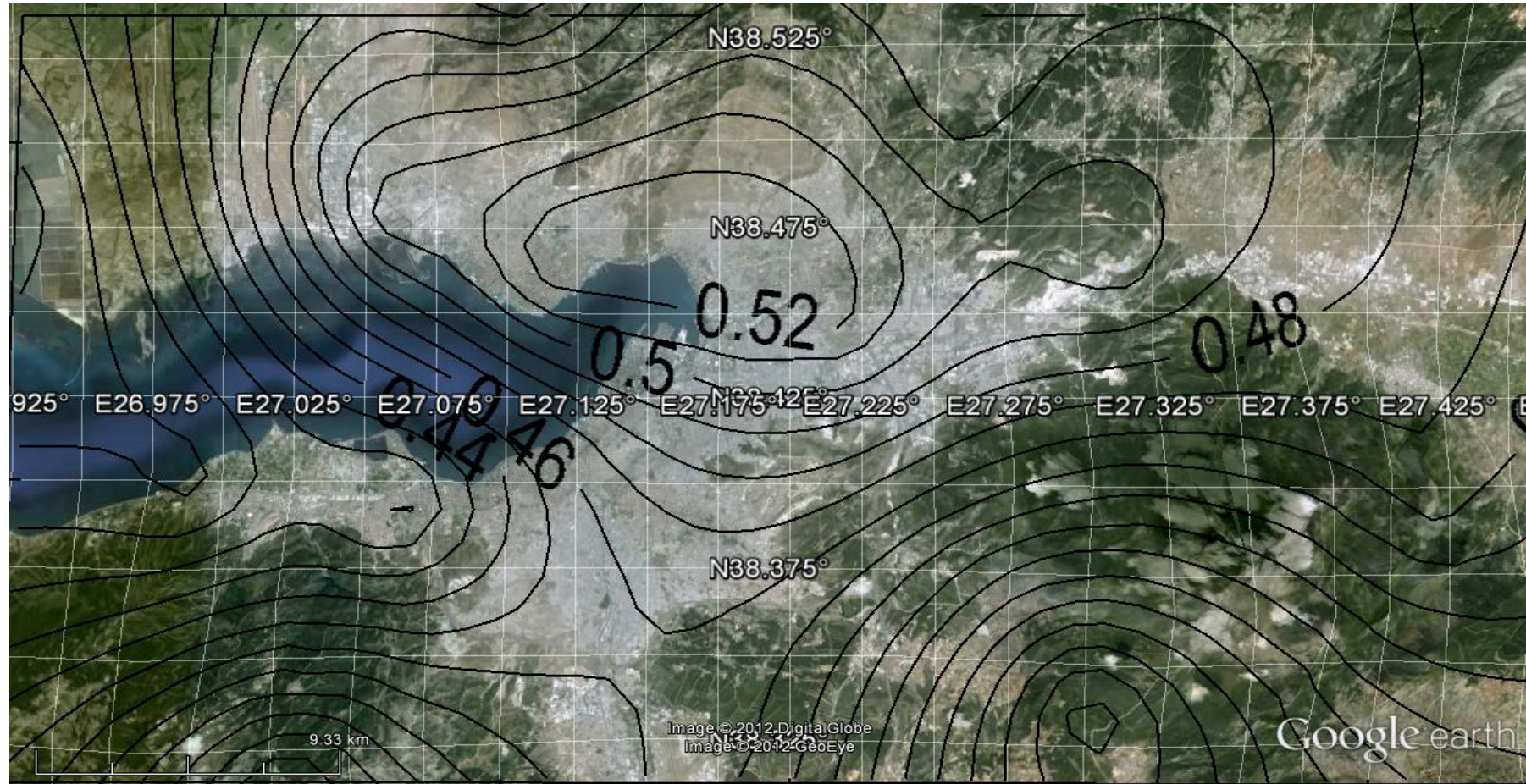
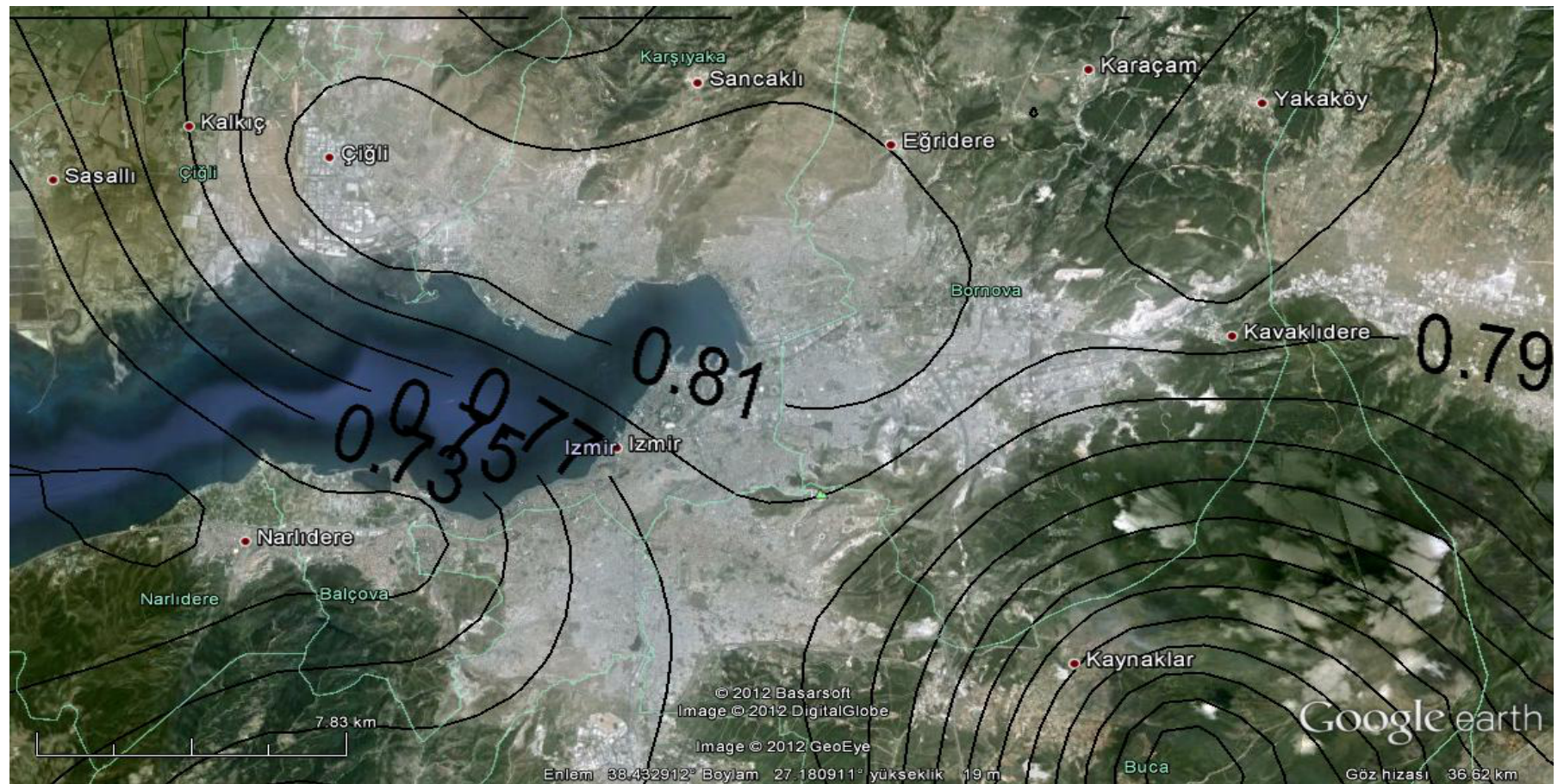


Figure E.4 (MAP 4): **Attenuation relationship:** Campbell & Bozorgnia (2008). **Probability of exceedance in 50 years:** 50%  
**Values:** Ground Acceleration (g) (Median)      **Spectral period** T=0.2s       $V_{s30}=760 \text{ m/s}$



**Figure E.5 (MAP 5): Attenuation relationship:** Campbell & Bozorgnia (2008). **Probability of exceedance in 50 years:** 10%  
**Values:** Ground Acceleration (g) (Median)      **Spectral period T=0.2s**     $V_{s30}=760 \text{ m/s}$

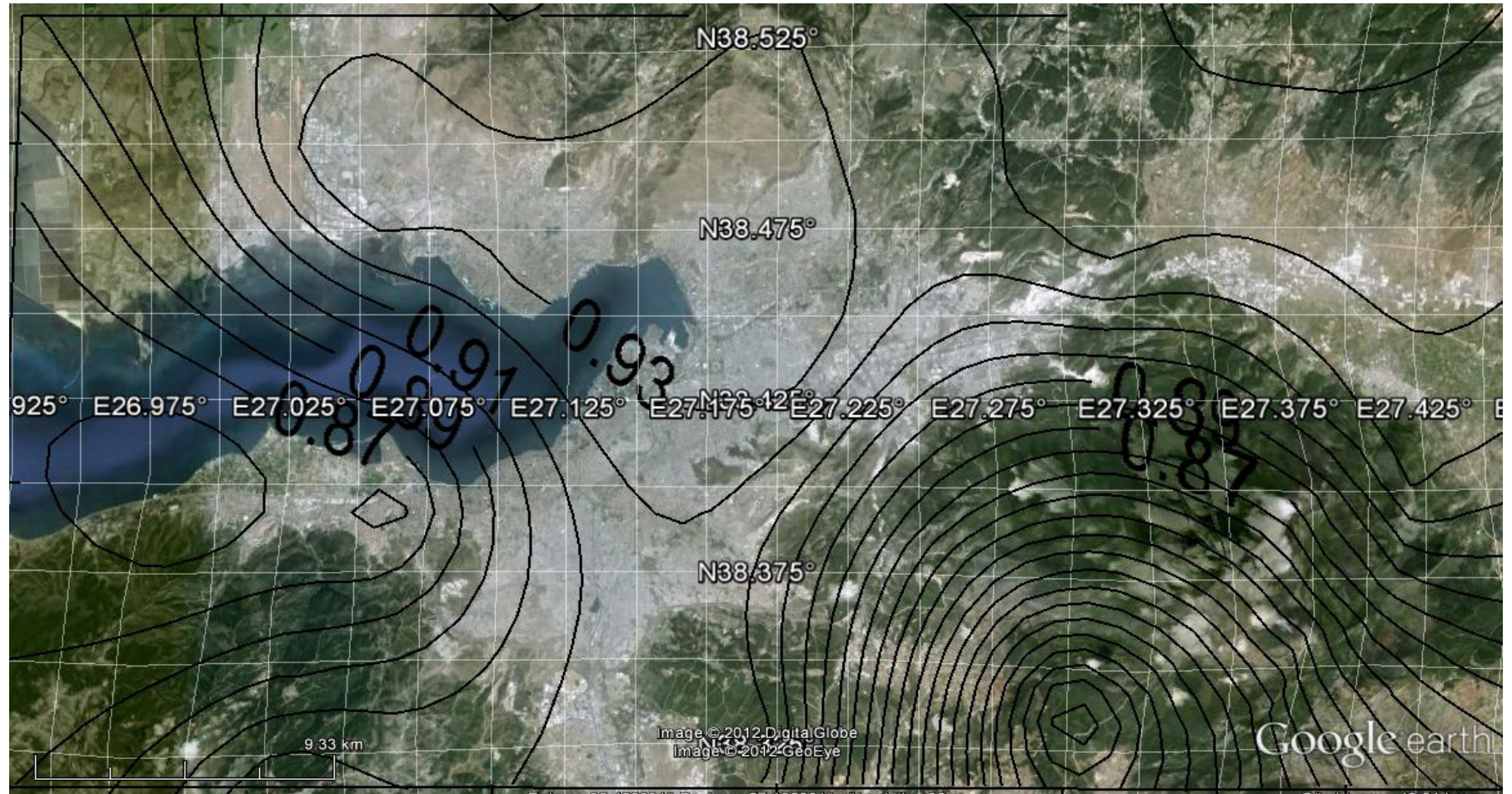


Figure E.6 (MAP 6): **Attenuation relationship:** Campbell & Bozorgnia (2008). **Probability of exceedance in 50 years: 2%**  
**Values:** Ground Acceleration (g) (Median)      **Spectral period T=0.2s**       $V_{s30}=760 \text{ m/s}$

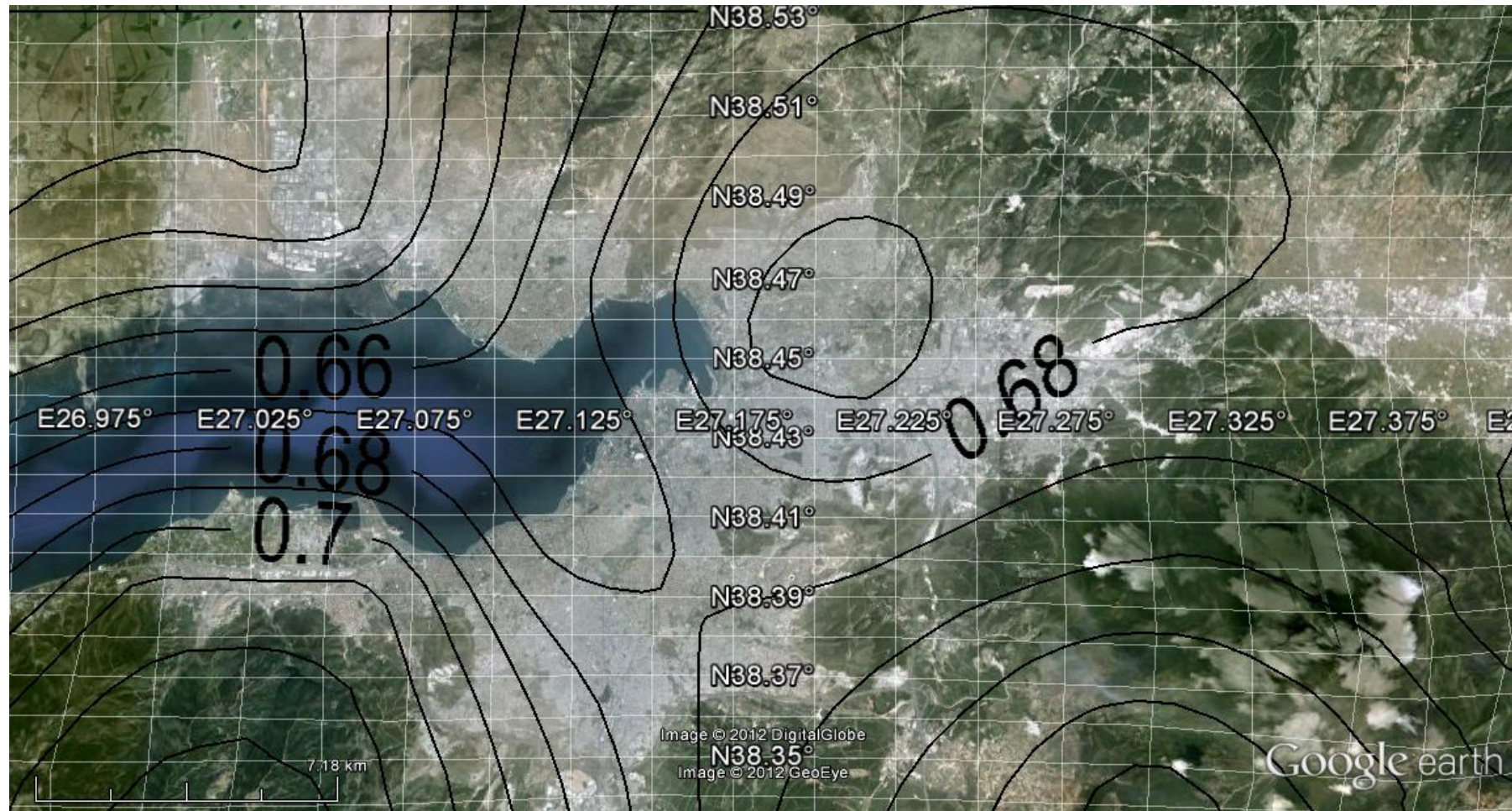


Figure E.7 (MAP 7): Attenuation relationship: Campbell & Bozorgnia (2008). Probability of exceedance in 50 years: 50% Values: Ground Acceleration (g) (Median +Standard Deviation). Spectral period T=0.2s V<sub>s30</sub>=760 m/s

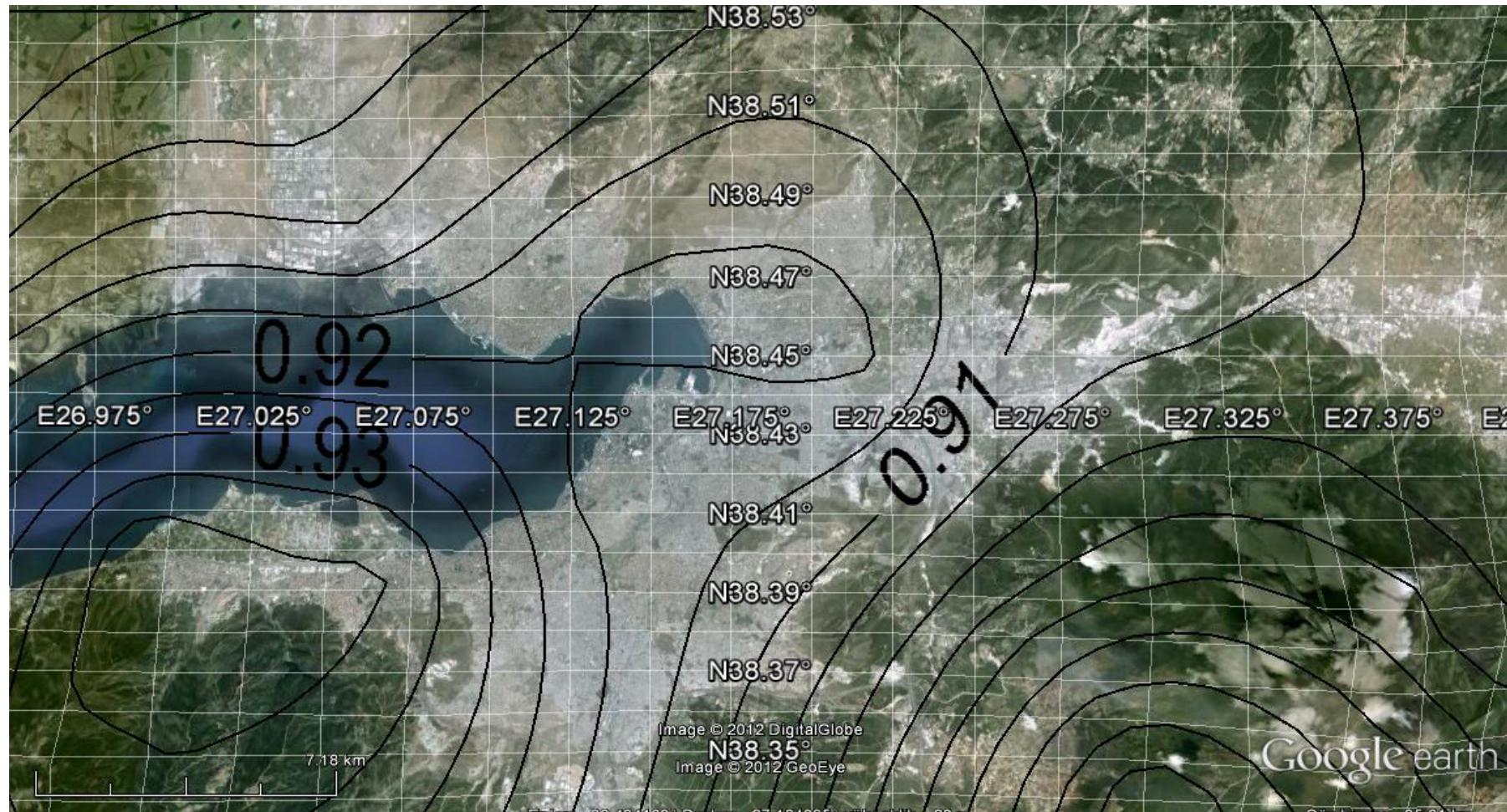


Figure E.8 (MAP 8): **Attenuation relationship:** Campbell & Bozorgnia (2008). **Probability of exceedance in 50 years:** 10%  
**Values:** Ground Acceleration (g) (Median +Standard Deviation). **Spectral period T=0.2s** **V<sub>s30</sub>=760 m/s**

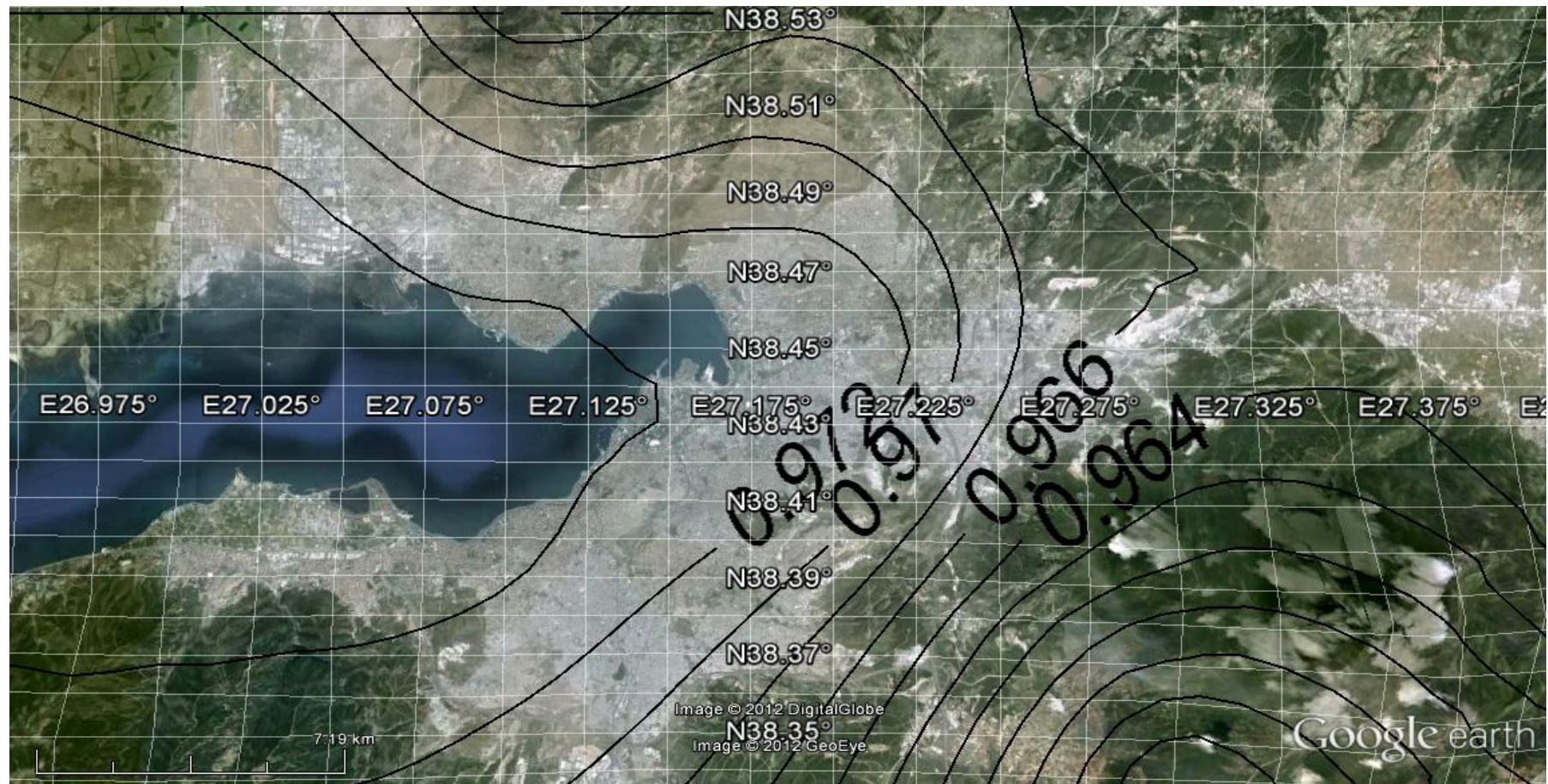


Figure E.9 (MAP 9): **Attenuation relationship:** Campbell & Bozorgnia (2008). **Probability of exceedance in 50 years:** 2%  
**Values:** Ground Acceleration (g) (Median +Standard Deviation). **Spectral period** T=0.2s  $V_{s30}=760$  m/s

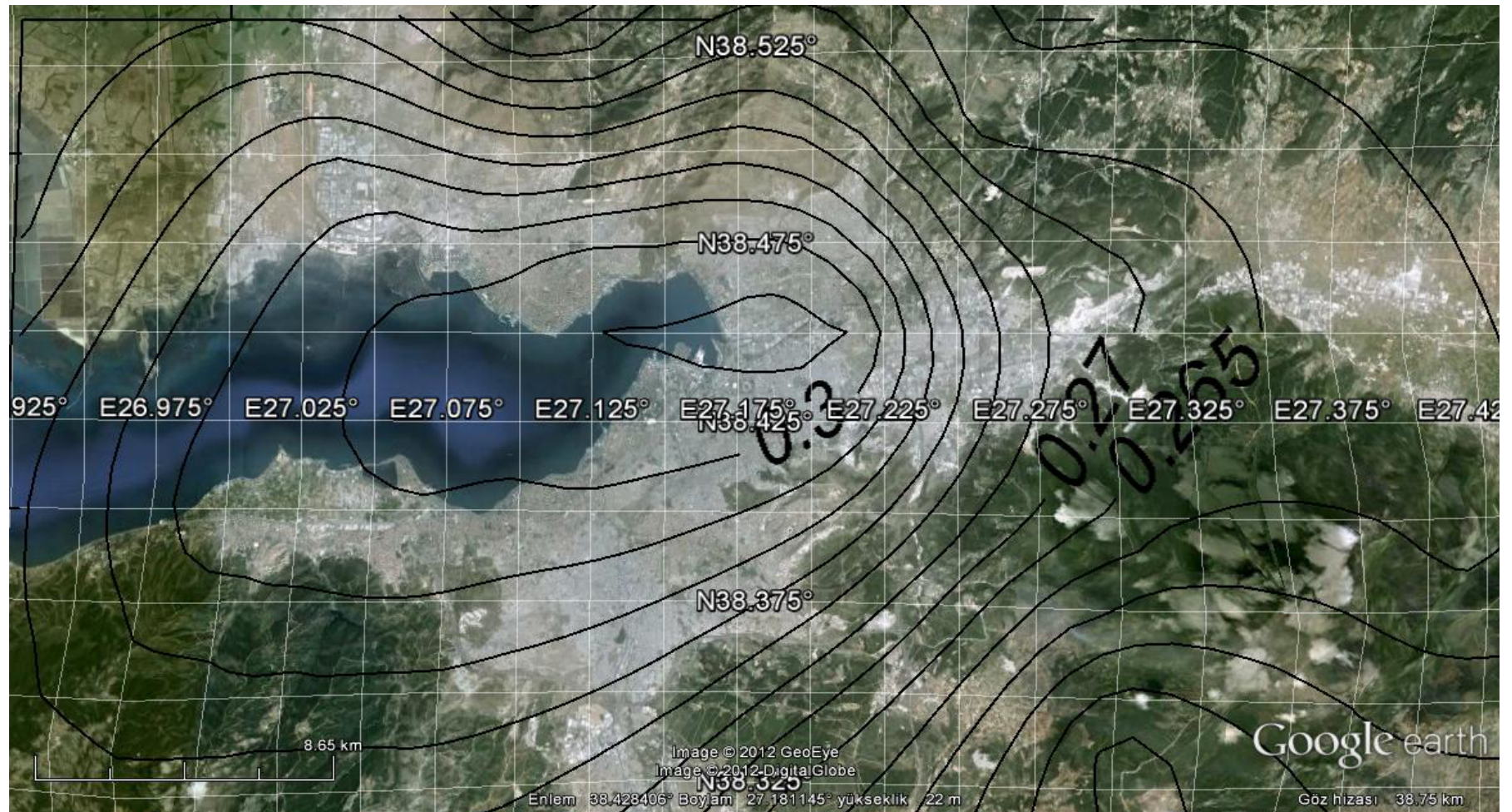


Figure E.10 (MAP 10): **Attenuation relationship:** Campbell & Bozorgnia (2008). **Probability of exceedance in 50 years:** 50%  
**Values:** Ground Acceleration (g) (Median +Standard Deviation). **Spectral period T=1 s**  $V_{s30}=760 \text{ m/s}$

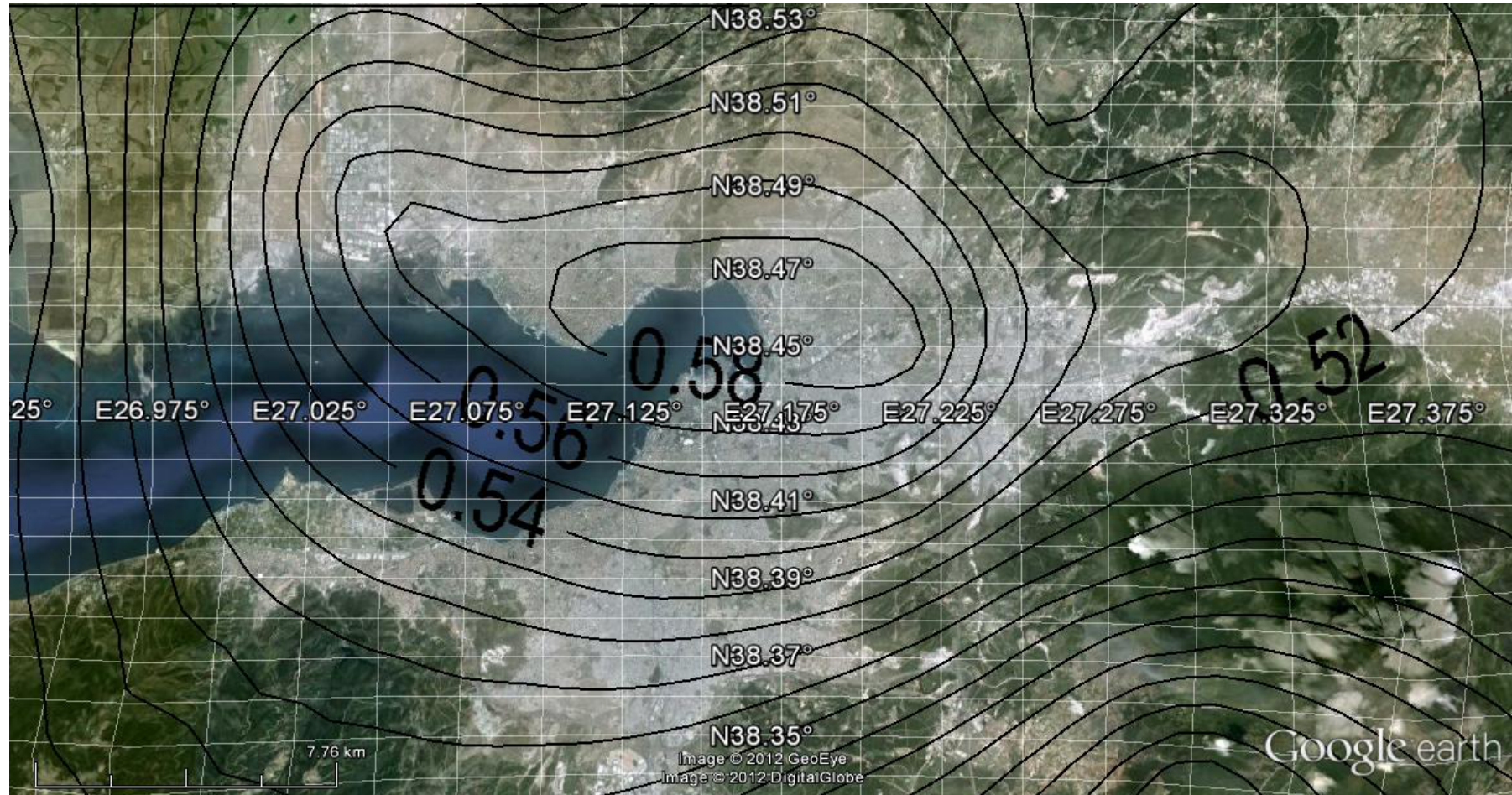


Figure E.11 (MAP 11): Attenuation relationship: Campbell & Bozorgnia (2008). Probability of exceedance in 50 years: 10% Values: Ground Acceleration (g) (Median +Standard Deviation). Spectral period T=1 s V<sub>s30</sub>=760 m/s

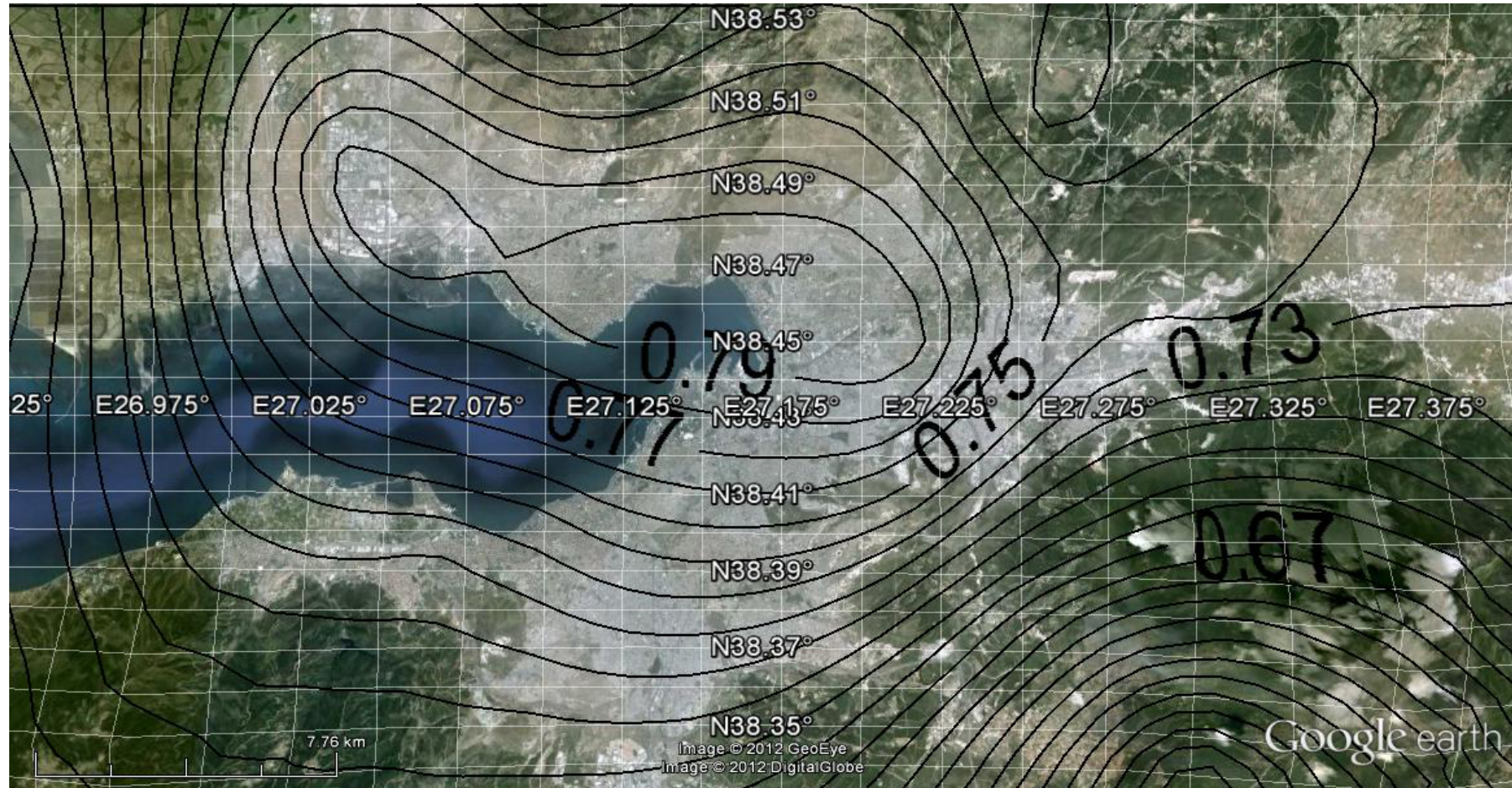


FIGURE 12 (MAP 12): **Attenuation relationship:** Campbell & Bozorgnia (2008). **Probability of exceedance in 50 years: 2%**  
**Values:** Ground Acceleration (g) (Median +Standard Deviation). **Spectral period T=1 s**  $V_{s30}=760 \text{ m/s}$

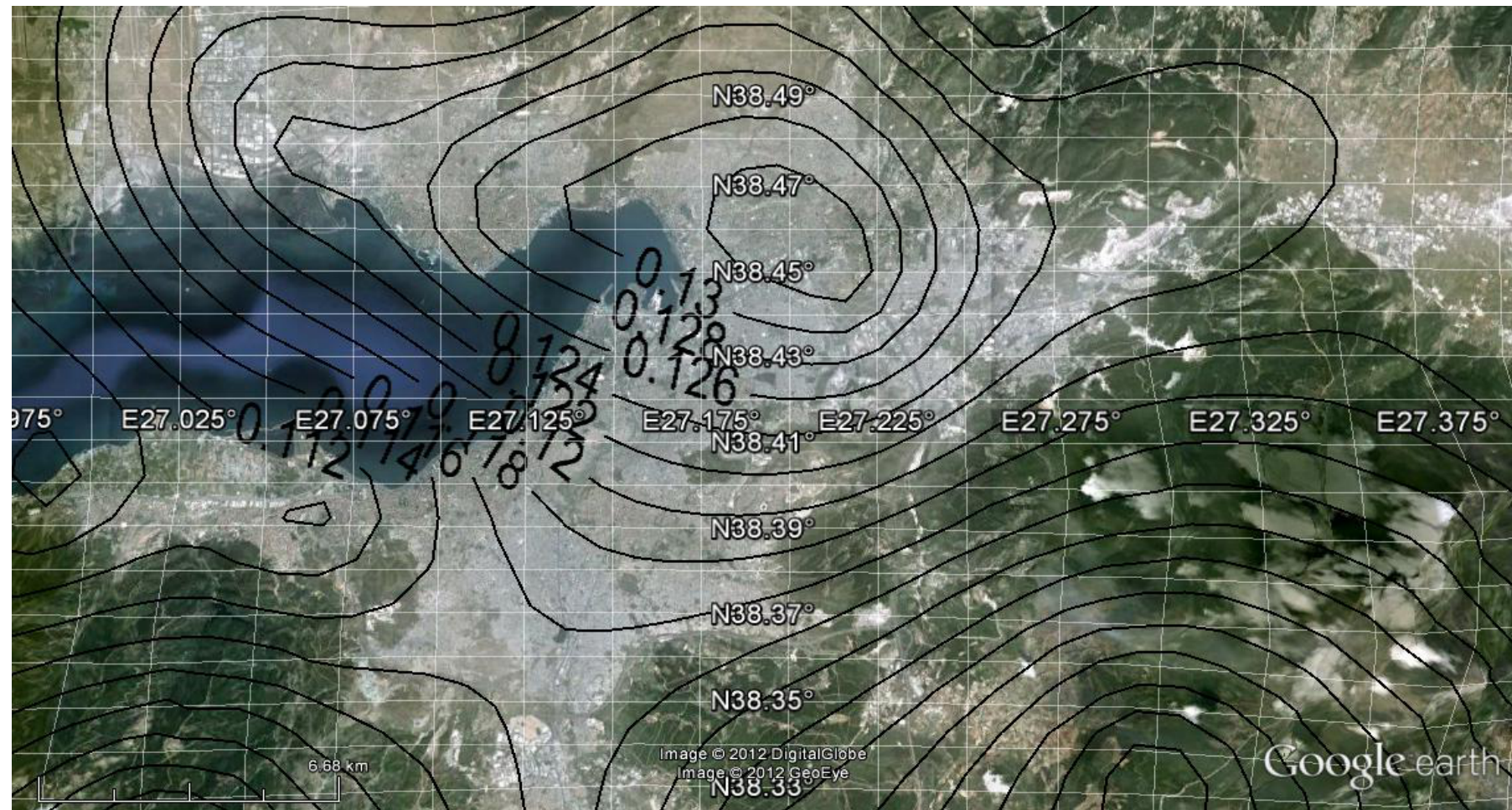


Figure E.13 (MAP 13): **Attenuation relationship**: Brian et al. (2008). **Probability of exceedance in 50 years**: 50%  
Ground Acceleration (g) (Median)    Spectral period T=1 s     $V_{s30}=760$  m/s

Values:

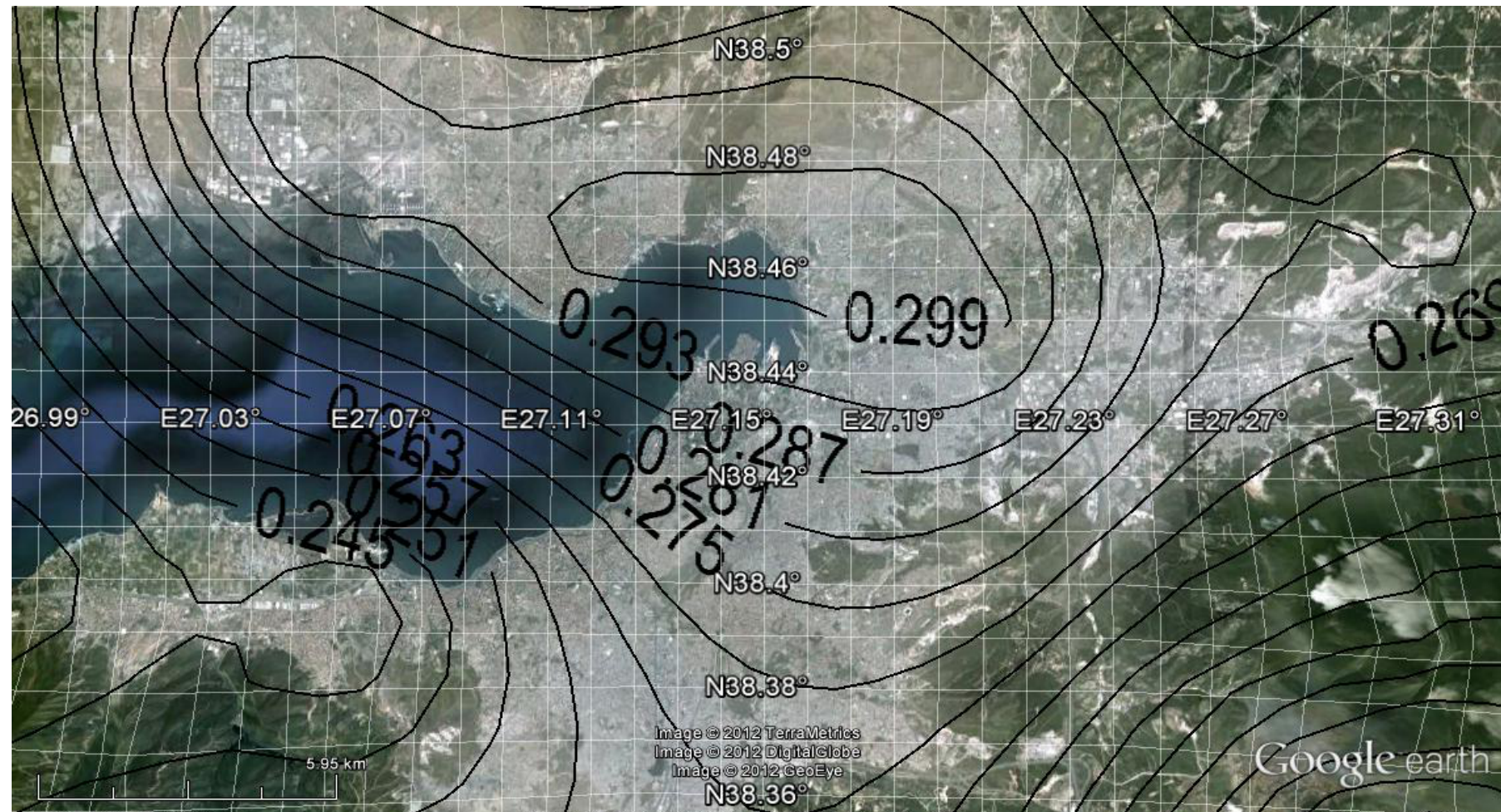


Figure E.14 (MAP 14): **Attenuation relationship:** Brian et al. (2008). **Probability of exceedance in 50 years:** 10%  
Ground Acceleration (g) (Median)      Spectral period T=1 s      V<sub>s30</sub>=760 m/s

Values:

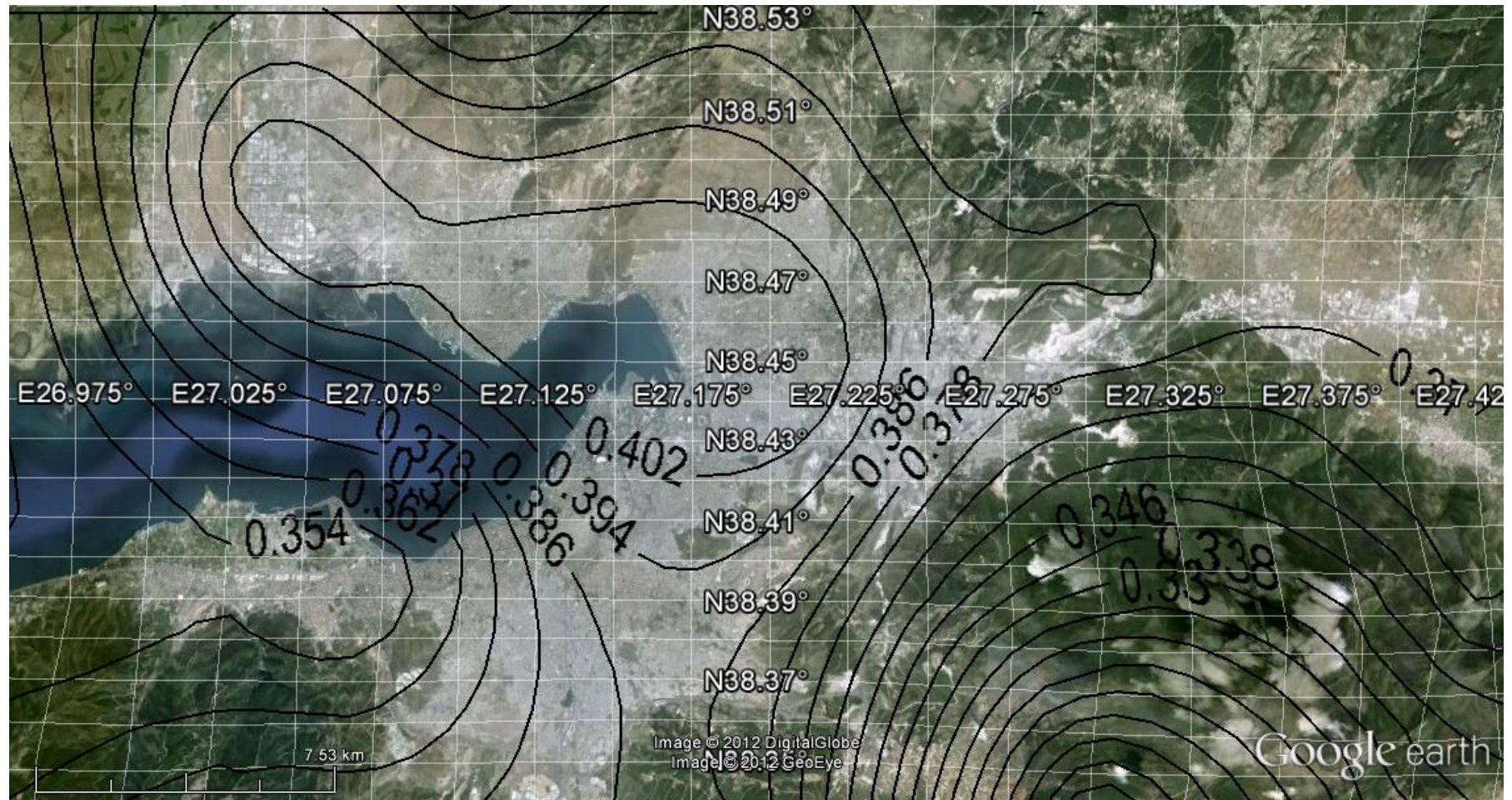


Figure E.15 (MAP 15): **Attenuation relationship:** Brian et al.(2008). **Probability of exceedance in 50 years: 2%**  
**Ground Acceleration (g) (Median)**    **Spectral period T=1 s**     $V_{s30}=760 \text{ m/s}$

**Values:**

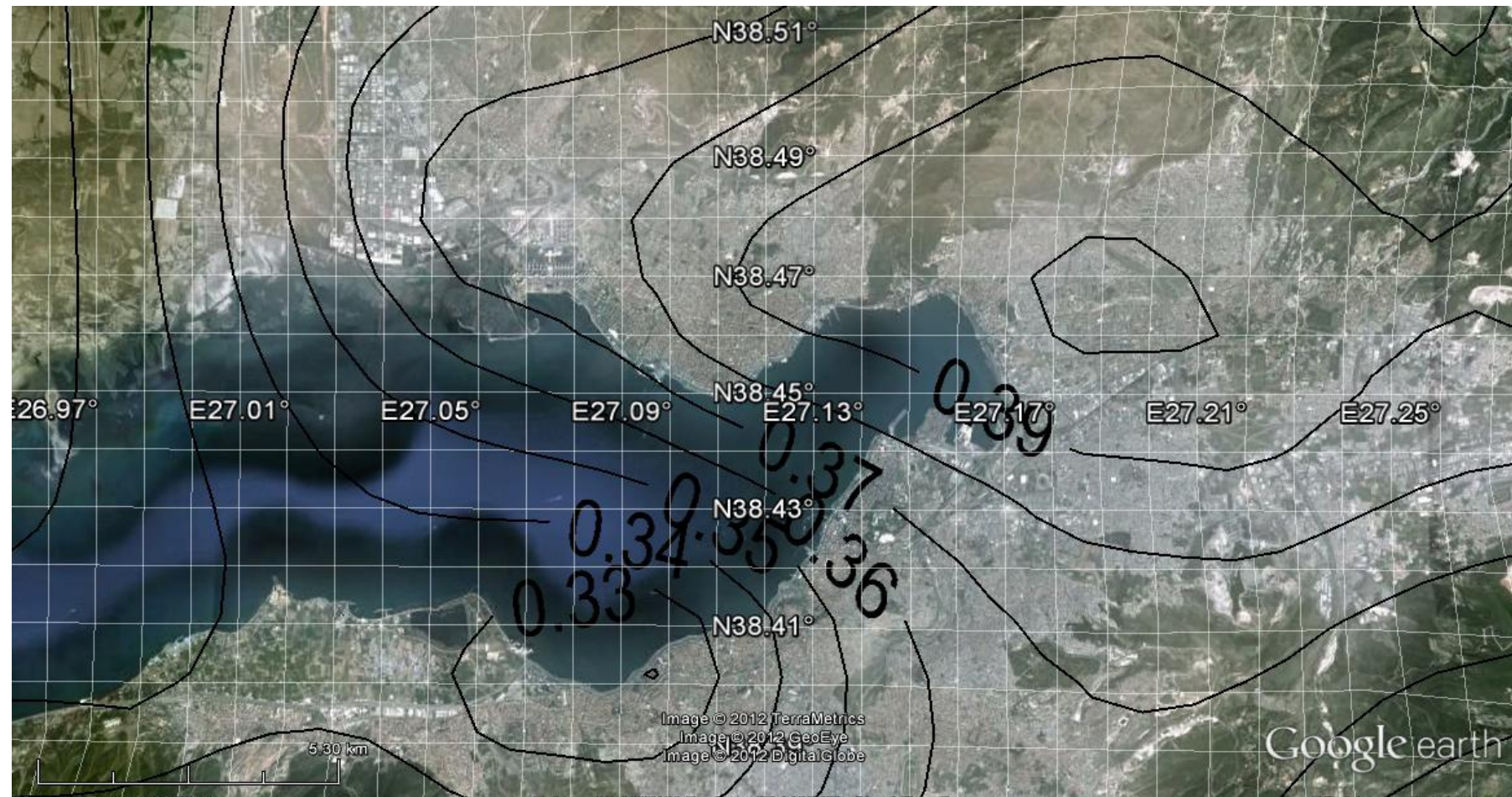
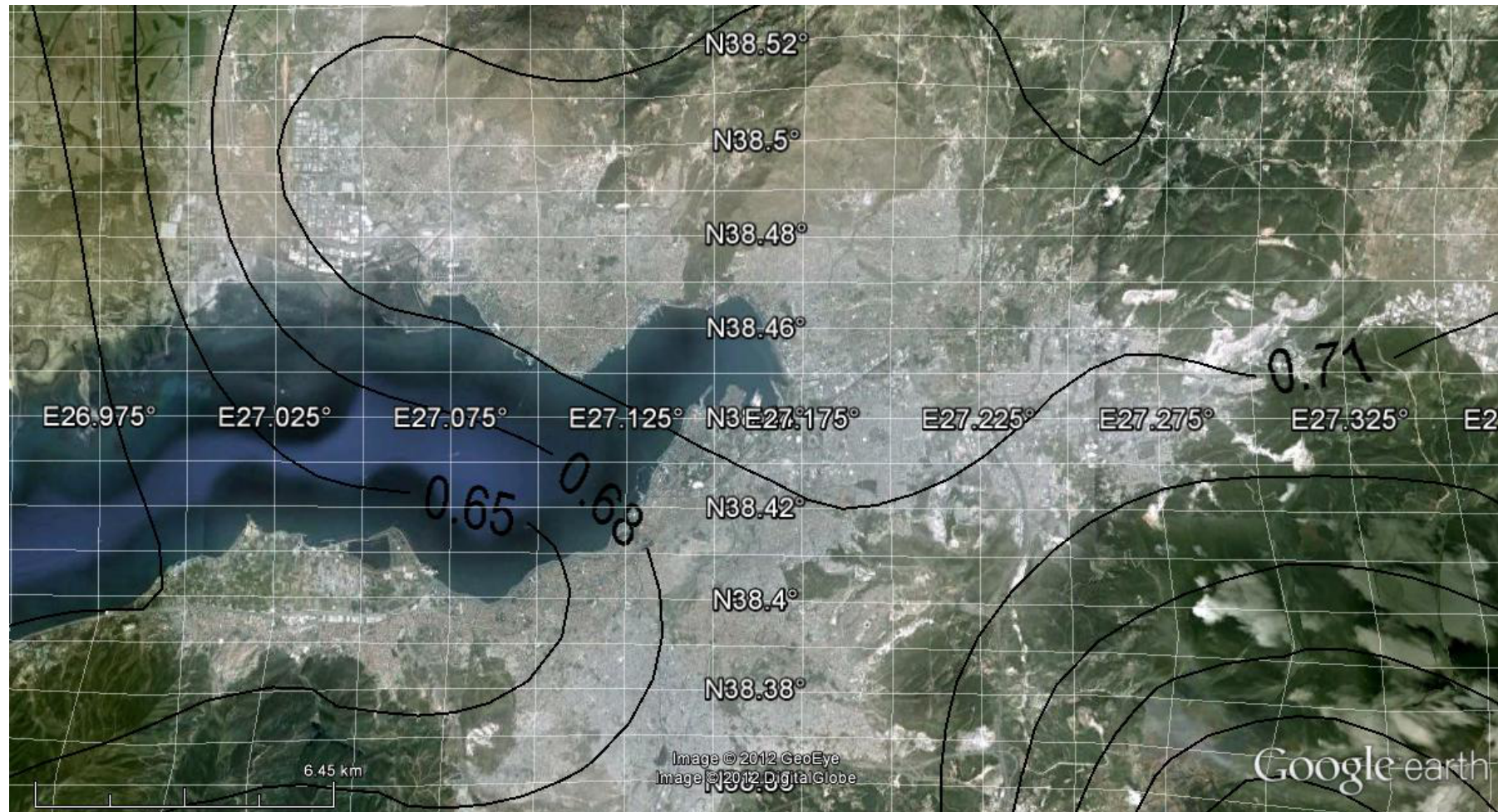


Figure E.16 (MAP 16): Attenuation relationship: Brian et al. (2008). Probability of exceedance in 50 years: 50%  
Ground Acceleration (g) (Median)      Spectral period T=0.2 s       $V_{s30}=760 \text{ m/s}$

Values:



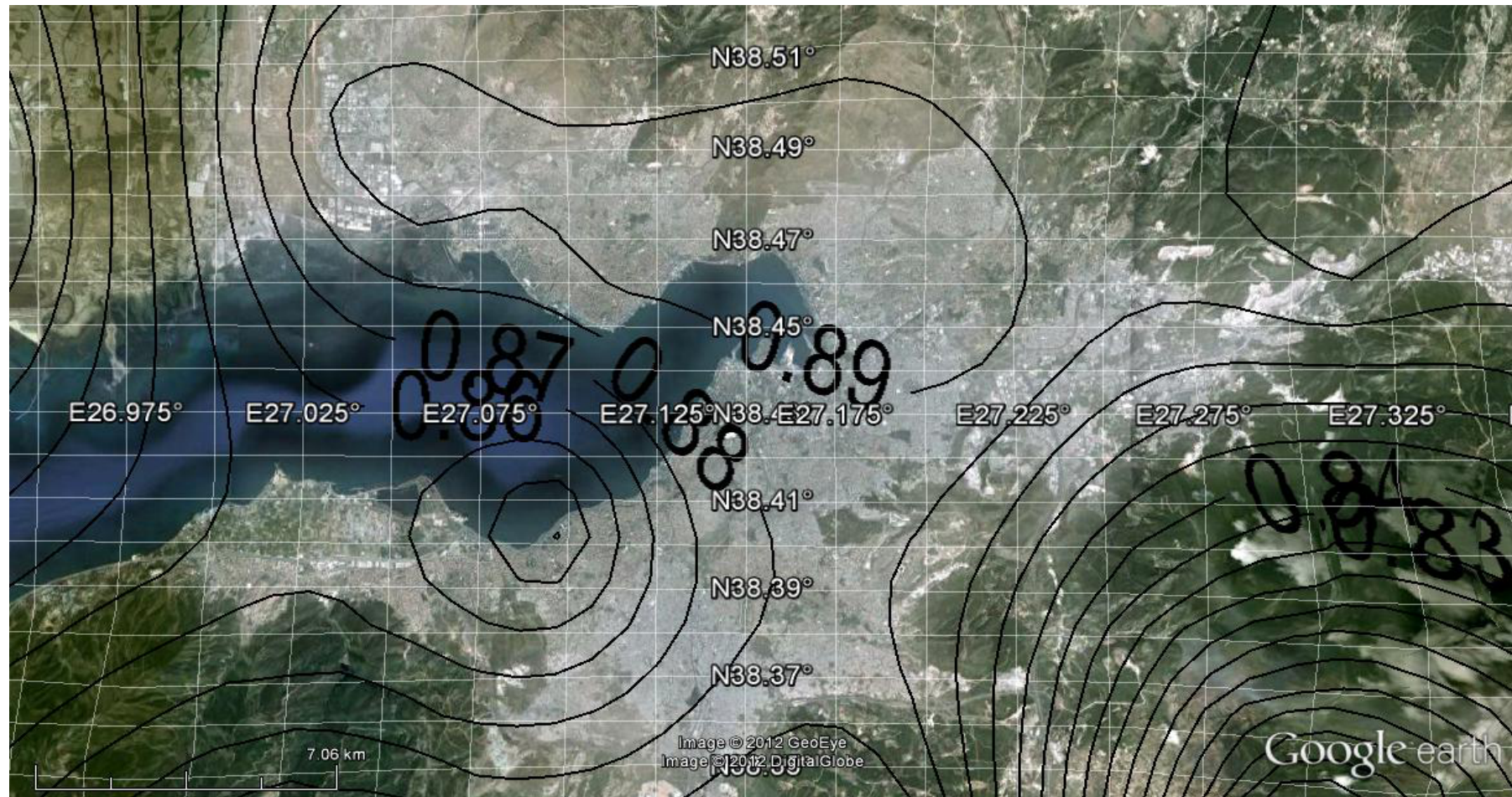


Figure E.18 (MAP 18): Attenuation relationship: Brian et al. (2008). Probability of exceedance in 50 years: 2%  
Ground Acceleration (g) (Median)    Spectral period T=0.2 s     $V_{s30}=760$  m/s

Values:

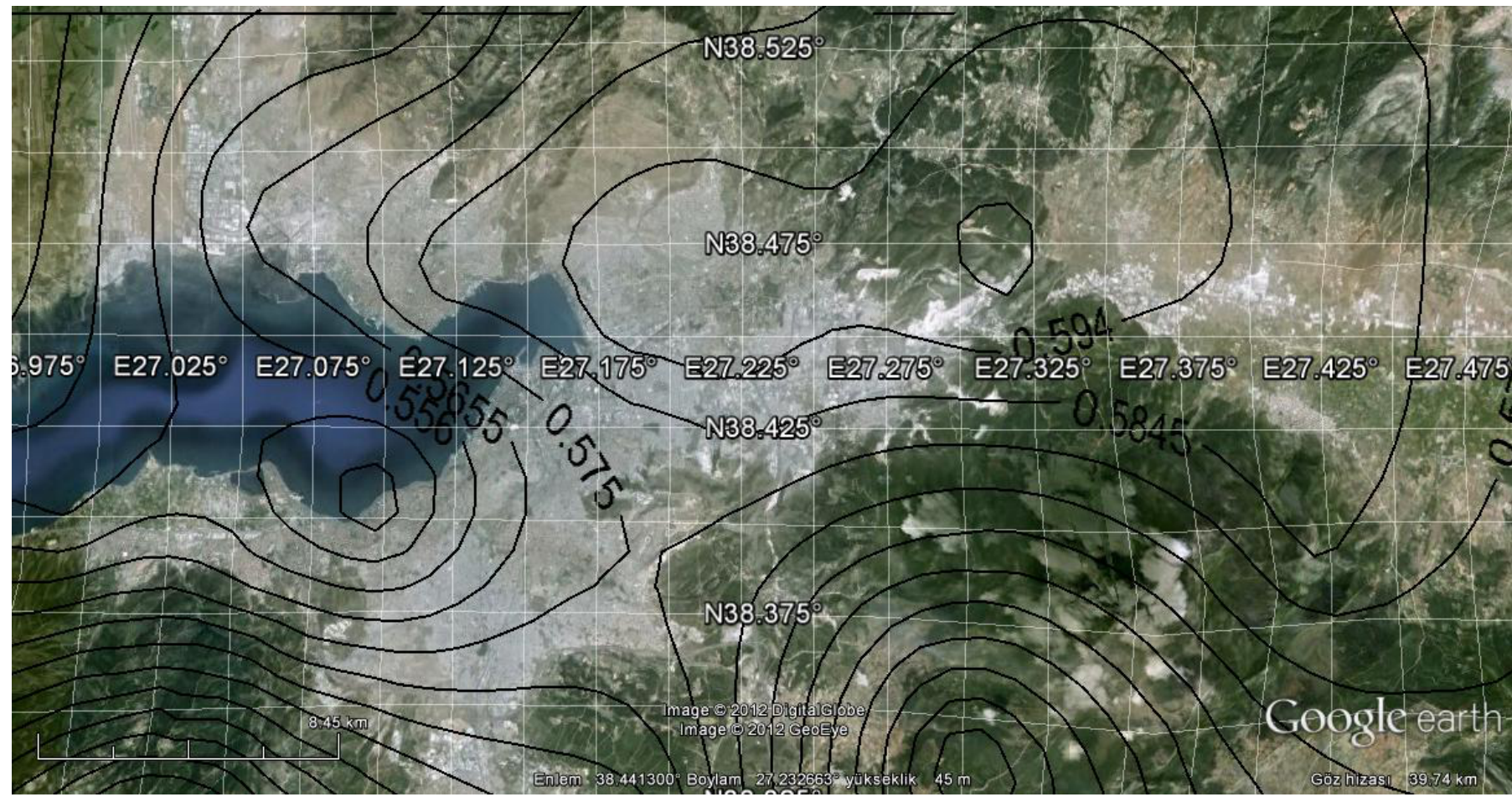


Figure E.19 (MAP 19): **Attenuation relationship:** Brian et al. (2008). **Probability of exceedance in 50 years:** 50%  
Ground Acceleration (g) (Median +Standard Deviation)    **Spectral period T=0.2 s**     $V_{s30}=760 \text{ m/s}$

**Values:**

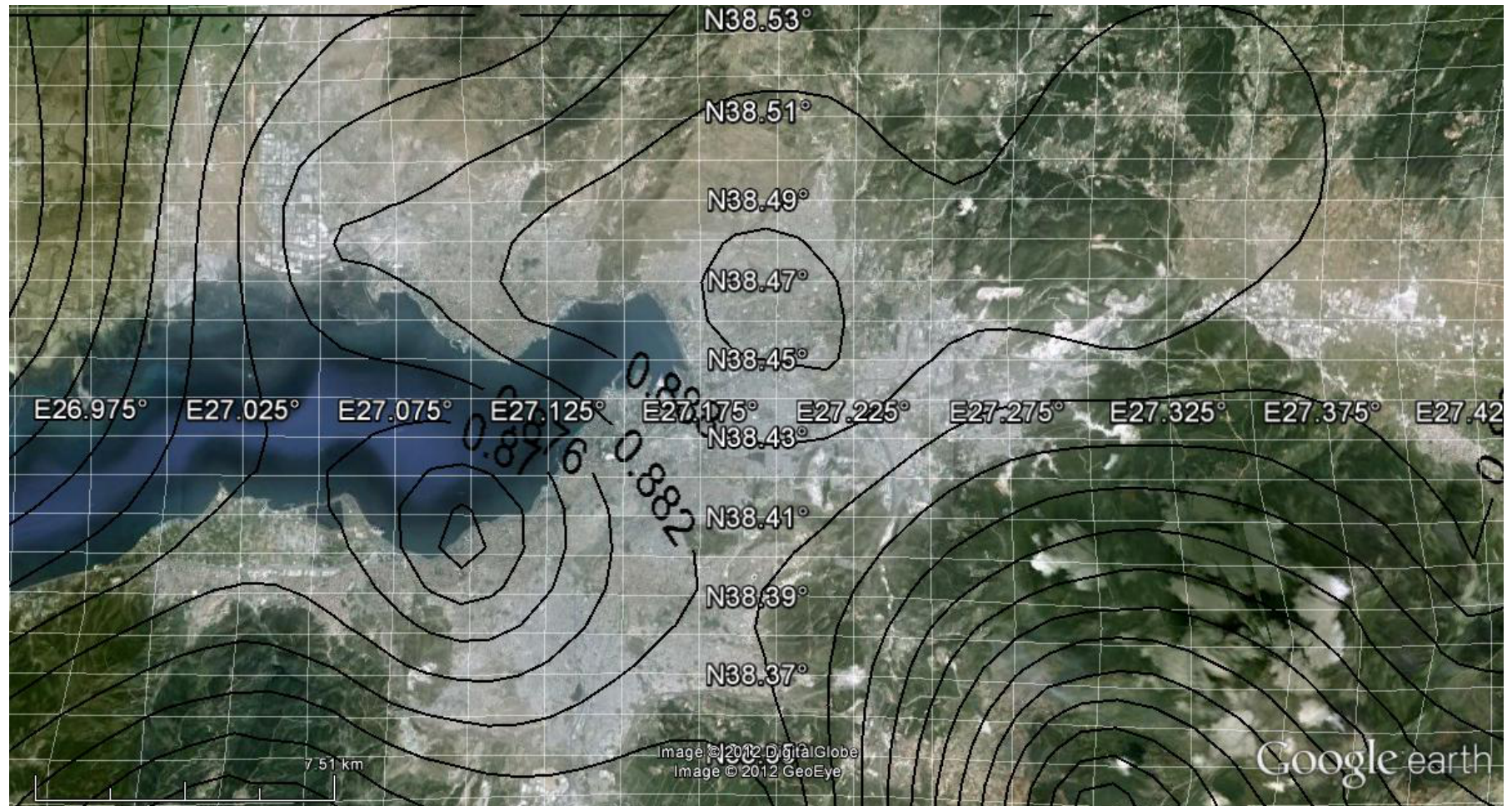


Figure E.20 (MAP 20): **Attenuation relationship:** Brian et al. (2008). **Probability of exceedance in 50 years:** 10%  
Ground Acceleration (g) (Median +Standard Deviation)      **Spectral period** T=0.2 s       $V_{s30}=760$  m/s

**Values:**

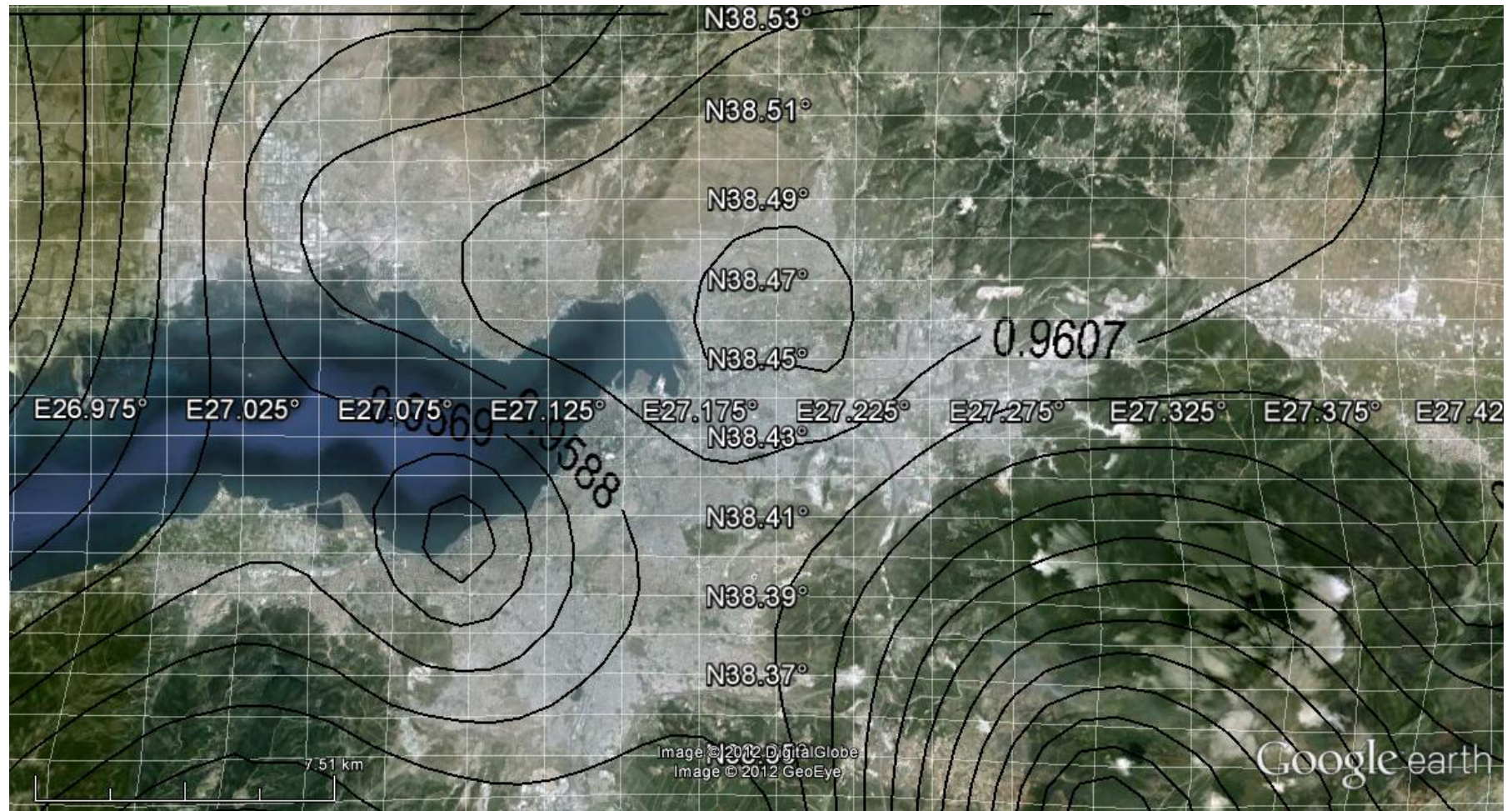


Figure E.21 (MAP 21): **Attenuation relationship:** Brian et al. (2008). **Probability of exceedance in 50 years:** 2%  
Ground Acceleration (g) (Median +Standard Deviation)    **Spectral period T=0.2 s**     $V_{s30}=760 \text{ m/s}$

**Values:**

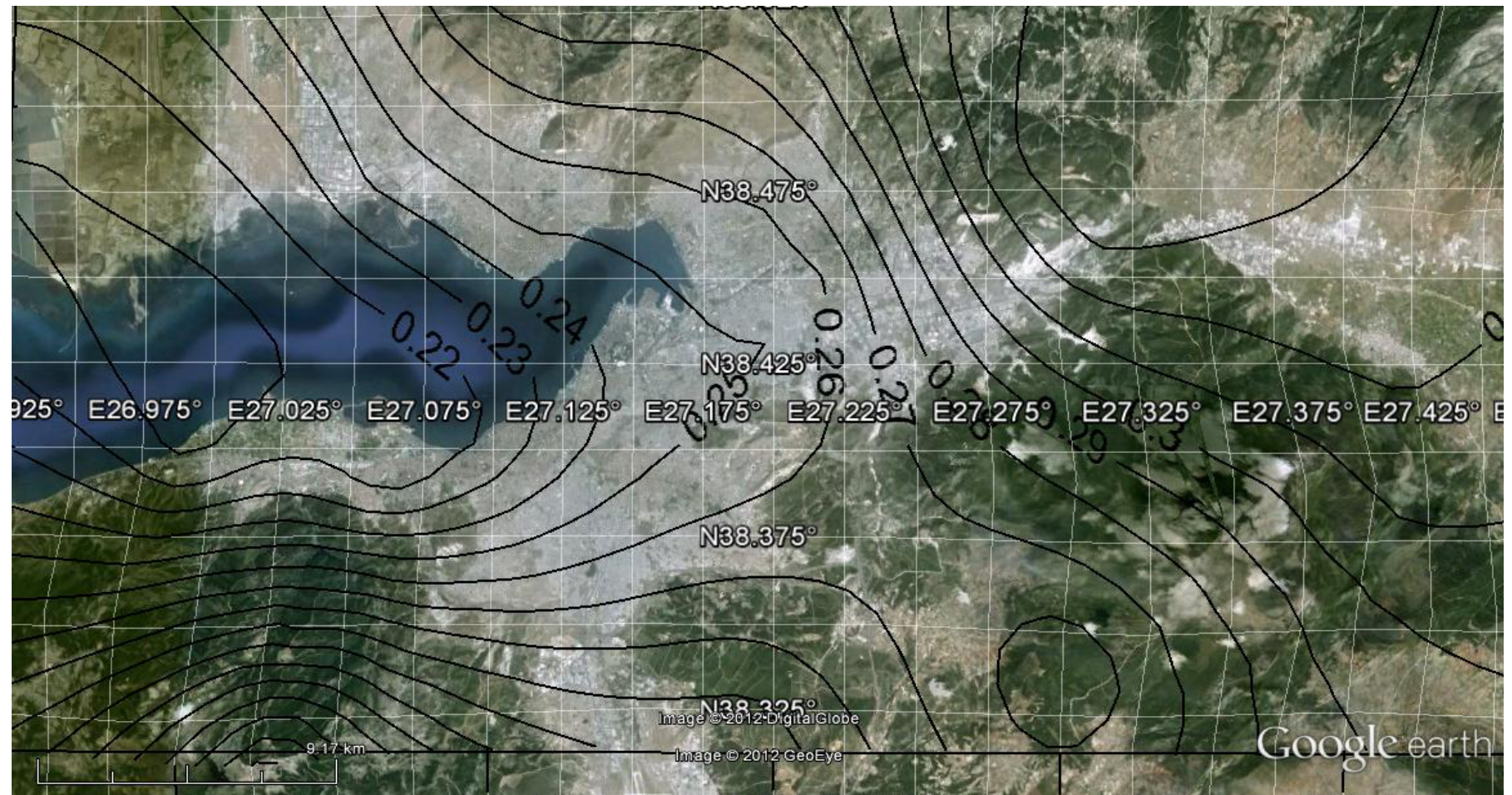


Figure E.22 (MAP 22): **Attenuation relationship:** Brian et al. (2008). **Probability of exceedance in 50 years: 50%**  
Ground Acceleration (g) (Median +Standard Deviation)      **Spectral period T=1 s**       $V_{s30}=760 \text{ m/s}$

Values:

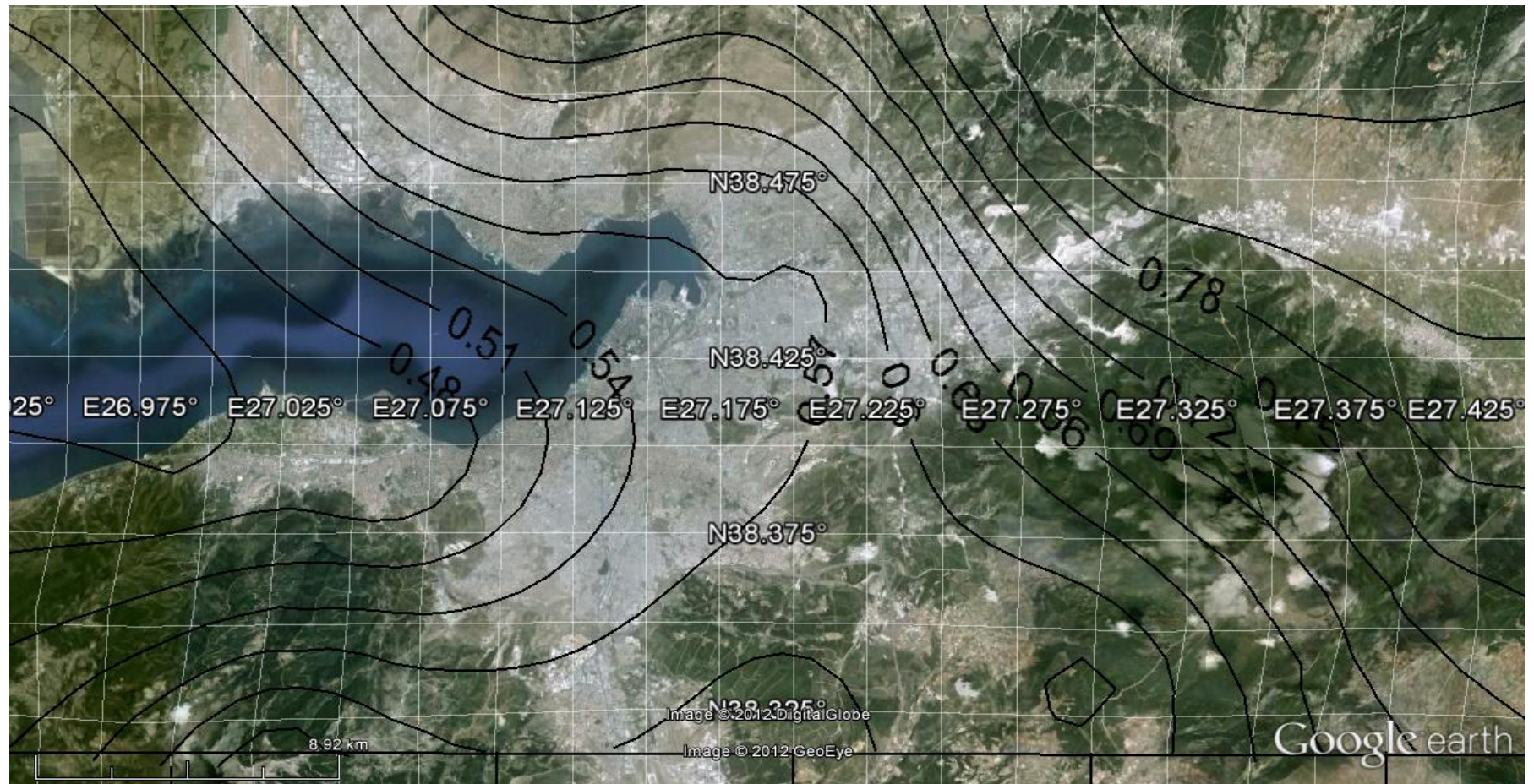


Figure E.23 (MAP 23): **Attenuation relationship:** Brian et al. (2008). **Probability of exceedance in 50 years:** 10%  
Ground Acceleration (g) (Median +Standard Deviation)    **Spectral period T=1 s**     $V_{s30}=760 \text{ m/s}$

**Values:**

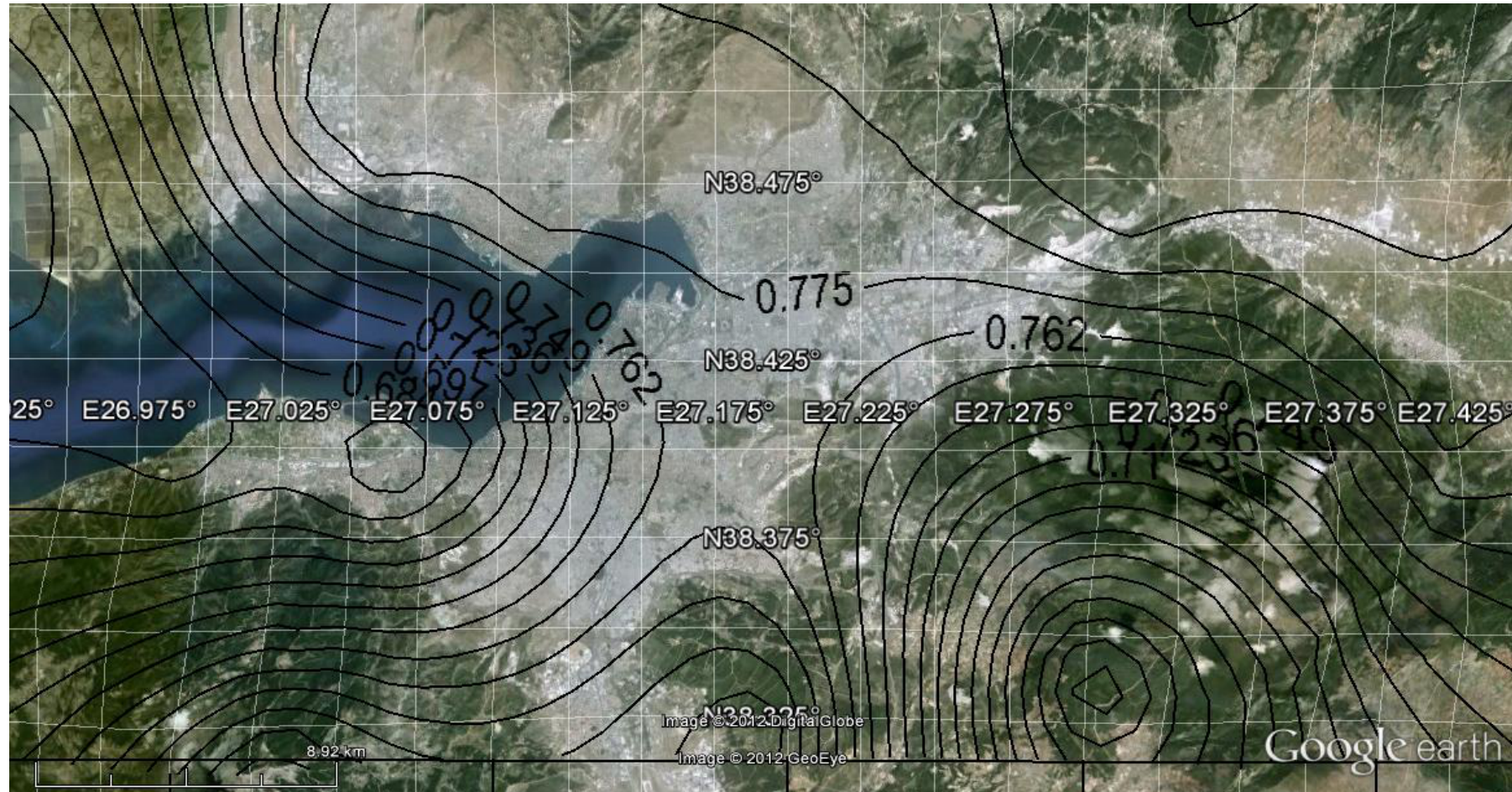


Figure E.24 (MAP 24): **Attenuation relationship:** Brian et al. (2008). **Probability of exceedance in 50 years:** 2%  
Ground Acceleration (g) (Median +Standard Deviation)    **Spectral period T=1 s**     $V_{s30}=760 \text{ m/s}$

**Values:**

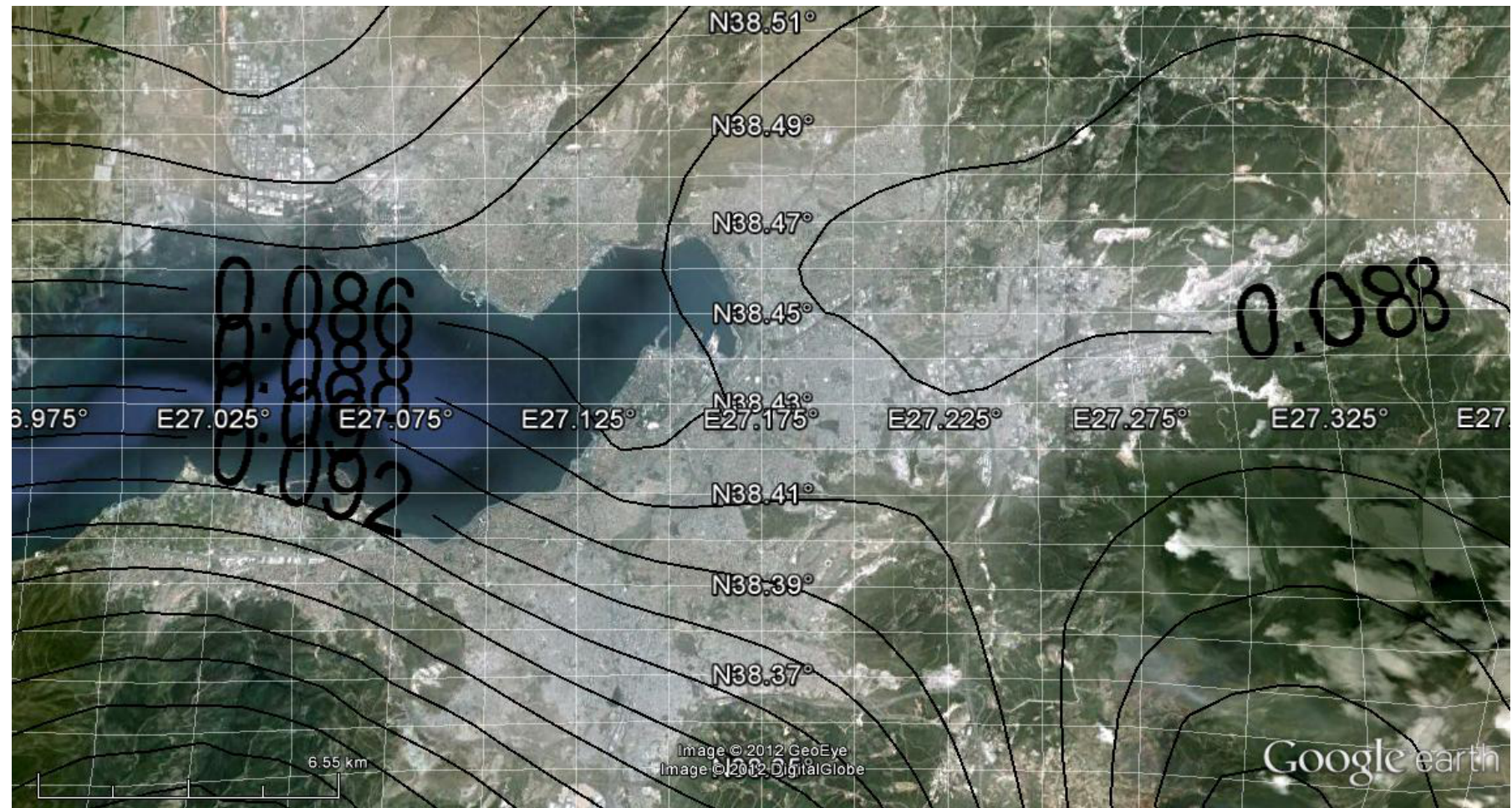


Figure E.25 (MAP 25): **Attenuation relationship:** Boore & Atkinson (2007). **Probability of exceedance in 50 years:** 50%  
**Values:** Ground Acceleration (g) (Median)    **Spectral period**  $T=1$  s     $V_{s30}=760$  m/s

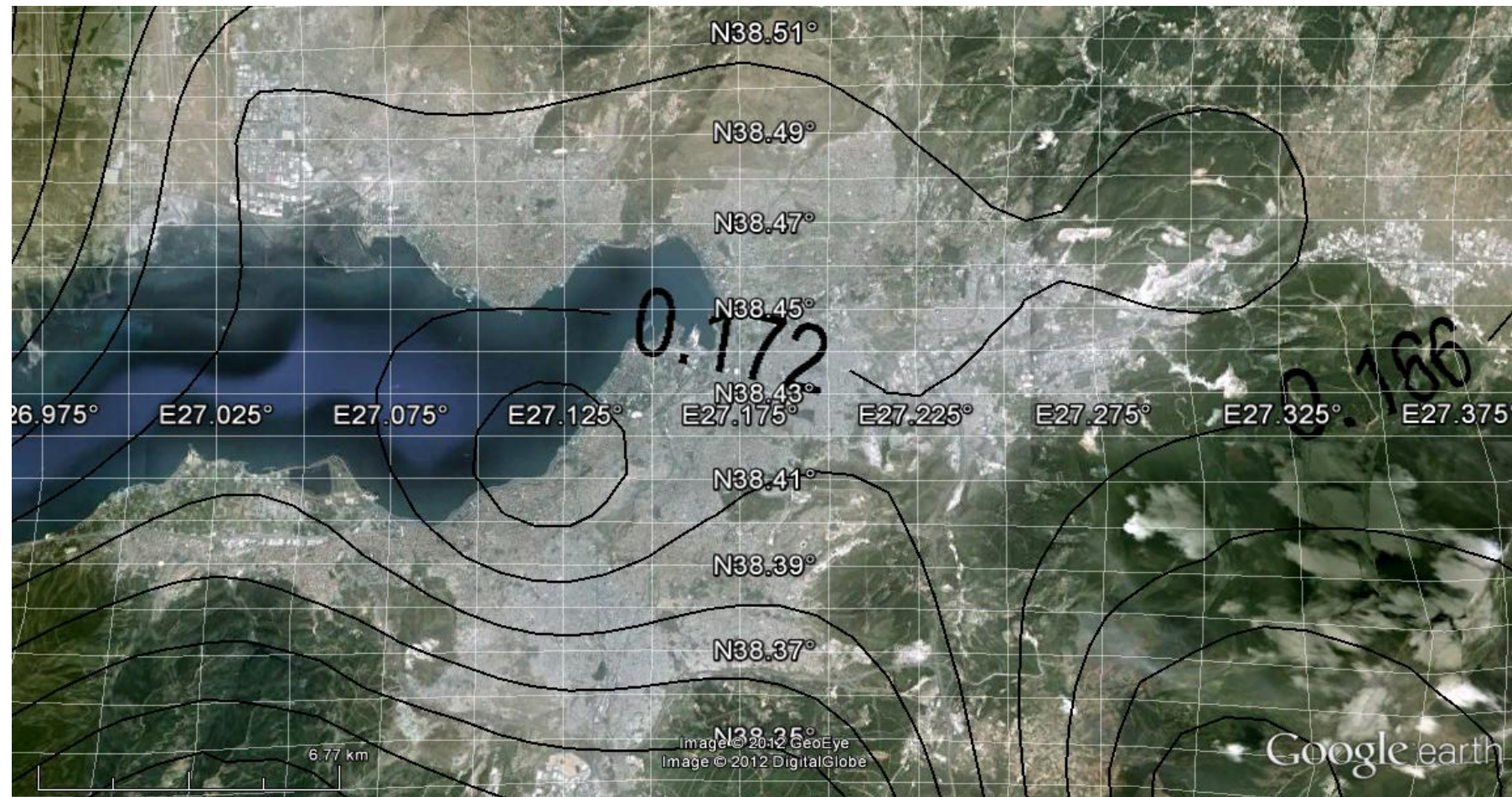


Figure E.26 (MAP 26): **Attenuation relationship:** Boore & Atkinson (2007). **Probability of exceedance in 50 years:** 10%

**Values:** Ground Acceleration (g) (Median)    **Spectral period** T=1 s     $V_{s30}=760$  m/s

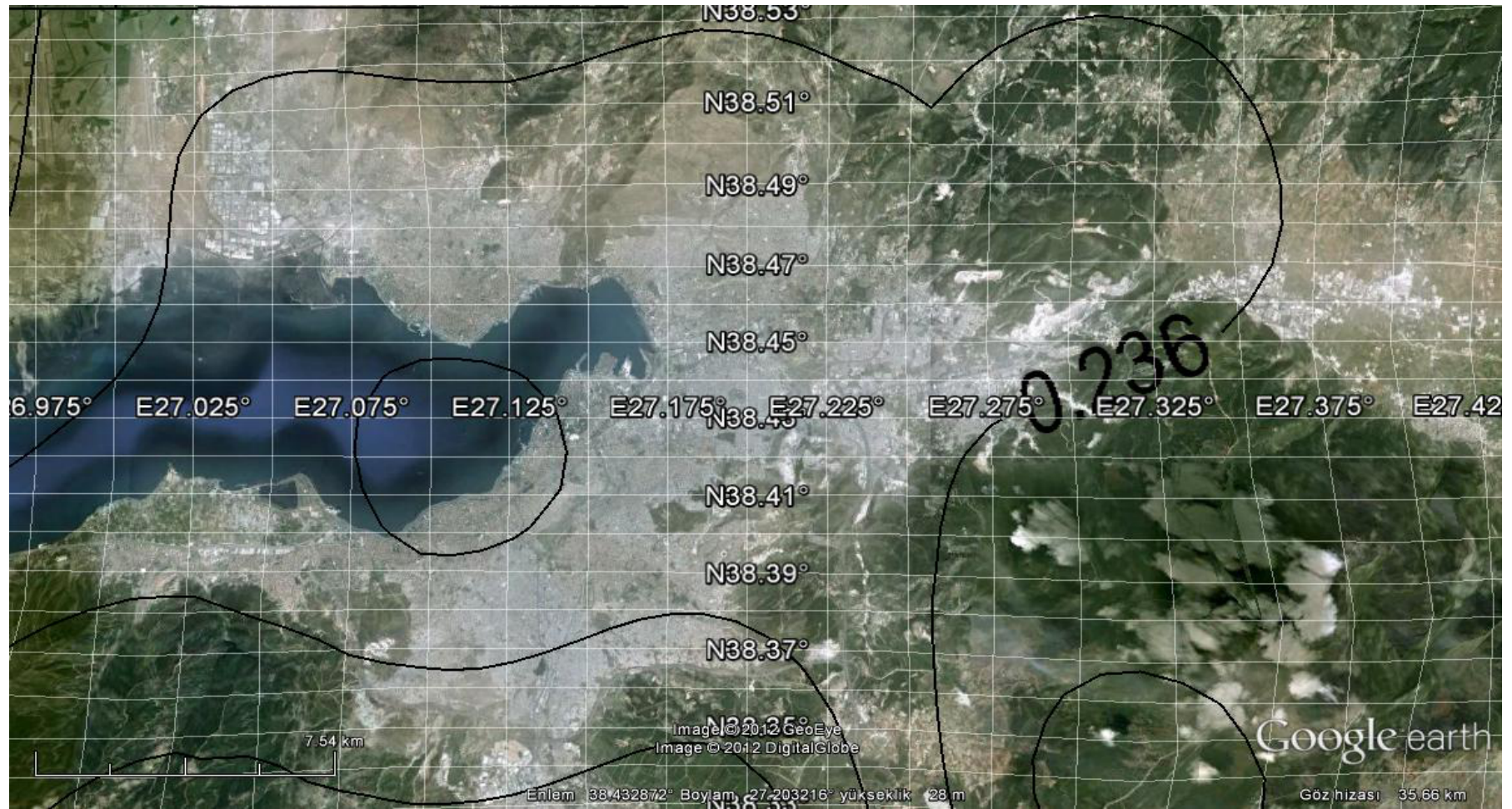


Figure E.27 (MAP 27): Attenuation relationship: Boore & Atkinson (2007). Probability of exceedance in 50 years: 2%

Values: Ground Acceleration (g) (Median)    Spectral period T=1 s     $V_{s30}=760$  m/s

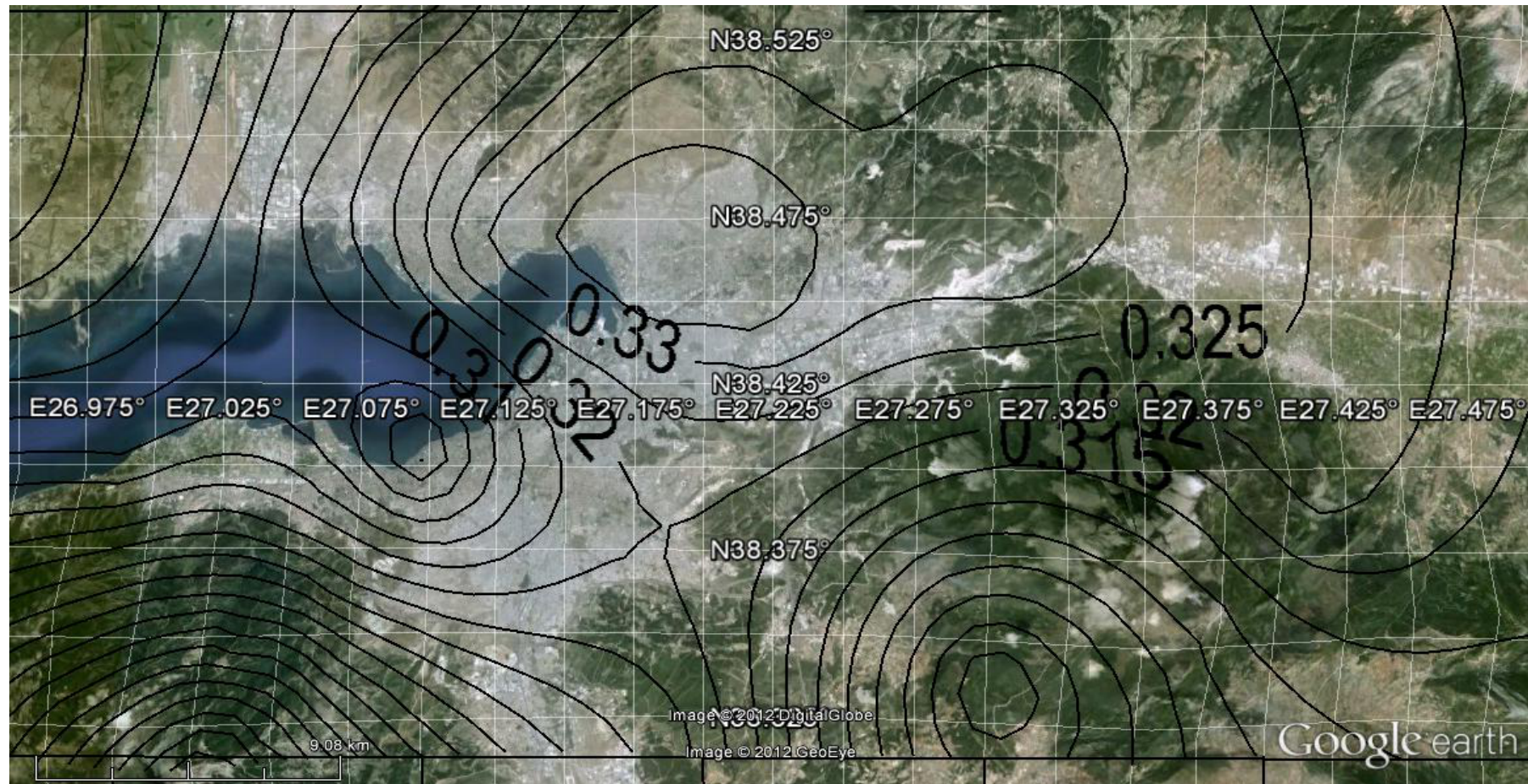


Figure E.28 (MAP 28): **Attenuation relationship:** Boore & Atkinson (2007). **Probability of exceedance in 50 years:** 50%

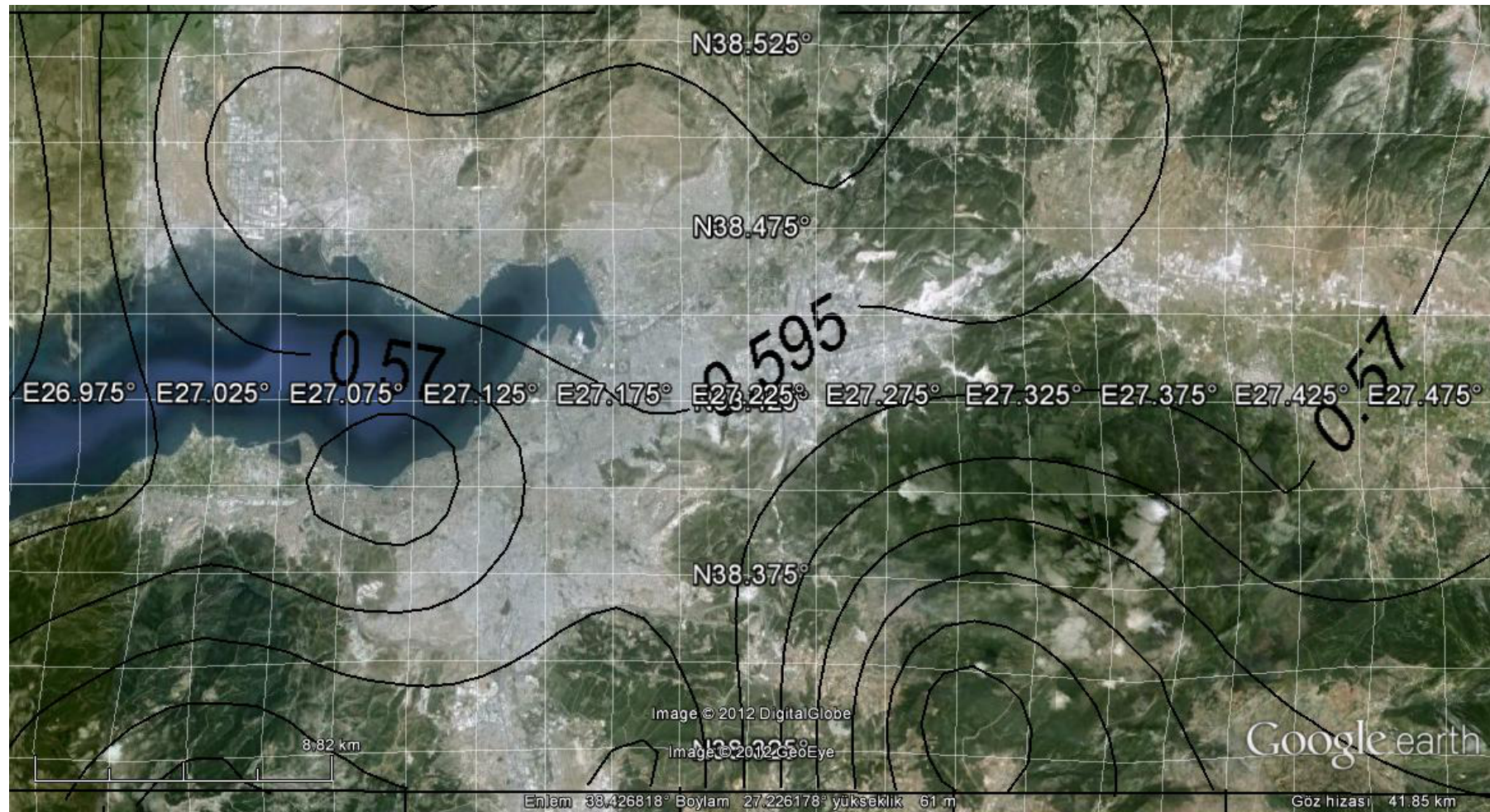


Figure E.29 (MAP 29): **Attenuation relationship:** Boore & Atkinson (2007). **Probability of exceedance in 50 years:** 10%  
**Values:** Ground Acceleration (g) (Median)    **Spectral period** T=0.2 s    V<sub>s30</sub>=760 m/s

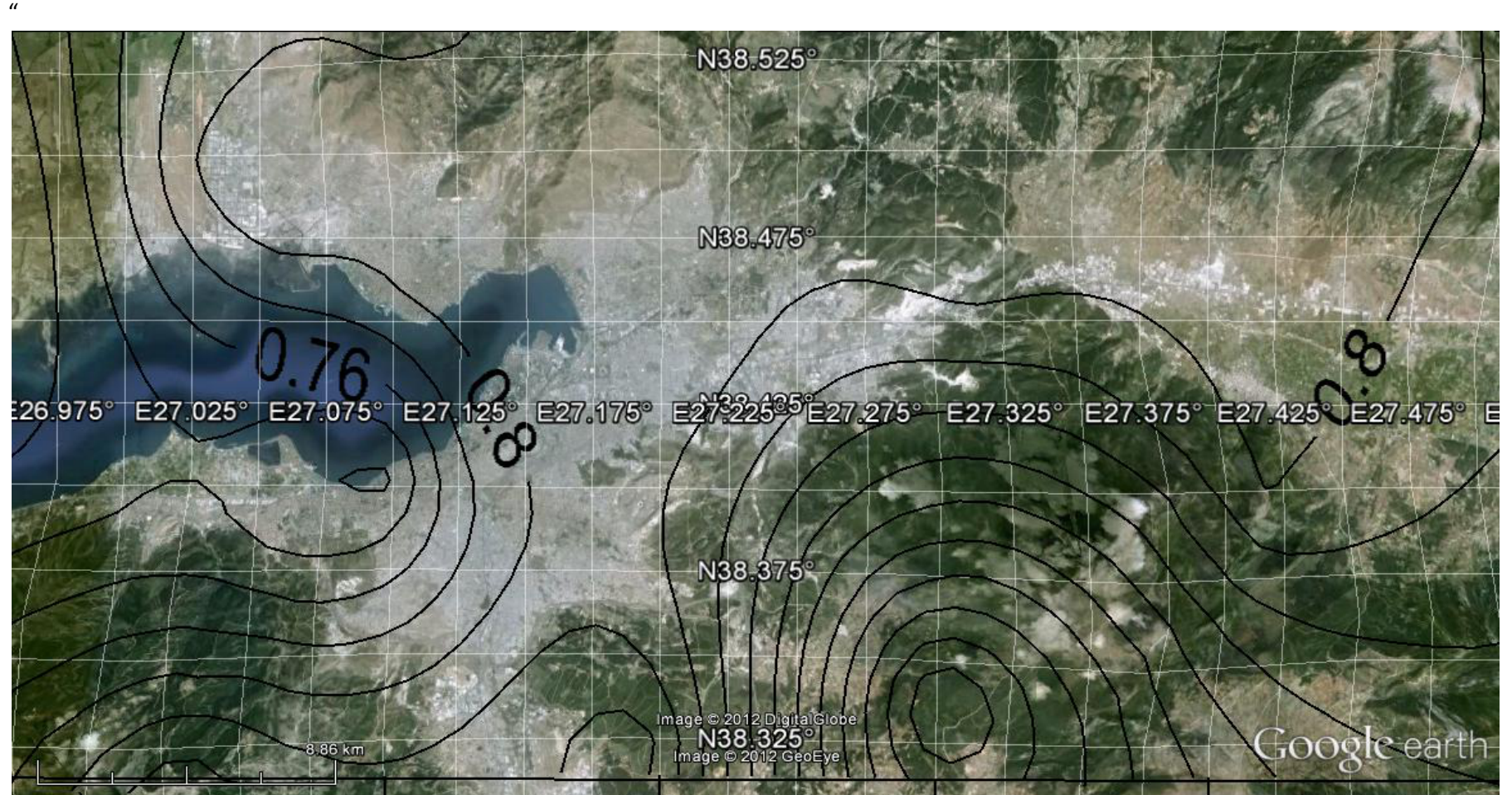


Figure E.30 (MAP 30): **Attenuation relationship:** Boore & Atkinson (2007). **Probability of exceedance in 50 years:** 2%  
**Values:** Ground Acceleration (g) (Median)    **Spectral period**  $T=0.2$  s     $V_{s30}=760$  m/s

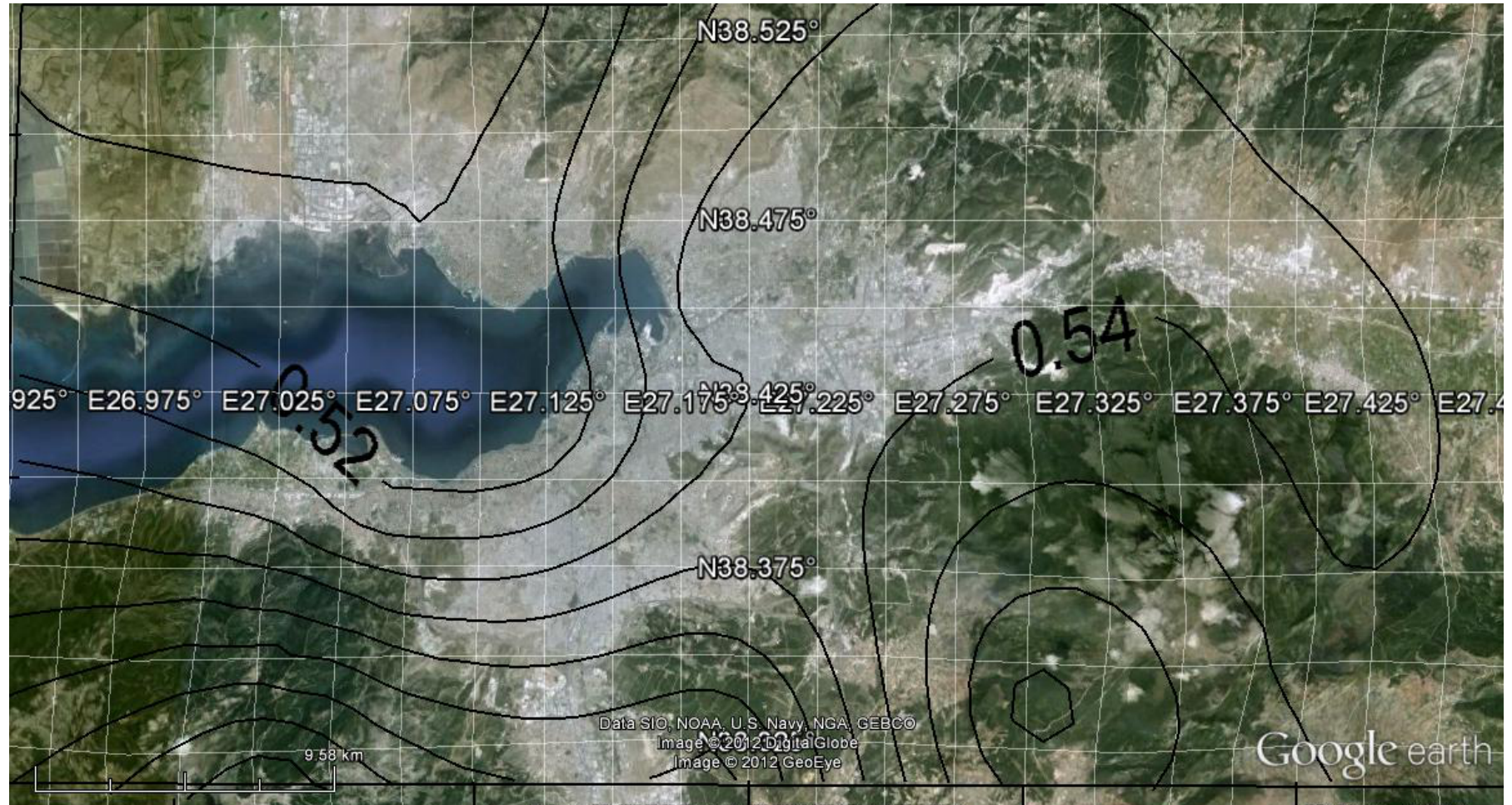


Figure E.31 (MAP 31): **Attenuation relationship**: Boore & Atkinson (2007). **Probability of exceedance in 50 years:** 50%  
**Values:** Ground Acceleration (g) (Median+ Standard Deviation)    **Spectral period** T=0.2 s     $V_{s30}=760$  m/s

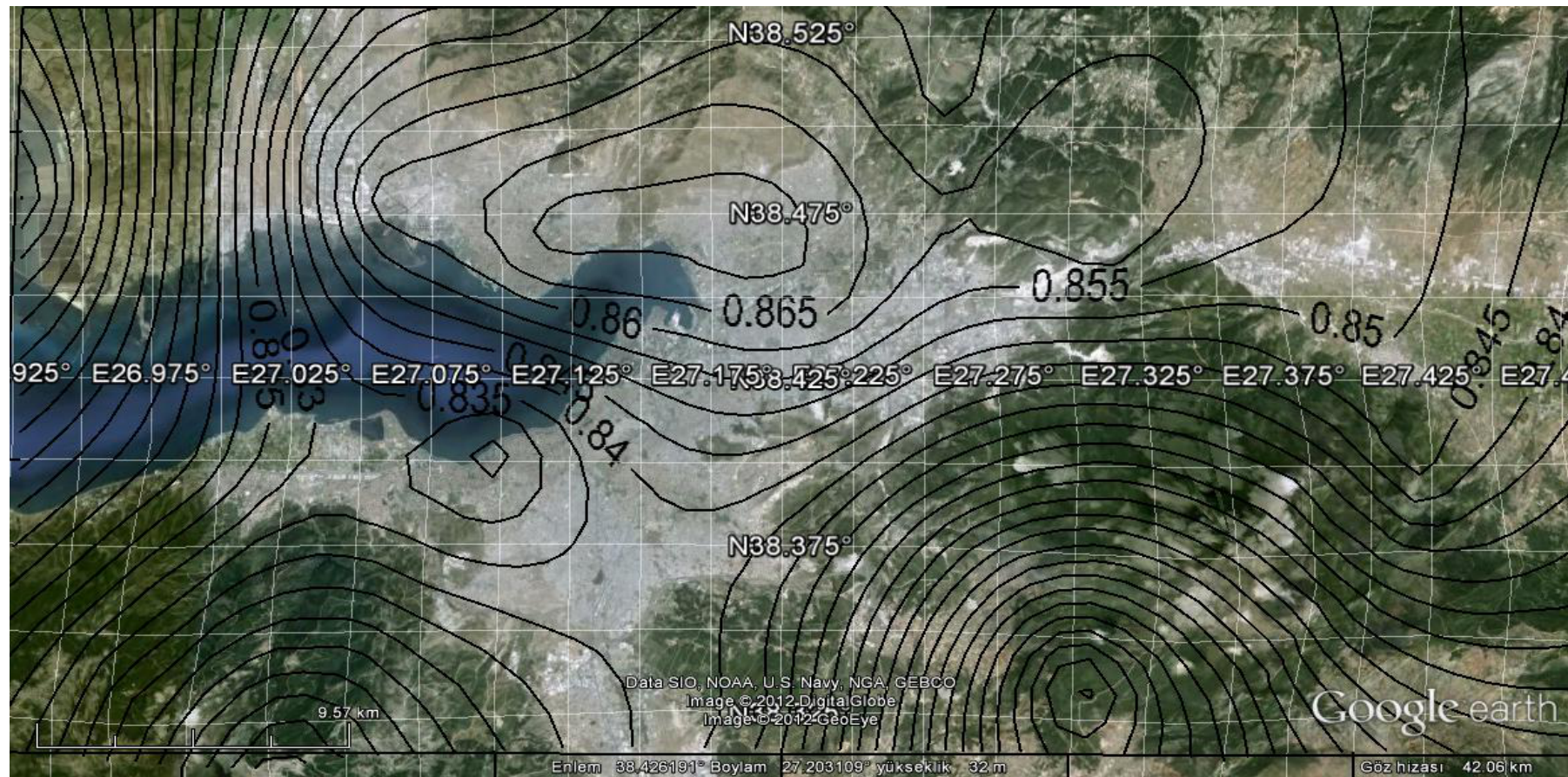


Figure E.32 (MAP 32): **Attenuation relationship:** Boore & Atkinson (2007). **Probability of exceedance in 50 years:** 10%  
**Values:** Ground Acceleration (g) (Median+ Standard Deviation)    **Spectral period** T=0.2 s    V<sub>s30</sub>=760 m/s

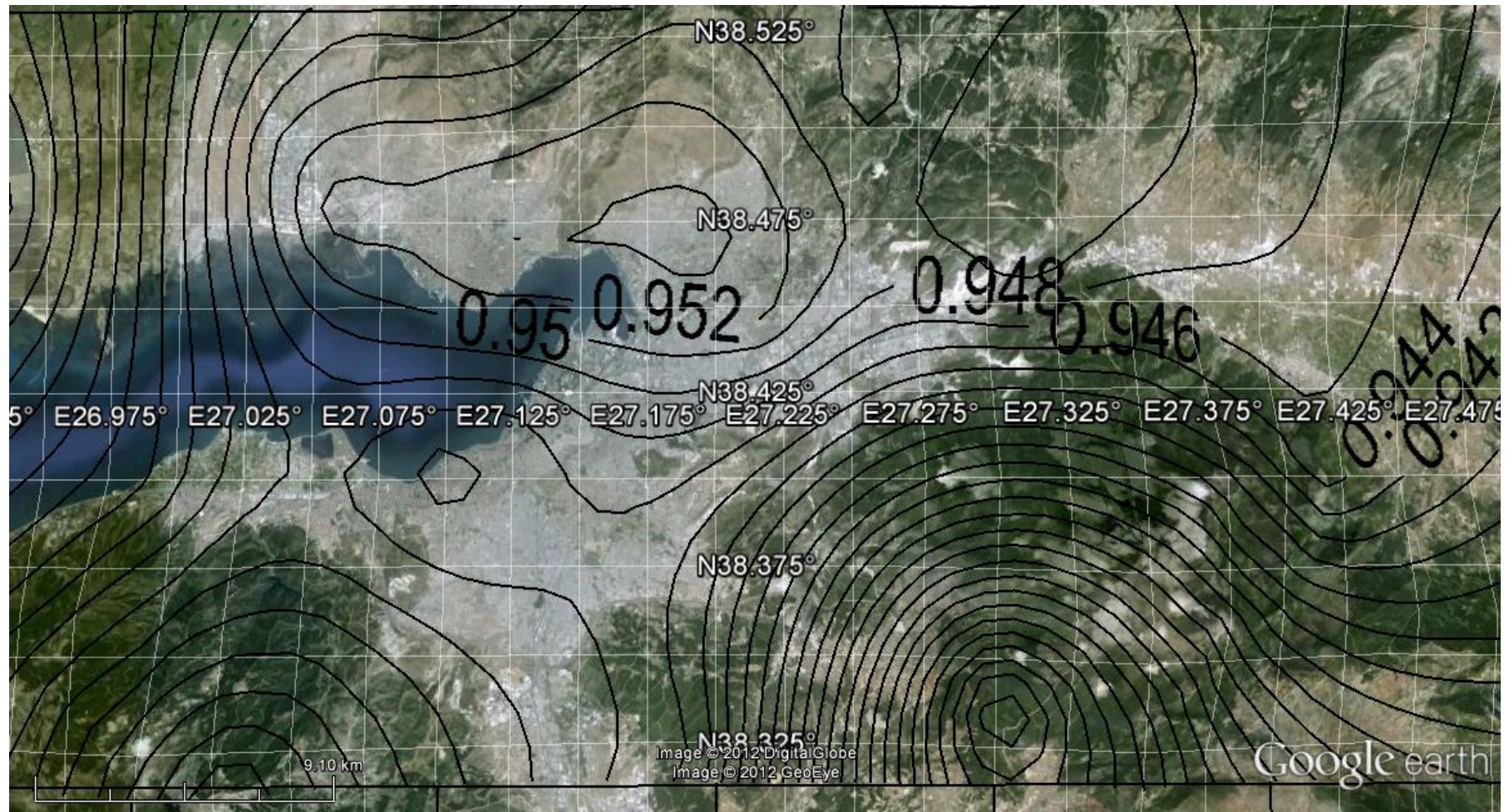


Figure E.33 (MAP 33): **Attenuation relationship:** Boore & Atkinson (2007). **Probability of exceedance in 50 years:** 2%  
**Values:** Ground Acceleration (g) (Median+ Standard Deviation)    **Spectral period** T=0.2 s    V<sub>s30</sub>=760 m/s

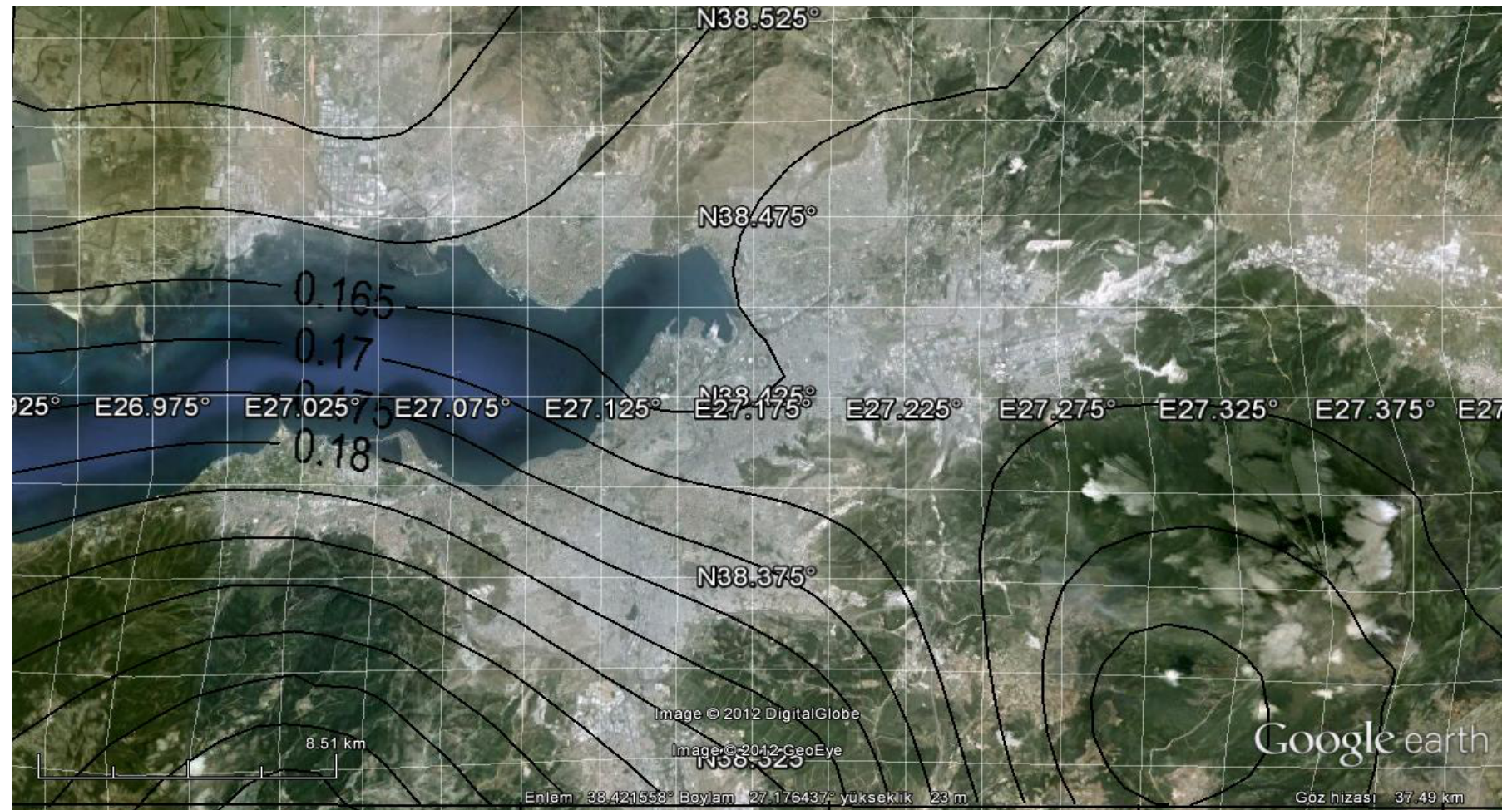


Figure E.34 (MAP 34): **Attenuation relationship:** Boore & Atkinson (2007). **Probability of exceedance in 50 years:** 50%  
**Values:** Ground Acceleration (g) (Median+ Standard Deviation)    **Spectral period** T=1 s     $V_{s30}=760$  m/s

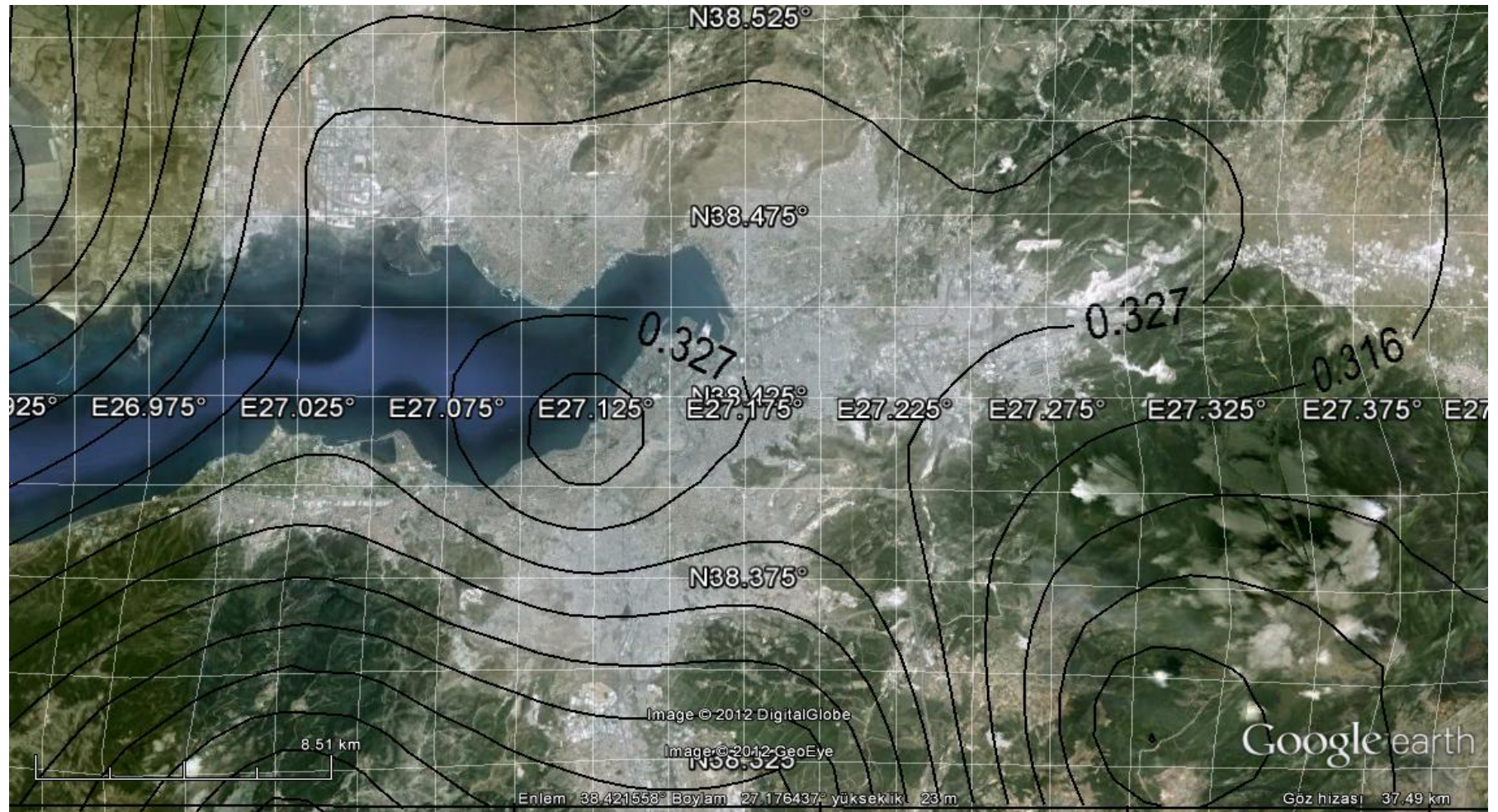


Figure E.35 (MAP 35): **Attenuation relationship:** Boore & Atkinson (2007). **Probability of exceedance in 50 years:** 10%  
**Values:** Ground Acceleration (g) (Median+ Standard Deviation)    **Spectral period T=1 s**     $V_{s30}=760 \text{ m/s}$

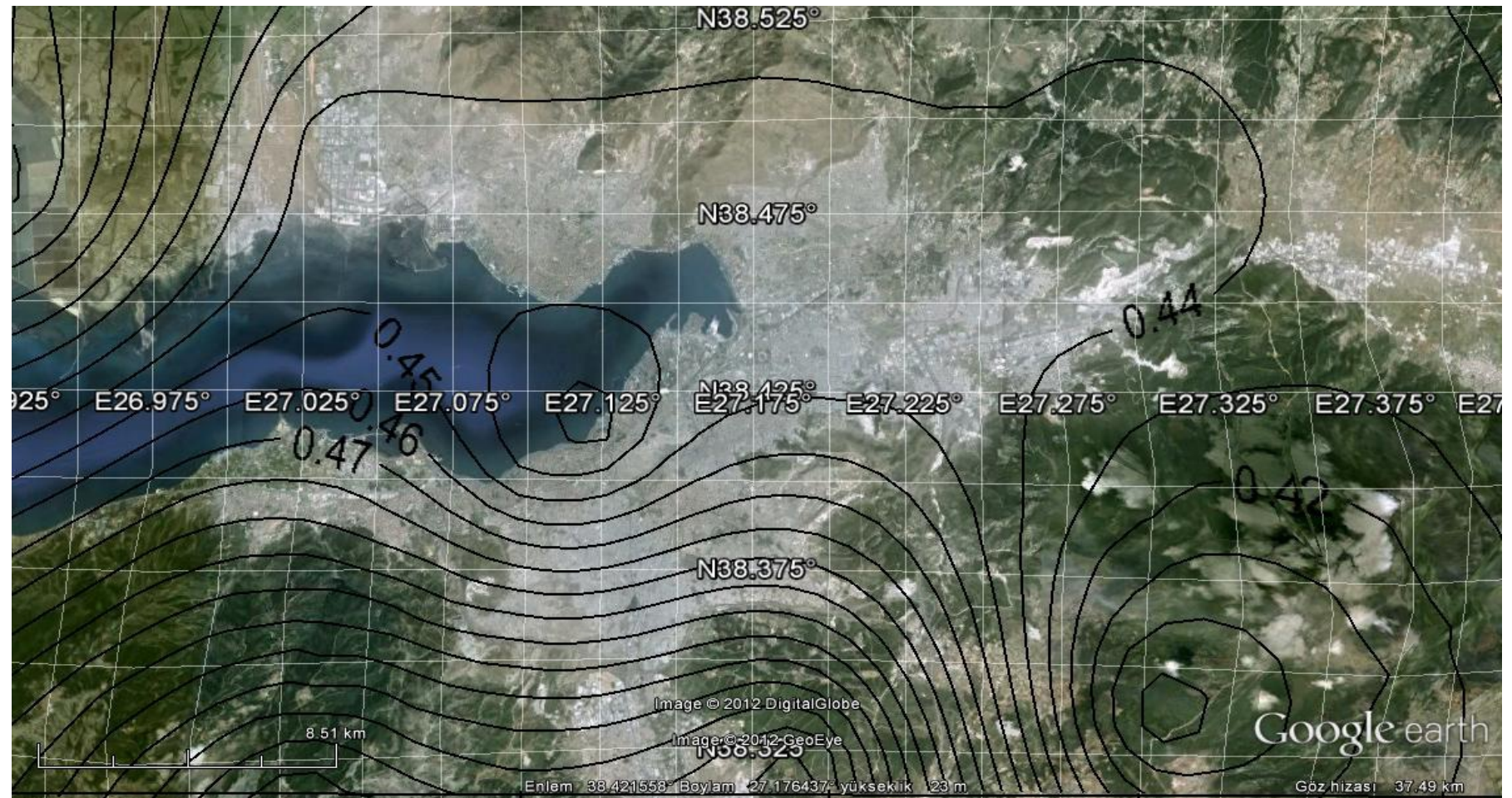


Figure E.36 (MAP 36): **Attenuation relationship:** Boore & Atkinson (2007). **Probability of exceedance in 50 years:** 2%  
**Values:** Ground Acceleration (g) (Median+ Standard Deviation)    **Spectral period T=1 s**     $V_{s30}=760 \text{ m/s}$